3-27-2014 12:00 AM

Distinct roles of BMP and LKB1/AMPK signalling impacting ovarian cancer spheroid biology

Teresa M. Peart
The University of Western Ontario

Supervisor
Dr. Trevor Shepherd
The University of Western Ontario Joint Supervisor
Dr. Gabriel DiMattia
The University of Western Ontario

Graduate Program in Anatomy and Cell Biology
A thesis submitted in partial fulfillment of the requirements for the degree in Doctor of Philosophy

DISTINCT ROLES OF BONE MORPHOGENETIC PROTEIN AND LIVER KINASE B1/AMP-ACTIVATED PROTEIN KINASE SIGNALLING IMPACTING OVARIAN CANCER SPHEROID BIOLOGY

(Thesis format: Integrated Article)

by

Teresa Marie Peart

Graduate Program in Anatomy and Cell Biology

A thesis submitted in partial fulfillment
of the requirements for the degree of
Doctor of Philosophy

The School of Graduate and Postdoctoral Studies
The University of Western Ontario
London, Ontario, Canada

Abstract

High-grade serous (HGS) carcinoma, the most prevalent and most deadly subtype of epithelial ovarian cancer (EOC), presents unique therapeutic challenges since the majority of cases are diagnosed at advanced, metastatic stage. At this point widespread intraperitoneal metastatic lesions are numerous, which is why models that recapitulate disease dissemination are critical to uncover novel therapeutic targets. One of the initiating events in ovarian cancer metastasis is shedding from the primary tumour into the peritoneal cavity where cells must survive in suspension in order to seed secondary tumours. This non-adherent population of cells exists as multicellular aggregates, or spheroids; data from our lab has demonstrated that cells within spheroids are dormant, yet are readily alter their phenotype upon reattachment to an adherent substratum. To further explore the pathobiology of ovarian cancer spheroids, my thesis work describes the functional characterization of two different signalling pathways—bone morphogenetic protein (BMP), and the liver kinase B1 (LKB1)/AMP-activated protein kinase (AMPK)—which mediate distinct and important aspects of spheroid formation and reattachment. Activated BMP signalling resulted in smaller, loosely-aggregated spheroids, which were more readily able to reattach and disperse. These phenotypic alterations observed as a result of active BMP signalling were mediated, at least in part, by cooperation with the AKT signalling pathway. These studies implicate inhibition of BMP and AKT signalling as potential strategies for therapeutic targeting of reattaching spheroids, which is critical for the formation of secondary metastatic lesions. Other work in our lab implicated the downregulation of AKT signalling in spheroid formation-induced dormancy. In an attempt to uncover additional pathways promoting the dormant phenotype of ovarian cancer spheroids, I investigated the LKB1/AMPK signalling cascade given its ability to alter cellular metabolism in response to nutrient and energy availability. Despite a dramatic enhancement in AMPK activity observed in ovarian cancer spheroids, targeted knockdown had no effect on viability of cells in this context. However, knockdown of its upstream kinase, LKB1, revealed a dramatic decrease in ovarian cancer spheroid viability, suggesting a role for this kinase in mediating anoikis-resistance in an AMPK-independent manner. Taken together, my results have uncovered two distinct and important signalling pathways that regulate unique aspects of spheroid formation, cell survival, and reattachment. By understanding the molecular mechanisms used by ovarian cancer spheroids to survive during dissemination and promote

secondary metastasis, my work has uncovered additional therapeutic targets for the potential treatment of advanced-stage ovarian cancer.

Keywords

Ovarian cancer, high-grade serous ovarian carcinoma, patient samples, spheroids, BMP, LKB1, AMPK

Co-Authorship Statement

All chapters were written by Teresa Peart and edited by Dr. Trevor Shepherd and Dr. Gabriel DiMattia.

The data presented in Chapter 2 appeared in the published manuscript "BMP signalling controls the malignant potential of ascites-derived human epithelial ovarian cancer spheroids via AKT kinase activation." Teresa Peart, Rohann Correa, Yudith Ramos-Valdes, Gabriel DiMattia, Trevor Shepherd. *Clin Exp Metastasis*. 2012. 29: 293-313. YRV and RC contributed to flow cytometry and reattachment assays respectively. All other data was generated and analyzed by TP. The manuscript was written by TP and edited by TS and GD.

In Chapter 3 analysis of TCGA dataset was performed by RC, immunofluorescence staining was performed by Dr. Elena Fazio, and the immunoblot in Figure 3.7 was performed by YRV. All other data appearing in this Chapter was generated and analyzed by TP.

Acknowledgments

The completion of this thesis would not be possible without the help and support of a number of different people. First, I'd like to thank my supervisor Dr. Trevor Shepherd for his continued support and guidance. Your mentorship has helped me to become more confident in my scientific abilities and to grow not only as a scientist, but also as a person. I would also like to thank my co-supervisor Dr. Gabriel DiMattia whose mentorship has been invaluable throughout this project. You have shown me what it means to be a truly dedicated scientist and I will continue to look up to you throughout my scientific career. Additionally, I would like to thank my advisory committee: Dr. Christopher Pin, Dr. Lynne Postovit and Dr. Alison Allan for sharing with me their knowledge and providing me guidance throughout this project.

Next I would like to thank the members of the Translational Ovarian Cancer Research laboratory, past and present, for making coming into work fun and for putting up with me all these years! Specifically, I would like to thank Yudith Ramos-Valdes who is not only a technician but also a dear friend.

I would also like to acknowledge the gynaecologic oncology surgeons Drs. Michel Préfontaine, Monique Bertrand, Jacob McGee, and Akira Sugimoto for providing us with patient specimens as well as insight into the clinical aspects of ovarian cancer. Carrie Thornton, Christine Gawlik and Kay Faroni have also been a tremendous help in collecting patient information for clinical specimens. Additionally, I would like to acknowledge all the women with ovarian cancer who participated in our study.

Finally, I would like to thank my entire family for their love and support throughout this process. I would not have been able to do it without you. Specifically, I would like to thank my parents, Robert and Kathy Peart. I could have not asked for more supportive, caring parents. Thank you for giving me the freedom to follow my dreams and helping me to grow into the person I am today. I love you more than you'll ever know.

Table of Contents

List of Abbreviations

ACC	Acetyl-CoA carboxylase
ADP	Adenosine diphosphate
AICAR	5-Aminoimidazole-4-carboxamide ribonucleotide
Alk	Activin receptor-like kinases
AMPK	Adenosine monophosphate-activated protein kinase
ARID1A	AT-rich interactive domain-containing protein 1A
ARKs	AMPK-related kinases
ATG 13	autophagy-related 13
ATP	Adenosine triphosphate
BAMBI	BMP and activin membrane-bound inhibitor
BMP	Bone morphogenetic protein
BRAF	v-Raf murine sarcoma viral oncogene homolog B1
CAMKKβ	Calmodulin-dependent protein kinase kinase β
CICs	Cortical inclusion cysts
CtBP	C-terminal binding protein
CTNNB1	catenin (cadherin-associated protein), beta 1
Dan	Differential screening-selected gene aberrative in neuroblastoma
E-Cadherin	Epithelial Cadherin
ECM	Extracellular matrix
EMT	Epithelial-to-mesenchymal transition

EOC	Epithelial Ovarian Cancer
GS domain	Glycine and serine rich domain
HGSCs	High-grade serous carcinomas
HMGR	3-hydroxy-3-methylglutaryl-CoA reductase
KRAS	v-Ki-ras2 Kirsten rat sarcoma viral oncogene homolog
LKB1	Liver kinase B1
MAPK	Mitogen-activated protein kinase
MARK4	microtubule affinity-regulating kinase 4
MEK	MAPK and ERK kinase
MO25	Mouse protein 25
mTORC1	mechanistic Target of Rapamycin 1
N-cadherin	Neural cadherin
NLS	Nuclear localization signal
NSCLC	Non-small-cell lung carcinoma
OSE	Ovarian surface epthelium
P-cadherin	Placental cadherin
PERK	protein kinase (PKR)-like endoplasmic reticulum kinase
PIK3CA	Phosphatidylinositol-4,5-bisphosphate 3-kinase, catalytic subunit alpha
PJS	Peutz-Jeghers syndrome
PKA	Protein kinase A

PTEN	Phosphatase and tensin homolog
RAPTOR	regulatory-associated protein of mTOR
RSK	p90 ribosomal S6 protein kinase
Smurf	Smad ubiquitination regulatory factors
STICs	Serous tubal intraepithelial carcinomas
STK11	Serine threonine kinase 11
STRAD	STE20-related adaptor
TCGA	The cancer genome atlas
TGF-β	Transforming growth factor beta
TP53	Tumour protein 53
TSC2	Tuberous sclerosis complex 2
ULK1	Unc-51 like autophagy activating kinase 1
UPR	Unfolded protein response
VEGF	Vascular endothelial growth factor

List of Tables

List of Figures

List of Appendices

Chapter 1

1 Introduction

1.1 Overview of Chapter 1

This thesis focuses on examining signalling pathways, which we believe mediate important aspects of ovarian cancer spheroid formation and survival. This chapter begins with a description of ovarian cancer (Section 1.2) specifically focusing on the origins, classification, and mortality associated with this very complex disease. The next section (Section 1.3) focuses on the multicellular spheroid as an *in vitro* model of ovarian cancer metastasis and the unique properties that spheroid cells acquire to avoid anoikis, including induction of cellular quiescence, altered cellular metabolism, and altered adhesion characteristics. The bone morphogenetic (BMP) (Section 1.4) and adenosine monophosphate-activated protein kinase (AMPK) (Section 1.5) signalling pathways will be described, and their relevance to ovarian cancer given my data in Chapters 2 and 3 showing that these pathways are important to the formation and survival of ovarian cancer spheroids. The final section provides rationale for our studies (Section 1.6) and outlines the studies presented in this thesis.

1.2 Ovarian Cancer

1.2.1 Ovarian Cancer Classification and Genetics

Ovarian cancers can be broadly characterized as epithelial and non-epithelial. Non-epithelial ovarian cancers, which are not the subject of my research, include granulosa cell tumours, fibrothecomas, teratomas and yolk sac tumours[1]. The most common form of ovarian cancer however is epithelial, comprising over 90% of cases[2].

Epithelial Ovarian Cancer (EOC) is not a single entity but rather consists of several subtypes that are distinguishable by unique histology and molecular aberrations[3,4]. The four main subtypes of ovarian cancer (mucinous, endometrioid, clear-cell and serous) can be further characterized as benign, malignant or borderline and classified as low or high-grade[5]. Each of these histologic subtypes has distinct clinical

characteristics and rates of occurrence. Serous carcinomas are the most common subtype and are typically high-grade neoplasms, which initially respond well to treatment with platinum/taxane-based chemotherapy but recur in the majority of cases[6,7]. Endometrioid and mucinous carcinomas are much less common (10% and 3-4% respectively) and are typically low-grade lesions with a relatively indolent course of progression, allowing them to be diagnosed at early stage[8,9]. Clear-cell carcinomas account for 10% of all cases of ovarian cancer and typically do not respond to conventional chemotherapeutics, resulting in a poor outcome for most patients[10,11].

In 2004, a dualistic model for the classification of ovarian cancer was proposed, which incorporated histopathological discoveries, clinical and molecular genetic findings [12]. In this model, the various types of ovarian cancer are broadly separated into two categories. Type I tumours include all of the major histotypes (serous, endometrioid, mucinous and clear-cell) but are low-grade and typically slow growing[10,13]. These tumours are associated with mutations in v-Ki-ras2 Kirsten rat sarcoma viral oncogene homolog (KRAS), v-Raf murine sarcoma viral oncogene homolog B1 (BRAF), phosphatase and tensin homolog (PTEN), phosphatidylinositol-4,5-bisphosphate 3-kinase, catalytic subunit alpha (PIK3CA), catenin (cadherin-associated protein), beta 1 (CTNNB1), and AT-rich interactive domain-containing protein 1A (ARID1A)[12,14]. Type II tumours, on the other hand, are comprised almost exclusively of high-grade serous carcinomas but also include high-grade endometrioid, undifferentiated carcinomas and carcinosarcomas[13]. These tumours are aggressive in nature and often present at an advanced, metastatic stage, owing to their relatively poor prognosis[15]. Type II tumours display a high degree of chromosomal aberrations and genomic instability unlike type I tumours which are relatively genetically stable[13]. An overwhelming proportion of these type II tumours (~95%) have mutated TP53[16-19](Table 1.1). This new classification takes into account the idea that low and high-grade ovarian tumours of the same subtype are not a spectrum of disease, but rather, two distinct entities with different origins, mutations and clinical course[1,20,21].

Table 1.1: Classification of type I and type II ovarian carcinomas

	Subtype	Precursor	Frequent Mutation(s)	Level of genomic instability
Type I	Low-grade serous	Serous borderline tumour	*KRAS, BRAF*	low
	Low-grade endometrioid	Endometriosis	*CTNNB1, PTEN, ARID1A*	low
	Clear-cell	Endometriosis	*PIK3CA, ARID1A, FBXW74*	low
	Mucinous	Mucinous borderline tumour (Gastrointestinal)	*KRAS*	low
Type II	High-grade serous	Fallopian tube	*TP53, BRCA1/2*	High
	High-grade endometrioid	Unknown	*TP53*	High
	Undifferentiated	Unknown	Unknown	Unknown
	Carcinosarcoma	Unknown	*TP53*	Unknown

*adapted from Nik et. al. (2013) and references therein

1.2.2 Origins of Ovarian Cancer

Many epithelial malignancies have well-defined precursor lesions and cells of origin[1]. This is not the case for EOC where until recently the origin and pathogenesis of this disease remained elusive[13]. The traditional view assumed that all ovarian cancer subtypes share a common site of origin within the ovarian surface epithelium (OSE). This is interesting, given the fact that the OSE is not a well-differentiated epithelium, but rather a mesothelial layer that originates embryonically from the mesodermally-derived coelomic epithelium[2]. This theory postulates that the process of damage and repair of the ovarian surface that occurs as a result of multiple ovulations throughout a woman's reproductive life increases the susceptibility of the OSE to transformation. In addition, multiple invaginations of the ovarian surface are also common as women age. These invaginations can pinch off over time and become entrapped within the ovarian stroma where they form cortical inclusion cysts (CICs). It is hypothesized that the epithelial cells lining these cysts undergo metaplasia in response to the hormone-rich environment within the ovary, differentiating into a Müllerian-like epithelium that eventually becomes dysplastic leading to ovarian carcinoma[2,5]. Although this model is consistent with epidemiologic evidence demonstrating that decreased ovulation is significantly correlated with a decreased risk of developing ovarian cancer, it does have many limitations[22]. One of the major drawbacks to this model is it does not address the significantly divergent phenotypes and genotypes that exist between tumour subtypes[5].

As technology has improved, so has our understanding of ovarian cancer where it is now established that it is a complex and heterogeneous disease without a single cell of origin[1]. Many studies have provided strong evidence indicating that endometriosis is the precursor lesion for clear-cell and endometrioid carcinomas[23-30]. Additionally, mucinous carcinomas have been shown to originate from appendicekal and other gastrointestinal origins[1]. In the late 1990s to early 2000s, pathologists identified occult non-invasive and invasive carcinomas in the fimbria of fallopian tubes collected from prophylactic salpingo-oophorectomy specimens in *BRCA1/2* mutation carriers[31-36]. Based on this, Piek and colleagues[37] proposed a model whereby occult tubal carcinomas shed malignant cells that implant and grow on the ovary, mimicking primary ovarian cancer. The hypothesis

that the fallopian tube is the primary site of high-grade serous carcinomas has since been supported by multiple studies[38-41]. In 2007, for example, a study performed on women with high-grade serous carcinomas (HGSCs) who did not harbor a *BRCA* mutation reported the presence of serous tubal intraepithelial carcinomas (STICs) in 48% of patients[41]. Additionally, studies matching STICs and HGSCs from the same patient not only reveal TP53 mutations in 92% of STICs but also show that these mutations match the mutation found in the ovarian carcinoma[13]. Most recently, the Drapkin and Dinulescu labs reported the development of an HGSC murine tumour model emanating specifically from the murine fallopian tube (oviduct) even after hysterectomy and oophorectomy[42]. This study provides additional support for the fallopian tube and STICs as the origin of HGSC. This new model defining the origin of high-grade serous ovarian cancer will open up new avenues for early detection and intervention as we gain a better understanding of STICs and their role in carcinogenesis. In fact, it may no longer be appropriate to categorize HGSCs as 'ovarian cancer' since it seems as though the ovary is simply a favourable microenvironment for these cancer cells to spread and grow.

1.2.3 Ovarian cancer treatment and prognosis

Ovarian cancer is the most lethal gynecologic malignancy in the western world, the overall survival of which has remained unchanged for more than 50 years[13,43]. Ovarian cancers that are diagnosed at an early-stage, before they have spread beyond the ovary (stage I) have a 90% cure rate through surgical resection. Unfortunately, the majority of cases (>75%) are diagnosed once the disease has metastasized to the pelvic organs, abdomen (stage III) or to distant sites (stage IV), at which point the chance of cure decreases substantially[44].

The high mortality rate associated with this disease is not only due to the lack of screening methods for early detection but also to the lack of effective therapies for advanced stage disease. Despite the high degree of heterogeneity associated with ovarian tumours, the majority of ovarian cancer patients are treated with cytoreductive surgery followed by platinum and taxane-based chemotherapy[5]. Although most tumours initially respond to chemotherapeutics, approximately 70% will develop platinum resistance and succumb to recurrent disease[45]. This results in a dismal five-year survival rate for

advanced-stage ovarian cancer patients of only 30%[46]. It is becoming obvious as we gain a better understanding of the molecular underpinnings of this complex disease that a "blanket approach" to treatment is not going be enough. Rather, we must use our knowledge of the molecular genetic characteristics of individual tumours to focus our efforts into developing more targeted therapeutics[5].

1.2.4 Ovarian cancer metastasis

Ovarian cancer metastasis is unique in that it rarely occurs through the bloodstream as is common for other solid tumours[3]. Instead, single cells or small clusters of cells are shed into the peritoneal cavity where they subsequently adhere to mesothelial cells of various abdominal organs to establish secondary lesions[47-49]. Since there is no anatomical barrier to prevent metastasis, tumour implants become widespread, blocking lymphatic vessels, and allowing ascites fluid to accumulate from leaky vasculature [44]. This peritoneal ascites fluid is a relatively unique environment in which tumour cells must survive in suspension[4]. The composition of ascites fluid from ovarian cancer patients has been shown to vary considerably; in fact, one study showed higher proportions of red blood cells when the fluid had rapidly accumulated[50]. A typical distribution of the cellular components of ascites fluid consists of 37% lymphocytes, 29% mesothelial cells, 32% macrophages, and <0.1% adenocarcinoma cells[51]. This fluid is a convenient source of tumour cells because it is routinely removed by paracentesis and is often of high volume facilitating isolation of tumour cells for study into the unique biological characteristics of cancer cells from different patients.

1.3 Multicellular spheroids

1.3.1 Spheroids as an *in vitro* model of metastasis

Multicellular spheroids have been recognized as a valuable tool in the fields of cell and developmental biology for over 50 years[52-55]. It wasn't until the 1970s, however, that Sutherland and colleagues established multicellular spheroids as a valuable *in vitro* model with which to study tumour biology[56-58]. Since then, tumour spheroids have been widely used to recapitulate the functional and microenvironmental features of human tumour tissue in order to study biological processes such as proliferation, metabolism,

differentiation, cell death, invasion, angiogenesis and immune response in an *in vitro* setting[59-66]. Spheroids exhibit many histologic similarities to their solid tumour counterparts including areas of necrosis as well as expression of ECM components[67].

1.3.1.1 ECM and cell adhesion

The ECM is a complex network made up of several proteins and polysaccharides such as fibronectin, collagen, laminin, hyaluronate, heparin sulfate, and elastin. These components are produced and secreted by cells, the combination of which depends on the functional requirements of a particular tissue[68].

The link between cell survival and adhesion to the extracellular matrix (ECM) has been well-established in the literature[69-72]. Anoikis, from the Greek word meaning "homelessness", refers to apoptosis induced by loss of cell adhesion to ECM[73]. This is an important physiological process as it prevents cells from reattaching to new matrices and growing in a dysplastic manner[74]. The ability to overcome anoikis has important implications for metastatic cancer. In fact, cancer cell lines are significantly less sensitive to anoikis than normal epithelial cells and in many cases have developed anchorage-independence, meaning they are able to survive and proliferate without attachment to ECM[75-78]. Integrins are important mediators of anchorage-independent survival that through their interaction with the ECM, stimulate numerous signalling pathways capable of modulating organization of the cytoskeleton, cell motility, and cell growth[79-81]. In addition to integrin-associated signalling molecules, many cancer cells also have alterations in cell-cell adhesion molecules, protein kinases, and cell cycle regulators. This also contributes to anoikis-resistance, allowing these cells to disseminate and become metastatic[77,78,82-84]. Epithelial cadherin (E-Cadherin), for example, has been shown to be a crucial mediator of cell-cell adhesion in multicellular spheroids. Oral squamous carcinoma cells, as well as mammary and prostate epithelial cells require E-cadherin in order to avoid anoikis in suspension[85,86]. These studies as well as others have shown that part of the pro-survival function of E-cadherin involves the induction of quiescence, or reversible exit from the cell cycle. When E-cadherin is overexpressed in the EMT/6 breast cancer cell line, which lacks endogenous E-cadherin expression, cells form

compact spheroids and the proportion of dividing cells is greatly reduced. This exit from the cell cycle is mediated by induction of $p27^{Kip1}$ activity in E-cadherin expressing cells[87].

Many tumour cells are not able to survive under anchorage-independent conditions if they remain as single cells. Rather, single cells must aggregate in order to avoid anoikis. In this context, survival signals arising from cell-cell contact substitute signals that normally come from matrix adhesion. Understanding the complex relationship between ECM components and cell-cell contact in multicellular spheroids is relevant in the field of tumour biology as they may more closely recapitulate the *in vivo* situation when tumour cells are detached from their tissue of origin[68]. In fact, the ECM profile and organization of glioma, osteosarcoma and melanoma spheroids have been shown to more closely resemble *in vivo* tumours than that of conventional monolayer cultures[88-90]. Additional studies in human epidermoid and colorectal carcinoma spheroids revealed a similar pattern with respect to integrin expression, whereby the expression pattern of various integrins observed in multicellular spheroids closely resembled that of solid tumours[91,92]. These results provide support for the use of multicellular spheroids as *in vitro* models with which to study the contribution of cell-matrix and cell-cell contacts in anoikis resistance.

1.3.1.2 Response to cytotoxic drugs

Many studies on multicellular spheroids have focused on the response of these structures to various tumour therapies[93-108]. The most extensively studied phenomenon is the response of spheroids to ionizing radiation. One of the most interesting findings from these studies was the observation that cells within multicellular spheroids are more resistant to ionizing radiation than monolayer cultures[109-111]. This was some of the first evidence to support the idea that spheroids mimic the *in vivo* response of cancer cells to treatment more closely than conventional monolayer cell cultures[67].

Multicellular spheroids remain an attractive model with which to examine the role of the tumour microenvironment on response to various therapeutic strategies. These structures maintain many of the metabolic and proliferative gradients that occur as a result of cellular interactions in a 3D context[112]. In fact, spatial variations in cellular

proliferation are quite common in solid tumours, where cellular proliferation is highest in areas adjacent to microvessels[113-116]. Decreased proliferation in areas with lower oxygen and nutrient concentrations is often associated with quiescence, reversible exit from the cell cycle[114,117]. These proliferation gradients common to solid tumours have not been demonstrated in monolayer cultures, but have been well-documented in multicellular spheroids[67,118]. In fact, cells toward the center of the spheroid exhibit prolonged cell-cycle times and often enter a non-proliferating or quiescent state[119]. Given the fact that the vast majority of therapeutics aimed at cancer cells target rapidly dividing cells, it is not surprising that multicellular spheroids are generally more resistant to cytotoxic drugs than the same cells in monolayer culture[58,120].

1.3.2 Multicellular spheroids in ovarian cancer

Multicellular spheroids are valuable tools for the study of ovarian cancer because, as described above, they more closely mimic the characteristics of solid tumours, but also because of the unique way ovarian cancer metastasizes. One of the early events in ovarian cancer metastasis is the proteinase-mediated shedding of cells from the primary tumour into the peritoneal cavity, which has now been elegantly demonstrated in a murine model of HGSC[4,42,121-123]. It is here, suspended within peritoneal ascites fluid, that this unique non-adherent population of ovarian cancer cells must respond to a series of unique environmental cues in order to survive and metastasize[4]. It is believed that in order to maintain cell-cell contact and avoid anoikis, cells under these conditions aggregate to form multicellular spheroids[124] (Figure 1.1). When forced into suspension, cells spontaneously aggregate as part of their natural survival response. Spheroid compaction is mediated by the interaction of key cell adhesion molecules such as integrins and cadherins[124]. E-cadherin expression, for example, has been shown to be lower in cells suspended within ascites fluid as compared to the primary tumour[125]. This loss of E-cadherin is part of a global "cadherin switch" whereby Neural Cadherin (N-Cadherin) and Placental cadherin (P-cadherin) are upregulated to compensate[121,126]. This switch in cadherin expression is indicative of an epithelial-to-mesenchymal transition (EMT), which has been shown to allow cells to survive under hypoxic conditions when cells are crowded together[127]. Integrins have also been shown to be important mediators

of survival when cells are in suspension. Ovarian cancer spheroid formation is greatly inhibited, for example, when cells are treated with a blocking antibody against β1 integrin[128]. Another important attribute of ovarian cancer spheroids is their ability to implant on mesothelial-lined peritoneal surfaces such as the peritoneum, omentum and pleural surface[49]. Skubitz and colleagues were the first to model this *in vitro*, demonstrating that ovarian cancer spheroids had the ability to reattach and invade live mesothelial cell monolayers[48]. More recently, the Brugge lab has shown that ovarian cancer spheroids use myosin-generated force in order to displace the mesothelial layer of cells and gain access to the underlying ECM to promote invasion[129].

These studies have taken the first steps towards gaining a better understanding of ovarian cancer spheroid biology, however, the stresses associated with ECM-detachment puts cells under a significant selection pressure. The cells that are able to survive within the peritoneal cavity and subsequently metastasize have likely altered many key signalling pathways. We have just begun to scratch the surface when it comes to understanding the adaptations of cells in this unique environment where they must exist in suspension. Since ovarian cancer mortality can be directly attributed to disseminated peritoneal mestastasis, it is critical that we identify signalling pathways which are important for spheroid formation, survival and reattachment[4]

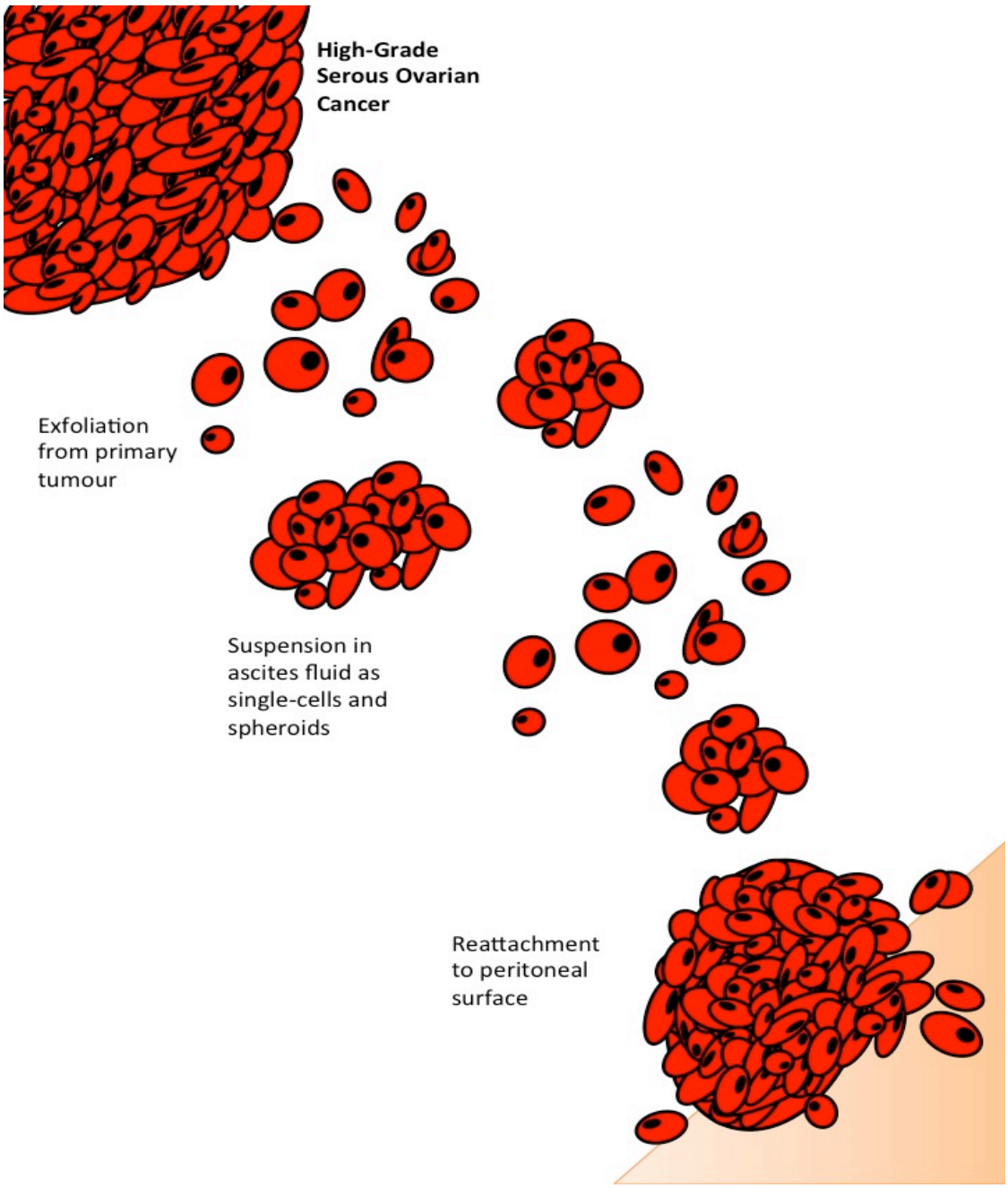

Figure 1.1: Mechanism of high-grade serous ovarian cancer metastasis.
During the process of ovarian cancer metastasis, malignant cells are shed from the primary tumour into the peritoneal cavity. It is here, suspended within ascites fluid, that single-cells and multicellular aggregates (spheroids) disperse throughout the peritoneal cavity. Widespread secondary metastatic lesions are formed when cells re-attach to mesothelial surfaces throughout the peritoneal cavity.

1.4 BMP/TGF-β signalling

1.4.1 Overview

Bone morphogenetic proteins (BMPs) belong to the transforming growth factor−β (TGF-β) superfamily and, as their name suggests, were originally identified based on their ability to induce bone and cartilage formation at extraskeletal sites[130-132]. These powerful cytokines have since become recognized for their role in other cellular processes such as, differentiation, apoptosis and migration[133-180]. Given the importance of BMP signalling in controlling proliferation and differentiation during development and in maintaining and regenerating tissue during adulthood, it is not surprising that this pathway has also been shown to play an important role in many types of cancer[157,180-187]. This section will discuss TGF-β/BMP signal transduction, how this pathway is regulated as well as its role in various different cancers, including ovarian cancer.

1.4.2 Pathway activation

BMP dimers are secreted to the extracellular environment, where they initiate signalling by cooperatively binding to two types of serine/threonine kinase receptors (type I and type II)[188,189]. These receptors are separated in the plasma membrane until a ligand binds and increases oligomerization, essentially acting as a bridge between the two receptors. Both types of receptors are structurally similar consisting of an extracellular domain, a single transmembrane-spanning domain, and an intracellular domain with serine/threonine kinase activity[190]. The type II receptors are constitutively active and are responsible for transphosphorylating the type I receptors when a signal is present[191]. This phosphorylation occurs on the GS domain (glycine and serine rich domain) which is located N-terminal to the serine/threonine kinase domain on the type I receptor (Figure 1.2). The activated type I receptor is responsible for binding and activating the downstream signalling mediators for this pathway, the Smads[190,191].

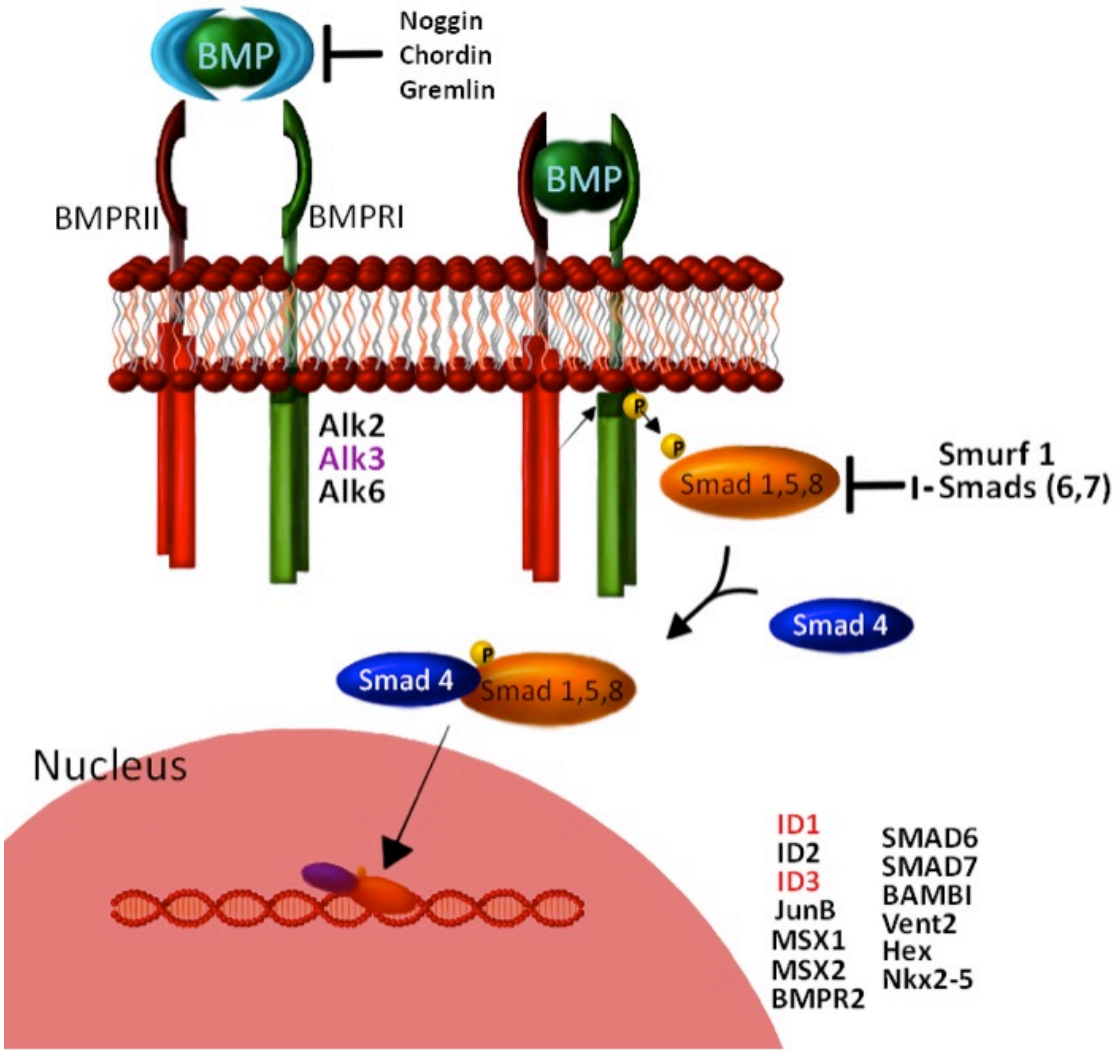

Figure 1.2: Activation of Bone Morphogenetic Protein (BMP) signalling.
Dimeric BMP ligands transduce their signal through a heterotetrameric complex composed of type I and type II transmembrane receptors. Following phosphorylation by the type II receptor, the type I receptor phosphorylates and activates Smads 1,5,8, allowing them to complex with Smad 4 and translocate to the nucleus to regulate target gene expression. Negative regulation of this pathway can occur through extracellular antagonists as well as intracellular inhibitory Smads.

1.4.2.1 Smad protein family

Eight different Smad proteins have been identified in mammals, each of which can be separated into three categories: Receptor-regulated Smads (R-Smads), Common-mediator Smad, or Inhibitory Smads (I-Smads)[192-194].

The Receptor-regulated Smads or R-Smads are those that interact with the type I receptor and are activated by phosphorylation. This interaction with the receptor is transient and once phosphorylation occurs, the R-Smad is released to the cytoplasm where it is free to form a complex with co-Smad[190]. The particular Smad that interacts with the receptor depends on the type of receptor as well as the ligand that triggers the signal. Smad2 and Smad3 transmit the signal from TGF-β, Nodal and activin ligands[195,196], whereas Smad1, 5 and 8 transduce the signal from BMP ligands[197-199].

The common-mediator Smad, of which there is only one, Smad4, has the ability to interact with any R-Smad, forming a heteromeric complex that can translocate to the nucleus to affect the expression of target genes[191]. This complex can be composed of one R-Smad bound to Smad4 or two R-Smads, depending on the target gene[200].

The third group of Smads, the inhibitory Smads (I-Smads), is comprised of Smad6 and Smad7. These Smads have the ability to modulate signalling by competing with R-Smads for binding to either the receptor or Smad4[201,202].

1.4.2.2. TGF-β/BMP receptors

Seven different type I receptors for the TGF-β family have been identified in mammals (activin receptor-like kinases 1-7; Alk 1-7). Of these, type I BMP receptors BMPR1A (Alk3) and BMPR1B (Alk6), as well as, type I activin receptor Acvr1 (Alk2) activate Smad 1,5, and 8 in response to BMP ligands. The remaining type I receptors activate Smad 2 or 3 and are responsible for transducing signal from TGF-β, Activin, or Nodal ligands[190]. Table 1.2 describes the various type I receptors and summarizes their expression patterns, their ligand-affinity and downstream signalling targets.

The binding preferences of a particular ligand for a type I receptor is determined by the presence of the type II receptor[203]. There are three type II receptors used by BMPs in mammals. BMPR-II is specific for BMPs, whereas, ActR-II and ActR-IIB are also used by activins and myostatin[190].

Table 1.2: Type I BMP receptors.

Receptors	Cell type	Ligands	Smads	References
BMPR-1A (Alk-3)	Ubiquitously expressed	BMP2,4	1,5,8	(ten Dijke, Yamashita et al. 1994; Dewulf, Verschueren et al. 1995; Miyazono, Kamiya et al. 2010)
BMPR-1B (Alk-6)	Brain	BMP2,4,6,7	1,5,8	(ten Dijke, Yamashita et al. 1994; Dewulf, Verschueren et al. 1995; Miyazono, Kamiya et al. 2010)
Alk-1	Endothelial cells, chondrocytes	TGF-β, BMP9	2,3 1,5,8	(Goumans and Mummery 2000; Oh, Seki et al. 2000; Seki, Hong et al. 2006; Finnson, Parker et al. 2008; Luo, Tang et al. 2010; Miyazono, Kamiya et al. 2010)
Alk-2	Ubiquitously expressed	BMP6,7,9	1,5,8	(Zhang, Schwarz et al. 2003; Luo, Tang et al. 2010; Miyazono, Kamiya et al. 2010)
ActR-1B (Alk-4)	Blood	TGF-β, Nodal	2,3	(Reissmann, Jornvall et al. 2001; Bianco, Adkins et al. 2002; Miyazono, Kamiya et al. 2010)
TβR-I (Alk-5)	Endothelial cells, chondrocytes	TGF-β	2,3	(Seki, Hong et al. 2006; Finnson, Parker et al. 2008; Miyazono, Kamiya et al. 2010)
ActR-IC (Alk-7)	Adipose tissue	Nodal	2,3	(Carlsson, Jacobson et al. 2009; Miyazono, Kamiya et al. 2010)

1.4.3 Pathway attenuation

Both BMP and TGF-β signalling are modulated at many different levels: outside the cell, inside the cell as well as at the membrane. In many instances, the expression of these inhibitory signals is controlled by the TGF-β/BMP signalling cascade, which creates a negative-feedback loop[204].

1.4.3.1 Extracellular modulation

At the extracellular level, secreted antagonists are capable of sequestering BMP ligands and preventing them from binding to the receptor. In vertebrates, more than seven of these antagonists have been identified[191,204]. These proteins are not redundant inhibitory signals as each antagonist displays a unique affinity for different ligands. Table 1.3 describes a number of BMP ligands and their antagonists in addition to knockout mouse models demonstrating their important embryonic functions.

Table 1.3: Knockout mouse models of BMP ligands and antagonists.

	Gene	Embryonic lethal?	Phenotype	Reference(s)
BMP ligands	*BMP2*	Yes	Amnion/chorion malformation Defects in cardiac development	(Zhang and Bradley 1996)
	BMP3	No	Increased tranbecular bone density	(Daluiski, Engstrand et al. 2001)
	BMP4	Yes	Defects in extraembryonic and posterior/ventral mesoderm formation	(Winnier, Blessing et al. 1995)
	BMP5	No	Abnormal skull and axial part of skeleton	(Green 1958; Kingsley, Bland et al. 1992)
	BMP6	No	Mild delay of sternum ossification in late gestation	(Solloway, Dudley et al. 1998)
	BMP7	Postnatal lethal	Holes in the basisphenoid bone and the xyphoid cartilage, retarded ossification of bones, fused ribs and vertebrae, underdeveloped neural arches of the lumbar and sacral vertebrae	(Jena, Martin-Seisdedos et al. 1997)
BMP Antagonists	*Noggin* (highest affinity for BMP 2,4)	Yes	Failure of neural tube closure, broad club-shaped limbs, loss of caudal vertebrae, shortened body axis and retention of small vestigial tail	(Brunet, McMahon et al. 1998; McMahon, Takada et al. 1998; Choi, Stottmann et al. 2007)
	Chordin (highest affinity for BMP2,4)	Still born	Normal early development and Neural induction, defects in inner and outer ear development, pharyngeal and cardiovascular organization at later stages of embryogenesis	(Bachiller, Klingensmith et al. 2000)
	Follistatin (highest affinity for BMP7)	Postnatal lethal	Smaller than heterozygotes, less muscle, fail to breath after birth	(Matzuk, Lu et al. 1995)
	DAN (highest affinity for BMP2)	No	No defects in head, mesoderm, somites, facial structures and limbs, normal neural tube development, viable and fertile	(Dionne, Skarnes et al. 2001)

All knockout mouse models described above are homozygous for gene of interest

1.4.3.2 Intracellular modulation

As mentioned above, inhibitory Smads or I-Smads (Smad 6 & 7) function within the cell to antagonize TGF-β/BMP signalling. These Smads have the ability to interact with type I receptors but are never released and thus prevent R-Smads from interacting with these same receptors[190]. Smad7 has the ability to inhibit TGF-β and BMP signalling, whereas Smad6 has been shown to preferentially inhibit BMP signalling[205]. I-Smads have also been shown to have activity within the nucleus. Smad7, for example, is able to bind to Smad-responsive DNA elements and disrupt the formation of a functional Smad-DNA complex[206]. On the other hand, Smad6, functions by recruiting transcriptional corepressors, such as histone deacetylases and C-terminal binding proteins (CtBP)[207,208].

Another way that Smad activity is regulated is through ubiquitin-mediated degradation. Smad ubiquitin regulatory factors 1 & 2 (Smurfs 1 & 2) are E3 ubiquitin ligases that selectively target R-Smads as well as activated type I receptors for degradation[209,210]. Smurf1 specifically interacts with Smads 1 and 5 to inhibit BMP signalling, whereas, Smurf2 acts more broadly to inhibit Smads 1 and 2 in order to repress both BMP and TGF-β signalling[188,204]. Smurf1 is also able to enhance the interaction between I-Smads and type I receptors in order to inhibit BMP signalling[211].

1.4.4 Smad-independent signalling

Smads are not only phosphorylated at the C-terminus by type I receptors in a ligand-dependent manner, but can also be phosphorylated within their linker region by kinases from other pathways (ie: MAPKs, ERKs, JNK, p38)[204]. The Smad linker region is easily accessed by a number of kinases since it is loosely organized and highly flexible. Specifically, epidermal growth factor (EGF) treatment, which activates Ras/MAPK signalling, results in phosphorylation of the Smad1 linker region. This phosphorylation blocks the nuclear translocation of Smad1, inhibiting BMP signalling[212]. Additionally, expression of a dominant negative mutant of Ras or treatment of intestinal epithelial cells with a MAP and ERK kinase (MEK) inhibitor decreased the ability of the BMP pathway in induce Smad1 phosphorylation[213]. From this it was proposed that these two pathways converge on Smad1 by phosphorylation of the C-terminus (BMP pathway) and the linker

region (Ras/MAPK pathway). It is the balance of these two inputs that determines Smad1 activation and nuclear translocation[214]. The crosstalk between BMP signalling and other signalling pathways could have important implications not only in development but also in cancer.

1.4.5 BMP signalling in cancer

The BMP signalling pathway can exhibit both tumour suppressive and oncogenic functions depending not only on the type of cancer but also the stage. In some cancers, BMP signaling is growth inhibitory and induces apoptosis[153,215-220] via activation of downstream Smad-dependent pathways that promote apoptosis or inhibition of pathways that prevent apoptosis. Alternatively, the BMP signaling pathway can also increase metastatic potential[221,222] and tumour angiogenesis[223]. In fact, it has been reported in different cancers that BMPs serve a dual role, acting as a tumour suppressor at early stages of carcinogenesis and as a promoter of tumour metastasis at later stages[224,225].

1.4.5.1 Cancer promoting activities

The BMP signalling pathway has been shown to increase metastatic potential[221,222] and tumour angiogenesis[223] in a number of different cancers. For example, BMP2 is expressed in non-small-cell lung carcinoma (NSCLC) and has the ability to enhance the growth of lung cancer cell lines *in vitro* and *in vivo*[226]. In addition to enhancing tumour growth, BMP2 has also been shown to play an important role in angiogenesis. Four days following injection of recombinant BMP2 a large increase in the size and number of blood vessels was observed in a NSCLC tumour xenograft model[223]. In addition to this, BMP7 has been shown to enhance vascular endothelial growth factor (VEGF) expression in metastatic prostate cancer cells[227]. The tumour-promoting properties of various components of the BMP signalling pathway have been illustrated in a number of other cancer sites including osteosarcoma, prostate, breast and colorectal[228-231].

1.4.5.2 Anti-cancer activities

The potential tumour suppressive function of the BMP signalling pathway was highlighted in the early 2000s with the discovery of germline mutations in the type I BMP receptor, BMPR1A (Alk3), and Smad4 in up to 40% of juvenile polyposis patients[232-237]. This is an autosomal dominant syndrome characterized by multiple hamartomatous polyps and predisposition for gastrointestinal cancers[233]. A role for the BMP signaling pathway in this inherited syndrome was further supported by a transgenic mouse model expressing the BMP inhibitor noggin. At two to three months of age, these mice displayed a phenotype similar to that observed in juvenile polyposis patients. At a later age (6 to 8 months), adenomatous polyps could be observed in these mice, resembling the syndrome in humans [238]. In addition to this, recent studies have suggested that the BMP signalling pathway may in fact be inactivated in a number of cases of sporadic colorectal cancer[239].

1.4.6 BMP signalling in ovarian cancer

BMPs serve critical functions in the normal ovary, controlling processes such as steroidogenesis, follicle formation, and apoptosis[240-244]. In addition to this, double knockout mouse models for either Smad 1 & 5 or BMPRIA & BMPRIB develop granulosa cell tumours by three and eight months of age respectively[245,246]. Given the importance of BMP signalling pathway in maintaining normal ovarian function, it is not surprising to that it may play a role in the development of ovarian cancer.

Human EOC cells have been reported to possess an autocrine BMP4 signalling loop[247] and treatment of EOC cells with exogenous BMP4 or constitutively-active type I BMP receptor ($Alk3^{QD}$) resulted in an increase in cell adhesion and invasion, as well as a cell spreading response indicative of enhanced cell motility[187,247]. Additionally, BMP2 expression has been shown to be elevated in malignant ascites cells and solid tumour samples with expression positively correlating with tumour grade[184]. Perhaps some of the most convincing evidence for the cancer promoting functions of the BMP signalling pathway in ovarian cancer came from the Buckanovich lab in 2011. They demonstrated that activation of BMP signalling significantly increased the proportion of ovarian cancer

stem cells. Additionally, inhibiting BMP signalling *in vivo* resulted in a decreased proportion of ovarian cancer stem cells and decreased tumour growth[248]. Taken together these results indicate a cellular response which could contribute to EOC progression in response to BMP signalling, however, given the complexity of this pathway, it is likely that it serves different functions throughout ovarian cancer pathogenesis. The use of relevant models to dissect the role of this pathway during ovarian cancer metastasis could provide additional insight into the therapeutic potential for targeting this pathway for treatment of ovarian cancer.

1.5 LKB1/AMPK signalling

1.5.1 Overview

As mentioned previously, the objective of my research was to identify signalling pathways that potentially interact and have a pro-survival effect on spheroid cells in ovarian cancer. In this vein, recent work uncovered a unique connection between the TGF-β/BMP signalling pathway and a tumour suppressor protein that plays an important role in the metabolic reprogramming of cancer cells, liver kinase B1 (LKB1). In this study they found that LKB1 is able to phosphorylate Smad4 and prevent it from binding to DNA, thus inhibiting both TGF- β/BMP signalling pathways[249].

Metabolic reprogramming of tumour cells is an important disease driver that allows cells to survive in unfavourable conditions where oxygen and nutrients are scarce[250-253]. This is especially relevant to the ovarian cancer environment where cancer cells are released into the ascites fluid an environment where oxygen and nutrient access is severely compromised which necessitates a unique metabolic response for survival. In this context, Adenosine monophosphate-activated protein kinase (AMPK) is important in that it functions as a sensor of cellular energy and allows cells to cope with various forms of metabolic stress, such as nutrient and energy deprivation[254]. AMPK is the only kinase that has the ability to respond to adenosine nucleotide levels within a cell and is thus one of the most important mediators of metabolic reprogramming. This section will discuss how the LKB1/AMPK signalling pathway is activated, how each of these kinases

contributes to oncogenesis, and the potential contribution of this pathway to ovarian cancer pathogenesis.

1.5.2 Pathway activation and attenuation

1.5.2.1 AMPK structure and activity

AMPK was originally discovered in 1987 as the protein kinase responsible for phosphorylating and inactivating acetyl-CoA carboxylase (ACC) and 3-hydroxy-3-methylglutaryl-CoA reductase (HMGR), enzymes crucial for fatty acid and sterol biosynthesis, respectively[255]. In response to cellular stress that results in ATP depletion either by inhibiting its production or accelerating its consumption, AMPK switches off ATP-consuming anabolic processes and turns on ATP-producing catabolic pathways in order to restore energy homeostasis[256]. This prevents cells from proliferating in situations where nutrients are scarce and allows them to survive periods of stress, an important attribute that many cancer cells have adapted especially ovarian cancer cells in ascites fluid.

AMPK is a highly conserved sensor of intracellular adenosine nucleotide levels that exists as a heterotrimeric complex consisting of catalytic α subunits and regulatory β and γ subunits[257]. In mammals, there are two isoforms of the α subunit (α1 and α2), two of the β (β1 and β2), and three of the γ subunit (γ1, γ2, and γ3), each of which is encoded by a distinct gene[258]. The α subunits contain a serine/threonine kinase domain in the N-terminus and are activated by phosphorylation of Threonine (Thr) 172 within the activation loop of this domain[259,260]. The γ subunits contain four tandem repeats known as CBS motifs. These repeats are arranged in a pseudo-symmetrical manner, yielding four potential adenosine nucleotide-binding clefts[256]. Site 4 binds only to AMP, site 2 appears to remain unoccupied while sites 1 and 3 competitively bind ADP, ATP or AMP[261,262]. The β subunits link the C-terminus of the α subunit to the N-terminal domain of the γ subunit[262-264]. In a cell that is not stressed and ATP:ADP ratios are high, sites 1 and 3 of the γ subunit are occupied primarily by ATP. However, when cells are exposed to metabolic stress and levels of ADP and AMP increase, ATP is gradually replaced at these sites[256]. When AMP or ADP is bound to the γ subunit a conformational change occurs in

the complex that promotes phosphorylation of the α subunit, which is required for its activation[257].

For many years the upstream kinase responsible for activating AMPK remained elusive. In 2003, after over 20 years of work and the combination of studies in yeast and mammals, three different groups published consecutive papers identifying liver kinase B1 (LKB1) as the primary kinase responsible for phosphorylating AMPK[265-267]. Since this time, calmodulin-dependent protein kinase β (CAMKKβ) has also been shown to phosphorylate AMPK at Thr172 in response to calcium flux[268-270] (Figure 1.3).

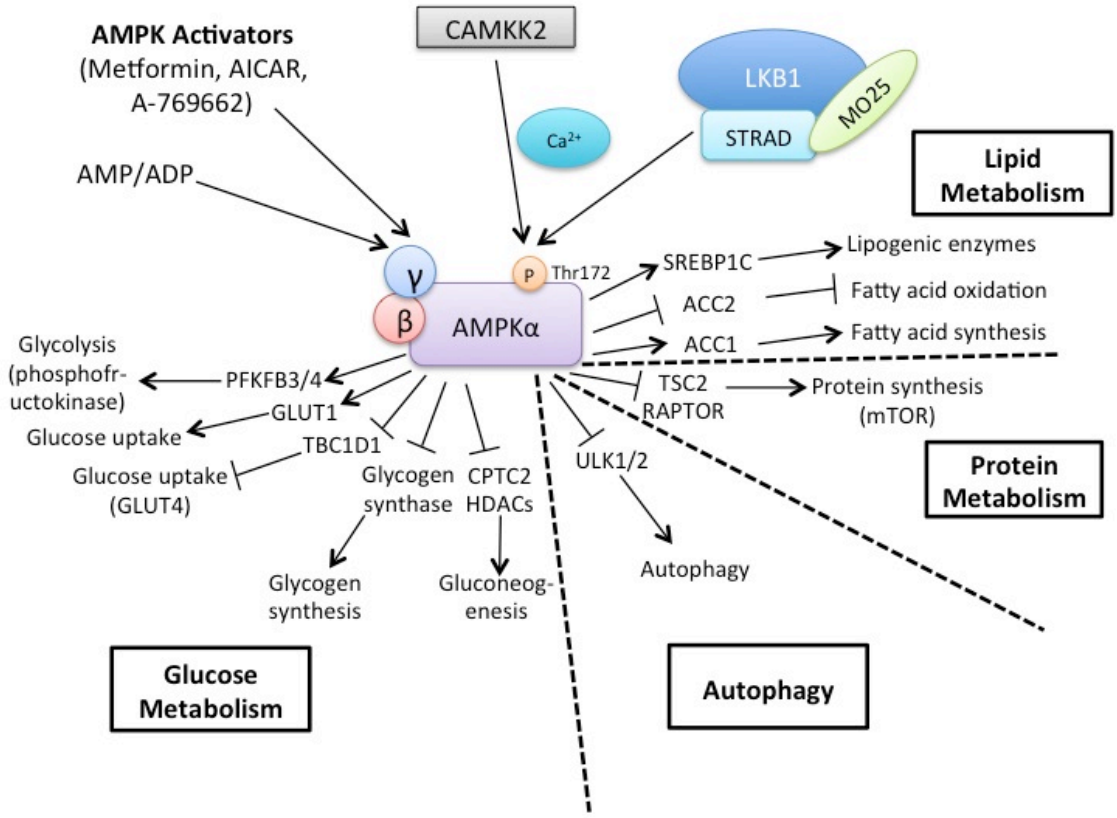

Figure 1.3: Activation of the LKB1/AMPK signalling cascade.
AMPK is activated when AMP or ADP levels increase due to a number of physiological stresses. It can also be activated pharmacologically (AICAR, A-769662). LKB1, in complex with STRAD and MO25, is the major upstream kinase that phosphorylates Thr172 on the α-subunit of AMPK in response to a rise in AMP or ADP. AMPK can also be phosphorylated by CAMKK2 in response to calcium flux. Activated AMPK directly phosphorylates a number of substrates to affect cellular metabolism and growth.

1.5.2.2 LKB1 structure and activity

The human LKB1 gene also referred to as serine threonine kinase 11 (*STK11*), spans 23kb with ten exons, nine of which are coding. LKB1 is phosphorylated on at least eight different residues, 4 of which are phosphorylated by upstream kinases (Ser31, Ser325, Thr366 and Ser428), while the other 4 are autophosphorylation sites (Thr185, Thr189, Thr336, and Ser 404)[271]. Mutation of these sites to an alanine (Ala) or glutamic acid (Glu) does not appear to have any effect on the catalytic activity or subcellular localization of LKB1[272-274]. However, mutation of Ser428 rendered LKB1 unable to suppress cell growth *in vitro*, suggesting that phosphorylation of this residue may contribute to LKB1 tumour suppressor function[274]. This particular site can be phosphorylated by the p90 ribosomal S6 protein kinase (RSK) as well as Protein kinase A (PKA), suggesting that phosphorylation of LKB1 may be an avenue through which these kinases can regulate cell growth[274,275].

LKB1 exists in mammalian cells in a complex with STE20-related adaptor (STRAD) and mouse protein 25 (MO25)[276-278]. STRADα and STRADβ are referred to as pseudokinases because although they exhibit high sequence homology to the STE20 family of protein kinases, they lack several key catalytic residues, rendering them inactive[276]. MO25α and MO25β are closely related to each other but don't appear to resemble any other protein. They were originally identified as genes expressed at the early cleavage stage during mouse embryogenesis[279]. STRAD and MO25 are required not only to enhance the activity of LKB1 but also to ensure proper localization within the cell.

LKB1 on its own is located predominantly in the nucleus, with only a small proportion in the cytoplasm[280,281]. This nuclear retention is mediated by a nuclear localization signal (NLS) located within the N-terminal non-catalytic region of LKB1[271,280,282-284]. When the NLS is mutated, LKB1 becomes distributed throughout the cell but retains its ability to suppress cell growth[285]. This suggests that the cytosolic pool of LKB1 may be the primary mediator of its tumour suppressive function[271]. When STRAD and MO25 are present LKB1 is relocalized to the cytoplasm where the catalytic

activity towards its substrates is 10-fold higher. When a mutant of LKB1 that is unable to bind STRAD is introduced into the G361 melanoma cell line, it is unable to induce cell cycle arrest. Thus, MO25/STRAD/LKB1 complex is essential for the tumour suppressive function of LKB1[272,276,282].

1.5.2.3 LKB1-mediated activation of AMPK

LKB1 does not respond to changes in AMP concentration, rather, it is constitutively active, constantly phosphorylating the Thr172 residue within the activation loop of AMPK[286,287]. When cells have an adequate supply of energy and nutrients, this site is immediately dephosphorylated, a process mediated by the conformational change induced in the γ subunit when adenosine nucleotides bind. This allows the phosphorylation state and activity of AMPK to change according to cellular energy status[288]. Specifically, in the presence of ADP or AMP, dephosphorylation of Thr172 by protein phosphatase 2C (PP2C) is inhibited[289,290], LKB1-mediated phosphorylation of Thr172 is promoted[291,292], and further activation is achieved by allosteric binding of AMP[288,293].

One of the initial papers identifying LKB1 as the upstream kinase for AMPK also highlighted the importance of this kinase in mediating AMPK stress responses. They showed that LKB1/*STK11*-null cells failed to activate AMPK in response to metabolic stress and that this response could be rescued by re-expression of LKB1[265]. This has more recently also been demonstrated *in vivo* where mice lacking LKB1 expression in skeletal muscle have significantly lower AMPK activity, fatty acid oxidation and glucose uptake in response to muscle contraction, a process which normally significantly enhances AMPK activation[294]. This was the first genetic evidence demonstrating the ability of the LKB1/AMPK pathway to regulate and maintain cellular energy levels.

1.5.2.4 LKB1-mediated activation of AMPK-related kinases (ARKs)

In the early 2000s, as we became more aware of various protein kinases and how they interact functionally as well as their sequence similarities, came the development of the human kinome dendogram[295]. It is from this that a group of 12 protein kinases closely related to AMPK were discovered and are now referred to as AMPK-related kinases

(ARKs; BRSK1/SAD-A, BRSK2/SAD-B, NUAK1/ARK5, NUAK2/SNARK, SIK1, OIK/SIK2, SIK3, SNRK, MARK1, MARK2, MARK3 and MARK4)[271]. LKB1 is the master kinase of this entire subfamily of protein kinases, phosphorylating and activating the residue equivalent to Thr172 within each AMPK-related kinase. Correspondingly, the activity of these kinases is decreased significantly in LKB1-deficient cells[286,296]. The catalytic subunits of the ARK subfamily do not interact with the γ subunits that provide AMPK with its ability to respond to changes in AMP/ADP concentrations, therefore, these kinases do not appear to be regulated by energy stress[256,297]. ARKs have been shown to play roles in cell polarity (MARK, BRSK/SAD)[298-301], cell proliferation (NUAKs)[271,302] and CREB-regulated gene transcription (SIKs)[303,304], although their regulation and function is poorly understood in comparison to AMPK[256]. Further study of the ARKs is important in cancer because they may mediate some of the tumour suppressor effects previously ascribed to LKB1 (Figure 1.4).

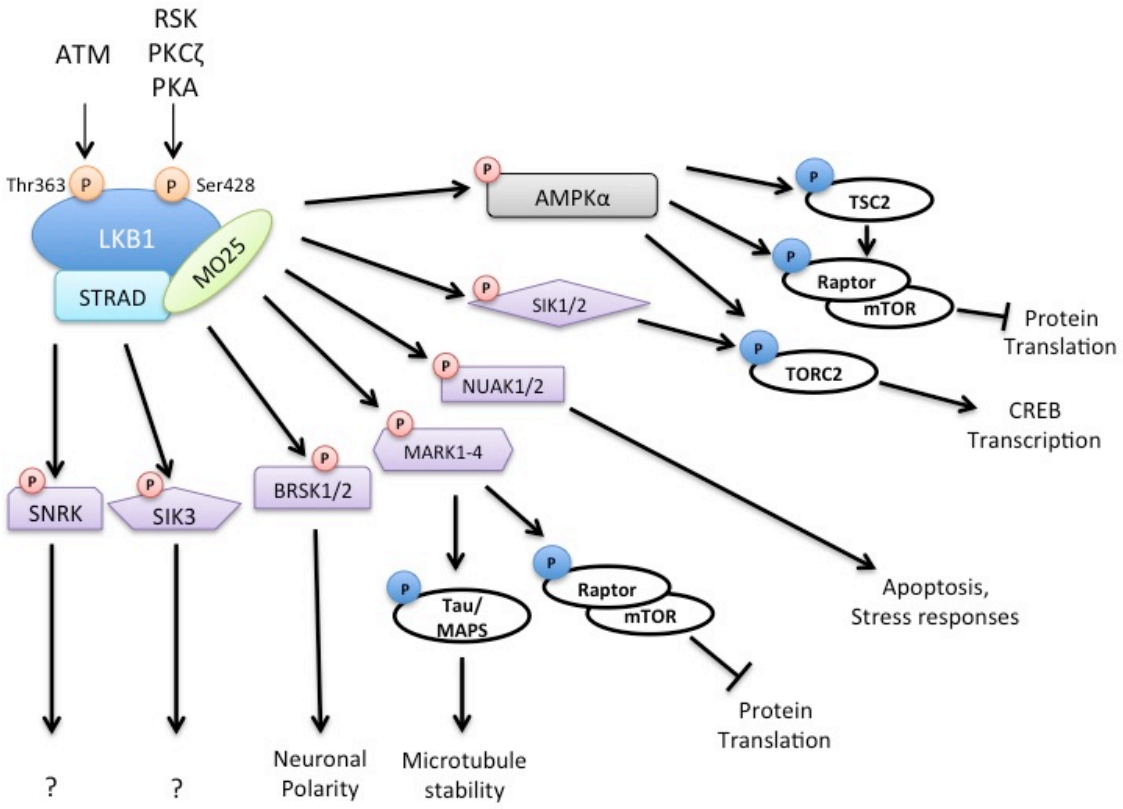

Figure 1.4: LKB1 is a master kinase, phosphorylating a number of AMPK-related kinases (ARKs).
LKB1, in a complex with STRAD and MO25, phosphorylates 12 AMPK-related kinases (ARKs) in addition to AMPK itself. These ARKs play roles in many important cellular processes, including microtubule stability, protein translation, CREB transcription and apoptosis. Upstream, LKB1 is phosphorylated by RSK, PKCζ or PKA at Ser428 and ATM at Thr 363.

1.5.3 LKB1/AMPK signalling in cancer

1.5.3.1 Peutz-Jeghers syndrome and LKB1

In 1922, Dr. Johannes Peutz was the first to describe Peutz-Jeghers Sydrome (PJS)[305]. This was followed by additional characterization provided by Dr. Harold Jeghers in the 1940s[306]. PJS is an autosomal dominant disorder characterized by development of benign hamartomatous polyps (benign tumour-like growths) within the gastrointestinal tract and marked cutaneous pigmentation (discolouration) of mucous membranes[271]. PJS patients also have a significantly greater chance of developing malignant tumours in a number of different tissues, including the breast, ovary, and pancreas[307-309]. In fact, 93% of PJS patients develop cancer by the age of 43 with 8% of patients developing a gynaecological cancer[310,311].

In 1998, parallel studies from two laboratories identified a number of mutations in the LKB1/STK11 gene in PJS families, providing the first evidence for LKB1's function as a tumour suppressor[312,313]. Since that time, 144 different mutations in the LKB1 gene have been identified in PJS families and a limited number of sporadic cancers. The majority of which result in significant truncation of the catalytic domain, impairing catalytic activity[314-326]. These findings indicate that the tumour suppressive functions of LKB1 are mediated by its downstream targets (AMPK and ARKs).

1.5.3.2 LKB1/AMPK function as tumour suppressors

Given the tumour suppressive function LKB1 plays in PJS, its mutation status in a number of sporadic cancers has also been examined. Surprisingly, the occurrence of somatic LKB1/STK11 mutations in sporadic cancers is relatively rare, except in the case of NSCLC and cervical cancers where mutations in this gene have been identified in 30% and 20% of tumours, respectively[327-329]. Additional evidence to support the tumour suppressive function of LKB1 was provided by overexpression studies whereby wild-type LKB1 induced a G1 cell-cycle arrest in the HeLa cervical cancer and G361 melanoma cell lines[330]. Mice heterozygous for $LKB1^{+/-}$ are viable with no overt phenotype until 45 weeks of age, at which point most animals develop polyps in the

gastrointestinal tract. Histology performed on these polyps revealed that they are remarkably similar to those found in PJS patients[271,331,332]. When LKB1/STK11$^{+/-}$mice are aged beyond 50 weeks of age, the majority of animals will develop hepatocellular carcinomas. These tumours have no LKB1 mRNA or protein expression, indicating that complete loss of LKB1 may be required for carcinogenesis[333].

Prior to the discovery that AMPK activation involves a tumour suppressor (LKB1), AMPK had solely been viewed as kinase with important roles in metabolism and was not on the radar of many cancer biologists. Although AMPK mediates some of the tumour suppressor functions of LKB1, some of these effects are also likely mediated by AMPK-related kinases[256]. A recent publication in which whole-animal knockout of AMPKα1 accelerates the development of B cell lymphomas in mice overexpressing c-myc supports the idea that AMPK may function as a tumour suppressor[334].

As part of its energy sensing capabilities, AMPK has a unique ability to control the cell-cycle under conditions of metabolic stress. This can occur through AMPK phosphorylation and stabilization of p53, which causes cells to arrest in the G1/S phase of the cell-cycle[335,336]. This effect was mediated by upregulation of cyclin-dependent kinase inhibitors p21$^{WAF1/CIP1}$, which is a transcriptional target of p53, and p27^{KIP1}, which is phosphorylated by AMPK[337].

Perhaps the best characterized mechanism through which AMPK controls cell growth is by suppressing the mechanistic Target of Rapamycin 1 (mTORC1) pathway. mTOR is a crucial hub through which a number of kinases signal, integrating signals from nutrient and energy sensors in order to ensure that growth and proliferation are only triggered when conditions are favourable[338]. AMPK is able to directly phosphorylate two crucial components of the mTORC1 signalling cascade, Tuberous sclerosis complex2 (TSC2/Tuberin)[339] and regulatory-associated protein of mTOR (RAPTOR)[340]. AMPK phosphorylation of both TSC2 and RAPTOR results in inhibition of mTORC1 signalling, thereby decreasing protein translation and inducing prosurvival process such as autophagy.

1.5.3.3 LKB1/AMPK pathway is tumour-promoting

Although many of the functions of the LKB1/AMPK pathway discussed above seem to support the idea that these kinases function as tumour suppressors, it has also been suggested that this may be highly context-dependent, based not only on the type of cancer but also the stage of metastasis. In fact, LKB1/AMPK may act as conditional tumour suppressors or oncogenes, depending on the magnitude or duration of stress[254,341].

It has also been suggested that LKB1 and AMPK may not always act in concert. Interestingly, unlike LKB1, AMPK subunits are more frequently amplified than mutated in human cancer and there is no evidence of a germline cancer predisposition syndrome involving AMPK subunits[254]. In addition to this, high levels of AMPK activity are observed in NSCLCs, where loss of LKB1 is common[342]. Given the lack of genetic evidence to support loss of AMPK function in cancer, AMPK may in fact be required for cancer cell survival in some instances[254]. In solid tumours, for example, AMPK is activated in areas of hypoxia allowing cells to tolerate nutrient starvation[253]. In this context, some of the aforementioned 'tumour suppressive' functions of AMPK can actually contribute to cell survival during periods of energetic stress. The prosurvival role of AMPK is likely mediated at least in part by its ability to inhibit mTORC1 signalling, thereby inducing proliferative quiescence and autophagy.

AMPK is able to induce autophagy, a highly conserved cellular process through which cellular content is degraded and recycled through lysosomal machinery. This process has been shown to be upregulated during periods of starvation in order to generate nutrients essential to maintain basic cellular function. mTORC1 activity suppresses autophagy by phosphorylating autophagy-related 13 (ATG 13) and Unc-51 like autophagy activating kinase 1 (ULK1) and preventing autophagosome initiation[343,344]. AMPK has the ability to indirectly induce autophagy when nutrients are scarce through its inhibition of mTORC1 signalling. It has also been reported that AMPK has the ability to directly phosphorylate ULK1[345,346], another mechanism through which AMPK directly promotes autophagy. The protective nature of AMPK activation and autophagy induction was illustrated in a recent study by Avivar *et al.*. In this study autophagy-induction mediated by the LKB1/AMPK/mTORC1 signalling axis promoted

anoikis-resistance in mammary epithelial cells. This effect was also found to be mediated by suspension-induced PERK activation, a member of the unfolded protein response (UPR) pathway[347].

1.5.3.4 Therapeutic manipulation of LKB1/AMPK signalling in cancer

Based on the proposed tumour suppressive function of the LKB1/AMPK pathway and its ability to suppress mTORC1 activity, it has been proposed that AMPK-activating drugs may be useful as cancer therapeutics[348]. One of the most commonly used AMPK agonists is the drug metformin, which is taken by approximately 120 million type 2 diabetics daily[349]. This activation, however, is not direct as metformin fails to activate AMPK in cell-free assays, rather it has been hypothesized to be through metformin's inhibition of the mitochondrial respiratory chain complex I[350]. Retrospective studies have demonstrated a strong correlation between metformin use and a reduction in cancer risk of up to 30%[351-353]. The most significant risk-reduction was observed for pancreatic and hepatocellular carcinomas[354]. It has been suggested that these associations between cancer incidence and metformin use may be due to other effects that metformin has on the tumour cells themselves, rather than AMPK activation alone. This provoked studies in tumour-prone $PTEN^{+/-}$ mice crossed to mice with decreased LKB1 expression (hypomorphic LKB1), in which development of lymphomas was delayed by administration of metformin or A-769662 (an allosteric AMPK agonist)[355]. Since metformin and A-769662 have completely different mechanisms through which they activate AMPK, it is unlikely that the effects of either of these compounds, is AMPK-independent[356]. Therefore, these data strongly suggest that metformin may be used as an AMPK-agonist in a therapeutic setting for cancer treatment.

As discussed above, the role of the LKB1/AMPK pathway largely depends on the stage of the tumour in question. In pre-neoplastic lesions, LKB1/AMPK may in fact function as a tumour suppressor through its ability to inhibit cell proliferation. Once a tumour is established, however, LKB1/AMPK may be needed to allow cells to survive periods of metabolic stress[256]. Before we use AMPK-activators as a cancer therapeutic, we need to better understand the unique metabolic requirements of cancer cells during

different stages of the carcinogenic process. In some cases, like when cells lose ECM-attachment or become hypoxic, specific inhibitors of LKB1 or AMPK may in fact be more appropriate.

1.5.4 LKB1/AMPK signalling in ovarian cancer

The observation that females with PJS have a significantly higher risk of developing gynecological cancers lead researchers to suspect that LKB1 may play an important role in the female reproductive tract[357]. In fact, 61% (176/288) of high-grade serous ovarian tumours analyzed within The Cancer Genome Atlas (TCGA) exhibit deletion of one or more of the alleles of the LKB1/STK11 gene. Correspondingly, immunofluorescence performed on 92 human high-grade serous ovarian carcinomas revealed complete loss of protein expression in 54% of samples and partial/scattered or no loss in the remaining specimens[358]. The consequences of LKB1 loss in high-grade serous ovarian cancer was examined using a conditional knockout mouse model in which LKB1 is lost in the OSE and stromal cells of the ovary using the Amhr2-cre driver mouse strain. Although adult $LKB1^{cko}$ mice exhibit a high degree of surface papillary hyperplasia of the ovary, tumour formation was not observed. Perhaps this was due to the fact that it is now well-recognized that the cell of origin of high grade serous cancer is the secretory cell of the fimbria in the fallopian tube. When $LKB1^{cko}$ mice are crossed to conditional knockout *PTEN* mice under control of the same promotor, however, adnexal (adnexa of uterus; i.e. fallopian tubes or ovaries) tumours were observed with 100% penetrance. When these tumours are examined histologically and compared to human ovarian cancer specimens, they strongly resemble that of high-grade serous ovarian carcinomas[358]. These studies provided the first evidence that LKB1 loss and its synergy with other tumour suppressors may be important for the initiation of high-grade serous ovarian cancer.

Contrary to LKB1, when tumour specimens from ovarian cancer patients were examined for expression of the various AMPK subunits, higher levels were observed in ovarian carcinomas compared to normal ovarian controls[359]. Additional studies have demonstrated that activation of AMPK by metformin or AMP mimetic, 5-Aminoimidazole-4-carboxamide ribonucleotide (AICAR) inhibits cell growth and

induces apoptosis[360,361]. The functional consequences of AMPK subunit overexpression in ovarian carcinoma specimens have yet to be determined with targeted knockdown experiments.

1.5.5 Summary

The LKB1/AMPK signalling pathway is unique in that it allows cells to respond to various forms of metabolic stress, such as nutrient deprivation, hypoxia, and energy depletion. The importance of metabolic reprogramming in allowing cancer cells to survive adverse microenvironments has become apparent over the last few years. It is clear that LKB1/AMPK may in fact play many context-specific roles throughout tumorigenesis and may not simply be classified as oncogenes or tumour suppressors. For example, loss of LKB1/AMPK signalling may be necessary during the initial stages of tumour development where there is need for rapid proliferation to support tumour growth. Subsequent to this, when this growth has stripped many of the available nutrient supplies, reactivation of LKB1/AMPK signalling may allow cells to survive until nutrients are replenished. Given the studies that have begun to implicate this pathway in ovarian carcinogenesis, there is a critical need for a more thorough molecular analysis and functional studies to determine the role of the LKB1/AMPK signalling pathway in ovarian cancer pathogenesis. This is particularly important given the unique way that ovarian cancer metastasizes and the crucial role that LKB1/AMPK signalling plays in mediating anoikis-resistance[347,362].

1.6 Scope of Thesis

Mechanisms of anoikis-resistance and spheroid formation are of particular importance when studying ovarian cancer given the way this disease metastasizes. Cells shed into the peritoneal cavity from the primary tumour must survive under non-adherent conditions until they reach the serosal surface of various abdominal organs at which point they are able to reattach and form secondary metastatic lesions. We developed an *in vitro* system with which to model suspension-induced spheroid formation and re-implantation to an adherent substratum. This allowed us to examine two signalling pathways we

hypothesized to play important, although not necessarily overlapping roles, in the process of ovarian cancer spheroid formation and re-implantation.

Our investigations began with the BMP signalling pathway, which we demonstrated is autonomously down-regulated during spheroid formation (Chapter 2). Correspondingly, over-activation of this pathway has a detrimental effect on the ability of cells to aggregate in suspension, resulting in much smaller spheroids. Further to this, we also demonstrate that when cells are reattached to an adherent substratum, BMP signalling is activated and enhances cell dispersion. Global gene expression analyses revealed a number of molecular aberrations associated with activated BMP signalling in ovarian cancer cells under both adherent and suspension conditions. Of these, Akt, which is also autonomously down-regulated when cells are in suspension, was shown to be enhanced in spheroids with activated BMP signalling. We also demonstrate that the BMP and Akt signalling pathways have the ability to act in concert to mediate suspension-induced cell aggregation and subsequent reattachment to an adherent surface. This study highlights the context-dependent role for the BMP signalling pathway throughout the various stages of ovarian cancer metastasis and provides a crucial link between this pathway and the PI3K/AKT signalling cascade. Given the important role that AKT plays in mediating the phenotypic alterations associated with activated BMP signalling in spheroids and other studies in our laboratory demonstrating that AKT signalling is a crucial mediator of reversible spheroid formation-induced dormancy, we became interested in other pathways that may cooperate with the PI3K/AKT pathway in our system.

AMPK is an important sensor of cellular energy status that converges with the PI3K/AKT signalling cascade on mTOR. These kinases have opposing regulatory effects on mTOR and therefore, may act in concert to allow ovarian cancer cells to survive in suspension. Indeed, in contrast to AKT, the activity of AMPK and its upstream kinase, LKB1, are enhanced in ovarian cancer spheroids (Chapter 3). Further pharmacological activation of the AMPK pathway is detrimental to adherent cells but much less so when cells are in suspension. Interestingly, targeted knockdown experiments demonstrated that LKB1 is crucial for suspension-induced spheroid formation and survival and that this

effect is AMPK-independent. These studies have begun to uncover the diverse range of signalling aberrations that occur when cells form multicellular spheroids and how these pathways interact to promote aggregation and survival in suspension.

1.7 References

1. Erickson, B.K., Conner, M.G. & Landen, C.N., Jr. The role of the fallopian tube in the origin of ovarian cancer. *Am J Obstet Gynecol* (2013).
2. Auersperg, N., Wong, A.S., Choi, K.C., Kang, S.K. & Leung, P.C. Ovarian surface epithelium: biology, endocrinology, and pathology. *Endocr Rev* **22**, 255-288 (2001).
3. Landen, C.N., Jr., Birrer, M.J. & Sood, A.K. Early events in the pathogenesis of epithelial ovarian cancer. *Journal of clinical oncology : official journal of the American Society of Clinical Oncology* **26**, 995-1005 (2008).
4. Lengyel, E.*, et al.* Epithelial ovarian cancer experimental models. *Oncogene* (2013).
5. Karst, A.M. & Drapkin, R. Ovarian cancer pathogenesis: a model in evolution. *J Oncol* **2010**, 932371 (2010).
6. Paclitaxel plus carboplatin versus standard chemotherapy with either single-agent carboplatin or cyclophosphamide, doxorubicin, and cisplatin in women with ovarian cancer: the ICON3 randomised trial. *Lancet* **360**, 505-515 (2002).
7. du Bois, A.*, et al.* A randomized clinical trial of cisplatin/paclitaxel versus carboplatin/paclitaxel as first-line treatment of ovarian cancer. *J Natl Cancer Inst* **95**, 1320-1329 (2003).
8. Gilks, C.B. Molecular abnormalities in ovarian cancer subtypes other than high-grade serous carcinoma. *J Oncol* **2010**, 740968 (2010).
9. Gilks, C.B. & Prat, J. Ovarian carcinoma pathology and genetics: recent advances. *Human pathology* **40**, 1213-1223 (2009).
10. Galic, V., Coleman, R.L. & Herzog, T.J. Unmet needs in ovarian cancer: dividing histologic subtypes to exploit novel targets and pathways. *Curr Cancer Drug Targets* **13**, 698-707 (2013).
11. Winter, W.E., 3rd*, et al.* Prognostic factors for stage III epithelial ovarian cancer: a Gynecologic Oncology Group Study. *Journal of clinical oncology : official journal of the American Society of Clinical Oncology* **25**, 3621-3627 (2007).
12. Shih Ie, M. & Kurman, R.J. Ovarian tumorigenesis: a proposed model based on morphological and molecular genetic analysis. *Am J Pathol* **164**, 1511-1518 (2004).
13. Nik, N.N., Vang, R., Shih, I.M. & Kurman, R.J. Origin and Pathogenesis of Pelvic (Ovarian, Tubal, and Primary Peritoneal) Serous Carcinoma. *Annu Rev Pathol* (2013).
14. Wiegand, K.C.*, et al.* ARID1A mutations in endometriosis-associated ovarian carcinomas. *N Engl J Med* **363**, 1532-1543 (2010).
15. Kurman, R.J. & Shih Ie, M. Molecular pathogenesis and extraovarian origin of epithelial ovarian cancer--shifting the paradigm. *Human pathology* **42**, 918-931 (2011).

16. Chan, W.Y.*, et al.* Bcl-2 and p53 protein expression, apoptosis, and p53 mutation in human epithelial ovarian cancers. *Am J Pathol* **156**, 409-417 (2000).
17. Kohler, M.F.*, et al.* Mutation and overexpression of p53 in early-stage epithelial ovarian cancer. *Obstet Gynecol* **81**, 643-650 (1993).
18. Kupryjanczyk, J.*, et al.* p53 gene mutations and protein accumulation in human ovarian cancer. *Proceedings of the National Academy of Sciences of the United States of America* **90**, 4961-4965 (1993).
19. Wen, W.H.*, et al.* p53 mutations and expression in ovarian cancers: correlation with overall survival. *Int J Gynecol Pathol* **18**, 29-41 (1999).
20. Singer, G., Shih Ie, M., Truskinovsky, A., Umudum, H. & Kurman, R.J. Mutational analysis of K-ras segregates ovarian serous carcinomas into two types: invasive MPSC (low-grade tumor) and conventional serous carcinoma (high-grade tumor). *Int J Gynecol Pathol* **22**, 37-41 (2003).
21. Singer, G.*, et al.* Patterns of p53 mutations separate ovarian serous borderline tumors and low- and high-grade carcinomas and provide support for a new model of ovarian carcinogenesis: a mutational analysis with immunohistochemical correlation. *Am J Surg Pathol* **29**, 218-224 (2005).
22. Permuth-Wey, J. & Sellers, T.A. Epidemiology of ovarian cancer. *Methods Mol Biol* **472**, 413-437 (2009).
23. Erzen, M. & Kovacic, J. Relationship between endometriosis and ovarian cancer. *Eur J Gynaecol Oncol* **19**, 553-555 (1998).
24. Goumenou, A., Matalliotakis, I., Mahutte, N. & Koumantakis, E. Endometriosis mimicking advanced ovarian cancer. *Fertil Steril* **86**, 219 e223-215 (2006).
25. Iwanari, O.*, et al.* Differential diagnosis of ovarian cancer, benign ovarian tumor and endometriosis by a combination assay of serum sialyl SSEA-1 antigen and CA125 levels. *Gynecol Obstet Invest* **29**, 71-74 (1990).
26. Mandai, M., Yamaguchi, K., Matsumura, N., Baba, T. & Konishi, I. Ovarian cancer in endometriosis: molecular biology, pathology, and clinical management. *Int J Clin Oncol* **14**, 383-391 (2009).
27. Steed, H., Chapman, W. & Laframboise, S. Endometriosis-associated ovarian cancer: a clinicopathologic review. *J Obstet Gynaecol Can* **26**, 709-715 (2004).
28. Vercellini, P.*, et al.* Endometriosis and ovarian cancer. *Am J Obstet Gynecol* **169**, 181-182 (1993).
29. Vlahos, N.F., Kalampokas, T. & Fotiou, S. Endometriosis and ovarian cancer: a review. *Gynecol Endocrinol* **26**, 213-219 (2010).
30. Yoshikawa, H.*, et al.* Prevalence of endometriosis in ovarian cancer. *Gynecol Obstet Invest* **50 Suppl 1**, 11-17 (2000).
31. Callahan, M.J.*, et al.* Primary fallopian tube malignancies in BRCA-positive women undergoing surgery for ovarian cancer risk reduction. *Journal of clinical oncology : official journal of the American Society of Clinical Oncology* **25**, 3985-3990 (2007).
32. Crum, C.P.*, et al.* Lessons from BRCA: the tubal fimbria emerges as an origin for pelvic serous cancer. *Clin Med Res* **5**, 35-44 (2007).
33. Crum, C.P.*, et al.* The distal fallopian tube: a new model for pelvic serous carcinogenesis. *Curr Opin Obstet Gynecol* **19**, 3-9 (2007).

34. Gross, A.L., Kurman, R.J., Vang, R., Shih Ie, M. & Visvanathan, K. Precursor lesions of high-grade serous ovarian carcinoma: morphological and molecular characteristics. *J Oncol* **2010**, 126295 (2010).
35. Piek, J.M.*, et al.* Dysplastic changes in prophylactically removed Fallopian tubes of women predisposed to developing ovarian cancer. *J Pathol* **195**, 451-456 (2001).
36. Saleemuddin, A.*, et al.* Risk factors for a serous cancer precursor ("p53 signature") in women with inherited BRCA mutations. *Gynecologic oncology* **111**, 226-232 (2008).
37. Piek, J.M.*, et al.* BRCA1/2-related ovarian cancers are of tubal origin: a hypothesis. *Gynecologic oncology* **90**, 491 (2003).
38. Erickson, B.K., Conner, M.G. & Landen, C.N., Jr. The role of the fallopian tube in the origin of ovarian cancer. *Am J Obstet Gynecol* **209**, 409-414 (2013).
39. Kessler, M., Fotopoulou, C. & Meyer, T. The molecular fingerprint of high grade serous ovarian cancer reflects its fallopian tube origin. *Int J Mol Sci* **14**, 6571-6596 (2013).
40. O'Shannessy, D.J.*, et al.* Gene expression analyses support fallopian tube epithelium as the cell of origin of epithelial ovarian cancer. *Int J Mol Sci* **14**, 13687-13703 (2013).
41. Kindelberger, D.W.*, et al.* Intraepithelial carcinoma of the fimbria and pelvic serous carcinoma: Evidence for a causal relationship. *Am J Surg Pathol* **31**, 161-169 (2007).
42. Perets, R.*, et al.* Transformation of the fallopian tube secretory epithelium leads to high-grade serous ovarian cancer in brca;tp53;pten models. *Cancer cell* **24**, 751-765 (2013).
43. Statistics, C.C.S.s.A.C.o.C. Canadian Cancer Statistics 2013. *Canadian Cancer Society* (2013).
44. Bast, R.C., Jr., Hennessy, B. & Mills, G.B. The biology of ovarian cancer: new opportunities for translation. *Nature reviews. Cancer* **9**, 415-428 (2009).
45. Herzog, T.J. & Pothuri, B. Ovarian cancer: a focus on management of recurrent disease. *Nat Clin Pract Oncol* **3**, 604-611 (2006).
46. Jemal, A.*, et al.* Cancer statistics, 2008. *CA Cancer J Clin* **58**, 71-96 (2008).
47. Burleson, K.M.*, et al.* Ovarian carcinoma ascites spheroids adhere to extracellular matrix components and mesothelial cell monolayers. *Gynecol Oncol* **93**, 170-181 (2004).
48. Burleson, K.M., Hansen, L.K. & Skubitz, A.P. Ovarian carcinoma spheroids disaggregate on type I collagen and invade live human mesothelial cell monolayers. *Clinical & experimental metastasis* **21**, 685-697 (2004).
49. Kenny, H.A., Nieman, K.M., Mitra, A.K. & Lengyel, E. The first line of intra-abdominal metastatic attack: breaching the mesothelial cell layer. *Cancer Discov* **1**, 100-102 (2011).
50. Milliken, D., Scotton, C., Raju, S., Balkwill, F. & Wilson, J. Analysis of chemokines and chemokine receptor expression in ovarian cancer ascites. *Clinical cancer research : an official journal of the American Association for Cancer Research* **8**, 1108-1114 (2002).

51. Kipps, E., Tan, D.S. & Kaye, S.B. Meeting the challenge of ascites in ovarian cancer: new avenues for therapy and research. *Nature reviews. Cancer* **13**, 273-282 (2013).
52. Holtfreter, J. A study of the mechanics of gastrulation. *J Exp Zool* **95**, 171-212 (1944).
53. Holtfreter, J. Neural induction in explants which have passed through sublethal cytolysis. *J Exp Zool* **106**, 197-222 (1947).
54. Moscana, A. Cell suspension from organ rudiments of chick embryos. *Exp Cell Res* **3**, 535-539 (1952).
55. Moscana, A. The development in vitro of chimeric aggregates of dissociated embryonic chick and mouse cells. *Proceedings of the National Academy of Sciences of the United States of America* **43**, 184-194 (1957).
56. Sutherland, R.M., Inch, W.R., McCredie, J.A. & Kruuv, J. A multi-component radiation survival curve using an in vitro tumour model. *Int J Radiat Biol Relat Stud Phys Chem Med* **18**, 491-495 (1970).
57. Sutherland, R.M., MacDonald, H.R. & Howell, R.L. Multicellular spheroids: a new model target for in vitro studies of immunity to solid tumor allografts. *J Natl Cancer Inst* **58**, 1849-1853 (1977).
58. Sutherland, R.M., McCredie, J.A. & Inch, W.R. Growth of multicell spheroids in tissue culture as a model of nodular carcinomas. *J Natl Cancer Inst* **46**, 113-120 (1971).
59. Ahammer, H., DeVaney, T.T. & Tritthart, H.A. Fractal dimension of K1735 mouse melanoma clones and spheroid invasion in vitro. *Eur Biophys J* **30**, 494-499 (2001).
60. Burleson, K.M., Boente, M.P., Pambuccian, S.E. & Skubitz, A.P. Disaggregation and invasion of ovarian carcinoma ascites spheroids. *Journal of translational medicine* **4**, 6 (2006).
61. Carey, S.P., Starchenko, A., McGregor, A.L. & Reinhart-King, C.A. Leading malignant cells initiate collective epithelial cell invasion in a three-dimensional heterotypic tumor spheroid model. *Clinical & experimental metastasis* **30**, 615-630 (2013).
62. de Ridder, L., Cornelissen, M. & de Ridder, D. Autologous spheroid culture: a screening tool for human brain tumour invasion. *Crit Rev Oncol Hematol* **36**, 107-122 (2000).
63. De Wever, O*., et al.* Single cell and spheroid collagen type I invasion assay. *Methods Mol Biol* **1070**, 13-35 (2014).
64. Del Duca, D., Werbowetski, T. & Del Maestro, R.F. Spheroid preparation from hanging drops: characterization of a model of brain tumor invasion. *J Neurooncol* **67**, 295-303 (2004).
65. Naber, H.P., Wiercinska, E., Ten Dijke, P. & van Laar, T. Spheroid assay to measure TGF-beta-induced invasion. *J Vis Exp* (2011).
66. Sutherland, R.M. Cell and environment interactions in tumor microregions: the multicell spheroid model. *Science* **240**, 177-184 (1988).
67. Mueller-Klieser, W. Multicellular spheroids. A review on cellular aggregates in cancer research. *Journal of cancer research and clinical oncology* **113**, 101-122 (1987).

68. Santini, M.T., Rainaldi, G. & Indovina, P.L. Apoptosis, cell adhesion and the extracellular matrix in the three-dimensional growth of multicellular tumor spheroids. *Crit Rev Oncol Hematol* **36**, 75-87 (2000).
69. Aoshiba, K., Rennard, S.I. & Spurzem, J.R. Cell-matrix and cell-cell interactions modulate apoptosis of bronchial epithelial cells. *Am J Physiol* **272**, L28-37 (1997).
70. Fukai, F*., et al.* Modulation of apoptotic cell death by extracellular matrix proteins and a fibronectin-derived antiadhesive peptide. *Experimental cell research* **242**, 92-99 (1998).
71. Rozzo, C., Chiesa, V., Caridi, G., Pagnan, G. & Ponzoni, M. Induction of apoptosis in human neuroblastoma cells by abrogation of integrin-mediated cell adhesion. *International journal of cancer. Journal international du cancer* **70**, 688-698 (1997).
72. Scott, G., Cassidy, L. & Busacco, A. Fibronectin suppresses apoptosis in normal human melanocytes through an integrin-dependent mechanism. *J Invest Dermatol* **108**, 147-153 (1997).
73. Frisch, S.M. & Francis, H. Disruption of epithelial cell-matrix interactions induces apoptosis. *The Journal of cell biology* **124**, 619-626 (1994).
74. Chiarugi, P. & Giannoni, E. Anoikis: a necessary death program for anchorage-dependent cells. *Biochemical pharmacology* **76**, 1352-1364 (2008).
75. Bissell, M.J. & Radisky, D. Putting tumours in context. *Nature reviews. Cancer* **1**, 46-54 (2001).
76. Eble, J.A. & Haier, J. Integrins in cancer treatment. *Curr Cancer Drug Targets* **6**, 89-105 (2006).
77. Reddig, P.J. & Juliano, R.L. Clinging to life: cell to matrix adhesion and cell survival. *Cancer Metastasis Rev* **24**, 425-439 (2005).
78. Valentijn, A.J., Zouq, N. & Gilmore, A.P. Anoikis. *Biochemical Society transactions* **32**, 421-425 (2004).
79. Frisch, S.M. & Ruoslahti, E. Integrins and anoikis. *Current opinion in cell biology* **9**, 701-706 (1997).
80. Ruoslahti, E. & Reed, J.C. Anchorage dependence, integrins, and apoptosis. *Cell* **77**, 477-478 (1994).
81. Giancotti, F.G. Complexity and specificity of integrin signalling. *Nat Cell Biol* **2**, E13-14 (2000).
82. Chiarugi, P. From anchorage dependent proliferation to survival: lessons from redox signalling. *IUBMB Life* **60**, 301-307 (2008).
83. Liotta, L.A. & Kohn, E. Anoikis: cancer and the homeless cell. *Nature* **430**, 973-974 (2004).
84. Wang, L.H. Molecular signaling regulating anchorage-independent growth of cancer cells. *Mt Sinai J Med* **71**, 361-367 (2004).
85. Day, M.L*., et al.* E-cadherin mediates aggregation-dependent survival of prostate and mammary epithelial cells through the retinoblastoma cell cycle control pathway. *J Biol Chem* **274**, 9656-9664 (1999).
86. Kantak, S.S. & Kramer, R.H. E-cadherin regulates anchorage-independent growth and survival in oral squamous cell carcinoma cells. *J Biol Chem* **273**, 16953-16961 (1998).

87. St Croix, B.*, et al.* E-Cadherin-dependent growth suppression is mediated by the cyclin-dependent kinase inhibitor p27(KIP1). *The Journal of cell biology* **142**, 557-571 (1998).
88. Davies, C.D., Muller, H., Hagen, I., Garseth, M. & Hjelstuen, M.H. Comparison of extracellular matrix in human osteosarcomas and melanomas growing as xenografts, multicellular spheroids, and monolayer cultures. *Anticancer research* **17**, 4317-4326 (1997).
89. Nederman, T., Norling, B., Glimelius, B., Carlsson, J. & Brunk, U. Demonstration of an extracellular matrix in multicellular tumor spheroids. *Cancer Res* **44**, 3090-3097 (1984).
90. Paulus, W., Huettner, C. & Tonn, J.C. Collagens, integrins and the mesenchymal drift in glioblastomas: a comparison of biopsy specimens, spheroid and early monolayer cultures. *International journal of cancer. Journal international du cancer* **58**, 841-846 (1994).
91. Hauptmann, S.*, et al.* Integrin expression on colorectal tumor cells growing as monolayers, as multicellular tumor spheroids, or in nude mice. *International journal of cancer. Journal international du cancer* **61**, 819-825 (1995).
92. Waleh, N.S.*, et al.* Selective down-regulation of integrin receptors in spheroids of squamous cell carcinoma. *Cancer Res* **54**, 838-843 (1994).
93. Boyd, M.*, et al.* Transfectant mosaic spheroids: a new model for evaluation of tumour cell killing in targeted radiotherapy and experimental gene therapy. *J Gene Med* **4**, 567-576 (2002).
94. Christensen, T., Moan, J., Sandquist, T. & Smedshammer, L. Multicellular spheroids as an in vitro model system for photoradiation therapy in the presence of Hpd. *Prog Clin Biol Res* **170**, 381-390 (1984).
95. Dubessy, C., Merlin, J.M., Marchal, C. & Guillemin, F. Spheroids in radiobiology and photodynamic therapy. *Crit Rev Oncol Hematol* **36**, 179-192 (2000).
96. Durand, R.E. & Olive, P.L. Resistance of tumor cells to chemo- and radiotherapy modulated by the three-dimensional architecture of solid tumors and spheroids. *Methods Cell Biol* **64**, 211-233 (2001).
97. Griffon, G.*, et al.* Radiosensitivity of multicellular tumour spheroids obtained from human ovarian cancers. *Eur J Cancer* **31A**, 85-91 (1995).
98. Guirado, D.*, et al.* Low-dose radiation hyper-radiosensitivity in multicellular tumour spheroids. *Br J Radiol* **85**, 1398-1406 (2012).
99. Ho, J.T.*, et al.* Effects of fractionated radiation therapy on human brain tumor multicellular spheroids. *Int J Radiat Oncol Biol Phys* **25**, 251-258 (1993).
100. Kelly, C.J., Hussien, K. & Muschel, R.J. 3D tumour spheroids as a model to assess the suitability of [18F]FDG-PET as an early indicator of response to PI3K inhibition. *Nucl Med Biol* **39**, 986-992 (2012).
101. Kim, T.H., Mount, C.W., Gombotz, W.R. & Pun, S.H. The delivery of doxorubicin to 3-D multicellular spheroids and tumors in a murine xenograft model using tumor-penetrating triblock polymeric micelles. *Biomaterials* **31**, 7386-7397.
102. Langmuir, V.K., Mendonca, H.L. & Woo, D.V. Comparisons between two monoclonal antibodies that bind to the same antigen but have differing affinities:

uptake kinetics and 125I-antibody therapy efficacy in multicell spheroids. *Cancer Res* **52**, 4728-4734 (1992).
103. Mandujano-Tinoco, E.A., Gallardo-Perez, J.C., Marin-Hernandez, A., Moreno-Sanchez, R. & Rodriguez-Enriquez, S. Anti-mitochondrial therapy in human breast cancer multi-cellular spheroids. *Biochimica et biophysica acta* **1833**, 541-551 (2013).
104. Mehta, G., Hsiao, A.Y., Ingram, M., Luker, G.D. & Takayama, S. Opportunities and challenges for use of tumor spheroids as models to test drug delivery and efficacy. *J Control Release* **164**, 192-204 (2012).
105. Nederman, T. & Twentyman, P. Spheroids for studies of drug effects. *Recent Results Cancer Res* **95**, 84-102 (1984).
106. Nichols, M.G. & Foster, T.H. Oxygen diffusion and reaction kinetics in the photodynamic therapy of multicell tumour spheroids. *Phys Med Biol* **39**, 2161-2181 (1994).
107. Perche, F. & Torchilin, V.P. Cancer cell spheroids as a model to evaluate chemotherapy protocols. *Cancer Biol Ther* **13**, 1205-1213 (2012).
108. Sutherland, R.M., Eddy, H.A., Bareham, B., Reich, K. & Vanantwerp, D. Resistance to adriamycin in multicellular spheroids. *Int J Radiat Oncol Biol Phys* **5**, 1225-1230 (1979).
109. Durand, R.E. & Sutherland, R.M. Effects of intercellular contact on repair of r adiation damage. *Experimental cell research* **71**, 75-80 (1972).
110. Durand, R.E. & Sutherland, R.M. Dependence of the radiation response of an in vitro tumor model on cell cycle effects. *Cancer Res* **33**, 213-219 (1973).
111. Sutherland, R.M. & Durand, R.E. Cell contact as a possible contribution to radiation resistance of some tumours. *Br J Radiol* **45**, 788-789 (1972).
112. Hirschhaeuser, F*., et al.* Multicellular tumor spheroids: an underestimated tool is catching up again. *Journal of biotechnology* **148**, 3-15.
113. Brammer, I., Zywietz, F. & Jung, H. Changes of histological and proliferative indices in the Walker carcinoma with tumour size and distance from blood vessel. *European journal of cancer* **15**, 1329-1336 (1979).
114. Burns, F.J. & Tannock, I.F. On the existence of a G 0 -phase in the cell cycle. *Cell Tissue Kinet* **3**, 321-334 (1970).
115. Denekamp, J. & Kallman, R.F. In vitro and in vivo labelling of animal tumours with tritiated thymidine. *Cell Tissue Kinet* **6**, 217-227 (1973).
116. Tannock, I.F. The relation between cell proliferation and the vascular system in a transplanted mouse mammary tumour. *British journal of cancer* **22**, 258-273 (1968).
117. Dethlefsen, L.A., Bauer, K.D. & Riley, R.M. Analytical cytometric approaches to heterogeneous cell populations in solid tumors: a review. *Cytometry* **1**, 89-108 (1980).
118. Hlatky, L. & Alpen, E.L. Two-dimensional diffusion limited system for cell growth. *Cell Tissue Kinet* **18**, 597-611 (1985).
119. Bauer, K.D., Keng, P., Sutherland, R.M. Isolation of quiescent cells from multicellular tumour spheroids using centrifugal elutriation. *Cancer Res* **42**, 72-78 (1982).

120. Inch, W.R., McCredie, J.A. & Sutherland, R.M. Growth of nodular carcinomas in rodents compared with multi-cell spheroids in tissue culture. *Growth* **34**, 271-282 (1970).
121. Hudson, L.G., Zeineldin, R. & Stack, M.S. Phenotypic plasticity of neoplastic ovarian epithelium: unique cadherin profiles in tumor progression. *Clinical & experimental metastasis* **25**, 643-655 (2008).
122. Sawada, K.*, et al.* Loss of E-cadherin promotes ovarian cancer metastasis via alpha 5-integrin, which is a therapeutic target. *Cancer Res* **68**, 2329-2339 (2008).
123. Symowicz, J.*, et al.* Engagement of collagen-binding integrins promotes matrix metalloproteinase-9-dependent E-cadherin ectodomain shedding in ovarian carcinoma cells. *Cancer Res* **67**, 2030-2039 (2007).
124. Shield, K., Ackland, M.L., Ahmed, N. & Rice, G.E. Multicellular spheroids in ovarian cancer metastases: Biology and pathology. *Gynecol Oncol* **113**, 143-148 (2009).
125. Valcarcel, M.*, et al.* Three-dimensional growth as multicellular spheroid activates the proangiogenic phenotype of colorectal carcinoma cells via LFA-1-dependent VEGF: implications on hepatic micrometastasis. *Journal of translational medicine* **6**, 57 (2008).
126. Patel, I.S., Madan, P., Getsios, S., Bertrand, M.A. & MacCalman, C.D. Cadherin switching in ovarian cancer progression. *International journal of cancer. Journal international du cancer* **106**, 172-177 (2003).
127. Imai, T.*, et al.* Hypoxia attenuates the expression of E-cadherin via up-regulation of SNAIL in ovarian carcinoma cells. *Am J Pathol* **163**, 1437-1447 (2003).
128. Casey, R.C.*, et al.* Beta 1-integrins regulate the formation and adhesion of ovarian carcinoma multicellular spheroids. *Am J Pathol* **159**, 2071-2080 (2001).
129. Iwanicki, M.P.*, et al.* Ovarian cancer spheroids use myosin-generated force to clear the mesothelium. *Cancer Discov* **1**, 144-157 (2011).
130. Sato, K. & Urist, M.R. Induced regeneration of calvaria by bone morphogenetic protein (BMP) in dogs. *Clin Orthop Relat Res*, 301-311 (1985).
131. Takahashi, S. & Urist, M.R. Differentiation of cartilage on three substrata under the influence of an aggregate of morphogenetic protein and other bone tissue noncollagenous proteins (BMP/iNCP). *Clin Orthop Relat Res*, 227-238 (1986).
132. Urist, M.R.*, et al.* Bone regeneration under the influence of a bone morphogenetic protein (BMP) beta tricalcium phosphate (TCP) composite in skull trephine defects in dogs. *Clin Orthop Relat Res*, 295-304 (1987).
133. Bin, S.*, et al.* BMP-7 attenuates TGF-beta1-induced fibroblast-like differentiation of rat dermal papilla cells. *Wound Repair Regen* **21**, 275-281 (2013).
134. Cai, J.*, et al.* BMP and TGF-beta pathway mediators are critical upstream regulators of Wnt signaling during midbrain dopamine differentiation in human pluripotent stem cells. *Dev Biol* **376**, 62-73 (2013).
135. Ghosh-Choudhury, N.*, et al.* Requirement of BMP-2-induced phosphatidylinositol 3-kinase and Akt serine/threonine kinase in osteoblast differentiation and Smad-dependent BMP-2 gene transcription. *J Biol Chem* **277**, 33361-33368 (2002).

136. Liu, D.D., Zhang, J.C., Zhang, Q., Wang, S.X. & Yang, M.S. TGF-beta/BMP signaling pathway is involved in cerium-promoted osteogenic differentiation of mesenchymal stem cells. *Journal of cellular biochemistry* **114**, 1105-1114 (2013).
137. Lorda-Diez, C.I., Montero, J.A., Choe, S., Garcia-Porrero, J.A. & Hurle, J.M. Ligand- and stage-dependent divergent functions of BMP signaling in the differentiation of embryonic skeletogenic progenitors in vitro. *J Bone Miner Res* (2013).
138. Matsumoto, T.*, et al.* BMP-2 Induced Expression of Alx3 That Is a Positive Regulator of Osteoblast Differentiation. *PLoS One* **8**, e68774 (2013).
139. Onishi, M., Fujita, Y., Yoshikawa, H. & Yamashita, T. Inhibition of Rac1 promotes BMP-2-induced osteoblastic differentiation. *Cell death & disease* **4**, e698 (2013).
140. Schneider, H., Sedaghati, B., Naumann, A., Hacker, M.C. & Schulz-Siegmund, M. Gene Silencing of Chordin Improves BMP-2 Effects on Osteogenic Differentiation of Human Adipose Tissue-Derived Stromal Cells. *Tissue Eng Part A* (2013).
141. Sharff, K.A.*, et al.* Hey1 basic helix-loop-helix protein plays an important role in mediating BMP9-induced osteogenic differentiation of mesenchymal progenitor cells. *J Biol Chem* **284**, 649-659 (2009).
142. Sui, L., Geens, M., Sermon, K., Bouwens, L. & Mfopou, J.K. Role of BMP signaling in pancreatic progenitor differentiation from human embryonic stem cells. *Stem Cell Rev* **9**, 569-577 (2013).
143. Vinals, F., Lopez-Rovira, T., Rosa, J.L. & Ventura, F. Inhibition of PI3K/p70 S6K and p38 MAPK cascades increases osteoblastic differentiation induced by BMP-2. *FEBS Lett* **510**, 99-104 (2002).
144. Wei, X.*, et al.* Effects of bone morphogenetic protein-4 (BMP-4) on adipocyte differentiation from mouse adipose-derived stem cells. *Cell Prolif* **46**, 416-424 (2013).
145. Yang, Z.*, et al.* Cessation of Epithelial Bmp Signaling Switches the Differentiation of Crown Epithelia to the Root Lineage in a beta-Catenin-Dependent Manner. *Mol Cell Biol* **33**, 4732-4744 (2013).
146. Zhang, J.*, et al.* BMP induces cochlin expression to facilitate self-renewal and suppress neural differentiation of mouse embryonic stem cells. *J Biol Chem* **288**, 8053-8060 (2013).
147. Guha, U., Gomes, W.A., Kobayashi, T., Pestell, R.G. & Kessler, J.A. In vivo evidence that BMP signaling is necessary for apoptosis in the mouse limb. *Dev Biol* **249**, 108-120 (2002).
148. Jernvall, J., Aberg, T., Kettunen, P., Keranen, S. & Thesleff, I. The life history of an embryonic signaling center: BMP-4 induces p21 and is associated with apoptosis in the mouse tooth enamel knot. *Development* **125**, 161-169 (1998).
149. Kawamura, C., Kizaki, M. & Ikeda, Y. Bone morphogenetic protein (BMP)-2 induces apoptosis in human myeloma cells. *Leuk Lymphoma* **43**, 635-639 (2002).
150. Pi, W., Guo, X., Su, L. & Xu, W. BMP-2 up-regulates PTEN expression and induces apoptosis of pulmonary artery smooth muscle cells under hypoxia. *PLoS One* **7**, e35283 (2012).

151. Shimizu, T., Kayamori, T., Murayama, C. & Miyamoto, A. Bone morphogenetic protein (BMP)-4 and BMP-7 suppress granulosa cell apoptosis via different pathways: BMP-4 via PI3K/PDK-1/Akt and BMP-7 via PI3K/PDK-1/PKC. *Biochemical and biophysical research communications* **417**, 869-873 (2012).
152. Smith, A. & Graham, A. Restricting Bmp-4 mediated apoptosis in hindbrain neural crest. *Dev Dyn* **220**, 276-283 (2001).
153. Wach, S., Schirmacher, P., Protschka, M. & Blessing, M. Overexpression of bone morphogenetic protein-6 (BMP-6) in murine epidermis suppresses skin tumor formation by induction of apoptosis and downregulation of fos/jun family members. *Oncogene* **20**, 7761-7769 (2001).
154. Wang, Z. & Guo, J. Mechanical Induction of BMP-7 in Osteocyte Blocks Glucocorticoid-Induced Apoptosis Through PI3K/AKT/GSK3beta Pathway. *Cell Biochem Biophys* **67**, 567-574 (2013).
155. Zhang, Y.*, et al.* Binding of carbon nanotube to BMP receptor 2 enhances cell differentiation and inhibits apoptosis via regulating bHLH transcription factors. *Cell death & disease* **3**, e308 (2012).
156. Zou, H. & Niswander, L. Requirement for BMP signaling in interdigital apoptosis and scale formation. *Science* **272**, 738-741 (1996).
157. Alarmo, E.L.*, et al.* BMP7 influences proliferation, migration, and invasion of breast cancer cells. *Cancer Lett* **275**, 35-43 (2009).
158. Busch, C., Drews, U., Garbe, C., Eisele, S.R. & Oppitz, M. Neural crest cell migration of mouse B16-F1 melanoma cells transplanted into the chick embryo is inhibited by the BMP-antagonist noggin. *International journal of oncology* **31**, 1367-1378 (2007).
159. Christiaen, L., Stolfi, A. & Levine, M. BMP signaling coordinates gene expression and cell migration during precardiac mesoderm development. *Dev Biol* **340**, 179-187 (2010).
160. Coles, E., Christiansen, J., Economou, A., Bronner-Fraser, M. & Wilkinson, D.G. A vertebrate crossveinless 2 homologue modulates BMP activity and neural crest cell migration. *Development* **131**, 5309-5317 (2004).
161. Crouzier, T., Fourel, L., Boudou, T., Albiges-Rizo, C. & Picart, C. Presentation of BMP-2 from a soft biopolymeric film unveils its activity on cell adhesion and migration. *Adv Mater* **23**, H111-118 (2011).
162. Fong, Y.C.*, et al.* BMP-2 increases migration of human chondrosarcoma cells via PI3K/Akt pathway. *J Cell Physiol* **217**, 846-855 (2008).
163. Fong, Y.C.*, et al.* BMP-2 increases migration of human chondrosarcoma cells via PI3K/Akt pathway. *J Cell Physiol* **217**, 846-855 (2008).
164. Fu, M., Vohra, B.P., Wind, D. & Heuckeroth, R.O. BMP signaling regulates murine enteric nervous system precursor migration, neurite fasciculation, and patterning via altered Ncam1 polysialic acid addition. *Dev Biol* **299**, 137-150 (2006).
165. Fu, M., Vohra, B.P., Wind, D. & Heuckeroth, R.O. BMP signaling regulates murine enteric nervous system precursor migration, neurite fasciculation, and patterning via altered Ncam1 polysialic acid addition. *Dev Biol* **299**, 137-150 (2006).

166. Gamell, C.*, et al.* BMP2 induction of actin cytoskeleton reorganization and cell migration requires PI3-kinase and Cdc42 activity. *J Cell Sci* **121**, 3960-3970 (2008).
167. Gamell, C., Susperregui, A.G., Bernard, O., Rosa, J.L. & Ventura, F. The p38/MK2/Hsp25 pathway is required for BMP-2-induced cell migration. *PLoS One* **6**, e16477 (2011).
168. Goldstein, A.M., Brewer, K.C., Doyle, A.M., Nagy, N. & Roberts, D.J. BMP signaling is necessary for neural crest cell migration and ganglion formation in the enteric nervous system. *Mech Dev* **122**, 821-833 (2005).
169. Ichikawa, T., Suenaga, Y., Koda, T., Ozaki, T. & Nakagawara, A. DeltaNp63/BMP-7-dependent expression of matrilin-2 is involved in keratinocyte migration in response to wounding. *Biochemical and biophysical research communications* **369**, 994-1000 (2008).
170. Inai, K., Burnside, J.L., Hoffman, S., Toole, B.P. & Sugi, Y. BMP-2 Induces Versican and Hyaluronan That Contribute to Post-EMT AV Cushion Cell Migration. *PLoS One* **8**, e77593 (2013).
171. Inai, K., Norris, R.A., Hoffman, S., Markwald, R.R. & Sugi, Y. BMP-2 induces cell migration and periostin expression during atrioventricular valvulogenesis. *Dev Biol* **315**, 383-396 (2008).
172. Inai, K., Norris, R.A., Hoffman, S., Markwald, R.R. & Sugi, Y. BMP-2 induces cell migration and periostin expression during atrioventricular valvulogenesis. *Dev Biol* **315**, 383-396 (2008).
173. Kim, M.*, et al.* Gremlin-1 induces BMP-independent tumor cell proliferation, migration, and invasion. *PLoS One* **7**, e35100 (2012).
174. Lenhart, K.F., Holtzman, N.G., Williams, J.R. & Burdine, R.D. Integration of nodal and BMP signals in the heart requires FoxH1 to create left-right differences in cell migration rates that direct cardiac asymmetry. *PLoS Genet* **9**, e1003109 (2013).
175. Li, B.*, et al.* Adenovirus-mediated overexpression of BMP-9 inhibits human osteosarcoma cell growth and migration through downregulation of the PI3K/AKT pathway. *International journal of oncology* **41**, 1809-1819 (2012).
176. Maegdefrau, U. & Bosserhoff, A.K. BMP activated Smad signaling strongly promotes migration and invasion of hepatocellular carcinoma cells. *Exp Mol Pathol* **92**, 74-81 (2012).
177. Park, J.E.*, et al.* BMP-9 induced endothelial cell tubule formation and inhibition of migration involves Smad1 driven endothelin-1 production. *PLoS One* **7**, e30075 (2012).
178. Pi, X.*, et al.* Sequential roles for myosin-X in BMP6-dependent filopodial extension, migration, and activation of BMP receptors. *The Journal of cell biology* **179**, 1569-1582 (2007).
179. Wang, X.Y.*, et al.* Construction of a eukaryotic expression vector pEGFP-C1-BMP-2 and its effect on cell migration. *J Zhejiang Univ Sci B* **13**, 356-363 (2012).
180. Wu, J.B., Fu, H.Q., Huang, L.Z., Liu, A.W. & Zhang, J.X. Effects of siRNA-targeting BMP-2 on the abilities of migration and invasion of human liver cancer SMMC7721 cells and its mechanism. *Cancer Gene Ther* **18**, 20-25 (2011).

181. Buijs, J.T.*, et al.* BMP7, a putative regulator of epithelial homeostasis in the human prostate, is a potent inhibitor of prostate cancer bone metastasis in vivo. *Am J Pathol* **171**, 1047-1057 (2007).
182. Darby, S., Cross, S.S., Brown, N.J., Hamdy, F.C. & Robson, C.N. BMP-6 over-expression in prostate cancer is associated with increased Id-1 protein and a more invasive phenotype. *J Pathol* **214**, 394-404 (2008).
183. Kang, M.H., Kim, J.S., Seo, J.E., Oh, S.C. & Yoo, Y.A. BMP2 accelerates the motility and invasiveness of gastric cancer cells via activation of the phosphatidylinositol 3-kinase (PI3K)/Akt pathway. *Exp Cell Res* **316**, 24-37.
184. Le Page, C.*, et al.* BMP-2 signaling in ovarian cancer and its association with poor prognosis. *J Ovarian Res* **2**, 4 (2009).
185. Peart, T.M., Correa, R.J., Valdes, Y.R., Dimattia, G.E. & Shepherd, T.G. BMP signalling controls the malignant potential of ascites-derived human epithelial ovarian cancer spheroids via AKT kinase activation. *Clinical & experimental metastasis* **29**, 293-313 (2012).
186. Shepherd, T.G., Theriault, B.L. & Nachtigal, M.W. Autocrine BMP4 signalling regulates ID3 proto-oncogene expression in human ovarian cancer cells. *Gene* **414**, 95-105 (2008).
187. Theriault, B.L., Shepherd, T.G., Mujoomdar, M.L. & Nachtigal, M.W. BMP4 induces EMT and Rho GTPase activation in human ovarian cancer cells. *Carcinogenesis* **28**, 1153-1162 (2007).
188. Derynck, R. & Zhang, Y.E. Smad-dependent and Smad-independent pathways in TGF-beta family signalling. *Nature* **425**, 577-584 (2003).
189. Heldin, C.H., Miyazono, K. & ten Dijke, P. TGF-beta signalling from cell membrane to nucleus through SMAD proteins. *Nature* **390**, 465-471 (1997).
190. Miyazono, K., Kamiya, Y. & Morikawa, M. Bone morphogenetic protein receptors and signal transduction. *J Biochem* **147**, 35-51 (2010).
191. Balemans, W. & Van Hul, W. Extracellular regulation of BMP signaling in vertebrates: a cocktail of modulators. *Dev Biol* **250**, 231-250 (2002).
192. Derynck, R. SMAD proteins and mammalian anatomy. *Nature* **393**, 737-739 (1998).
193. Kawabata, M. & Miyazono, K. Signal transduction of the TGF-beta superfamily by Smad proteins. *J Biochem* **125**, 9-16 (1999).
194. Raftery, L.A. & Sutherland, D.J. TGF-beta family signal transduction in Drosophila development: from Mad to Smads. *Dev Biol* **210**, 251-268 (1999).
195. Macias-Silva, M.*, et al.* MADR2 is a substrate of the TGFbeta receptor and its phosphorylation is required for nuclear accumulation and signaling. *Cell* **87**, 1215-1224 (1996).
196. Zhang, Y., Feng, X., We, R. & Derynck, R. Receptor-associated Mad homologues synergize as effectors of the TGF-beta response. *Nature* **383**, 168-172 (1996).
197. Hoodless, P.A.*, et al.* MADR1, a MAD-related protein that functions in BMP2 signaling pathways. *Cell* **85**, 489-500 (1996).
198. Kawai, S.*, et al.* Mouse smad8 phosphorylation downstream of BMP receptors ALK-2, ALK-3, and ALK-6 induces its association with Smad4 and transcriptional activity. *Biochemical and biophysical research communications* **271**, 682-687 (2000).

199. Nishimura, R.*, et al.* Smad5 and DPC4 are key molecules in mediating BMP-2-induced osteoblastic differentiation of the pluripotent mesenchymal precursor cell line C2C12. *J Biol Chem* **273**, 1872-1879 (1998).
200. Massague, J., Seoane, J. & Wotton, D. Smad transcription factors. *Genes & development* **19**, 2783-2810 (2005).
201. Casellas, R. & Brivanlou, A.H. Xenopus Smad7 inhibits both the activin and BMP pathways and acts as a neural inducer. *Dev Biol* **198**, 1-12 (1998).
202. Imamura, T.*, et al.* Smad6 inhibits signalling by the TGF-beta superfamily. *Nature* **389**, 622-626 (1997).
203. Yu, P.B., Beppu, H., Kawai, N., Li, E. & Bloch, K.D. Bone morphogenetic protein (BMP) type II receptor deletion reveals BMP ligand-specific gain of signaling in pulmonary artery smooth muscle cells. *J Biol Chem* **280**, 24443-24450 (2005).
204. Blanco Calvo, M.*, et al.* Biology of BMP signalling and cancer. *Clin Transl Oncol* **11**, 126-137 (2009).
205. Goto, K., Kamiya, Y., Imamura, T., Miyazono, K. & Miyazawa, K. Selective inhibitory effects of Smad6 on bone morphogenetic protein type I receptors. *J Biol Chem* **282**, 20603-20611 (2007).
206. Zhang, S.*, et al.* Smad7 antagonizes transforming growth factor beta signaling in the nucleus by interfering with functional Smad-DNA complex formation. *Mol Cell Biol* **27**, 4488-4499 (2007).
207. Bai, S., Shi, X., Yang, X. & Cao, X. Smad6 as a transcriptional corepressor. *J Biol Chem* **275**, 8267-8270 (2000).
208. Lin, X.*, et al.* Smad6 recruits transcription corepressor CtBP to repress bone morphogenetic protein-induced transcription. *Mol Cell Biol* **23**, 9081-9093 (2003).
209. Ebisawa, T.*, et al.* Smurf1 interacts with transforming growth factor-beta type I receptor through Smad7 and induces receptor degradation. *J Biol Chem* **276**, 12477-12480 (2001).
210. Kavsak, P.*, et al.* Smad7 binds to Smurf2 to form an E3 ubiquitin ligase that t argets the TGF beta receptor for degradation. *Mol Cell* **6**, 1365-1375 (2000).
211. Gazzerro, E. & Canalis, E. Bone morphogenetic proteins and their antagonists. *Rev Endocr Metab Disord* **7**, 51-65 (2006).
212. Kretzschmar, M., Doody, J. & Massague, J. Opposing BMP and EGF signalling pathways converge on the TGF-beta family mediator Smad1. *Nature* **389**, 618-622 (1997).
213. Yue, J., Frey, R.S. & Mulder, K.M. Cross-talk between the Smad1 and Ras/MEK signaling pathways for TGFbeta. *Oncogene* **18**, 2033-2037 (1999).
214. Massague, J. Integration of Smad and MAPK pathways: a link and a linker revisited. *Genes & development* **17**, 2993-2997 (2003).
215. Buckley, S.*, et al.* BMP4 signaling induces senescence and modulates the oncogenic phenotype of A549 lung adenocarcinoma cells. *Am J Physiol Lung Cell Mol Physiol* **286**, L81-86 (2004).
216. Hjertner, O.*, et al.* Bone morphogenetic protein-4 inhibits proliferation and induces apoptosis of multiple myeloma cells. *Blood* **97**, 516-522 (2001).

217. Kawamura, C.*, et al.* Bone morphogenetic protein-2 induces apoptosis in human myeloma cells with modulation of STAT3. *Blood* **96**, 2005-2011 (2000).
218. Yamada, N.*, et al.* Bone morphogenetic protein type IB receptor is progressively expressed in malignant glioma tumours. *British journal of cancer* **73**, 624-629 (1996).
219. Ide, H.*, et al.* Growth regulation of human prostate cancer cells by bone morphogenetic protein-2. *Cancer Res* **57**, 5022-5027 (1997).
220. Ro, T.B.*, et al.* Bone morphogenetic protein-5, -6 and -7 inhibit growth and induce apoptosis in human myeloma cells. *Oncogene* **23**, 3024-3032 (2004).
221. Autzen, P.*, et al.* Bone morphogenetic protein 6 in skeletal metastases from prostate cancer and other common human malignancies. *British journal of cancer* **78**, 1219-1223 (1998).
222. Kim, I.Y.*, et al.* Expression of bone morphogenetic protein receptors type-IA, -IB and -II correlates with tumor grade in human prostate cancer tissues. *Cancer Res* **60**, 2840-2844 (2000).
223. Langenfeld, E.M. & Langenfeld, J. Bone morphogenetic protein-2 stimulates angiogenesis in developing tumors. *Mol Cancer Res* **2**, 141-149 (2004).
224. Buijs, J.T.*, et al.* TGF-beta and BMP7 interactions in tumour progression and bone metastasis. *Clinical & experimental metastasis* **24**, 609-617 (2007).
225. Kodach, L.L.*, et al.* The bone morphogenetic protein pathway is active in human colon adenomas and inactivated in colorectal cancer. *Cancer* **112**, 300-306 (2008).
226. Langenfeld, E.M.*, et al.* The mature bone morphogenetic protein-2 is aberrantly expressed in non-small cell lung carcinomas and stimulates tumor growth of A549 cells. *Carcinogenesis* **24**, 1445-1454 (2003).
227. Dai, J.*, et al.* Vascular endothelial growth factor contributes to the prostate cancer-induced osteoblast differentiation mediated by bone morphogenetic protein. *Cancer Res* **64**, 994-999 (2004).
228. Guo, W.*, et al.* Expression of bone morphogenetic proteins and receptors in sarcomas. *Clin Orthop Relat Res*, 175-183 (1999).
229. Deng, H.*, et al.* Bone morphogenetic protein-4 is overexpressed in colonic adenocarcinomas and promotes migration and invasion of HCT116 cells. *Experimental cell research* **313**, 1033-1044 (2007).
230. Clement, J.H.*, et al.* Bone morphogenetic protein 2 (BMP-2) induces in vitro invasion and in vivo hormone independent growth of breast carcinoma cells. *International journal of oncology* **27**, 401-407 (2005).
231. Hamdy, F.C.*, et al.* Immunolocalization and messenger RNA expression of bone morphogenetic protein-6 in human benign and malignant prostatic tissue. *Cancer Res* **57**, 4427-4431 (1997).
232. Friedl, W.*, et al.* Juvenile polyposis: massive gastric polyposis is more common in MADH4 mutation carriers than in BMPR1A mutation carriers. *Hum Genet* **111**, 108-111 (2002).
233. Howe, J.R.*, et al.* Germline mutations of the gene encoding bone morphogenetic protein receptor 1A in juvenile polyposis. *Nat Genet* **28**, 184-187 (2001).

234. Howe, J.R.*, et al.* The prevalence of MADH4 and BMPR1A mutations in juvenile polyposis and absence of BMPR2, BMPR1B, and ACVR1 mutations. *J Med Genet* **41**, 484-491 (2004).
235. Sayed, M.G.*, et al.* Germline SMAD4 or BMPR1A mutations and phenotype of juvenile polyposis. *Ann Surg Oncol* **9**, 901-906 (2002).
236. Zhou, X.P.*, et al.* Germline mutations in BMPR1A/ALK3 cause a subset of cases of juvenile polyposis syndrome and of Cowden and Bannayan-Riley-Ruvalcaba syndromes. *Am J Hum Genet* **69**, 704-711 (2001).
237. Rahimi, R.A. & Leof, E.B. TGF-beta signaling: a tale of two responses. *Journal of cellular biochemistry* **102**, 593-608 (2007).
238. Haramis, A.P.*, et al.* De novo crypt formation and juvenile polyposis on BMP inhibition in mouse intestine. *Science* **303**, 1684-1686 (2004).
239. Kodach, L.L.*, et al.* The bone morphogenetic protein pathway is inactivated in the majority of sporadic colorectal cancers. *Gastroenterology* **134**, 1332-1341 (2008).
240. Otsuka, F., Moore, R.K. & Shimasaki, S. Biological function and cellular mechanism of bone morphogenetic protein-6 in the ovary. *J Biol Chem* **276**, 32889-32895 (2001).
241. Shimasaki, S.*, et al.* A functional bone morphogenetic protein system in the ovary. *Proceedings of the National Academy of Sciences of the United States of America* **96**, 7282-7287 (1999).
242. Shimizu, T.*, et al.* Involvement of the bone morphogenetic protein/receptor system during follicle development in the bovine ovary: Hormonal regulation of the expression of bone morphogenetic protein 7 (BMP-7) and its receptors (ActRII and ALK-2). *Mol Cell Endocrinol* **249**, 78-83 (2006).
243. Lee, W.S.*, et al.* Effects of bone morphogenetic protein-7 (BMP-7) on primordial follicular growth in the mouse ovary. *Mol Reprod Dev* **69**, 159-163 (2004).
244. Sun, R.Z.*, et al.* Expression of GDF-9, BMP-15 and their receptors in mammalian ovary follicles. *J Mol Histol* **41**, 325-332 (2010).
245. Edson, M.A.*, et al.* Granulosa cell-expressed BMPR1A and BMPR1B have unique functions in regulating fertility but act redundantly to suppress ovarian tumor development. *Mol Endocrinol* **24**, 1251-1266 (2010).
246. Pangas, S.A.*, et al.* Conditional deletion of Smad1 and Smad5 in somatic cells of male and female gonads leads to metastatic tumor development in mice. *Mol Cell Biol* **28**, 248-257 (2008).
247. Shepherd, T.G. & Nachtigal, M.W. Identification of a putative autocrine bone morphogenetic protein-signaling pathway in human ovarian surface epithelium and ovarian cancer cells. *Endocrinology* **144**, 3306-3314 (2003).
248. McLean, K.*, et al.* Human ovarian carcinoma-associated mesenchymal stem cells regulate cancer stem cells and tumorigenesis via altered BMP production. *The Journal of clinical investigation* **121**, 3206-3219 (2011).
249. Moren, A., Raja, E., Heldin, C.H. & Moustakas, A. Negative regulation of TGFbeta signaling by the kinase LKB1 and the scaffolding protein LIP1. *J Biol Chem* **286**, 341-353 (2011).
250. Caino, M.C.*, et al.* Metabolic stress regulates cytoskeletal dynamics and metastasis of cancer cells. *The Journal of clinical investigation* **123**, 2907-2920 (2013).

251. Buchakjian, M.R. & Kornbluth, S. The engine driving the ship: metabolic steering of cell proliferation and death. *Nature reviews. Molecular cell biology* **11**, 715-727 (2010).
252. Kroemer, G. & Pouyssegur, J. Tumor cell metabolism: cancer's Achilles' heel. *Cancer cell* **13**, 472-482 (2008).
253. Laderoute, K.R.*, et al.* 5'-AMP-activated protein kinase (AMPK) is induced by low-oxygen and glucose deprivation conditions found in solid-tumor microenvironments. *Mol Cell Biol* **26**, 5336-5347 (2006).
254. Liang, J. & Mills, G.B. AMPK: a contextual oncogene or tumor suppressor? *Cancer Res* **73**, 2929-2935 (2013).
255. Carling, D., Zammit, V.A. & Hardie, D.G. A common bicyclic protein kinase cascade inactivates the regulatory enzymes of fatty acid and cholesterol biosynthesis. *FEBS Lett* **223**, 217-222 (1987).
256. Hardie, D.G. & Alessi, D.R. LKB1 and AMPK and the cancer-metabolism link - ten years after. *BMC Biol* **11**, 36 (2013).
257. Mihaylova, M.M. & Shaw, R.J. The AMPK signalling pathway coordinates cell growth, autophagy and metabolism. *Nat Cell Biol* **13**, 1016-1023 (2011).
258. Hardie, D.G. AMP-activated protein kinase: an energy sensor that regulates all aspects of cell function. *Genes & development* **25**, 1895-1908 (2011).
259. Hawley, S.A.*, et al.* Characterization of the AMP-activated protein kinase kinase from rat liver and identification of threonine 172 as the major site at which it phosphorylates AMP-activated protein kinase. *J Biol Chem* **271**, 27879-27887 (1996).
260. Stein, S.C., Woods, A., Jones, N.A., Davison, M.D. & Carling, D. The regulation of AMP-activated protein kinase by phosphorylation. *The Biochemical journal* **345 Pt 3**, 437-443 (2000).
261. Scott, J.W.*, et al.* CBS domains form energy-sensing modules whose binding of adenosine ligands is disrupted by disease mutations. *The Journal of clinical investigation* **113**, 274-284 (2004).
262. Xiao, B.*, et al.* Structural basis for AMP binding to mammalian AMP-activated protein kinase. *Nature* **449**, 496-500 (2007).
263. Amodeo, G.A., Rudolph, M.J. & Tong, L. Crystal structure of the heterotrimer core of Saccharomyces cerevisiae AMPK homologue SNF1. *Nature* **449**, 492-495 (2007).
264. Townley, R. & Shapiro, L. Crystal structures of the adenylate sensor from fission yeast AMP-activated protein kinase. *Science* **315**, 1726-1729 (2007).
265. Hawley, S.A.*, et al.* Complexes between the LKB1 tumor suppressor, STRAD alpha/beta and MO25 alpha/beta are upstream kinases in the AMP-activated protein kinase cascade. *J Biol* **2**, 28 (2003).
266. Shaw, R.J.*, et al.* The tumor suppressor LKB1 kinase directly activates AMP-activated kinase and regulates apoptosis in response to energy stress. *Proceedings of the National Academy of Sciences of the United States of America* **101**, 3329-3335 (2004).
267. Woods, A.*, et al.* LKB1 is the upstream kinase in the AMP-activated protein kinase cascade. *Current biology : CB* **13**, 2004-2008 (2003).

268. Hawley, S.A., *et al.* Calmodulin-dependent protein kinase kinase-beta is an alternative upstream kinase for AMP-activated protein kinase. *Cell Metab* **2**, 9-19 (2005).
269. Hurley, R.L., *et al.* The Ca2+/calmodulin-dependent protein kinase kinases are AMP-activated protein kinase kinases. *J Biol Chem* **280**, 29060-29066 (2005).
270. Woods, A., *et al.* Ca2+/calmodulin-dependent protein kinase kinase-beta acts upstream of AMP-activated protein kinase in mammalian cells. *Cell Metab* **2**, 21-33 (2005).
271. Alessi, D.R., Sakamoto, K. & Bayascas, J.R. LKB1-dependent signaling pathways. *Annu Rev Biochem* **75**, 137-163 (2006).
272. Boudeau, J., *et al.* Functional analysis of LKB1/STK11 mutants and two aberrant isoforms found in Peutz-Jeghers Syndrome patients. *Hum Mutat* **21**, 172 (2003).
273. Sapkota, G.P., *et al.* Identification and characterization of four novel phosphorylation sites (Ser31, Ser325, Thr336 and Thr366) on LKB1/STK11, the protein kinase mutated in Peutz-Jeghers cancer syndrome. *The Biochemical journal* **362**, 481-490 (2002).
274. Sapkota, G.P., *et al.* Phosphorylation of the protein kinase mutated in Peutz-Jeghers cancer syndrome, LKB1/STK11, at Ser431 by p90(RSK) and cAMP-dependent protein kinase, but not its farnesylation at Cys(433), is essential for LKB1 to suppress cell vrowth. *J Biol Chem* **276**, 19469-19482 (2001).
275. Collins, S.P., Reoma, J.L., Gamm, D.M. & Uhler, M.D. LKB1, a novel serine/threonine protein kinase and potential tumour suppressor, is phosphorylated by cAMP-dependent protein kinase (PKA) and prenylated in vivo. *The Biochemical journal* **345 Pt 3**, 673-680 (2000).
276. Baas, A.F., *et al.* Activation of the tumour suppressor kinase LKB1 by the STE20-like pseudokinase STRAD. *The EMBO journal* **22**, 3062-3072 (2003).
277. Boudeau, J., *et al.* MO25alpha/beta interact with STRADalpha/beta enhancing their ability to bind, activate and localize LKB1 in the cytoplasm. *The EMBO journal* **22**, 5102-5114 (2003).
278. Brajenovic, M., Joberty, G., Kuster, B., Bouwmeester, T. & Drewes, G. Comprehensive proteomic analysis of human Par protein complexes reveals an interconnected protein network. *J Biol Chem* **279**, 12804-12811 (2004).
279. Miyamoto, H., Matsushiro, A. & Nozaki, M. Molecular cloning of a novel mRNA sequence expressed in cleavage stage mouse embryos. *Mol Reprod Dev* **34**, 1-7 (1993).
280. Nezu, J., Oku, A. & Shimane, M. Loss of cytoplasmic retention ability of mutant LKB1 found in Peutz-Jeghers syndrome patients. *Biochemical and biophysical research communications* **261**, 750-755 (1999).
281. Smith, D.P., Spicer, J., Smith, A., Swift, S. & Ashworth, A. The mouse Peutz-Jeghers syndrome gene Lkb1 encodes a nuclear protein kinase. *Human molecular genetics* **8**, 1479-1485 (1999).
282. Boudeau, J., *et al.* Analysis of the LKB1-STRAD-MO25 complex. *J Cell Sci* **117**, 6365-6375 (2004).
283. Karos, M. & Fischer, R. Molecular characterization of HymA, an evolutionarily highly conserved and highly expressed protein of Aspergillus nidulans. *Mol Gen Genet* **260**, 510-521 (1999).

284. Nozaki, M., Onishi, Y., Togashi, S. & Miyamoto, H. Molecular characterization of the Drosophila Mo25 gene, which is conserved among Drosophila, mouse, and yeast. *DNA Cell Biol* **15**, 505-509 (1996).
285. Tiainen, M., Vaahtomeri, K., Ylikorkala, A. & Makela, T.P. Growth arrest by the LKB1 tumor suppressor: induction of p21(WAF1/CIP1). *Human molecular genetics* **11**, 1497-1504 (2002).
286. Lizcano, J.M.*, et al.* LKB1 is a master kinase that activates 13 kinases of the AMPK subfamily, including MARK/PAR-1. *The EMBO journal* **23**, 833-843 (2004).
287. Sakamoto, K., Goransson, O., Hardie, D.G. & Alessi, D.R. Activity of LKB1 and AMPK-related kinases in skeletal muscle: effects of contraction, phenformin, and AICAR. *Am J Physiol Endocrinol Metab* **287**, E310-317 (2004).
288. Gowans, G.J., Hawley, S.A., Ross, F.A. & Hardie, D.G. AMP is a true physiological regulator of AMP-activated protein kinase by both allosteric activation and enhancing net phosphorylation. *Cell Metab* **18**, 556-566 (2013).
289. Davies, S.P., Helps, N.R., Cohen, P.T. & Hardie, D.G. 5'-AMP inhibits dephosphorylation, as well as promoting phosphorylation, of the AMP-activated protein kinase. Studies using bacterially expressed human protein phosphatase-2C alpha and native bovine protein phosphatase-2AC. *FEBS Lett* **377**, 421-425 (1995).
290. Park, S., Scheffler, T.L., Rossie, S.S. & Gerrard, D.E. AMPK activity is regulated by calcium-mediated protein phosphatase 2A activity. *Cell Calcium* **53**, 217-223 (2013).
291. Hawley, S.A.*, et al.* 5'-AMP activates the AMP-activated protein kinase cascade, and Ca2+/calmodulin activates the calmodulin-dependent protein kinase I cascade, via three independent mechanisms. *J Biol Chem* **270**, 27186-27191 (1995).
292. Oakhill, J.S.*, et al.* beta-Subunit myristoylation is the gatekeeper for initiating metabolic stress sensing by AMP-activated protein kinase (AMPK). *Proceedings of the National Academy of Sciences of the United States of America* **107**, 19237-19241 (2010).
293. Corton, J.M., Gillespie, J.G., Hawley, S.A. & Hardie, D.G. 5-aminoimidazole-4-carboxamide ribonucleoside. A specific method for activating AMP-activated protein kinase in intact cells? *Eur J Biochem* **229**, 558-565 (1995).
294. Sakamoto, K.*, et al.* Deficiency of LKB1 in skeletal muscle prevents AMPK activation and glucose uptake during contraction. *The EMBO journal* **24**, 1810-1820 (2005).
295. Manning, G., Whyte, D.B., Martinez, R., Hunter, T. & Sudarsanam, S. The protein kinase complement of the human genome. *Science* **298**, 1912-1934 (2002).
296. Jaleel, M.*, et al.* Identification of the sucrose non-fermenting related kinase SNRK, as a novel LKB1 substrate. *FEBS Lett* **579**, 1417-1423 (2005).
297. Al-Hakim, A.K.*, et al.* 14-3-3 cooperates with LKB1 to regulate the activity and localization of QSK and SIK. *J Cell Sci* **118**, 5661-5673 (2005).
298. Martin, S.G. & St Johnston, D. A role for Drosophila LKB1 in anterior-posterior axis formation and epithelial polarity. *Nature* **421**, 379-384 (2003).

299. Munro, E.M. PAR proteins and the cytoskeleton: a marriage of equals. *Current opinion in cell biology* **18**, 86-94 (2006).
300. Nance, J. PAR proteins and the establishment of cell polarity during C. elegans development. *Bioessays* **27**, 126-135 (2005).
301. Kishi, M., Pan, Y.A., Crump, J.G. & Sanes, J.R. Mammalian SAD kinases are required for neuronal polarization. *Science* **307**, 929-932 (2005).
302. Sun, X., Rikkerink, E.H., Jones, W.T. & Uversky, V.N. Multifarious Roles of Intrinsic Disorder in Proteins Illustrate Its Broad Impact on Plant Biology. *Plant Cell* (2013).
303. Katoh, Y.*, et al.* Salt-inducible kinase-1 represses cAMP response element-binding protein activity both in the nucleus and in the cytoplasm. *Eur J Biochem* **271**, 4307-4319 (2004).
304. Screaton, R.A.*, et al.* The CREB coactivator TORC2 functions as a calcium- and cAMP-sensitive coincidence detector. *Cell* **119**, 61-74 (2004).
305. Peutz, J.L.A. Over een zeer merkwaardige, gecombineerde familiaire polyposis van de slijmvliezen van den tractus intestinalis met die van de neuskeelholte en gepaard met eigenaardige pigmentaties van huiden slijmvliezen. *Ned Maandschr v Geneesk* **10**, 134-146 (1921).
306. Jeghers, H., Mc, K.V. & Katz, K.H. Generalized intestinal polyposis and melanin spots of the oral mucosa, lips and digits; a syndrome of diagnostic significance. *N Engl J Med* **241**, 993, illust; passim (1949).
307. Hemminki, A. The molecular basis and clinical aspects of Peutz-Jeghers syndrome. *Cellular and molecular life sciences : CMLS* **55**, 735-750 (1999).
308. Tomlinson, I.P. & Houlston, R.S. Peutz-Jeghers syndrome. *J Med Genet* **34**, 1007-1011 (1997).
309. Westerman, A.M.*, et al.* Peutz-Jeghers syndrome: 78-year follow-up of the original family. *Lancet* **353**, 1211-1215 (1999).
310. Giardiello, F.M.*, et al.* Very high risk of cancer in familial Peutz-Jeghers syndrome. *Gastroenterology* **119**, 1447-1453 (2000).
311. Giardiello, F.M.*, et al.* Increased risk of cancer in the Peutz-Jeghers syndrome. *N Engl J Med* **316**, 1511-1514 (1987).
312. Hemminki, A.*, et al.* A serine/threonine kinase gene defective in Peutz-Jeghers syndrome. *Nature* **391**, 184-187 (1998).
313. Jenne, D.E.*, et al.* Peutz-Jeghers syndrome is caused by mutations in a novel serine threonine kinase. *Nat Genet* **18**, 38-43 (1998).
314. Abed, A.A., Gunther, K., Kraus, C., Hohenberger, W. & Ballhausen, W.G. Mutation screening at the RNA level of the STK11/LKB1 gene in Peutz-Jeghers syndrome reveals complex splicing abnormalities and a novel mRNA isoform (STK11 c.597(insertion mark)598insIVS4). *Hum Mutat* **18**, 397-410 (2001).
315. Alhopuro, P.*, et al.* Mutation analysis of three genes encoding novel LKB1-interacting proteins, BRG1, STRADalpha, and MO25alpha, in Peutz-Jeghers syndrome. *British journal of cancer* **92**, 1126-1129 (2005).
316. Chen, C.*, et al.* One novel deletion and one splicing mutation of the LKB1 gene in two Chinese patients with Peutz-Jeghers syndrome. *DNA Cell Biol* **31**, 1535-1540 (2012).

317. Guldberg, P.*, et al.* Somatic mutation of the Peutz-Jeghers syndrome gene, LKB1/STK11, in malignant melanoma. *Oncogene* **18**, 1777-1780 (1999).
318. Hastings, M.L.*, et al.* An LKB1 AT-AC intron mutation causes Peutz-Jeghers syndrome via splicing at noncanonical cryptic splice sites. *Nat Struct Mol Biol* **12**, 54-59 (2005).
319. Hernan, I.*, et al.* De novo germline mutation in the serine-threonine kinase STK11/LKB1 gene associated with Peutz-Jeghers syndrome. *Clin Genet* **66**, 58-62 (2004).
320. Liu, L., Du, X. & Nie, J. A novel de novo mutation in LKB1 gene in a Chinese Peutz Jeghers syndrome patient significantly diminished p53 activity. *Clin Res Hepatol Gastroenterol* **35**, 221-226 (2011).
321. Qiu, W., Schonleben, F., Thaker, H.M., Goggins, M. & Su, G.H. A novel mutation of STK11/LKB1 gene leads to the loss of cell growth inhibition in head and neck squamous cell carcinoma. *Oncogene* **25**, 2937-2942 (2006).
322. Scott, R.J.*, et al.* Mutation analysis of the STK11/LKB1 gene and clinical characteristics of an Australian series of Peutz-Jeghers syndrome patients. *Clin Genet* **62**, 282-287 (2002).
323. Su, G.H.*, et al.* Germline and somatic mutations of the STK11/LKB1 Peutz-Jeghers gene in pancreatic and biliary cancers. *Am J Pathol* **154**, 1835-1840 (1999).
324. Takahashi, M.*, et al.* A novel germline mutation of the LKB1 gene in a patient with Peutz-Jeghers syndrome with early-onset gastric cancer. *J Gastroenterol* **39**, 1210-1214 (2004).
325. Tate, G., Suzuki, T. & Mitsuya, T. A new mutation of LKB1 gene in a Japanese patient with Peutz-Jeghers syndrome. *Acta Med Okayama* **57**, 305-308 (2003).
326. Zhong, D.*, et al.* LKB1 mutation in large cell carcinoma of the lung. *Lung Cancer* **53**, 285-294 (2006).
327. Ding, L.*, et al.* Somatic mutations affect key pathways in lung adenocarcinoma. *Nature* **455**, 1069-1075 (2008).
328. Sanchez-Cespedes, M.*, et al.* Inactivation of LKB1/STK11 is a common event in adenocarcinomas of the lung. *Cancer Res* **62**, 3659-3662 (2002).
329. Wingo, S.N.*, et al.* Somatic LKB1 mutations promote cervical cancer progression. *PLoS One* **4**, e5137 (2009).
330. Tiainen, M., Ylikorkala, A. & Makela, T.P. Growth suppression by Lkb1 is mediated by a G(1) cell cycle arrest. *Proceedings of the National Academy of Sciences of the United States of America* **96**, 9248-9251 (1999).
331. Jishage, K.*, et al.* Role of Lkb1, the causative gene of Peutz-Jegher's syndrome, in embryogenesis and polyposis. *Proceedings of the National Academy of Sciences of the United States of America* **99**, 8903-8908 (2002).
332. Miyoshi, H.*, et al.* Gastrointestinal hamartomatous polyposis in Lkb1 heterozygous knockout mice. *Cancer Res* **62**, 2261-2266 (2002).
333. Nakau, M.*, et al.* Hepatocellular carcinoma caused by loss of heterozygosity in Lkb1 gene knockout mice. *Cancer Res* **62**, 4549-4553 (2002).
334. Faubert, B.*, et al.* AMPK is a negative regulator of the Warburg effect and suppresses tumor growth in vivo. *Cell Metab* **17**, 113-124 (2013).

335. Imamura, K., Ogura, T., Kishimoto, A., Kaminishi, M. & Esumi, H. Cell cycle regulation via p53 phosphorylation by a 5'-AMP activated protein kinase activator, 5-aminoimidazole- 4-carboxamide-1-beta-D-ribofuranoside, in a human hepatocellular carcinoma cell line. *Biochemical and biophysical research communications* **287**, 562-567 (2001).
336. Jones, K.R.*, et al.* p53-Dependent accelerated senescence induced by ionizing radiation in breast tumour cells. *Int J Radiat Biol* **81**, 445-458 (2005).
337. Liang, J.*, et al.* The energy sensing LKB1-AMPK pathway regulates p27(kip1) phosphorylation mediating the decision to enter autophagy or apoptosis. *Nat Cell Biol* **9**, 218-224 (2007).
338. Efeyan, A. & Sabatini, D.M. mTOR and cancer: many loops in one pathway. *Current opinion in cell biology* **22**, 169-176.
339. Inoki, K.*, et al.* TSC2 integrates Wnt and energy signals via a coordinated phosphorylation by AMPK and GSK3 to regulate cell growth. *Cell* **126**, 955-968 (2006).
340. Pacholec, M.*, et al.* SRT1720, SRT2183, SRT1460, and resveratrol are not direct activators of SIRT1. *J Biol Chem* **285**, 8340-8351 (2010).
341. Herrmann, J.L., Byekova, Y., Elmets, C.A. & Athar, M. Liver kinase B1 (LKB1) in the pathogenesis of epithelial cancers. *Cancer Lett* **306**, 1-9 (2011).
342. William, W.N.*, et al.* The impact of phosphorylated AMP-activated protein kinase expression on lung cancer survival. *Annals of oncology : official journal of the European Society for Medical Oncology / ESMO* **23**, 78-85 (2012).
343. Chan, E.Y. mTORC1 phosphorylates the ULK1-mAtg13-FIP200 autophagy regulatory complex. *Science signaling* **2**, pe51 (2009).
344. Hosokawa, N.*, et al.* Nutrient-dependent mTORC1 association with the ULK1-Atg13-FIP200 complex required for autophagy. *Mol Biol Cell* **20**, 1981-1991 (2009).
345. Kim, J., Kundu, M., Viollet, B. & Guan, K.L. AMPK and mTOR regulate autophagy through direct phosphorylation of Ulk1. *Nat Cell Biol* **13**, 132-141 (2011).
346. Egan, D.F.*, et al.* Phosphorylation of ULK1 (hATG1) by AMP-activated protein kinase connects energy sensing to mitophagy. *Science* **331**, 456-461 (2011).
347. Avivar-Valderas, A.*, et al.* Regulation of autophagy during ECM detachment is linked to a selective inhibition of mTORC1 by PERK. *Oncogene* **32**, 4932-4940 (2013).
348. Hardie, D.G. AMP-activated protein kinase as a drug target. *Annu Rev Pharmacol Toxicol* **47**, 185-210 (2007).
349. Shackelford, D.B. Unravelling the connection between metabolism and tumorigenesis through studies of the liver kinase B1 tumour suppressor. *J Carcinog* **12**, 16 (2013).
350. Hardie, D.G. Neither LKB1 nor AMPK are the direct targets of metformin. *Gastroenterology* **131**, 973; author reply 974-975 (2006).
351. Bowker, S.L., Majumdar, S.R., Veugelers, P. & Johnson, J.A. Increased cancer-related mortality for patients with type 2 diabetes who use sulfonylureas or insulin. *Diabetes Care* **29**, 254-258 (2006).

352. Evans, J.M., Donnelly, L.A., Emslie-Smith, A.M., Alessi, D.R. & Morris, A.D. Metformin and reduced risk of cancer in diabetic patients. *Bmj* **330**, 1304-1305 (2005).
353. Pollak, M. Metformin and other biguanides in oncology: advancing the research agenda. *Cancer Prev Res (Phila)* **3**, 1060-1065 (2010).
354. Decensi, A.*, et al.* Metformin and cancer risk in diabetic patients: a systematic review and meta-analysis. *Cancer Prev Res (Phila)* **3**, 1451-1461 (2010).
355. Huang, X.*, et al.* Important role of the LKB1-AMPK pathway in suppressing tumorigenesis in PTEN-deficient mice. *The Biochemical journal* **412**, 211-221 (2008).
356. Hawley, S.A.*, et al.* Use of cells expressing gamma subunit variants to identify diverse mechanisms of AMPK activation. *Cell Metab* **11**, 554-565 (2010).
357. Sanchez-Cespedes, M. A role for LKB1 gene in human cancer beyond the Peutz-Jeghers syndrome. *Oncogene* **26**, 7825-7832 (2007).
358. Tanwar, P.S.*, et al.* Loss of LKB1 and PTEN tumor suppressor genes in the ovarian surface epithelium induces papillary serous ovarian cancer. *Carcinogenesis* (2013).
359. Li, C., Liu, V.W., Chiu, P.M., Chan, D.W. & Ngan, H.Y. Over-expressions of AMPK subunits in ovarian carcinomas with significant clinical implications. *BMC cancer* **12**, 357 (2012).
360. Gotlieb, W.H.*, et al.* In vitro metformin anti-neoplastic activity in epithelial ovarian cancer. *Gynecologic oncology* **110**, 246-250 (2008).
361. Yasmeen, A.*, et al.* Induction of apoptosis by metformin in epithelial ovarian cancer: involvement of the Bcl-2 family proteins. *Gynecologic oncology* **121**, 492-498 (2011).
362. Ng, T.L.*, et al.* The AMPK stress response pathway mediates anoikis resistance through inhibition of mTOR and suppression of protein synthesis. *Cell Death Differ* **19**, 501-510 (2012).

Chapter 2

2 BMP signalling controls the malignant potential of ascites-derived human epithelial ovarian cancer spheroids via AKT kinase activation

2.1 Introduction

Metastasis of epithelial ovarian cancer (EOC) is unique among most carcinomas in that spread occurs by direct dissemination of malignant cells from the primary tumour into the peritoneal cavity. EOC cells exist in suspension as single cells or aggregates called spheroids, until they adhere to the serosal surfaces of abdominal organs to establish and grow as secondary tumours[1,2]. It is becoming increasingly evident that EOC spheroids harbour unique characteristics that render them more resistant to chemotherapeutics, and perhaps more aggressive in establishing metastatic implants[3]. From an experimental perspective, we know that the gene expression patterns of cancer cells within multicellular spheroids more closely resemble that of the tumour, when compared with adherent monolayer cell cultures [4,5]. Therefore, cell culture systems that better mimic this metastatic program of EOC are favoured because they will more accurately reflect the pathophysiology of native EOC spheroids and provide relevant data regarding the signalling pathways important for spheroid formation and survival.

The transforming growth factor beta (TGF-β)/bone morphogenetic protein (BMP) signalling superfamily has been implicated in numerous aspects of the pathogenesis of many different cancers including EOC [4,5]. Both normal human ovarian surface epithelial (OSE) cells and EOC cells possess the signalling components necessary for activation of this pathway in response to ligands of this superfamily, including TGF-β, BMPs, activin and Mullerian inhibiting substance (MIS)[6-13]. For example, EOC cells respond to exogenous TGF-β by inducing growth arrest due to upregulation of p15 expression [14]. MIS treatment targets EOC-initiating cells of both cell lines and patient ascites cells by reducing their stem-like characteristics and thereby blocking their tumour-forming ability when injected in mice [15]. BMP signalling through BMP4 increases the adhesion, motility and invasiveness of ascites-derived primary human EOC cells and induces epithelial-

mesenchymal transition (EMT); treatment with the BMP2/4 antagonist Noggin blocks these activities as well as autocrine BMP4 signalling [13]. In addition, BMP2 expression in EOC cells from ascites fluid is elevated compared to matched solid tumour samples [7]. Regulated expression of a constitutively-active BMP2/4 receptor in the human OVCA429 ovarian cancer cell line recapitulates many of the changes modulated by BMP ligands, however, the ability of these cells to form ascites and secondary tumours in immuno-compromised mice is dramatically reduced [11]. Thus, we propose that BMP signalling has different effects at specific stages of EOC progression including dissemination from the primary tumour, spread through the ascites as spheroids, and reattachment to form secondary tumours. Determining the molecular changes controlled by activated BMP signalling in an *in vitro* cell culture system that closely mimics EOC pathogenesis would provide additional mechanistic insight into the functional implications of this pathway during the disease process in patients.

Herein, we describe the characterization of activated BMP signalling using a three-dimensional cell culture system whereby ascites-derived primary human EOC cells are grown in suspension where they naturally and rapidly form viable multicellular aggregates that closely resemble those observed directly in the malignant ascites collected from patients. Endogenous BMP signalling is decreased during EOC spheroid formation yet re-established during the process of spheroid reattachment. Ectopic expression of the constitutively-active BMP type I receptor $ALK3^{QD}$, however, reduces the formation of large multicellular spheroids, yet enhances the immediate reattachment of EOC spheroids via increased cell motility. In addition, we provide evidence that activated BMP signalling in EOC cells and spheroids induces AKT phosphorylation, which is a necessary intracellular mediator of activated BMP signalling regulating the malignant features of metastatic disease.

2.2 Materials and Methods

2.2.1 Cell culture

Ascitic fluid collected from chemotherapy-naive patients at time of paracentesis or debulking surgery was used to generate primary ascites cell cultures from patients with

stage III or IV ovarian cancer as described previously [16]. Briefly, ascitic fluid containing cells was mixed 1:1 with growth medium [MCDB105 (Sigma, St. Louis, MO)/M199 (Invitrogen, Carlsbad, CA) supplemented with 10% fetal bovine serum (FBS) (Wisent, St. Bruno, Quebec, Canada) and 50 µg/ml penicillin-streptomycin]. Cells were grown in a 37°C humidified atmosphere of 95% air and 5% CO_2. All experiments with primary EOC cells were performed between passages 3 and 5.

Adherent cells were maintained on tissue culture-treated polystyrene (Sarstedt, Newton, NC). Non-adherent cells were maintained on Ultra Low-Attachment (ULA®) cultureware (Corning, Corning, NY) which is coated with a hydrophilic, neutrally charged hydrogel to prevent cell attachment. Single-cell suspensions of 5 x 10^4 cells/mL were seeded to ULA plates to form spheroids over time.

2.2.2 Adenovirus vectors and cell transduction

The virus Ad-ALK3^{QD}, which encodes constitutively-active BMP type IA receptor was previously constructed using the AdEasy Vector System (Qbiogene, Irvine, CA, USA) [11]. Adenovirus expressing green fluorescent protein (Ad-GFP) was a kind gift from Dr. B. C. Vanderhyden (Ottawa Health Research Institute). Primary ovarian cancer cells were transduced at 80% confluence with a multiplicity of infection of 25 with either Ad-ALK3^{QD} or Ad-GFP in a minimal volume of medium containing 10% FBS for 2 hours with occasional agitation. Following transduction, complete growth medium was replenished. ALK3^{QD} is tagged with a hemagglutinin (HA) epitope at the carboxyl-terminus, therefore expression was detected by western analysis using anti-HA. All experiments were performed or initiated 24 hours following transduction.

2.2.3 RNA expression analysis

Total RNA was isolated from cells grown either as a monolayer on tissue-culture-treated polystyrene or as spheroids on ULA® cultureware using Qiagen RNeasy Mini Kit (Qiagen, Valencia, CA). Quantity and quality of purified RNA was determined using an ND-1000 spectrophotometer (NanoDrop Technologies, Wilmington, DE) and Agilent 2100 bioanalyzer (Agilent Technologies, Santa Clara, CA). Monolayer and spheroid

RNA samples from five different primary EOC patient samples that were transduced with either Ad-GFP (control) or Ad-ALK3^{QD} (activated BMP signalling) were hybridized to Affymetrix® Human Genome U133A GeneChips (Affymetrix, Santa Clara, CA) at Precision Biomarker Resources Inc. (Evanston, IL).

2.2.4 Real-time quantitative RT-PCR

Reverse transcription was performed using total RNA isolated from five independent patient samples (adherent & spheroid, Ad-GFP & Ad-ALK3^{QD}-transduced) and Superscript II reverse transcriptase (Invitrogen) as per manufacturer's instructions. PCR reactions were carried out using Brilliant® SYBR® Green QPCR Master Mix (Agilent Technologies/Stratagene) and a Stratagene Mx3000P machine with data exported to Microsoft® Excel for data analysis. Human-specific primers sequences and annealing temperatures used for *CDH1*, *SNAI1*, *SNAI2*, *TWIST1*, *TWIST2*, *ZEB2*, *SMAD6*, *NOG*, *MSX2*, *TBX3*, *HEY1* and *DLX2* are available upon request. *GAPDH* served as an internal control for RNA input using previously published primer sequences [11].

2.2.5 Cell number a viability assays

Primary EOC cells were transduced in complete growth medium with either Ad-GFP or Ad-ALK3^{QD}. Twenty-four hours following transduction, cells were seeded to either tissue-culture treated or ULA cultureware. Adherent cells were exposed to 0.25% trypsin-EDTA for 3 minutes and, following detachment, trypsin was inactivated using complete growth medium. Spheroids were exposed to 0.25% trypsin-EDTA for 10 minutes with vortexing and trituration to disaggregate spheroids. Trypsin was then inactivated using a small volume of FBS. To evaluate total cell number, single-cell suspensions were counted in a hemacytometer. To assess cell viability, single-cell suspensions were first diluted 1:1 in Trypan Blue reagent (Invitrogen, Carlsbad, CA) and all dye-excluding, viable cells counted in a hemacytometer. All treatments were performed in triplicate and two hemacytometer counts were performed per replicate.

2.2.6 Spheroid formation and reattachment assays

Primary EOC cells were transduced at 80% confluence with either Ad-GFP or Ad-ALK3QD. Twenty four hours later, spheroids were formed on ULA cultureware for three days at which point phase contrast images were captured of each well containing spheroids using an Olympus IX70 inverted microscope and ImagePro image capture software. The size of each of the spheroids was quantified for each image using the area measurement tool in the *ImageJ* image processing program (NIH, Bethesda, MD). In some cases, instead of transduction with virus, cells were incubated in media with minimal serum (0.5%-1%) for 24 hours prior to seeding to ULA culture ware, at which point, cells were treated with either Fc-Noggin or LDN-193189.

Spheroids were collected and re-plated to: (i) 18 mm diameter round glass coverslips placed in 22 mm diameter culture dishes for subsequent BrdU immunocytochemical analysis (see below), or (ii) directly to tissue-culture-treated 24-well polystyrene plates to quantify spheroid reattachment and dispersion. Phase contrast images were captured using an Olympus IX70 inverted microscope and ImagePro software of individual reattaching spheroids at initial point of attachment prior to dispersion (3 hours) and 24 hours following re-attachment. At this point, the experiment was terminated and re-attached spheroids were fixed and stained with using Hema-3 Stain kit (Fisher, Kalamazoo, MI). Spheroid dispersion was quantified using the area measurement tool in *ImageJ* (NIH, Bethesda, MD). Dispersion area at 24 hours was calculated as a percentage of the original spheroid size at 3 hours of attachment.

2.2.7 Spheroid disaggregation assay

Primary EOC cells were transduced as described above with either virus (Ad-GFP or Ad-ALK3^{QD}) and 24 hours later plated to ULA cultureware to form spheroids. Spheroids that had formed for 3 days were then exposed to 0.25% trypsin-EDTA for specified periods of time (*i.e.*, 2-30mins) at which point the trypsin was inactivated with a small volume of FBS and single cells were counted in a hemacytometer. All treatments were performed in triplicate and two hemacytometer counts were performed per replicate.

2.2.8 Flow cytometry

Primary EOC cells were transduced with Ad-GFP or Ad-ALK3^{QD} and 24 hours later plated to ULA culture ware to form spheroids or to standard tissue culture plastic for adherent culture. After three days in culture, adherent cells and spheroids were detached and disaggregated, respectively, using 0.25% trypsin-EDTA. Cells were rinsed with PBS and fixed for 5 minutes using 10% neutral-buffered formalin. Cells were then rinsed with PBS/1% BSA and incubated with primary anti-E-cadherin antibody (#3195; Cell Signalling) for 1 hour, rinsed in PBS/1% BSA, and incubated with AlexaFluor 488-conjugated anti-rabbit secondary antibody (#4412; Cell Signalling). The proportion of E-cadherin-positive cells was determined using a Beckman Coulter Epics XL-MCL flow cytometer with at least 10,000 events counted per test. Four independent patient samples were tested in triplicate and included cells-only and secondary antibody-only controls for each.

2.2.9 BrdU cytochemistry

Spheroids formed over a 3 day period were allowed to re-attach and disperse on glass coverslips for 24 hours at which point they were pulse labelled overnight with 10μM bromodeoxyuridine (BrdU; GE Healthcare, Buckinghamshire, UK). Spheroids on coverslips were then fixed in a buffered 10% formalin solution, washed with PBS, and permeabilized with 0.1% TritonX-100 in PBS. This was followed by sequential washes and incubations in 2N HCl/0.5% TritonX-100 for DNA denaturation, 0.1M NaB_4O_4 pH 8.5 for neutralization, mouse anti-BrdU primary antibody (1:100; Becton Dickinson), anti-Mouse FITC-conjugated secondary antibody (1:100; Vector Laboratories), and 4',6-diamidino-2-phenylindole (DAPI; 1:5000; Sigma). Stained coverslips were washed in PBS, inverted and mounted on glass slides with VectaShield mounting medium (Vector Laboratories). Fluorescence images were captured using an Olympus AX70 upright microscope and ImagePro image capture software.

2.2.10 Western blotting

Total cellular protein was isolated from adherent and non-adherent EOC cells. Cells were washed once briefly in ice-cold PBS, dissolved in lysis buffer [50 mM HEPES

pH7.4, 150 mM NaCl, 10% glycerol, 1.5 mM $MgCl_2$, 1 mM EGTA, 1 mM sodium orthovanadate, 10 mM sodium pyrophosphate, 10 mM NaF, 1% Triton X-100, 1% sodium deoxycholate, 0.1% SDS, 1 mM PMSF, 1X protease inhibitor cocktail (Roche, Laval, Quebec, Canada)], clarified by centrifugation (20 min at 15,000 x *g*), and quantified by Bradford analysis (Bio-Rad Laboratories, Mississauga, Ontario, Canada). Thirty to fifty micrograms of protein extract per lane were separated by SDS-PAGE in the presence of 1% β-mercaptoethanol using 8% or 12% gels. Proteins were then transferred to a polyvinylidene difluoride membrane (PVDF; Roche, Laval, Quebec, Canada), blocked with 5% skim milk in Tris-buffered saline with Tween-20 [TBST; 10 mM Tris.HCl, pH 8.0, 150 mM NaCl, 0.1% Tween-20]. Membranes were washed in TBST and incubated (overnight, 4°C) with appropriate antibodies (1:1000 in 5% skim milk/TBST or 5% BSA/TBST). Immunoreactive bands were visualized by incubating (1h, room temperature) with a peroxidase-conjugated anti-rabbit (1:10,000 in 1% skim milk/TBST; GE Healthcare) followed by exposure to enhanced chemiluminescence reagent (ECL Plus; GE Healthcare).

2.2.11 Antibodies and other reagents

Antibodies against phospho-Smad1/5/8 (#9511), phospho-Smad2 (#3108), phospho-Smad3 (#9520), total Smad1 (#9743), total Smad2 (#3122), total Smad3 (#9528), Smurf1 (#2174), and E-cadherin (#3195) were purchased from Cell Signaling Technologies (Danvers, MA). HA-probe (Y-11; sc-805) and Smad4 (H-552; sc-7154) antibodies were purchased from Santa Cruz Biotechnology (Santa Cruz, CA). The antibody against ID1 was purchased from Biocheck (Foster City, CA). Antibody to detect phosphorylated AKT (Ser473) was purchased from Cell Signaling Technology (#9271; Danvers, MA), and for total AKT1/2/3 from Santa Cruz Biotechnology (H-136 sc-8312; Santa Cruz, CA). Anti-actin antibody (A 2066) was purchased from Sigma (Mississauga, ON).

Recombinant human Noggin (Fc-NG; 6057-NG) was purchased from R&D systems (Minneapolis, MN) and used at 50 or 100 ng/mL, as indicated. The BMP type I receptor inhibitor LDN-193189 was purchased from Stemgent (San Diego, CA) and prepared in DMSO: chloroform (3:1) according to manufacturer's instructions, and used at a concentration of 10 or 100 nM, as indicated. Akt inhibitor VIII (Akti-1/2) was purchased

from EMD/Calbiochem (Merck, Darmstadt, Germany), prepared in DMSO according to manufacturer's instructions, and used at a concentration of 5 mM. The PI3K inhibitor LY294002 was purchased from (Cell Signaling)) and used at a concentration of 50 mM. Mammalian target of rapamycin inhibitors were used at a concentration of 20 nM for rapamycin (Sigma) and 500 nM for temsirolimus (Torisel®; Pfizer).

2.2.12 Statistical analysis

Statistical analysis was performed using GraphPad Prism® software. Data were expressed as mean ± SEM. Statistical analysis was performed using two-tailed Student's *t*-tests or one-way ANOVA and Tukey's *post-hoc* test with significances set at $*p < 0.05$, $** p < 0.01$ and $*** p < 0.001$ as indicated.

2.3 Results

2.3.1 Reduced BMP signalling activity in primary human EOC spheroids

We have previously reported that primary human EOC cells possess an intact BMP signalling pathway [11,12,17]. To determine whether the critical BMP signalling components are present in EOC spheroids we prepared protein extracts from several independent primary human EOC cells that were grown as suspension cultures for three days. We have selected this time point because primary EOC cells will autonomously form multi-cellular aggregates or spheroids with morphological characteristics mimicking those observed directly in patient ascites within this time frame. Western blotting using protein lysates isolated from EOC spheroids and matched adherent cultures demonstrated expression of phosphorylated Smad1/5/8 levels. Interestingly, total Smad1/5 protein was significantly increased in all primary EOC spheroids as compared with their adherent cell counterparts (Figure 2.1A). Thus, when BMP-activated R-Smad levels are normalized to total Smad1/5 protein, endogenous BMP signalling activity is in effect decreased by >50% upon spheroid formation.

To follow this observation, we performed quantitative RT-PCR on RNA isolated from primary EOC adherent cells and spheroids and directly measured the expression of

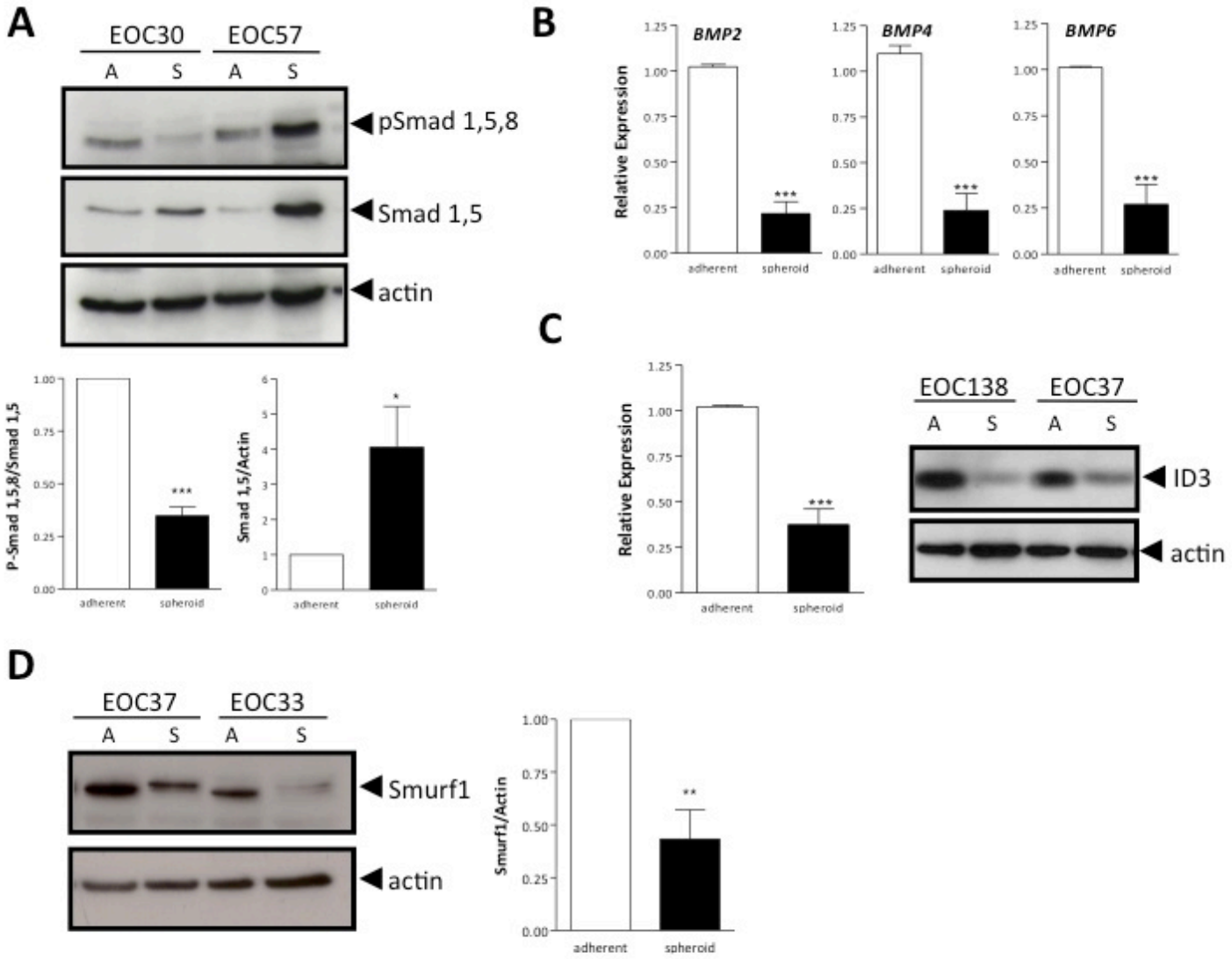

Figure 2.1: BMP signalling is decreased during EOC spheroid formation.
(A) Western blot analysis of phosphorylated and total Smad1/5/8 in adherent [A] and spheroid [S] samples in two independent EOC patient samples. Densitometric quantification of phosphorylated and total Smad1/5/8 (n=8) levels from Western blots. (B) Quantitative RT-PCR analysis of *BMP2*, *BMP4*, *BMP6* and *ID3* mRNA in adherent and spheroid samples in four independent EOC patient samples. (C, D) Western blot and densitometric quantification of ID3 and SMURF1 levels respectively in spheroids compared to adherent EOC cells (n=6). **p*<0.05; ***p*<0.01;****p*<0.001 as determined by Student's *t*-test.

ligands BMP 2, 4 and 6, known to be present in EOC cells [7,9,17]. The mRNA levels of all three of these BMP ligands were significantly reduced in EOC spheroids compared with matched adherent cells (Figure 2.1B). Quantitative RT-PCR analysis of BMP7, however, did not yield a consistently detectable product in all samples analyzed (data not shown). In addition, the expression of the BMP signalling target gene *ID3* [12,17] was significantly reduced in EOC spheroids (Figure 2.1C). To address the potential mechanism by which EOC spheroids exhibit increased Smad1/5 protein, we assessed the expression level of the E3 ubiquitin-protein ligase SMURF1. SMURF1 is a Smad1/5-specific ubiquitin ligase and functions to target the degradation of R-Smad1/5/8 as a form of negative feedback regulation [18,19]. Indeed, SMURF1 protein levels were significantly decreased in EOC spheroids as compared to adherent cells from multiple patient samples (Figure 2.1D), which could account for the observed increase in total Smad1/5 in EOC spheroids.

To determine whether this phenomenon of downregulated signalling could be applied broadly to the TGFβ superfamily, we also assessed the levels of the related R-Smad2/3. Phosphorylated Smad2 and Smad3 were detectable in both adherent EOC cells and spheroids, but there was no statistically significant difference in expression between culture conditions (Figure 2.2). Additionally, levels of the common-mediator Smad4 were not significantly altered in EOC spheroids (data not shown). Thus, it appears that differential R-Smad expression and activity in three-dimensional EOC spheroids is specific to the BMP pathway, with the net result being a downregulation of its endogenous signalling capacity in EOC spheroids.

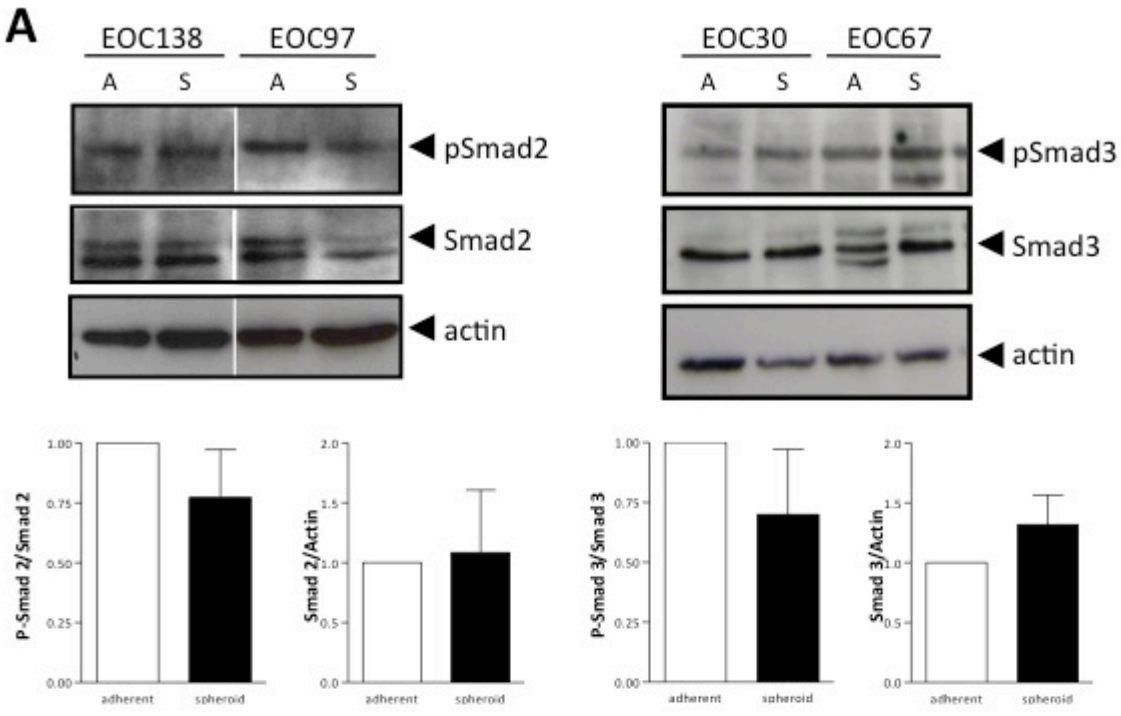

Figure 2.2: TGF-β signalling is not altered during EOC spheroid formation.
(A) Western blot and densitometric analysis of Smad2 and Smad3 levels in adherent [A] and spheroid [S] EOC cells (n=4).

2.3.2 Forced BMP activity in EOC spheroids alters cell adhesion

Given that endogenous BMP signalling activity was decreased in EOC spheroids, we postulated that this change was important for the optimal formation of spheroids. To examine this further, we tested the effect of ectopic re-activation of BMP signalling within these structures. To accomplish this, we transduced primary human EOC cells grown as adherent monolayer with adenovirus constructs expressing an HA-tagged constitutively-active mutant of the BMP type I receptor ALK3 (Ad-ALK3^{QD}), or control virus expressing green fluorescent protein (Ad-GFP). We chose this method to sustain BMP signalling during spheroid formation and reattachment experiments to ensure cell autonomous BMP signalling without the limitation of BMP ligand access to all cells within the three-dimensional multicellular aggregate during the time course of the experiment. Transducing cells as adherent cultures ensured homogeneous and efficient transduction and resultant expression of ALK3^{QD} (Figure 2.3A); direct transduction of established spheroids yielded uptake of virus into surface cells only, as visualized by Ad-GFP (data not shown). To confirm that ALK3^{QD} expression resulted in activation of BMP signalling in transduced EOC cells, western immunoblotting was performed to detect downstream targets of the pathway. As predicted, forced ALK3^{QD} expression resulted in increased phosphorylated Smad1/5/8 and ID1 protein levels as compared with EOC cells transduced with Ad-GFP (Figure 2.3B).

Since endogenous BMP signalling is naturally reduced in EOC spheroids, we hypothesized that sustained BMP signalling activity via ALK3^{QD} would abrogate their formation and resultant morphological phenotype. Indeed, primary human EOC cells expressing ALK3^{QD} generates EOC spheroids that are much smaller in size as compared with Ad-GFP transduced control spheroids (Figure 2.3C&D). This result is consistent with previous results using OVCA429 cells expressing ALK3^{QD} [11].

In addition, we noted that ALK3^{QD}-expressing spheroids consist of cells that are much more loosely-aggregated than the compact spheroids observed from control cells (Figure 2.3C). To verify that this phenotype is not just due to decreased cell viability from overexpression of ALK3^{QD}, we performed viable cell counting of Trypan blue-excluding cells over 72 hours of spheroid formation. ALK3^{QD} signalling had no effect on

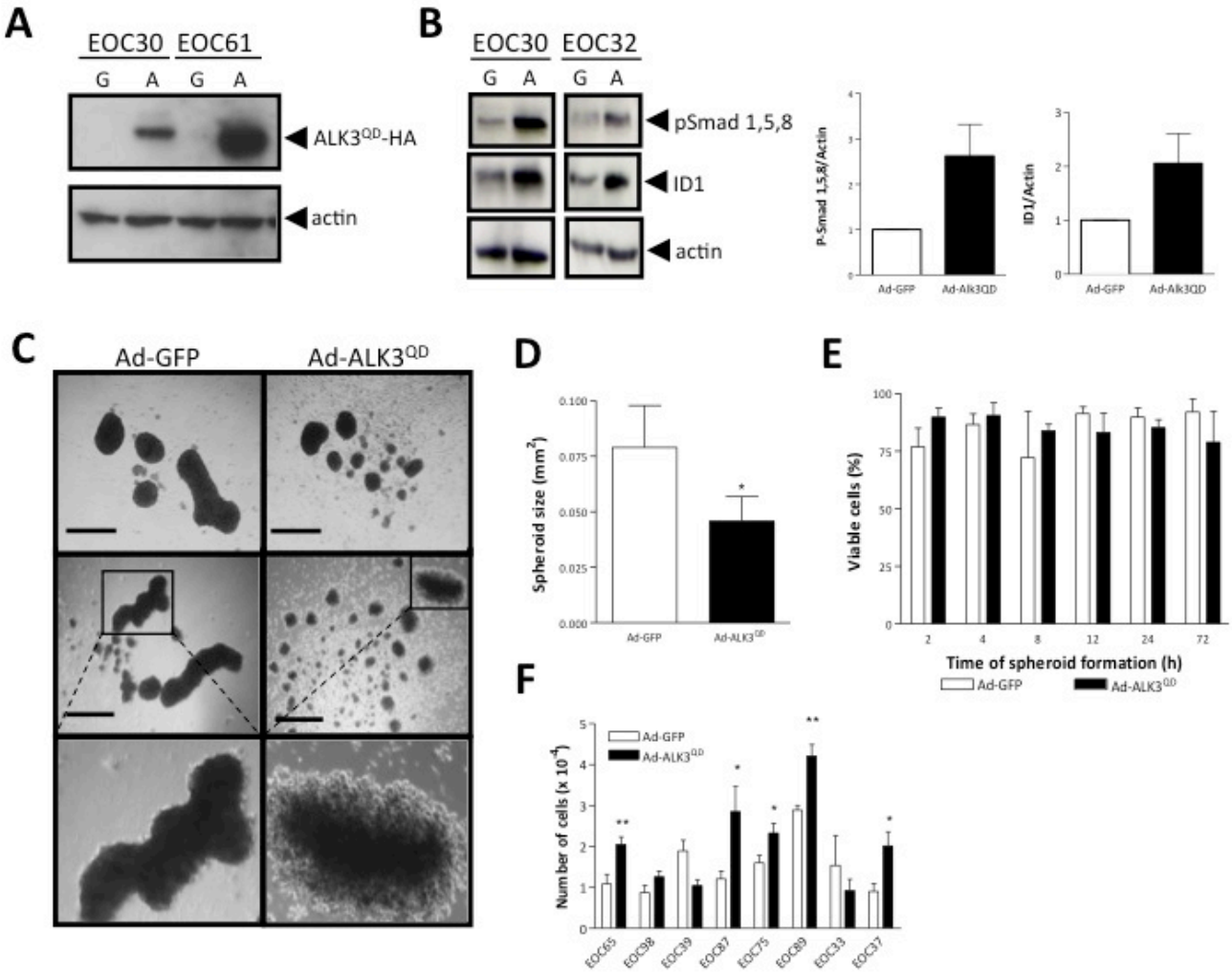

Figure 2.3: Activated BMP signalling results in smaller EOC spheroids that are more loosely aggregated.

(A) ALK3^{QD} expression was achieved by adenoviral transduction of primary EOC cells using Ad-ALK3^{QD} [A] and compared to Ad-GFP [G] control vector. (B) ALK3^{QD} expression results in activation of BMP signalling pathway as confirmed by increased phosphorylated Smad1/5/8 and ID1 protein levels 24 hours following transduction. (C) ALK3^{QD} dramatically reduces the ability of primary EOC cells to form large multicellular spheroids as compared with Ad-GFP transduced controls. Scale bar = 200 μm. (D) ALK3^{QD} reduces the size of EOC spheroids as quantified using *ImageJ* software and averaged among seven experiments using independent patient samples. (E) ALK3^{QD} expression in EOC cells has no effect on cell viability within the first 72 hours of seeding to non-adherent culture as determined by Trypan blue exclusion. (F) ALK3^{QD}-expressing primary EOC spheroids (5 out of 8 individual patient samples) are more readily disaggregated compared to Ad-GFP controls, as determined by single-cell counting after a 2-minute trypsinization. *p<0.05; **p<0.01 as determined by Student's t-test.

EOC cell viability in suspension culture, indicating that enhanced anoikis is not triggered by elevated BMP signalling during spheroid formation (Figure 2.2E). To assay cell cohesion directly, spheroid disaggregation experiments were performed on several patient samples (n=8) expressing $ALK3^{QD}$, or Ad-GFP controls. Timed exposure to trypsin followed by quantification of single cells demonstrated that activated BMP signalling caused decreased cell cohesion of spheroids in 5 of 8 independent primary EOC samples (Figure 2.3F).

Activated BMP signalling in adherent EOC cells induces epithelial-mesenchymal transition (EMT), a hallmark of which is the downregulation of E-cadherin [11,13]. Since E-cadherin may be involved in mediating cell-cell interactions in 3D spheroids [2,20], we sought to determine if $ALK3^{QD}$ was downregulating E-cadherin expression via inducing EMT in EOC spheroids, thereby resulting in decreased cell cohesion. Using real-time quantitative RT-PCR analysis of several EMT markers, we observed that EOC cells naturally undergo an EMT response during spheroid formation with an upregulation of Snail, Slug, ZEB2, Twist1 and Twist2 transcriptional repressors and concomitant downregulation of E-cadherin (*CDH1*) expression (Figure 2.4A). In contrast, we observed that spheroid cells expressing $ALK3^{QD}$ possess increased E-cadherin mRNA expression compared with control cells, and this correlated with an increase in the proportion of cells that were E-cadherin positive as determined by flow cytometry (Figure 2.4B). Therefore, constitutively active BMP signalling appeared to counteract the natural dynamics of transitions between epithelial and mesenchymal cell phenotypes in EOC spheroids.

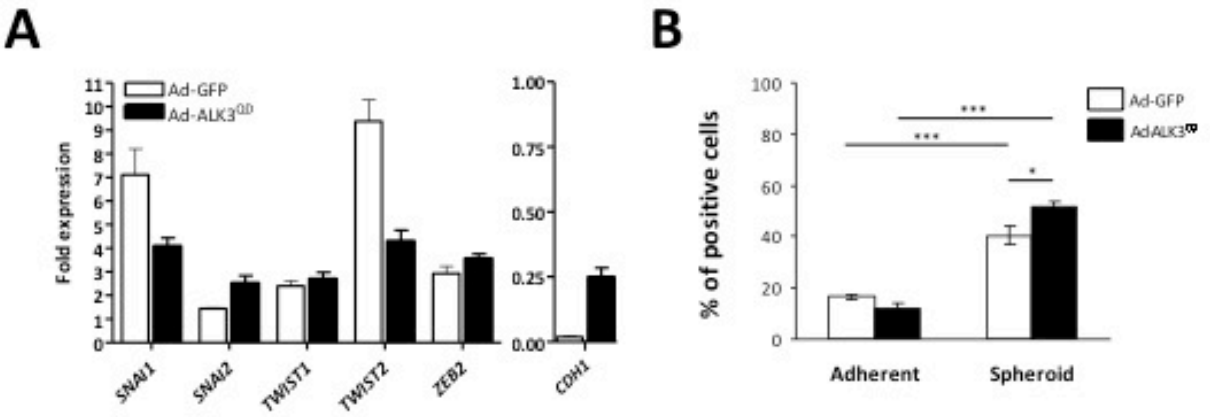

Figure 2.4: EMT is induced during EOC spheroid formation.
(A) EMT is induced in EOC spheroids, both in the absence or presence of activated ALK3^{QD} signalling, as determined by real-time quantitative RT-PCR of E-cadherin (*CDH1*), Snail (*SNAI1*), Slug (*SNAI2*), *TWIST1*, *TWIST2* and *ZEB2*. Fold expression was quantified against adherent cultures (set to 1) using pooled data from 5 independent patient samples performed in duplicate; *GAPDH* served as an internal control. (B) Flow cytometry for E-cadherin protein expression across 5 independent patient samples in the presence or absence of Alk3^{QD} signalling. *p<0.05; ***p<0.001 as determined by Student's *t*-test.

The capacity of EOC spheroids for reattachment, growth and motility defines their ability to form secondary metastases[2]. Since activated BMP signalling consistently reduces cell-cell cohesion within EOC spheroids, we next sought to determine whether activated BMP signalling affects the ability of EOC spheroid cells to reattach and migrate. $ALK3^{QD}$-expressing EOC spheroids and GFP controls were plated for reattachment using standard tissue culture-treated plastic by directly transferring spheroids into new dishes with fresh growth medium. We observed an increased cell dispersion area and number of motile cells emanating from $ALK3^{QD}$-expressing EOC spheroids within the first 24 hours of replating, as compared with controls (Figure 2.5A&B). This was not due to cell proliferation since there was no significant difference in BrdU-incorporated cytochemistry in dispersing cells of $ALK3^{QD}$-expressing spheroids compared to GFP controls (data not shown). This observed effect on EOC cell motility upon spheroid reattachment was consistent with our previous results of increased motility in adherent primary human EOC cells using recombinant human BMP4 and $ALK3^{QD}$ expression in conventional scratch wound assays [11,13].

2.3.3 Inhibition of endogenous BMP signalling affects EOC spheroid adhesion

Given the enhanced effect of activated BMP signalling during EOC spheroid reattachment, we wanted to determine if the reduction in endogenous BMP signalling, which was observed during EOC spheroid formation, would be restored during reattachment. Indeed, there is a significant increase in the levels of phosphorylated Smad1/5/8 when normalized to total protein levels in a number of different EOC patient samples (Figure 2.5C). These results indicate that the activity of the BMP signalling pathway is restored during EOC spheroid reattachment.

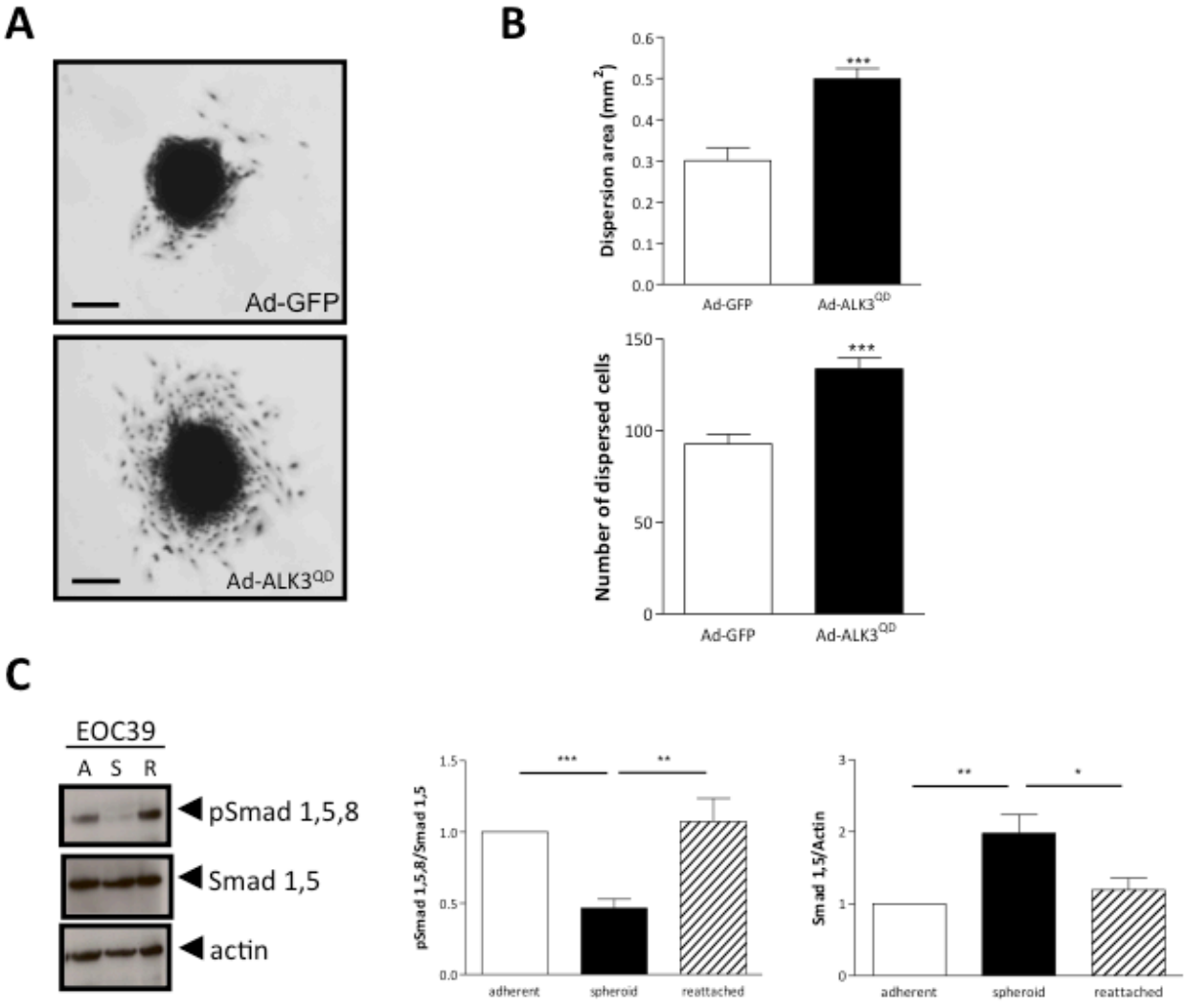

Figure 2.5: Alk3^{QD} expression enhances the movement of EOC cells from spheroids after reattachment.

(A) ALK3^{QD} enhances the ability of EOC spheroids to migrate from the spheroid. (B) ALK3^{QD} increases the dispersion area generated by reattached EOC spheroids as quantified using *ImageJ* software and averaged among six experiments using independent patient samples. Dispersion area was calculated 24 hours after spheroids have been replated to standard tissue culture plastic and normalized to the size of original spheroid. ALK3^{QD} increases the number of dispersed cells 24 hours following spheroid reattachment as determined by counting DAPI-stained nuclei. (C) Western blot and densitometric analysis of phosphorylated and total Smad1/5/8 in adherent, spheroid and reattached EOC spheroid cells (n=7). (*p<0.05;** p<0.001;***p<0.001 as determined by Student's t-test). Scale Bar: 200μm.

Given our results in EOC spheroids thus far, we postulated that blocking endogenous BMP activity may further facilitate spheroid formation yet decrease subsequent reattachment and dispersion. Primary human EOC cells express several BMP ligands, chiefly BMP2, BMP4 and BMP6 (Figure 2.1B) and their ability to promote signalling in EOC cells can be efficiently blocked using natural antagonists such as Noggin (NG) and Chordin [9,13]. Additionally, LDN-193189 is a small molecule that selectively inhibits BMP type I receptors and can be used to block this pathway [21,22]. Treatment of EOC cells with a single bolus of 50 ng/mL Fc-NG or with a range of concentrations of LDN-193189 resulted in a rapid and sustained reduction in phosphorylated BMP R-Smad1/5/8 over 72 hours (Figure 2.6A). Primary EOC cells were seeded to Ultra-Low Attachment dishes and treatment with Fc-NG (50 ng/mL) or LDN-193189 (10 nM and 100 nM) was initiated immediately. From this, we observed a statistically significant increase in the average size of EOC spheroids as compared with control cultures (Figure 2.6B&C). In addition to this, when EOC spheroids were treated with either Fc-NG or LDN-193189 upon reattachment, dispersion areas were significantly reduced. A reduction in the number of dispersing cells was observed at 100 nM of LDN-193189, but no difference in the number of cells arising from the attached spheroids by treatment with Fc-NG. Taken together, these results suggest a functional requirement for differential regulation of EOC spheroid formation and subsequent motility of EOC cells upon spheroid reattachment by BMP signalling.

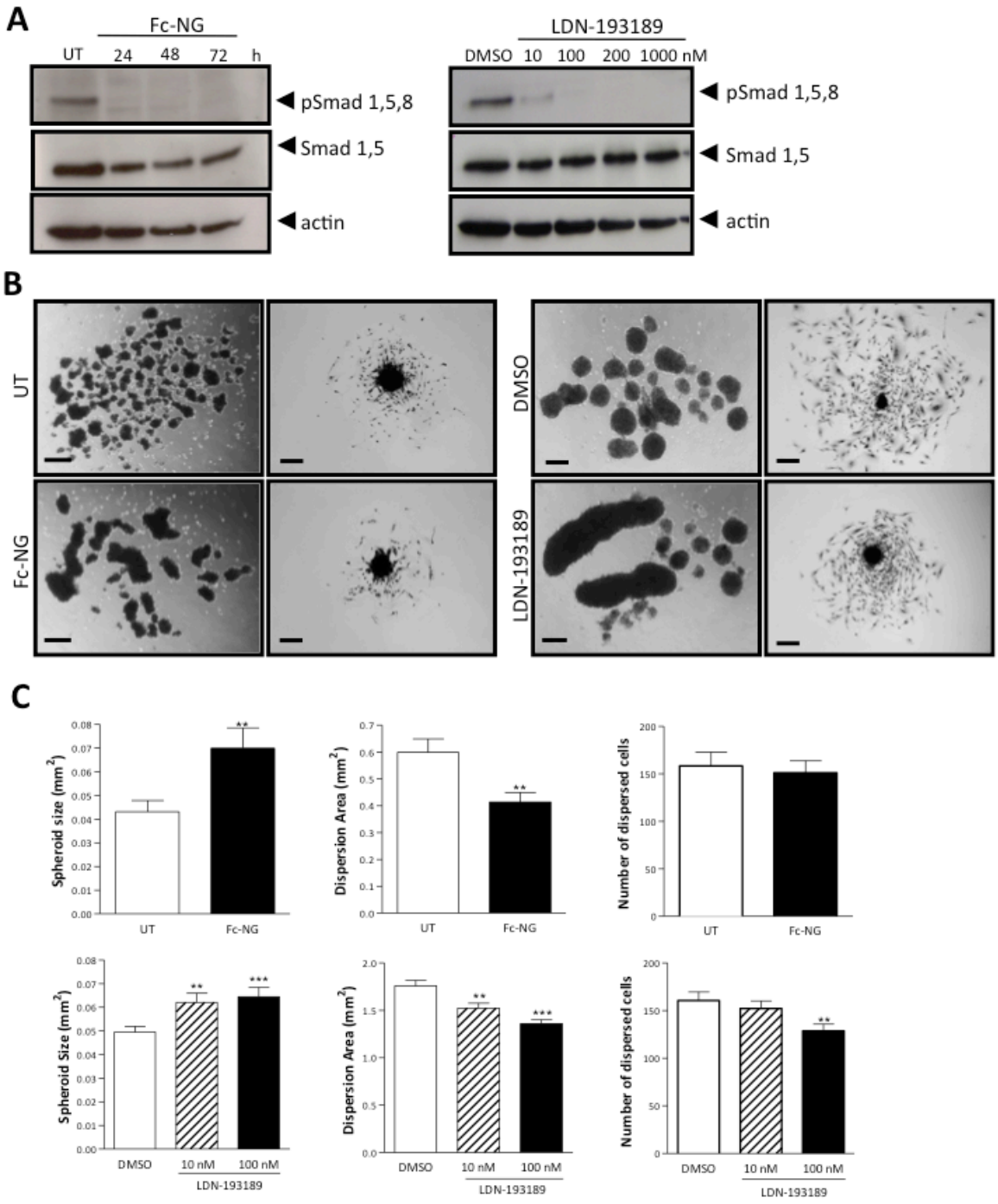

Figure 2.6: Inhibition of BMP signalling enhances EOC spheroid formation and decreases reattachment.

(A) Treatment of primary EOC cells with extracellular antagonist of BMP signalling Fc-Noggin (Fc-NG, 50 ng/mL) and small molecule inhibitor LDN-193189 results in potent inhibition of BMP signalling as visualized by Western blot analysis of pSmad1/5/8. (B) Treatment with Fc-NG (50 ng/mL) or LDN-193189 (100 nM) increases the ability of EOC cells to form large multicellular spheroids and a subsequent decreased ability to disperse on tissue culture plastic. Scale bar=50 μm. (C) Quantification of spheroid size and dispersion area following treatment with Fc-NG or LDN-193189 using *ImageJ* software (n=3; n=7 respectively). (**p<0.01; ***p<0.001 using Student's t-test).

2.3.4 BMP signalling activates the AKT pathway in EOC cells & spheroids

The phenotypic changes in EOC spheroid adhesion and motility due to $ALK3^{QD}$ signalling likely result from a combination of both direct and indirect alterations in expression of many genes and their products. Activation of BMP signalling leads to the regulation of target gene expression primarily via Smad-dependent mechanisms. Several genes are direct targets of BMP signalling in EOC cells, including genes encoding the inhibitory Smad6/7 and the helix-loop-helix negative regulatory transcription factors ID1 and ID3[12,17]. Thus, to uncover many potential targets on a genome-wide scale, we performed an expression microarray using Ad-$ALK3^{QD}$- and Ad-GFP-transduced cells of five independent EOC patient samples, and compared mRNA expression between adherent and spheroid cultures as well. We selected primary human EOC cells from patients with high-grade serous adenocarcinoma since they represent the most common histologic subtype of EOC and also to minimize potential experimental variability among patient samples. Using Affymetrix® Human U133A 2.0 plus arrays, we uncovered a plethora of altered gene expression characteristics which were consistent among all five patient samples ($p<0.05$): 444 annotated genes were elevated in expression due to $ALK3^{QD}$ in EOC spheroids compared to GFP controls, and 314 annotated genes were reduced (Table S2.1). The subset of genes that were commonly-regulated by $ALK3^{QD}$ in both adherent EOC cells and spheroids, comprising 96 up-regulated and 45 down-regulated genes (Tables 2.1 & 2.2 and Figure 2.7A) were used to focus our analysis. Some known BMP target genes were identified in this subset, namely the transcription factors *SMAD6* and *SMAD7*, *MSX2*, *DLX2*, and *JUND*. In addition, the BMP signalling antagonists *NOG* (Noggin) and *GREM2* (Gremlin 2) were also increased due to $ALK3^{QD}$ signalling in both adherent cells and spheroids. We have since validated the expression of several of these genes, with *SMAD6*, *NOG*, *MSX2*, *HEY1 and TBX3* demonstrating reproducible upregulation by $ALK3^{QD}$ signalling as determined by qRT-PCR (Figure S2.1).

Table 2.1: Up-regulated genes in response to Alk3QD expression and common between adherent and spheroid EOC cells.

Gene Name	Gene Description	Probe Set	Adherent Fold Change	Spheroid Fold Change
BMP signalling & target genes				
*DLX2**	distal-less homeobox 2	207147_at	8.543	20.206
*SMAD6**	SMAD family member 6	207069_s_at	5.782	10.538
SMAD7	SMAD family member 7	204790_at	2.078	2.813
GREM2	gremlin 2	235504_at	5.071	2.982
		240509_s_at	4.665	2.535
*NOG**	noggin	231798_at	3.683	10.343
*MSX2**	msh homeobox 2	210319_x_at	2.581	4.527
		205555_s_at	2.118	4.689
JUND	jun D proto-oncogene	203751_x_at	2.146	2.291
ECM & cell adhesion				
GJD3	gap junction protein, delta 3, 31.9kDa	230025_at	7.533	10.917
HAS2	hyaluronan synthase 2	206432_at	4.122	2.696
CD24	CD24 molecule	209772_s_at	4.078	39.195
		208650_s_at	3.376	24.444
		266_s_at	2.927	37.327
		208651_x_at	2.861	21.376
LRRC4	leucine rich repeat containing 4	223552_at	4.043	6.963
PCDH10	protocadherin 10	1552925_at	3.641	2.624
CD300LG	CD300 molecule-like family member g	1552509_a_at	3.316	6.675
SSX2IP	synovial sarcoma, X breakpoint 2 interacting protein	203018_s_at	2.858	3.122
		210871_x_at	2.788	3.153
		203016_s_at	2.759	3.056
		203015_s_at	2.675	3.625
		203019_x_at	2.655	3.195
		203017_s_at	2.19	2.175
FBLN2	fibulin 2	203886_s_at	2.542	2.905
CDH24	cadherin-like 24	1553166_at	2.321	2.181
CNTNAP2	contactin associated protein-like 2	219301_s_at	2.309	25.559
Ligands				
TNFSF9	tumor necrosis factor, member 9	206907_at	4.802	8.53
CCL26	chemokine (C-C motif) ligand 26	223710_at	4.725	11.408
CCK	cholecystokinin	205827_at	7.97	3.831
JAG1	jagged 1	231183_s_at	3.146	2.306
		209098_s_at	2.639	2.546
PGF	placental growth factor	209652_s_at	2.84	3.963
INSL3	insulin-like 3	1553594_a_at	2.472	2.875
Receptors & membrane proteins				
FOLR3	folate receptor 3	206371_at	6.787	12.253
SYT15	synaptotagmin XV	1560879_a_at	6.497	6.516
		1560878_at	3.835	2.825
FIBCD1	fibrinogen C domain containing 1	240042_at	4.27	4.389

Table 2.1 cont'd

SEMA7A	semaphorin 7A	230345_at	4.226	2.382
TMEM132E	transmembrane protein 132E	243708_at	4.196	3.56
MALL	mal, T-cell differentiation protein-like	209373_at	3.705	4.481
SLC25A15	solute carrier family 25, member 15	222705_s_at	3.524	2.879
KCNQ5	potassium voltage-gated channel, member 5	244623_at	3.489	6.034
STRA6	stimulated by retinoic acid gene 6	221701_s_at	3.465	3.08
PLXNA2	plexin A2	213030_s_at	2.758	4.575
		227032_at	2.413	2.938
PAQR9	progestin and adipoQ receptor family member IX	1558322_a_at	2.7	2.681
LIN7B	lin-7 homolog B	241957_x_at	2.583	4.773
FZD8	frizzled homolog 8	227405_s_at	2.513	3.713
PITPNM2	phosphatidylinositol transfer protein, membrane-associated 2	1552924_a_at	2.476	2.579
TRPC3	transient receptor potential cation channel, subfamily C, member 3	210814_at	2.223	4.341
TRPV2	transient receptor potential cation channel, subfamily V, member 2	219282_s_at	2.1	2.149
FGFR3	fibroblast growth factor receptor 3	204379_s_at	2.184	2.227
Intracellular signalling proteins				
DUSP5P	dual specificity phosphatase 5	1553299_at	2.305	3.296
DUSP26	dual specificity phosphatase 26	219144_at	4.234	2.56
SPRY2	sprouty homolog 2	204011_at	2.598	2.061
SOCS2	suppressor of cytokine signaling 2	203372_s_at	2.473	6.416
		203373_at	2.065	4.938
SHC4	SHC family, member 4	230538_at	2.132	2.765
NCLN	nicalin	222206_s_at	2.007	2.055
Structural proteins				
LOR	loricrin	207720_at	63.124	49.49
IVL	involucrin	214599_at	4.612	14.951
KRTAP2-4	keratin associated protein 2-4	1555673_at	4.146	3.112
KIF7	kinesin family member 7	229405_at	4.102	2.224
EML1	echinoderm microtubule associated protein like 1	204797_s_at	3.853	2.712
ACTC1	actin, alpha, cardiac muscle 1	205132_at	3.766	40.174
DCDC5	doublecortin domain containing 5	232603_at	3.346	4.783
TUBB2A /// TUBB2B	tubulin, beta 2A /// tubulin, beta 2B	209372_x_at	2.684	2.546
TPM1	tropomyosin 1	206117_at	2.454	3.223
SPTBN1	spectrin, beta, non-erythrocytic 1	226342_at	2.437	2.422
TLN2	talin 2	212701_at	2.239	3.438
MAP1B	microtubule-associated protein 1B	212233_at	2.193	3.056
Transcription factors				
FEZF2	FEZ family zinc finger 2	233972_s_at	5.611	16.35
MYB	v-myb myeloblastosis viral oncogene	204798_at	3.721	3.094
ATOH8	atonal homolog 8	1558706_a_at	3.716	4.353
		228890_at	2.873	4.266
KLF4	Kruppel-like factor 4	220266_s_at	3.638	3.033
		221841_s_at	2.701	2.962
LMO2	LIM domain only 2	204249_s_at	3.592	4.971
AFF2	AF4/FMR2 family, member 2	206105_at	3.356	3.267

Table 2.1 cont'd

*TBX3**	T-box 3	225544_at	2.737	2.183
		229576_s_at	2.707	2.416
GATA2	GATA binding protein 2	209710_at	2.422	2.501
GATA3	GATA binding protein 3	209604_s_at	2.123	2.301
*HEY1**	hairy/enhancer-of-split related with YRPW motif 1	44783_s_at	2.053	3.736
		218839_at	2.047	3.216
PRRX2	paired related homeobox 2	219729_at	2.037	4.659
Other				
AKR1C1	aldo-keto reductase family 1, member C1	204151_x_at	4.2	4.254
		216594_x_at	3.321	3.725
AKR1C2	aldo-keto reductase family 1, member C2	211653_x_at	5.339	4.759
		209699_x_at	3.62	3.771
CCDC68	coiled-coil domain containing 68	220180_at	2.022	2.067
CCDC85A	coiled-coil domain containing 85A	235228_at	3.596	5.131
TRNP1	TMF1-regulated nuclear protein 1	227862_at	3.268	4.095
CRYAB	crystallin, alpha B	209283_at	3.058	4.708
GPX3	glutathione peroxidase 3	214091_s_at	3.03	4.534
THAP2	THAP domain containing, apoptosis associated protein 2	230380_at	2.893	4.04
DNAJA4	DnaJ homolog, subfamily A, member 4	1554334_a_at	2.89	3.921
PEG10	paternally expressed 10	212092_at	2.875	2.108
RPA4	replication protein A4	221143_at	2.733	4.239
KANK4	KN motif and ankyrin repeat domains 4	229125_at	2.522	2.414
DCBLD2	discoidin, CUB and LCCL domain containing 2	213873_at	2.497	3.841
		213865_at	2.323	2.769
NHEDC2	Na+/H+ exchanger domain containing 2	1564746_at	2.438	3.347
		229491_at	2.358	4.648
ALAS2	aminolevulinate synthase 2	244205_at	2.355	2.621
HSPD1 /// HSPD1P4	heat shock 60kDa protein 1 /// pseudogene 4	243372_at	2.34	2.642
HSPA1A /// HSPA1B	heat shock 70kDa protein 1A /// 1B	200800_s_at	2.145	7.074
MEX3C	mex-3 homolog C	1556874_a_at	2.326	2.37
CASQ1	calsequestrin 1	219645_at	2.285	3.64
PSG6	pregnancy specific beta-1-glycoprotein 6	208106_x_at	2.195	2.017
YWHAH	tyrosine 3-monooxygenase/ tryptophan 5-monooxygenase activation protein, eta polypeptide	201020_at	2.188	2.704
ME2	malic enzyme 2	210154_at	2.068	2.187
HECW2	HECT, C2 and WW domain containing	232080_at	2.04	3.641
ATP13A3	ATPase type 13A3	219558_at	2.018	3.262

*- Expression was validated by real-time quantitative RT-PCR as described in Materials & Methods.

Table 2.2: Down-regulated genes in response to Alk3QD expression common between adherent and spheroid EOC cells.

Gene Name	Gene Description	Probe Sets	Adherent Fold Change	Spheroid Fold Change
ECM & cell adhesion				
CHI3L1	chitinase 3-like 1	209396_s_at	23.81	4.35
		209395_at	14.08	3.25
VCAM1	vascular cell adhesion molecule 1	203868_s_at	3.82	3.38
CCDC80	coiled-coil domain containing 80	225241_at	3	3.27
		225242_s_at	2.38	2.72
Ligands				
PDGFD	platelet derived growth factor D	219304_s_at	4.55	3.3
CXCL16	chemokine (C-X-C motif) ligand 16	223454_at	3.57	2.85
Receptors & membrane proteins				
PDPN	podoplanin	221898_at	5.88	3.64
		204879_at	3.46	2.72
KCNH2	potassium voltage-gated channel, subfamily H, member 2	210036_s_at	4.37	3.21
KCNJ12	potassium inwardly-rectifying channel, subfamily J, member 12	232289_at	2.51	2
		207110_at	2.5	2.01
VNN1	vanin 1	205844_at	3.48	3.72
PLSCR4	phospholipid scramblase 4	218901_at	3.17	2.43
EPHB3	EPH receptor B3	204600_at	2.91	5.95
PLSCR1	phospholipid scramblase 1	202430_s_at	2.81	2.1
PTGFRN	prostaglandin F2 receptor negative regulator	224937_at	2.66	2.43
TNFRSF21	tumor necrosis factor receptor superfamily,	218856_at	2.39	2.72
ITGB8	integrin, beta 8	226189_at	2.21	2.41
SORT1	sortilin 1	224818_at	2.17	2.57
PGRMC2	progesterone receptor membrane component 2	213227_at	2.04	2.32
Intracellular signalling proteins				
RAP1A	RAP1A, member of RAS oncogene family	1555340_x_at	1000	333.33
		1555339_at	333.33	333.33
PKIB	protein kinase inhibitor beta	231120_x_at	18.18	3.23
REPS2	RALBP1 associated Eps domain containing 2	227425_at	6.21	5.08
		205645_at	4.61	3.19
CASP10	caspase 10	205467_at	2.43	2.28
ELMO1	engulfment and cell motility 1	204513_s_at	2.22	2.15
ARHGEF3	Rho guanine nucleotide exchange factor 3	218501_at	2.19	2.01
Structural proteins				
PPL	periplakin	203407_at	15.15	4.42
MYO5B	myosin VB	225299_at	3.04	3.1
		225301_s_at	3.04	3.7
MBP	myelin basic protein	210136_at	2.97	2.51

Table 2.2 cont'd.

		1554544_a_at	2.56	3.15
MAP7	microtubule-associated protein 7	202890_at	2.5	2.39
Transcription factors				
NFE2L3	nuclear factor (erythroid-derived 2)-like 3	204702_s_at	3.06	2.19
KAT2B	lysine acetyltransferase 2B	203845_at	2.39	2.75
BNC1	basonuclin 1	1552487_a_at	2.1	2.2
Other				
LRIG3	leucine-rich repeats and immunoglobulin-like domains 3	226908_at	4.31	3.65
SLC46A3	solute carrier family 46, member 3	214719_at	3.77	2.22
ALDH6A1	aldehyde dehydrogenase 6 family, member A1	221589_s_at	3.68	2.86
ALDH6A1		221588_x_at	2.84	2.39
ALDH6A1		204290_s_at	2.51	2.31
CYP7B1	cytochrome P450, family 7, subfamily B, polypeptide 1	207386_at	3.64	2.67
CYP39A1	cytochrome P450, family 39, subfamily A, polypeptide 1	1553977_a_at	2.73	2.12
IFIT1	interferon-induced protein with tetratricopeptide repeats 1	203153_at	3.19	2.7
ERO1LB	ERO1-like beta	231944_at	2.69	2.06
FTH1	ferritin, heavy polypeptide 1	214211_at	2.59	2.16
FTH1				
FTH1				
CMBL	carboxymethylenebutenolidase	227522_at	2.46	2.74
AOX1	aldehyde oxidase 1	205083_at	2.28	6.25
SLC27A1	solute carrier family 27, member 1	226728_at	2.2	2.15
ZFYVE16	zinc finger, FYVE domain containing 16	1555982_at	2.14	2.14
B3GNT1	beta-1,3-N-acetylglucosaminyl-transferase 1	203188_at	2.07	2.92
PS1TP4	HBV preS1-transactivated protein 4	226381_at	2.06	2.04
FUCA1	fucosidase, alpha-L-1, tissue	202838_at	2.02	2.06

Uncovering potential novel mechanisms of disease hidden within a gene expression signature is more readily attainable when compared to the large number of published datasets available. One such useful resource is Connectivity Map (CMAP) that was established and made available by the Broad Institute and MIT (http://www.broadinstitute.org/cmap) [23-25]. CMAP facilitates the discovery of connections among human diseases, chiefly cancer, with gene expression changes and drug action. By uploading the up-regulated and down-regulated probe set lists (*i.e*. 96 up- and 45 down-regulated genes) from our microarray study to CMAP (Figure 2.7A), we identified that three of the top ten drugs are inhibitors targeting the phosphatidylinositol 3-kinase (PI3K)-mammalian target of rapamycin (mTOR) pathway (Figure 2.7B). The PI3K inhibitors LY294002 and wortmannin were ranked first and seventh respectively, and the mTOR inhibitor sirolimus, also known as rapamycin, was ranked second. Interestingly, the compiled data of these three drugs from CMAP had a strong negative correlation with our $ALK3^{QD}$ gene expression signature. Given that the $ALK3^{QD}$ gene expression dataset was negatively-correlated with those from all three of the PI3K-mTOR pathway inhibitors, we reasoned that activated BMP signalling induces the PI3K-mTOR pathway in primary EOC cells. To determine if this was the case, we performed western blotting to detect phosphorylated AKT levels as a direct readout of PI3K-mTOR pathway activity in EOC cells and spheroids expressing the constitutively-active BMP receptor. Indeed, $ALK3^{QD}$ expression significantly increased phospho-AKT in EOC cells (Figure 2.8C).

We and others have demonstrated that active PI3K-mTOR signalling is vital to promoting the metastatic potential of EOC cells and spheroids[26-29] [26-29]. Indeed, treatment of reattaching primary EOC spheroids with any of three different inhibitors of the PI3K-mTOR pathway, LY294002, rapamycin and temsirolimus (Torisel®), resulted in a significant reduction in cell dispersion (Figure S2.2). To address whether this pathway is required for the phenotypic changes imparted by active BMP signalling, we targeted its central mediator AKT directly and specifically using the AKT inhibitor, Akti-1/2. Reattaching EOC spheroids transduced with either Ad-$ALK3^{QD}$ or Ad-GFP were treated with 5 μM AKTi-1/2, or DMSO as a vehicle control. As early as 24 hours after treatment with Akti-1/2, the dispersion area of $ALK3^{QD}$ spheroids was reduced, although not

A

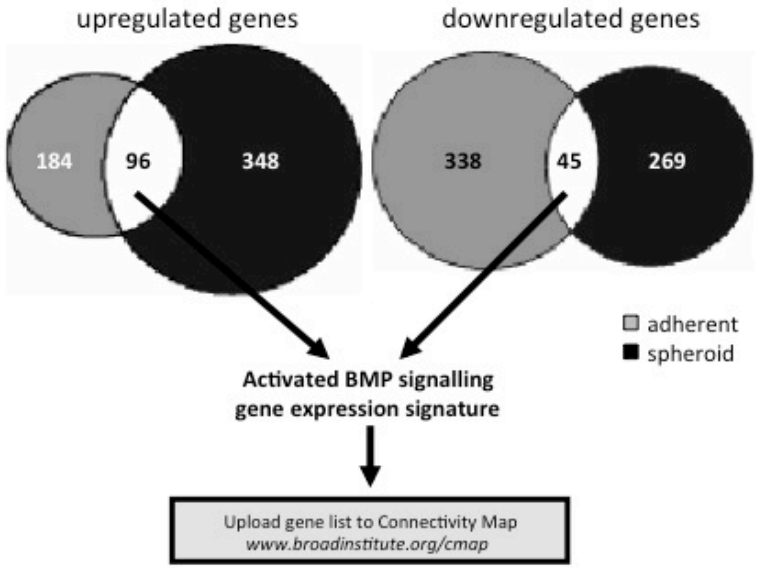

B

CMAP Rank	Drug Treatment	Mean Score	n	Enrichment	p	Specificity
1	LY-294002	-0.295	61	-0.474	0	0.0614
2	sirolimus	-0.327	44	-0.397	0	0.1986
3	monensin	-0.58	6	-0.877	0.00002	0
4	CP-690334-01	-0.43	8	-0.689	0.00024	0.0068
5	isotretinoin	-0.521	4	-0.842	0.00107	0.0079
6	cefadroxil	-0.454	4	-0.84	0.00117	0
7	wortmannin	-0.322	18	-0.425	0.00229	0.2038
8	bicuculline	0.506	4	0.782	0.00418	0.0074
9	tracazolate	0.521	4	0.775	0.00491	0.0168
10	glipizide	-0.448	5	-0.698	0.00545	0

Figure 2.7: The PI3K-AKT-mTOR pathway is activated by BMP signalling in EOC cells and spheroids.

(A) Venn diagrams (based on Genespring analysis of microarray data using Affymetrix Human U133 plus 2.0 arrays) representing a total of 96 genes which are increased and 45 genes which are decreased in expression in response to ALK3QD in both EOC cells and spheroids. The up-regulated and down-regulated probe set lists from the microarray study were uploaded to Connectivity Map (CMAP) which was established and made available by the Broad Institute and MIT (http://www.broadinstitute.org/cmap). (B) The top ten drugs with gene expression signatures correlating with the ALK3QD gene expression signatures. Inhibitors targeting the PI3K-AKT-mTOR pathway, specifically LY294002, sirolimus, and wortmannin, result in gene expression patterns exhibiting a negative correlation with the ALK3QD gene expression signature.

completely down to levels observed in Ad-GFP control spheroids (Figure 2.8D). This suggests that enhanced AKT activity is required, at least in part, for the enhanced reattachment and dispersion of EOC cells observed as a result of active BMP signalling.

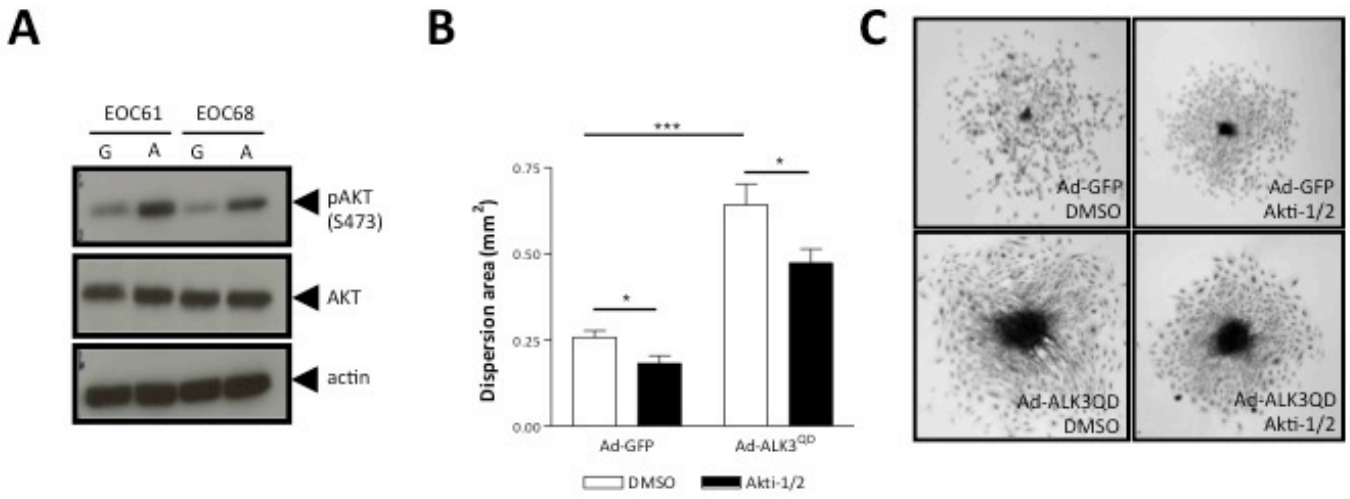

Figure 2.8: BMP-enhanced spheroid reattachment is partially mediated by AKT signalling.
(A) ALK3QD results in increased levels of phosphorylated AKT (at residue Ser473) in EOC cells. (B, C) Enhanced EOC spheroid dispersion due to ALK3QD is decreased by treatment with the AKT inhibitor, Akti-1/2 (5 mM).

2.4 Discussion

The multicellular spheroids found in EOC malignant ascites possess distinct biological properties due to their 3D architecture and downstream signalling afforded by the tumour sphere structure[2,30]. For example, the formation of EOC multi-cellular clusters provides protection against anoikis allowing these cancer cells to survive in ascites and seed metastatic tumours[31]. Therefore, identifying signalling pathways that contribute to the formation or disruption of EOC spheroids will provide new potential therapeutic targets that may also facilitate killing of solid tumour cells given their common 3D structure. We have shown previously that EOC cells express an intact and functional BMP signalling pathway, which directly impacts several key characteristics of a transformed cell phenotype[12,13]. Here we have exploited the *in vitro* EOC spheroid model system, to uncover novel actions of the BMP signalling pathway in EOC pathobiology (Figure 2.9). Interestingly, we have found that endogenous BMP signalling in EOC cells is down-regulated during spheroid formation. To determine whether this reduction in BMP signalling has functional implications for the formation of EOC spheroids we generated cells with constitutive activation of the pathway. Indeed, expression of the constitutively-active BMP type I receptor ALK3QD caused a decrease in EOC cell cohesion during spheroid formation. Additionally, enhanced BMP signalling activity subsequently resulted in increased motility of EOC cells dispersing from spheroids that attached to the culture dish. At the protein level we determined that activated BMP signalling resulted in activation of the AKT signalling pathway in human EOC cells. Therefore, the phenotypic changes induced by BMP signalling in EOC spheroids may, in part, be mediated by its effects on AKT signalling.

The process of forming multi-cellular aggregates in suspension, akin to what occurs in malignant ascites, results in the down-regulation of endogenous BMP signalling. The genes encoding several BMP ligands showed significantly reduced expression during spheroid formation when compared to proliferating adherent monolayer cells, which was directly correlated with reduced levels of phosphorylated BMP R-Smad protein, thus implying that autocrine activation of the pathway is reduced in spheroid EOC cells. The downregulation of BMP signalling in EOC spheroid cells could occur through several

mechanisms. Several extracellular antagonists exist for BMP signalling, including Noggin, Chordin and Gremlin and other related proteins [32]. Moreover, BMP signalling induces the transcriptional activation of target genes encoding inhibitory Smad proteins, Smad6 and Smad7. Smad6/7 function at several points in the pathway, namely to inhibit R-Smad phosphorylation, and Smad complex formation and its transcriptional activity[33-35]. This mechanism is likely not operational in EOC spheroid cells because Smad6/7 mRNA expression does not change in EOC spheroids, and Smad6 protein levels are not consistent among EOC cells and spheroids generated from patient samples (data not shown). We also demonstrate that increased turnover of R-Smads by SMURF1-mediated ubiquitinylation is not a likely mechanism, since SMURF1 levels are in fact decreased in expression in EOC spheroids. This indicates that turnover of Smads is reduced in spheroids leading to the subsequent accumulation of Smad1/5 as we observed. This increase in BMP R-Smad protein levels may represent a compensatory response to the decrease in endogenous BMP signalling during EOC cell spheroid formation. Consequently, the reduction in expression of the major BMP ligands expressed in EOC cells, *i.e*. BMP4, BMP2, and BMP6, likely represents the mechanism for downregulated BMP signalling in EOC spheroids. This is the first time that decreased endogenous BMP signalling has been observed during spheroid formation. This is in contrast to the data demonstrating that BMP signalling is elevated in primary EOC cells and in solid tumour samples compared to normal ovarian surface epithelial cells[7,12,17]. Thus, our results provide new insight about the dynamics of BMP signalling within EOC spheroids, which represent a unique transitional step for malignant cells between the primary tumour and secondary metastases[2].

The process of multicellular spheroid formation is complex and involves the coordinated action of different cell adhesion molecules. During the initial stages of spheroid formation, cell-cell adhesion is primarily mediated by the actions of integrins and cadherins[20,36,37]. By analysing several markers for EMT, we observed that EOC cells induce an EMT phenotype during spheroid formation, defined by a substantial decrease in the gene expression of the cell-cell adhesion molecule E-cadherin. This implies that EOC spheroid compaction likely depends on additional molecules or processes, such as fibronectin, vimentin or actomyosin-mediated contractility as seen in other spheroid

systems[2,37-39]. Since endogenous BMP signalling is reduced during spheroid formation, we propose that induction of the EMT phenotype in EOC spheroid cells does not require activation of BMP signalling. We noted, however, that the general induction of EMT in EOC spheroids is sustained in the presence of ectopic activated BMP signalling, a result which is supported by previous studies showing that BMP stimulation can induce EMT[11,13,40]. We also observed an unexpected slight but significantly greater increase in the induction of E-cadherin expression in $ALK3^{QD}$ expressing patient derived EOC spheroid cells relative to GFP transduced cells. This up regulation may be related to the unique microenvironment of the spheroid counteracting the EMT inducing properties of activated BMP signalling to maintain cell-cell contacts. The decreased spheroid integrity that occurs as a result of activated BMP signalling may be due to the lack of typical late-step spheroid compaction. In fact, the reduction in EOC spheroid compaction in the presence of activated BMP signalling may provide cells with an increased propensity to attach and disperse during secondary metastasis formation (as modeled by spheroid re-attachment and dispersion *in vitro*).

Reattachment of EOC spheroids to a hospitable substratum and the subsequent dispersion of cells and expansion via cell proliferation and motility are necessary to achieve secondary metastasis[2,41,42]. In response to activated BMP signalling, EOC spheroids have a significantly increased ability to reattach and disperse due to increased cell adhesion and motility and not cell proliferation. This result conforms to previous data indicating that BMP signalling has no effect on EOC cell proliferation, but induces a cell spreading phenotype, enhances motility and adhesion to several ECM components[13,17].

The phenotypic response of altered cell motility due to BMP signalling usually occurs in a Smad-independent manner utilizing other converging intracellular signalling pathways[43,44]. In this report, we determined that levels of phosphorylated AKT were significantly elevated in EOC cells and spheroids in response to activated BMP signalling, thus providing a further mechanism for BMP-mediated changes in cell adhesion and motility. There has been growing evidence for crosstalk between the BMP and PI3K-AKT-mTOR signalling pathways. For example, AKT kinase is activated by BMP2 stimulation of mouse myoblast C2C12 cells, an effect that is inhibited by the BMP

type I receptor specific inhibitor LDN-193189 [21]. Stimulation of vascular smooth muscle cells with BMP2 induces cell motility in a phospho-AKT dependent manner via the action of Rac1 and RhoA GTPases[45]. In addition, activated BMP signalling enhances cell motility, invasion and EMT via the PI3K-AKT pathway in other cancer cell types [46-50]. Thus, it will be important to identify whether BMP activation of AKT employs common or different mechanisms in EOC cells and spheroids, as well as the functional implications of this signalling on the malignant characteristics of EOC.

Our laboratory has independent evidence that the PI3K-AKT pathway is down-regulated endogenously during EOC spheroid formation, yet its activation is required again during spheroid reattachment and cell dispersion. Taken together, AKT and BMP signalling are co-ordinately down-regulated during EOC spheroid formation. Perhaps sustained AKT activity due to enforced BMP signalling leads to less-cohesive spheroid formation yet enhances cell dispersion after re-attachment (Figure 2.9). This idea is supported by our studies in which treatment of $ALK3^{QD}$-expressing spheroids with an Akt1/2 inhibitor results in a partial restoration of spheroid dispersion area to that of controls. Thus, we believe that activation of the AKT pathway is functionally required and plays an important role in BMP-induced changes in spheroid behaviour and ultimately EOC metastasis. As mentioned previously, the presence of BMP signalling in EOC is correlated with significantly shorter survival periods for patients with advanced stage disease[7]. One mechanism for the deleterious effects of active BMP signalling in EOC may be downstream activation of the AKT pathway, another established marker for poor patient prognosis[51,52]. Thus, further exploration of the interaction between these two pathways is currently underway and may determine the therapeutic potential of targeting BMP signalling or AKT activity during EOC metastasis.

Our previous and current studies implicate disparate roles for BMP signalling during different steps of the metastatic cascade in EOC pathogenesis. Overall, the data supports the notion that BMP signalling has bi-phasic influences: reduced activity may be required for EOC spheroid formation during dissemination of cells from the primary tumour, yet reactivation is required for more efficient establishment of secondary metastases (Figure 2.9). As such, the conflicting roles for BMP signalling during EOC progression are

similar to the multifaceted effects of the related TGFβ pathway at early and late stages of multiple human cancers[53]. Collectively our data indicates the critical necessity to assess the effects of signalling systems at each step of the EOC metastatic process to assess the overall therapeutic potential of targeting a particular pathway.

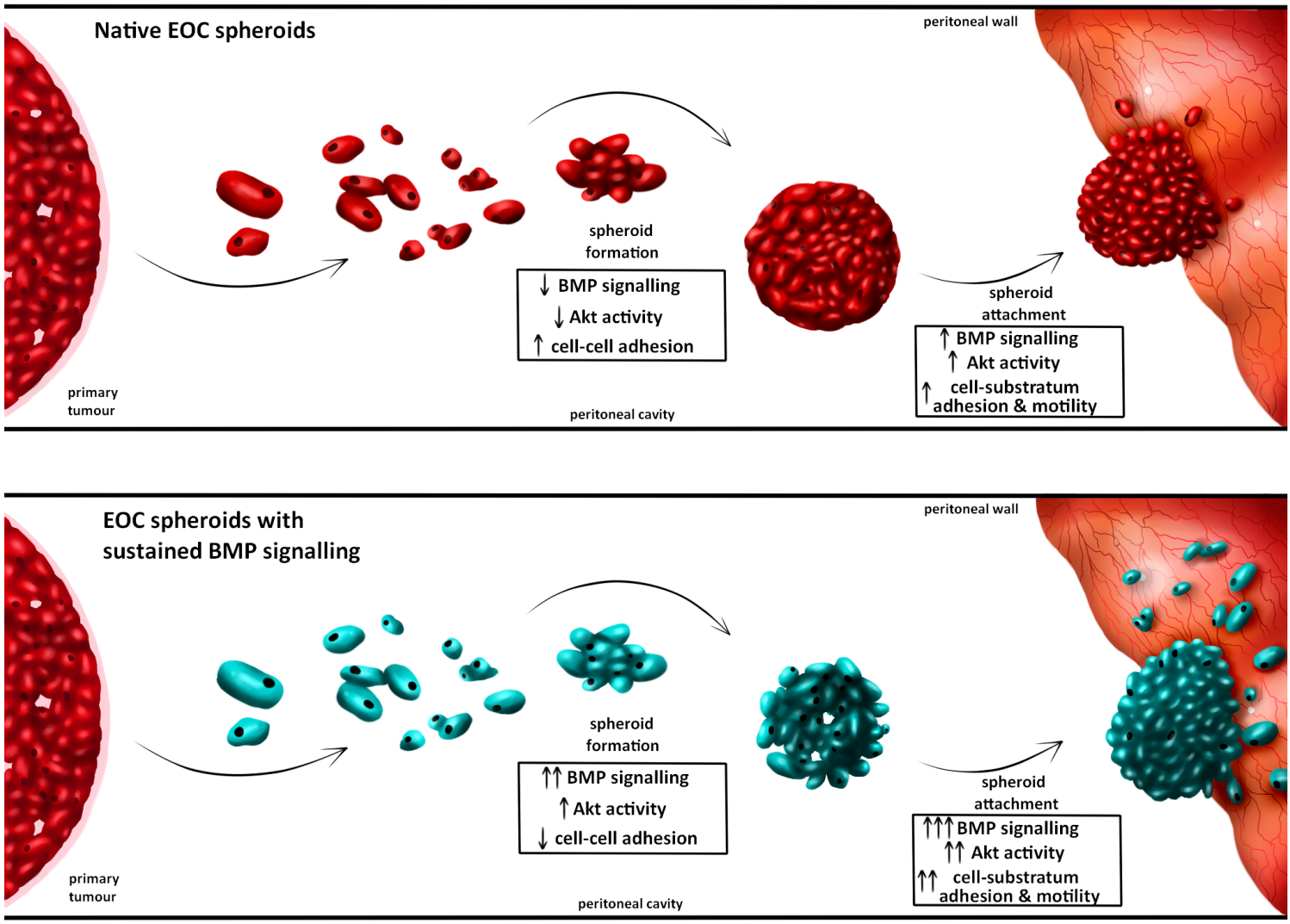

Figure 2.9: Proposed model of BMP signalling in EOC metastasis.
Metastatic EOC cells disseminating from the primary tumour naturally aggregate to form multicellular spheroids while in suspension in ascites in the peritoneal cavity. EOC spheroids endogenously down-regulate both BMP and AKT signalling, which may be required for tight cell-cell cohesion. Upon reattachment of EOC spheroids, however, cells reactivate the BMP and AKT pathways for efficient adhesion and dispersion to establish secondary metastases (*e.g.* on peritoneal wall). Ectopic activation of BMP signalling using $ALK3^{QD}$, with the concomitant increase in AKT activity, alters this dynamic process by rendering EOC spheroids more loosely-aggregated while in suspension, which ultimately enhances their ability to disperse upon reattachment.

2.5 References

1. Lengyel, E. Ovarian cancer development and metastasis. *American Journal of Pathology* **177**, 1053-1064 (2010).
2. Shield, K., Ackland, M.L., Ahmed, N. & Rice, G.E. Multicellular spheroids in ovarian cancer metastases: Biology and pathology. *Gynecol Oncol* **113**, 143-148 (2009).
3. Kim, T.H., Mount, C.W., Gombotz, W.R. & Pun, S.H. The delivery of doxorubicin to 3-D multicellular spheroids and tumors in a murine xenograft model using tumor-penetrating triblock polymeric micelles. *Biomaterials* **31**, 7386-7397 (2010).
4. Grun, B.*, et al.* Three-dimensional in vitro cell biology models of ovarian and endometrial cancer. *Cell Prolif* **42**, 219-228 (2009).
5. Kim, J.B. Three-dimensional tissue culture models in cancer biology. *Seminars in cancer biology* **15**, 365-377 (2005).
6. Herrera, B., van Dinther, M., Ten Dijke, P. & Inman, G.J. Autocrine bone morphogenetic protein-9 signals through activin receptor-like kinase-2/Smad1/Smad4 to promote ovarian cancer cell proliferation. *Cancer Res* **69**, 9254-9262 (2009).
7. Le Page, C.*, et al.* BMP-2 signaling in ovarian cancer and its association with poor prognosis. *Journal of ovarian research* **2**, 4 (2009).
8. Ma, Y., Ma, L., Guo, Q. & Zhang, S. Expression of bone morphogenetic protein-2 and its receptors in epithelial ovarian cancer and their influence on the prognosis of ovarian cancer patients. *J Exp Clin Cancer Res* **29**, 85.
9. Moll, F.*, et al.* Chordin is underexpressed in ovarian tumors and reduces tumor cell motility. *Faseb J* **20**, 240-250 (2006).
10. Pils, D.*, et al.* BAMBI is overexpressed in ovarian cancer and co-translocates with Smads into the nucleus upon TGF-beta treatment. *Gynecol Oncol* **117**, 189-197.
11. Shepherd, T.G., Mujoomdar, M.L. & Nachtigal, M.W. Constitutive activation of BMP signalling abrogates experimental metastasis of OVCA429 cells via reduced cell adhesion. *Journal of ovarian research* **3**, 5 (2010).
12. Shepherd, T.G., Theriault, B.L. & Nachtigal, M.W. Autocrine BMP4 signalling regulates ID3 proto-oncogene expression in human ovarian cancer cells. *Gene* **414**, 95-105 (2008).
13. Theriault, B.L., Shepherd, T.G., Mujoomdar, M.L. & Nachtigal, M.W. BMP4 induces EMT and Rho GTPase activation in human ovarian cancer cells. *Carcinogenesis* **28**, 1153-1162 (2007).
14. Dunfield, L.D., Dwyer, E.J. & Nachtigal, M.W. TGF beta-induced Smad signaling remains intact in primary human ovarian cancer cells. *Endocrinology* **143**, 1174-1181 (2002).
15. Wei, X.*, et al.* Mullerian inhibiting substance preferentially inhibits stem/progenitors in human ovarian cancer cell lines compared with chemotherapeutics. *Proceedings of the National Academy of Sciences of the United States of America* **107**, 18874-18879 (2010).

16. Shepherd, T.G., Theriault, B.L., Campbell, E.J. & Nachtigal, M.W. Primary culture of ovarian surface epithelial cells and ascites-derived ovarian cancer cells from patients. *Nature protocols* **1**, 2643-2649 (2006).
17. Shepherd, T.G. & Nachtigal, M.W. Identification of a putative autocrine bone morphogenetic protein-signaling pathway in human ovarian surface epithelium and ovarian cancer cells. *Endocrinology* **144**, 3306-3314 (2003).
18. Murakami, G., Watabe, T., Takaoka, K., Miyazono, K. & Imamura, T. Cooperative inhibition of bone morphogenetic protein signaling by Smurf1 and inhibitory Smads. *Mol Biol Cell* **14**, 2809-2817 (2003).
19. Zhu, H., Kavsak, P., Abdollah, S., Wrana, J.L. & Thomsen, G.H. A SMAD ubiquitin ligase targets the BMP pathway and affects embryonic pattern formation. *Nature* **400**, 687-693 (1999).
20. Ivascu, A. & Kubbies, M. Diversity of cell-mediated adhesions in breast cancer spheroids. *International journal of oncology* **31**, 1403-1413 (2007).
21. Boergermann, J.H., Kopf, J., Yu, P.B. & Knaus, P. Dorsomorphin and LDN-193189 inhibit BMP-mediated Smad, p38 and Akt signalling in C2C12 cells. *International Journal of Biochemistry and Cell Biology* **42**, 1802-1807 (2010).
22. Cuny, G.D.*, et al.* Structure-activity relationship study of bone morphogenetic protein (BMP) signaling inhibitors. *Bioorg Med Chem Lett* **18**, 4388-4392 (2008).
23. Lamb, J. The Connectivity Map: a new tool for biomedical research. *Nature reviews* **7**, 54-60 (2007).
24. Lamb, J.*, et al.* The Connectivity Map: using gene-expression signatures to connect small molecules, genes, and disease. *Science* **313**, 1929-1935 (2006).
25. Zhang, S.D. & Gant, T.W. A simple and robust method for connecting small-molecule drugs using gene-expression signatures. *BMC bioinformatics* **9**, 258 (2008).
26. Bast, R.C., Jr., Hennessy, B. & Mills, G.B. The biology of ovarian cancer: new opportunities for translation. *Nature reviews* **9**, 415-428 (2009).
27. Correa, R.J., Peart, T., Valdes, Y.R., Dimattia, G.E. & Shepherd, T.G. Modulation of AKT activity is associated with reversible dormancy in ascites-derived epithelial ovarian cancer spheroids. *Carcinogenesis* **33**, 49-58 (2012).
28. Arboleda, M.J.*, et al.* Overexpression of AKT2/protein kinase Bbeta leads to up-regulation of beta1 integrins, increased invasion, and metastasis of human breast and ovarian cancer cells. *Cancer Res* **63**, 196-206 (2003).
29. Meng, Q., Xia, C., Fang, J., Rojanasakul, Y. & Jiang, B.H. Role of PI3K and AKT specific isoforms in ovarian cancer cell migration, invasion and proliferation through the p70S6K1 pathway. *Cell Signal* **18**, 2262-2271 (2006).
30. Ahmed, N., Thompson, E.W. & Quinn, M.A. Epithelial-mesenchymal interconversions in normal ovarian surface epithelium and ovarian carcinomas: an exception to the norm. *J Cell Physiol* **213**, 581-588 (2007).
31. Tang, M.K., Zhou, H.Y., Yam, J.W. & Wong, A.S. c-Met overexpression contributes to the acquired apoptotic resistance of nonadherent ovarian cancer cells through a cross talk mediated by phosphatidylinositol 3-kinase and extracellular signal-regulated kinase 1/2. *Neoplasia* **12**, 128-138 (2010).
32. Balemans, W. & Van Hul, W. Extracellular regulation of BMP signaling in vertebrates: a cocktail of modulators. *Dev Biol* **250**, 231-250 (2002).

33. Goto, K., Kamiya, Y., Imamura, T., Miyazono, K. & Miyazawa, K. Selective inhibitory effects of Smad6 on bone morphogenetic protein type I receptors. *J Biol Chem* **282**, 20603-20611 (2007).
34. Itoh, F*., et al.* Promoting bone morphogenetic protein signaling through negative regulation of inhibitory Smads. *Embo J* **20**, 4132-4142 (2001).
35. Kamiya, Y., Miyazono, K. & Miyazawa, K. Smad7 inhibits transforming growth factor-beta family type i receptors through two distinct modes of interaction. *Journal of Biological Chemistry* **285**, 30804-30813 (2010).
36. Casey, R.C*., et al.* Beta 1-integrins regulate the formation and adhesion of ovarian carcinoma multicellular spheroids. *Am J Pathol* **159**, 2071-2080 (2001).
37. Kim, Y.J*., et al.* Modulating the strength of cadherin adhesion: evidence for a novel adhesion complex. *J Cell Sci* **118**, 3883-3894 (2005).
38. Napolitano, A.P., Chai, P., Dean, D.M. & Morgan, J.R. Dynamics of the self-assembly of complex cellular aggregates on micromolded nonadhesive hydrogels. *Tissue Eng* **13**, 2087-2094 (2007).
39. Tzanakakis, E.S., Hansen, L.K. & Hu, W.S. The role of actin filaments and microtubules in hepatocyte spheroid self-assembly. *Cell Motil Cytoskeleton* **48**, 175-189 (2001).
40. Gamell, C*., et al.* BMP2 induction of actin cytoskeleton reorganization and cell migration requires PI3-kinase and Cdc42 activity. *J Cell Sci* **121**, 3960-3970 (2008).
41. Burleson, K.M., Boente, M.P., Pambuccian, S.E. & Skubitz, A.P. Disaggregation and invasion of ovarian carcinoma ascites spheroids. *Journal of translational medicine* **4**, 6 (2006).
42. Iwanicki, M*., et al.* Ovarian cancer spheroids use myosin-generated force to clear the mesothelium. *Cancer Discov* (2011).
43. Derynck, R. & Zhang, Y.E. Smad-dependent and Smad-independent pathways in TGF-beta family signalling. *Nature* **425**, 577-584 (2003).
44. Guo, X. & Wang, X.F. Signaling cross-talk between TGF-beta/BMP and other pathways. *Cell Res* **19**, 71-88 (2009).
45. Perez, V.A*., et al.* BMP promotes motility and represses growth of smooth muscle cells by activation of tandem Wnt pathways. *Journal of Cell Biology* **192**, 171-188 (2011).
46. Chen, X., Liao, J., Lu, Y., Duan, X. & Sun, W. Activation of the PI3K/Akt Pathway Mediates Bone Morphogenetic Protein 2-Induced Invasion of Pancreatic Cancer Cells Panc-1. *Pathology Oncology Research* (2011).
47. Graham, T.R*., et al.* PI3K/Akt-dependent transcriptional regulation and activation of BMP-2-Smad signaling by NF-kappaB in metastatic prostate cancer cells. *Prostate* **69**, 168-180 (2009).
48. Kang, M.H*., et al.* Inhibition of PI3 kinase/Akt pathway is required for BMP2-induced EMT and invasion. *Oncol Rep* **22**, 525-534 (2009).
49. Kang, M.H., Kim, J.S., Seo, J.E., Oh, S.C. & Yoo, Y.A. BMP2 accelerates the motility and invasiveness of gastric cancer cells via activation of the phosphatidylinositol 3-kinase (PI3K)/Akt pathway. *Experimental cell research* **316**, 24-37 (2010).

50. Langenfeld, E.M., Kong, Y. & Langenfeld, J. Bone morphogenetic protein-2-induced transformation involves the activation of mammalian target of rapamycin. *Mol Cancer Res* **3**, 679-684 (2005).
51. Davidson, B.*, et al.* Proteomic analysis of malignant ovarian cancer effusions as a tool for biologic and prognostic profiling. *Clinical Cancer Research* **12**, 791-799 (2006).
52. Schilder, R.J.*, et al.* Phase II evaluation of imatinib mesylate in the treatment of recurrent or persistent epithelial ovarian or primary peritoneal carcinoma: a Gynecologic Oncology Group Study. *Journal of Clinical Oncology* **26**, 3418-3425 (2008).
53. Massague, J. TGFbeta in Cancer. *Cell* **134**, 215-230 (2008).

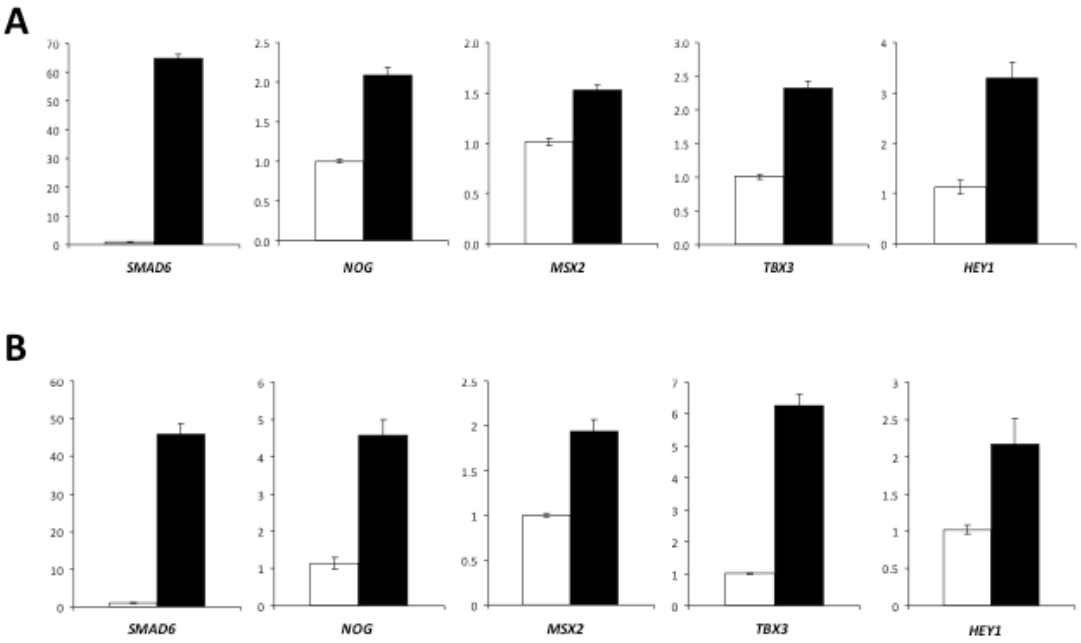

Figure S2.1: Validation of microarray results by quantitative RT-PCR analysis of specific up-regulated genes.
SMAD6, *NOG*, *MSX2*, *TBX3*, and *HEY1* mRNA expression was detected using human-specific primers for each and cDNA samples generated from adherent primary human EOC cells (A) and spheroids (B) transduced with either Ad-ALK3^{QD} or Ad-GFP control virus. Relative expression was normalized to Ad-GFP transduced cells (set to 1) and *GAPDH* mRNA served as an internal control.

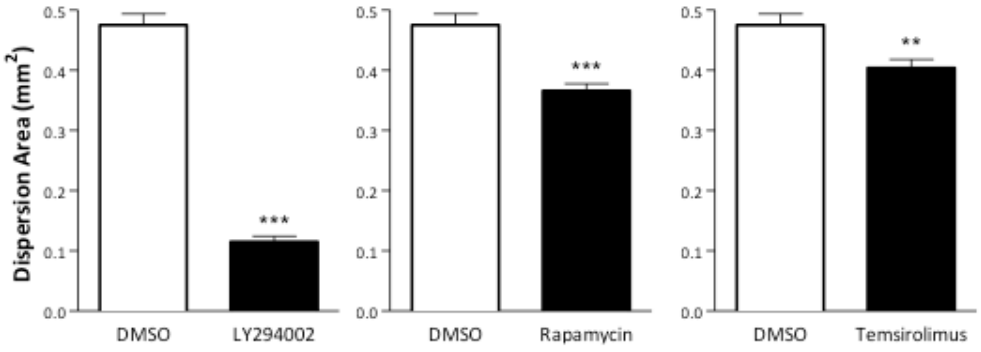

Figure S2.2: Inhibition of PI3K-mTOR signalling reduces EOC cell dispersion upon spheroid reattachment.
EOC cells from patient ascites samples (EOC30 and EOC67) were seeded to ULA cluster plates to generate spheroids over three days. EOC spheroids were individually seeded to standard tissue culture plastic and treated with LY294002, rapamycin, or temsirolimus (Torisel®) or DMSO vehicle control. Images of spheroids were captured (>40 per treatment group) at 24 h post-reattachment and dispersion area was quantified using *ImageJ* software. (**p<0.01; ***p<0.001 using Student's t-test).

Table S2.1: Genes with increased expression due to Alk3QD in adherent EOC cells.

Gene Title	Gene Symbol	Probe Set ID	Fold Change
loricrin	LOR	207720_at	63.124
calcitonin-related polypeptide beta	CALCB	214636_at	17.708
S100 calcium binding protein P	S100P	204351_at	14.716
heat shock 70kDa protein 6 (HSP70B)	HSPA6	213418_at	9.249
distal-less homeobox 2	DLX2	207147_at	8.543
cholecystokinin	CCK	205827_at	7.97
pregnancy specific beta-1-glycoprotein 5	PSG5	204830_x_at	7.951
FLJ35409 protein	FLJ35409	1559506_x_at	7.665
gap junction protein, delta 3, 31.9kDa	GJD3	230025_at	7.533
acetoacetyl-CoA synthetase-like	AACSL	1570020_at	6.901
pregnancy specific beta-1-glycoprotein 3	PSG3	211741_x_at	6.892
folate receptor 3 (gamma)	FOLR3	206371_at	6.787
synaptotagmin XV	SYT15	1560879_a_at	6.497
similar to hCG2038656	LOC100129058	1564300_at	6.285
KIT ligand	KITLG	211124_s_at	6.282
dual specificity phosphatase 2	DUSP2	204794_at	6.138
podocalyxin-like	PODXL	201578_at	6.085
claudin 4	CLDN4	201428_at	6.019
SMAD family member 6	SMAD6	207069_s_at	5.782
FEZ family zinc finger 2	FEZF2	233972_s_at	5.611
keratin associated protein 4-12	KRTAP4-12	224269_at	5.553
chloride intracellular channel 2	CLIC2	213415_at	5.416
aldo-keto reductase family 1, member C2 (dihydrodiol dehydrogenase 2; bile acid binding protein; 3-alpl	AKR1C2	211653_x_at	5.339
glutamate receptor, ionotropic, AMPA 2	GRIA2	241172_at	5.324
solute carrier family 16, member 14 (monocarboxylic acid transporter 14)	SLC16A14	238029_s_at	5.109
interleukin 9	IL9	208193_at	5.086
gremlin 2, cysteine knot superfamily, homolog (Xenopus laevis)	GREM2	235504_at	5.071
tumor necrosis factor (ligand) superfamily, member 9	TNFSF9	206907_at	4.802
chemokine (C-C motif) ligand 26	CCL26	223710_at	4.725
gremlin 2, cysteine knot superfamily, homolog (Xenopus laevis)	GREM2	240509_s_at	4.665
involucrin	IVL	214599_at	4.612
hypothetical protein MGC16121	MGC16121	228235_at	4.348
XK, Kell blood group complex subunit-related family, member 6	XKR6	1557436_at	4.344
hemicentin 2	HMCN2	241650_x_at	4.341
ameloblastin (enamel matrix protein)	AMBN	221114_at	4.3
fibrinogen C domain containing 1	FIBCD1	240042_at	4.27
dual specificity phosphatase 26 (putative)	DUSP26	219144_at	4.234
semaphorin 7A, GPI membrane anchor (John Milton Hagen blood group)	SEMA7A	230345_at	4.226
aldo-keto reductase family 1, member C1 (dihydrodiol dehydrogenase 1; 20-alpha (3-alpha)-hydroxyster	AKR1C1	204151_x_at	4.2
transmembrane protein 132E	TMEM132E	243708_at	4.196
keratin associated protein 2-4	KRTAP2-4	1555673_at	4.146
hypothetical LOC441052	LOC441052	232443_at	4.131
hyaluronan synthase 2	HAS2	206432_at	4.122
kinesin family member 7	KIF7	229405_at	4.102
keratin associated protein 4-1	KRTAP4-1	234635_at	4.082
CD24 molecule	CD24	209772_s_at	4.078
leucine rich repeat containing 4	LRRC4	223552_at	4.043
polymerase (RNA) II (DNA directed) polypeptide A, 220kDa	POLR2A	217415_at	4.005
G protein-coupled receptor 56	GPR56	212070_at	3.941
gremlin 2, cysteine knot superfamily, homolog (Xenopus laevis)	GREM2	220794_at	3.908
folate receptor 2 (fetal)	FOLR2	204829_s_at	3.882
hypothetical protein LOC284542	LOC284542	230920_at	3.88
zinc finger protein 114	ZNF114	1552946_at	3.878
echinoderm microtubule associated protein like 1	EML1	204797_s_at	3.853
neuregulin 1	NRG1	206343_s_at	3.837
synaptotagmin XV	SYT15	1560878_at	3.835
hypothetical protein MGC16121	MGC16121	227488_at	3.823
neuronal cell adhesion molecule	NRCAM	204105_s_at	3.777
actin, alpha, cardiac muscle 1	ACTC1	205132_at	3.766
zinc finger protein 831	ZNF831	1558826_at	3.752
extra spindle pole bodies homolog 1 (S. cerevisiae)	ESPL1	204817_at	3.747
v-myb myeloblastosis viral oncogene homolog (avian)	MYB	204798_at	3.721
Atonal homolog 8 (Drosophila)	ATOH8	1558706_a_at	3.716
pregnancy specific beta-1-glycoprotein 9	PSG9	209594_x_at	3.712
mal, T-cell differentiation protein-like	MALL	209373_at	3.705
synaptopodin	SYNPO	235914_at	3.697
noggin	NOG	231798_at	3.683
synapsin I	SYN1	221914_at	3.657

Table S2.1 cont'd.

protocadherin 10	PCDH10	1552925_at	3.641
Kruppel-like factor 4 (gut)	KLF4	220266_s_at	3.638
clusterin	CLU	222043_at	3.632
aldo-keto reductase family 1, member C2 (dihydrodiol dehydrogenase 2; bile acid binding protein; 3-alpl	AKR1C2	209699_x_at	3.62
GIPC PDZ domain containing family, member 3	GIPC3	236730_at	3.617
glutathione peroxidase 3 (plasma)	GPX3	201348_at	3.601
coiled-coil domain containing 85A	CCDC85A	235228_at	3.596
LIM domain only 2 (rhombotin-like 1)	LMO2	204249_s_at	3.592
vasoactive intestinal peptide	VIP	206577_at	3.532
solute carrier family 25 (mitochondrial carrier; ornithine transporter) member 15	SLC25A15	222705_s_at	3.524
DIRAS family, GTP-binding RAS-like 3	DIRAS3	215506_s_at	3.49
potassium voltage-gated channel, KQT-like subfamily, member 5	KCNQ5	244623_at	3.489
trafficking protein particle complex 2	TRAPPC2	1562349_at	3.483
WD repeat domain 33	WDR33	243832_at	3.466
stimulated by retinoic acid gene 6 homolog (mouse)	STRA6	221701_s_at	3.465
acidic (leucine-rich) nuclear phosphoprotein 32 family, member C	ANP32C	208538_at	3.454
pappalysin 2	PAPPA2	228237_at	3.404
CD24 molecule	CD24	208650_s_at	3.376
hypothetical gene supported by AK026773	LOC440863	234478_at	3.368
myosin binding protein H	MYBPH	206304_at	3.363
RASD family, member 2	RASD2	223634_at	3.36
AF4/FMR2 family, member 2	AFF2	206105_at	3.356
doublecortin domain containing 5	DCDC5	232603_at	3.346
aldo-keto reductase family 1, member C1 (dihydrodiol dehydrogenase 1; 20-alpha (3-alpha)-hydroxyster	AKR1C1	216594_x_at	3.321
CD300 molecule-like family member g	CD300LG	1552509_a_at	3.316
pleckstrin homology domain containing, family A member 7	PLEKHA7	228450_at	3.276
TMF1-regulated nuclear protein 1	TRNP1	227862_at	3.268
myosin, heavy chain 13, skeletal muscle	MYH13	208208_at	3.243
hypothetical LOC100126784	LOC100126784	240407_at	3.228
hypothetical protein LOC254057	LOC254057	232370_at	3.226
RAB39B, member RAS oncogene family	RAB39B	230075_at	3.204
UPF0632 protein A	LOC388630	244472_at	3.199
ankyrin repeat domain 20 family, member A pseudogene	LOC375010	1566147_a_at	3.182
small nucleolar RNA host gene 4 (non-protein coding)	SNHG4	1565325_at	3.172
TIMP metallopeptidase inhibitor 4	TIMP4	206243_at	3.169
similar to Primase, DNA, polypeptide 2 (58kDa) /// primase, DNA, polypeptide 2 (58kDa)	LOC100134355 /	215709_at	3.162
family with sequence similarity 83, member G	FAM83G	228587_at	3.158
Jagged 1 (Alagille syndrome)	JAG1	231183_s_at	3.146
neural cell adhesion molecule 1	NCAM1	212843_at	3.145
solute carrier family 6 (neutral amino acid transporter), member 15	SLC6A15	232263_at	3.138
X-ray repair complementing defective repair in Chinese hamster cells 4	XRCC4	210812_at	3.109
breast cancer 1, early onset	BRCA1	211851_x_at	3.096
similar to TLK2 protein /// similar to TLK2 protein /// similar to Serine/threonine-protein kinase tousled-lik	LOC100128729 /	232585_at	3.088
echinoderm microtubule associated protein like 1	EML1	204796_at	3.062
crystallin, alpha B	CRYAB	209283_at	3.058
exoribonuclease 2	ERI2	240604_at	3.048
retinoic acid induced 2	RAI2	219440_at	3.039
glutathione peroxidase 3 (plasma)	GPX3	214091_s_at	3.03
IGF-like family member 2	IGFL2	231148_at	3.027
retinitis pigmentosa 1 (autosomal dominant)	RP1	224021_at	3.013
chromosome 14 open reading frame 145	C14orf145	244033_at	3.01
Hypothetical LOC150538	FLJ32063	235147_at	3.005
ELMO/CED-12 domain containing 1	ELMOD1	231930_at	2.984
jagged 1 (Alagille syndrome)	JAG1	216268_s_at	2.974
glycerol-3-phosphate dehydrogenase 2 (mitochondrial)	GPD2	211613_s_at	2.971
extra spindle pole bodies homolog 1 (S. cerevisiae)	ESPL1	38158_at	2.953
chromosome 14 open reading frame 145	C14orf145	1557755_at	2.936
CD24 molecule	CD24	266_s_at	2.927
aurora kinase B	AURKB	209464_at	2.912
dynein, axonemal, heavy chain 12	DNAH12	1563097_at	2.91
hypothetical protein LOC283278	LOC283278	242417_at	2.907
fatty acid binding protein 5 (psoriasis-associated)	FABP5	202345_s_at	2.898
THAP domain containing, apoptosis associated protein 2	THAP2	230380_at	2.893
DnaJ (Hsp40) homolog, subfamily A, member 4	DNAJA4	1554334_a_at	2.89
formin 2	FMN2	1555471_a_at	2.877
paternally expressed 10	PEG10	212092_at	2.875
atonal homolog 8 (Drosophila)	ATOH8	228890_at	2.873
T-box 3	TBX3	219682_s_at	2.871
X-ray repair complementing defective repair in Chinese hamster cells 4	XRCC4	210813_s_at	2.866
CD24 molecule	CD24	208651_x_at	2.861

Table S2.1 cont'd.

synovial sarcoma, X breakpoint 2 interacting protein	SSX2IP	203018_s_at	2.858
RGD motif, leucine rich repeats, tropomodulin domain and proline-rich containing	RLTPR	227216_at	2.854
placental growth factor	PGF	209652_s_at	2.84
transketolase	TKT	228205_at	2.83
formin 2	FMN2	223618_at	2.826
cancer susceptibility candidate 4	CASC4	1559635_at	2.798
t-complex 11 homolog (mouse)	TCP11	220378_at	2.798
synovial sarcoma, X breakpoint 2 interacting protein	SSX2IP	210871_x_at	2.788
cholecystokinin A receptor	CCKAR	211174_s_at	2.772
Na+/K+ transporting ATPase interacting 2	NKAIN2	242002_at	2.762
matrix metallopeptidase 3 (stromelysin 1, progelatinase)	MMP3	205828_at	2.762
synovial sarcoma, X breakpoint 2 interacting protein	SSX2IP	203016_s_at	2.759
plexin A2	PLXNA2	213030_s_at	2.758
ATP-binding cassette, sub-family C (CFTR/MRP), member 9	ABCC9	208561_at	2.758
hypothetical protein LOC144481	LOC144481	1559315_s_at	2.755
T-box 3	TBX3	225544_at	2.737
replication protein A4, 34kDa	RPA4	221143_at	2.733
WD repeat domain 4	WDR4	241937_s_at	2.725
X-ray repair complementing defective repair in Chinese hamster cells 4	XRCC4	205071_x_at	2.713
T-box 3	TBX3	229576_s_at	2.707
transient receptor potential cation channel, subfamily C, member 4	TRPC4	224219_s_at	2.703
pyrophosphatase (inorganic) 2	PPA2	1554499_s_at	2.701
Kruppel-like factor 4 (gut)	KLF4	221841_s_at	2.701
progestin and adipoQ receptor family member IX	PAQR9	1558322_a_at	2.7
v-maf musculoaponeurotic fibrosarcoma oncogene homolog B (avian)	MAFB	218559_s_at	2.691
tubulin, beta 2A /// tubulin, beta 2B	TUBB2A /// TUBI	209372_x_at	2.684
cysteine-rich protein 2	CRIP2	208978_at	2.682
pregnancy specific beta-1-glycoprotein 9	PSG9	207733_x_at	2.681
actinin, alpha 2	ACTN2	203861_s_at	2.678
synovial sarcoma, X breakpoint 2 interacting protein	SSX2IP	203015_s_at	2.675
RNA binding motif protein, Y-linked, family 3, member A pseudogene	RBMY3AP	1565320_at	2.669
synovial sarcoma, X breakpoint 2 interacting protein	SSX2IP	203019_x_at	2.655
serine/threonine/tyrosine kinase 1	STYK1	220030_at	2.649
transforming growth factor, alpha	TGFA	211258_s_at	2.642
jagged 1 (Alagille syndrome)	JAG1	209098_s_at	2.639
sperm specific antigen 2	SSFA2	236207_at	2.639
v-maf musculoaponeurotic fibrosarcoma oncogene homolog B (avian)	MAFB	222670_s_at	2.619
zinc finger and BTB domain containing 45	ZBTB45	240551_at	2.602
regulator of G-protein signaling 4	RGS4	204339_s_at	2.602
sprouty homolog 2 (Drosophila)	SPRY2	204011_at	2.598
X-ray repair complementing defective repair in Chinese hamster cells 4	XRCC4	205072_s_at	2.593
E2F transcription factor 7	E2F7	228033_at	2.586
lin-7 homolog B (C. elegans)	LIN7B	241957_x_at	2.583
msh homeobox 2	MSX2	210319_x_at	2.581
MAP/microtubule affinity-regulating kinase 2	MARK2	211082_x_at	2.581
cystic fibrosis transmembrane conductance regulator (ATP-binding cassette sub-family C, member 7)	CFTR	234706_x_at	2.581
solute carrier family 4, sodium bicarbonate cotransporter, member 4	SLC4A4	210738_s_at	2.565
regulator of G-protein signaling 4	RGS4	204338_s_at	2.563
synaptotagmin-like 3	SYTL3	238423_at	2.558
fibulin 2	FBLN2	203886_s_at	2.542
Hypothetical protein LOC100132244	LOC100132244	229438_at	2.538
ELOVL family member 6, elongation of long chain fatty acids (FEN1/Elo2, SUR4/Elo3-like, yeast)	ELOVL6	204256_at	2.531
Fc receptor-like A	FCRLA	235401_s_at	2.527
KN motif and ankyrin repeat domains 4	KANK4	229125_at	2.522
jagged 1 (Alagille syndrome)	JAG1	209099_x_at	2.519
Sperm specific antigen 2	SSFA2	229744_at	2.516
chromosome 10 open reading frame 116	C10orf116	203571_s_at	2.516
frizzled homolog 8 (Drosophila)	FZD8	227405_s_at	2.513
cerebellin 2 precursor	CBLN2	242301_at	2.508
potassium voltage-gated channel, subfamily G, member 1	KCNG1	214595_at	2.507
diacylglycerol kinase, gamma 90kDa	DGKG	206395_at	2.504
olfactory receptor, family 2, subfamily J, member 2	OR2J2	208508_s_at	2.502
microtubule-associated protein 1A	MAP1A	203151_at	2.502
discoidin, CUB and LCCL domain containing 2	DCBLD2	213873_at	2.497
ELOVL family member 6, elongation of long chain fatty acids (FEN1/Elo2, SUR4/Elo3-like, yeast)	ELOVL6	210868_s_at	2.493
solute carrier family 29 (nucleoside transporters), member 2	SLC29A2	1560149_at	2.484
ubiquitin-like with PHD and ring finger domains 1	UHRF1	225655_at	2.484
angiotensin II receptor, type 2	AGTR2	222321_at	2.481
phosphatidylinositol transfer protein, membrane-associated 2	PITPNM2	1552924_a_at	2.476
suppressor of cytokine signaling 2	SOCS2	203372_s_at	2.473

Table S2.1 cont'd.

insulin-like 3 (Leydig cell)	INSL3	1553594_a_at	2.472
peroxisome proliferator-activated receptor gamma	PPARG	208510_s_at	2.47
non-protein coding RNA 161	NCRNA00161	1554405_a_at	2.467
phosphatidylinositol-5-phosphate 4-kinase, type II, beta	PIP4K2B	1553047_at	2.464
integrin, alpha 2 (CD49B, alpha 2 subunit of VLA-2 receptor)	ITGA2	205032_at	2.456
tropomyosin 1 (alpha)	TPM1	206117_at	2.454
TOX high mobility group box family member 2	TOX2	228737_at	2.446
kelch-like 17 (Drosophila)	KLHL17	229792_at	2.44
Na+/H+ exchanger domain containing 2	NHEDC2	1564746_at	2.438
spectrin, beta, non-erythrocytic 1	SPTBN1	226342_at	2.437
TruB pseudouridine (psi) synthase homolog 1 (E. coli)	TRUB1	236020_s_at	2.432
p21 protein (Cdc42/Rac)-activated kinase 7	PAK7	213990_s_at	2.428
GATA binding protein 2	GATA2	209710_at	2.422
similar to hCG2042915	LOC100129673	236611_at	2.419
plexin A2	PLXNA2	227032_at	2.413
testis specific, 14	TSGA14	215637_at	2.403
acyl-CoA thioesterase 7	ACOT7	215728_s_at	2.399
Spectrin repeat containing, nuclear envelope 1	SYNE1	232027_at	2.391
hypothetical locus MGC42157	MGC42157	1552987_a_at	2.376
transcription factor 19	TCF19	223274_at	2.369
Na+/H+ exchanger domain containing 2	NHEDC2	229491_at	2.358
aminolevulinate, delta-, synthase 2	ALAS2	244205_at	2.355
claudin domain containing 2	CLDND2	231162_at	2.343
heat shock 60kDa protein 1 (chaperonin) /// heat shock 60kDa protein 1 (chaperonin) pseudogene 4	HSPD1 /// HSPD	243372_at	2.34
purinergic receptor P2Y, G-protein coupled, 8	P2RY8	229686_at	2.336
GINS complex subunit 4 (Sld5 homolog)	GINS4	211767_at	2.332
ADAMTS-like 1	ADAMTSL1	229585_at	2.33
mex-3 homolog C (C. elegans)	MEX3C	1556874_a_at	2.326
discoidin, CUB and LCCL domain containing 2	DCBLD2	213865_at	2.323
cadherin-like 24	CDH24	1553166_at	2.321
homeobox A4	HOXA4	206289_at	2.321
erythrocyte membrane protein band 4.2	EPB42	210746_s_at	2.315
contactin associated protein-like 2	CNTNAP2	219301_s_at	2.309
dual specificity phosphatase 5 pseudogene	DUSP5P	1553299_at	2.305
choroideremia (Rab escort protein 1)	CHM	1569183_a_at	2.303
interleukin 21 receptor	IL21R	221658_s_at	2.301
FERM domain containing 8	FRMD8	227964_at	2.293
nuclear factor of kappa light polypeptide gene enhancer in B-cells inhibitor-like 2	NFKBIL2	1558329_at	2.286
calsequestrin 1 (fast-twitch, skeletal muscle)	CASQ1	219645_at	2.285
OTU domain, ubiquitin aldehyde binding 2	OTUB2	222878_s_at	2.281
sterile alpha motif domain containing 11	SAMD11	1560477_a_at	2.28
leucine-rich repeats and WD repeat domain containing 1	LRWD1	225680_at	2.28
aquaporin 5	AQP5	213611_at	2.268
high mobility group AT-hook 2	HMGA2	1567224_at	2.267
acyl-Coenzyme A dehydrogenase, long chain	ACADL	206068_s_at	2.265
A kinase (PRKA) anchor protein 6	AKAP6	205359_at	2.262
tetraspanin 13	TSPAN13	217979_at	2.262
minichromosome maintenance complex component 5	MCM5	201755_at	2.257
calcium activated nucleotidase 1	CANT1	1554327_a_at	2.252
plexin A2	PLXNA2	207290_at	2.239
talin 2	TLN2	212701_at	2.239
pregnancy specific beta-1-glycoprotein 3	PSG3	203399_x_at	2.233
carbohydrate (chondroitin 6) sulfotransferase 3	CHST3	32094_at	2.228
Janus kinase 2	JAK2	205842_s_at	2.224
pre-B-cell leukemia homeobox 4	PBX4	230536_at	2.223
transient receptor potential cation channel, subfamily C, member 3	TRPC3	210814_at	2.223
poliovirus receptor	PVR	214443_at	2.221
retinoic acid receptor, gamma	RARG	204188_s_at	2.217
clusterin	CLU	208791_at	2.211
ADAM metallopeptidase domain 11	ADAM11	207880_at	2.204
FERM domain containing 8	FRMD8	1554903_at	2.196
pregnancy specific beta-1-glycoprotein 6	PSG6	208106_x_at	2.195
microtubule-associated protein 1B	MAP1B	212233_at	2.193
synovial sarcoma, X breakpoint 2 interacting protein	SSX2IP	203017_s_at	2.19
prolactin	PRL	205445_at	2.19
connector enhancer of kinase suppressor of Ras 2	CNKSR2	1554607_at	2.189
tyrosine 3-monooxygenase/tryptophan 5-monooxygenase activation protein, eta polypeptide	YWHAH	201020_at	2.188
MyoD family inhibitor domain containing	MDFIC	1559942_at	2.186
fibroblast growth factor receptor 3	FGFR3	204379_s_at	2.184
cadherin 6, type 2, K-cadherin (fetal kidney)	CDH6	205532_s_at	2.183

Table S2.1 cont'd.

annexin A10	ANXA10	210143_at	2.183
intermediate filament family orphan 2	IFFO2	225615_at	2.179
coiled-coil-helix-coiled-coil-helix domain containing 10	CHCHD10	224932_at	2.176
monoglyceride lipase	MGLL	211026_s_at	2.175
oxysterol binding protein-like 6	OSBPL6	223805_at	2.169
glycerol-3-phosphate acyltransferase, mitochondrial	GPAM	225420_at	2.162
collagen, type XIII, alpha 1	COL13A1	211343_s_at	2.157
SHC (Src homology 2 domain containing) family, member 4	SHC4	235238_at	2.156
FERM domain containing 3	FRMD3	230645_at	2.153
carbonic anhydrase I	CA1	205949_at	2.148
small VCP/p97-interacting protein	SVIP	230005_at	2.148
jun D proto-oncogene	JUND	203751_x_at	2.146
heat shock 70kDa protein 1A /// heat shock 70kDa protein 1B	HSPA1A /// HSP/	200800_s_at	2.145
Ankyrin-repeat and fibronectin type III domain containing 1	ANKFN1	1559640_at	2.139
arylsulfatase B	ARSB	1554032_at	2.139
nucleolar and coiled-body phosphoprotein 1	NOLC1	205895_s_at	2.133
SHC (Src homology 2 domain containing) family, member 4	SHC4	230538_at	2.132
TRM1 tRNA methyltransferase 1 homolog (S. cerevisiae)	TRMT1	203701_s_at	2.127
GATA binding protein 3	GATA3	209604_s_at	2.123
heme oxygenase (decycling) 1	HMOX1	203665_at	2.123
chromosome 14 open reading frame 34	C14orf34	1555786_s_at	2.123
similar to HSPC047 protein	LOC100134722	220692_at	2.122
ATP-binding cassette, sub-family C (CFTR/MRP), member 4	ABCC4	203196_at	2.121
msh homeobox 2	MSX2	205555_s_at	2.118
Insulin receptor substrate 1	IRS1	235392_at	2.112
chondroitin sulfate synthase 3	CHSY3	242100_at	2.106
transient receptor potential cation channel, subfamily V, member 2	TRPV2	219282_s_at	2.1
RGM domain family, member B	RGMB	227339_at	2.099
TRM1 tRNA methyltransferase 1 homolog (S. cerevisiae)	TRMT1	210463_x_at	2.099
BTB (POZ) domain containing 11	BTBD11	238692_at	2.097
ATPase family, AAA domain containing 3A /// ATPase family, AAA domain containing 3B /// similar to A/	ATAD3A /// ATAI	1552641_s_at	2.092
notchless homolog 1 (Drosophila)	NLE1	203867_s_at	2.086
FERM domain containing 3	FRMD3	229893_at	2.079
SMAD family member 7	SMAD7	204790_at	2.078
Sp8 transcription factor	SP8	239743_at	2.072
clusterin	CLU	208792_s_at	2.071
ATP-binding cassette, sub-family C (CFTR/MRP), member 4	ABCC4	1554918_a_at	2.069
malic enzyme 2, NAD(+)-dependent, mitochondrial	ME2	210154_at	2.068
thromboxane A2 receptor	TBXA2R	336_at	2.068
KIAA1609	KIAA1609	221843_s_at	2.067
suppressor of cytokine signaling 2	SOCS2	203373_at	2.065
myosin VA (heavy chain 12, myoxin)	MYO5A	204527_at	2.06
hairy/enhancer-of-split related with YRPW motif 1	HEY1	44783_s_at	2.053
solute carrier family 4, sodium bicarbonate cotransporter, member 4	SLC4A4	1554027_a_at	2.051
YOD1 OTU deubiquinating enzyme 1 homolog (S. cerevisiae)	YOD1	215150_at	2.049
hairy/enhancer-of-split related with YRPW motif 1	HEY1	218839_at	2.047
glutamate receptor, ionotropic, kainate 2	GRIK2	1560265_at	2.046
smoothelin	SMTN	207390_s_at	2.046
BTB (POZ) domain containing 11	BTBD11	228570_at	2.044
protein phosphatase 3 (formerly 2B), catalytic subunit, beta isoform	PPP3CB	209817_at	2.043
septin 13	13-Sep	230355_at	2.042
potassium inwardly-rectifying channel, subfamily J, member 8	KCNJ8	205304_s_at	2.042
HECT, C2 and WW domain containing E3 ubiquitin protein ligase 2	HECW2	232080_at	2.04
Kruppel-like factor 2 (lung)	KLF2	226646_at	2.037
paired related homeobox 2	PRRX2	219729_at	2.037
gamma-aminobutyric acid (GABA) A receptor, gamma 1	GABRG1	241805_at	2.032
acyl-CoA thioesterase 7	ACOT7	208002_s_at	2.026
coiled-coil domain containing 68	CCDC68	220180_at	2.022
SET domain and mariner transposase fusion gene	SETMAR	1554060_s_at	2.021
ATPase type 13A3	ATP13A3	219558_at	2.018
glycerol-3-phosphate acyltransferase, mitochondrial	GPAM	225424_at	2.018
KIAA1609	KIAA1609	65438_at	2.013
zinc finger protein 175	ZNF175	205497_at	2.01
prominin 2	PROM2	1552797_s_at	2.009
nicalin homolog (zebrafish)	NCLN	222206_s_at	2.007
BAI1-associated protein 2	BAIAP2	205293_x_at	2.005
P antigen family, member 1 (prostate associated)	PAGE1	206897_at	2.004
monoglyceride lipase	MGLL	225102_at	2
collagen, type IV, alpha 6	COL4A6	210945_at	2

Table S2.2: Genes with increased expression due to Alk3QD in EOC spheroids.

Gene Title	Gene Symbol	Probe Set ID	Fold Change
lipopolysaccharide binding protein	LBP	214461_at	72.27
loricrin	LOR	207720_at	49.49
hairy/enhancer-of-split related with YRPW motif 2	HEY2	222921_s_at	48.379
actin, alpha, cardiac muscle 1	ACTC1	205132_at	40.174
CD24 molecule	CD24	209772_s_at	39.195
CD24 molecule	CD24	266_s_at	37.327
CD24 molecule	CD24	209771_x_at	34.274
CD24 molecule	CD24	216379_x_at	30.311
contactin associated protein-like 2	CNTNAP2	219301_s_at	25.559
CD24 molecule	CD24	208650_s_at	24.444
cut-like homeobox 2	CUX2	213920_at	24.245
CD24 molecule	CD24	208651_x_at	21.376
distal-less homeobox 2	DLX2	207147_at	20.206
FEZ family zinc finger 2	FEZF2	233972_s_at	16.35
involucrin	IVL	214599_at	14.951
dickkopf homolog 1 (Xenopus laevis)	DKK1	204602_at	13.536
cannabinoid receptor 1 (brain)	CNR1	213436_at	13.412
gamma-aminobutyric acid (GABA) B receptor, 2	GABBR2	209990_s_at	12.811
folate receptor 3 (gamma)	FOLR3	206371_at	12.253
chromosome 5 open reading frame 23	C5orf23	219054_at	11.902
chemokine (C-C motif) ligand 26	CCL26	223710_at	11.408
gap junction protein, delta 3, 31.9kDa	GJD3	230025_at	10.917
SMAD family member 9	SMAD9	206320_s_at	10.709
SMAD family member 6	SMAD6	207069_s_at	10.538
noggin	NOG	231798_at	10.343
chromosome 2 open reading frame 88	C2orf88	223754_at	10.294
guanine nucleotide binding protein (G protein), gamma transducing activity polypeptide 1	GNGT1	207166_at	9.878
lipopolysaccharide binding protein	LBP	211652_s_at	9.867
keratin 81	KRT81	213711_at	9.186
Interleukin 1 receptor-like 1	IL1RL1	234066_at	9.109
distal-less homeobox 1	DLX1	242138_at	8.579
tumor necrosis factor (ligand) superfamily, member 9	TNFSF9	206907_at	8.53
chemokine (C-C motif) ligand 2	CCL2	216598_s_at	8.503
solute carrier family 25 (mitochondrial carrier; ornithine transporter) member 2	SLC25A2	224166_at	8.37
hypothetical protein LOC90246	LOC90246	233835_at	7.669
neural cell adhesion molecule 1	NCAM1	227394_at	7.19
Inhibitor of growth family, member 2	ING2	213544_at	7.105
heat shock 70kDa protein 1A /// heat shock 70kDa protein 1B	HSPA1A /// HS	200800_s_at	7.074
hypothetical gene supported by BC011527; BC021928; BC011527; BC021928	LOC284260	1570208_at	7.018
leucine rich repeat containing 4	LRRC4	223552_at	6.963
protocadherin 9	PCDH9	219738_s_at	6.945
neutrophil cytosolic factor 2	NCF2	209949_at	6.843
tubulin, beta 2B	TUBB2B	214023_x_at	6.831
hypothetical LOC100127940	LOC100127940	1564299_at	6.828
calcitonin-related polypeptide alpha	CALCA	217561_at	6.805
CD300 molecule-like family member g	CD300LG	1552509_a_at	6.675
FEZ family zinc finger 2	FEZF2	221086_s_at	6.65
chromosome 2 open reading frame 88	C2orf88	228195_at	6.64
Tropomyosin 4	TPM4	1559989_at	6.591
neurofilament, medium polypeptide	NEFM	205113_at	6.543
synaptotagmin XV	SYT15	1560879_a_at	6.516
heparan sulfate 6-O-sulfotransferase 3	HS6ST3	232275_s_at	6.499
myozenin 2	MYOZ2	207148_x_at	6.44
suppressor of cytokine signaling 2	SOCS2	203372_s_at	6.416
UPF0632 protein A	LOC388630	244472_at	6.388
hypothetical protein LOC254057	LOC254057	232370_at	6.369
hypothetical protein LOC284542	LOC284542	230920_at	6.349
collagen, type XXIII, alpha 1	COL23A1	229168_at	6.304
hypothetical LOC84983	MGC14436	1553811_at	6.267
contactin associated protein-like 2	CNTNAP2	219302_s_at	6.263
sterile alpha motif domain containing 4A	SAMD4A	215120_s_at	6.246
A kinase (PRKA) anchor protein 5	AKAP5	230846_at	6.169
myozenin 2	MYOZ2	213782_s_at	6.144
potassium voltage-gated channel, KQT-like subfamily, member 5	KCNQ5	244623_at	6.034
solute carrier family 37 (glycerol-3-phosphate transporter), member 1	SLC37A1	218928_s_at	6.029
pyruvate dehydrogenase kinase, isozyme 4	PDK4	225207_at	5.985
matrix metallopeptidase 24 (membrane-inserted)	MMP24	213171_s_at	5.825
NEL-like 1 (chicken)	NELL1	206089_at	5.742
cartilage oligomeric matrix protein	COMP	205713_s_at	5.662
hedgehog interacting protein	HHIP	1556037_s_at	5.573
cyclic AMP-regulated phosphoprotein, 21 kD /// hypothetical protein LOC100130503	ARPP-21 /// LO	1556599_s_at	5.243
KIAA1128	KIAA1128	1554131_at	5.23
ribonuclease, RNase A family, 1 (pancreatic)	RNASE1	201785_at	5.165

Table S2.2 cont'd.

SV2 related protein homolog (rat)	SVOP	229818_at	5.14
coiled-coil domain containing 85A	CCDC85A	235228_at	5.131
heat shock 70kDa protein 1A /// heat shock 70kDa protein 1B	HSPA1A /// HSI	202581_at	5.082
chromosome 14 open reading frame 81	C14orf81	1564499_at	5.047
LIM domain only 2 (rhombotin-like 1)	LMO2	204249_s_at	4.971
keratin associated protein 19-3	KRTAP19-3	240967_at	4.965
retinol binding protein 2, cellular	RBP2	231734_at	4.96
suppressor of cytokine signaling 2	SOCS2	203373_at	4.938
chromosome 1 open reading frame 14	C1orf14	220996_s_at	4.936
neuron navigator 2	NAV2	218330_s_at	4.868
Syntrophin, gamma 1	SNTG1	1562287_at	4.854
G protein-coupled receptor 83	GPR83	222953_at	4.849
doublecortin domain containing 5	DCDC5	232603_at	4.783
lin-7 homolog B (C. elegans)	LIN7B	241957_x_at	4.773
acyl-CoA thioesterase 11	ACOT11	214763_at	4.76
aldo-keto reductase family 1, member C2 (dihydrodiol dehydrogenase 2; bile acid binding protein; 3-alpha	AKR1C2	211653_x_at	4.759
UDP-Gal:betaGlcNAc beta 1,3-galactosyltransferase, polypeptide 5	B3GALT5	206947_at	4.757
crystallin, alpha B	CRYAB	209283_at	4.708
tachykinin, precursor 1	TAC1	206552_s_at	4.698
msh homeobox 2	MSX2	205555_s_at	4.689
epiplakin 1	EPPK1	232165_at	4.664
paired related homeobox 2	PRRX2	219729_at	4.659
chromosome 10 open reading frame 126	C10orf126	1553915_at	4.65
Na+/H+ exchanger domain containing 2	NHEDC2	229491_at	4.648
complement component (3b/4b) receptor 1-like	CR1L	239206_at	4.631
chromosome 12 open reading frame 59	C12orf59	236646_at	4.616
chromosome 12 open reading frame 47	C12orf47	212868_x_at	4.586
plexin A2	PLXNA2	213030_s_at	4.575
heparan sulfate 6-O-sulfotransferase 3	HS6ST3	232276_at	4.547
glutathione peroxidase 3 (plasma)	GPX3	214091_s_at	4.534
neural cell adhesion molecule 1	NCAM1	209968_s_at	4.53
msh homeobox 2	MSX2	210319_x_at	4.527
pyruvate dehydrogenase kinase, isozyme 4	PDK4	1562321_at	4.525
G protein-coupled receptor 137C	GPR137C	242592_at	4.515
mal, T-cell differentiation protein-like	MALL	209373_at	4.481
phospholipase C, eta 1	PLCH1	216634_at	4.47
G protein-coupled receptor 158	GPR158	232195_at	4.448
kynurenine 3-monooxygenase (kynurenine 3-hydroxylase)	KMO	205306_x_at	4.438
fibrinogen C domain containing 1	FIBCD1	240042_at	4.389
uronyl-2-sulfotransferase	UST	205138_s_at	4.359
Atonal homolog 8 (Drosophila)	ATOH8	1558706_a_at	4.353
chromosome 13 open reading frame 38	C13orf38	234085_at	4.351
hypothetical protein LOC641364	LOC641364	1562253_at	4.35
transient receptor potential cation channel, subfamily C, member 3	TRPC3	210814_at	4.341
neurofilament, light polypeptide	NEFL	221801_x_at	4.293
placenta-specific 1	PLAC1	219702_at	4.286
maestro	MRO	224324_at	4.283
atonal homolog 8 (Drosophila)	ATOH8	228890_at	4.266
aldo-keto reductase family 1, member C1 (dihydrodiol dehydrogenase 1; 20-alpha (3-alpha)-hydroxysteroi	AKR1C1	204151_x_at	4.254
replication protein A4, 34kDa	RPA4	221143_at	4.239
hypothetical protein LOC652821 /// variable charge, Y-linked /// variable charge, Y-linked 1B	LOC652821 /// '	206922_at	4.209
serpin peptidase inhibitor, clade B (ovalbumin), member 5	SERPINB5	1555551_at	4.159
hypothetical protein MGC16121	MGC16121	228235_at	4.159
par-3 partitioning defective 3 homolog B (C. elegans)	PARD3B	1555113_at	4.144
slit homolog 3 (Drosophila)	SLIT3	216216_at	4.107
caspase 12 (gene/pseudogene)	CASP12	1564736_a_at	4.104
DnaJ (Hsp40) homolog, subfamily A, member 4	DNAJA4	225061_at	4.102
A kinase (PRKA) anchor protein 5	AKAP5	207800_at	4.1
activating transcription factor 3	ATF3	202672_s_at	4.099
TMF1-regulated nuclear protein 1	TRNP1	227862_at	4.095
arginine-glutamic acid dipeptide (RE) repeats	RERE	200939_s_at	4.089
solute carrier family 23 (nucleobase transporters), member 3	SLC23A3	1553265_at	4.076
Cell division cycle 20 homolog B (S. cerevisiae)	CDC20B	240161_s_at	4.069
coiled-coil domain containing 3	CCDC3	223316_at	4.062
THAP domain containing, apoptosis associated protein 2	THAP2	230380_at	4.04
calponin 1, basic, smooth muscle	CNN1	203951_at	4.023
natriuretic peptide receptor A/guanylate cyclase A (atrionatriuretic peptide receptor A)	NPR1	204648_at	4.018
glycoprotein V (platelet)	GP5	211525_s_at	3.984
interleukin 8	IL8	211506_s_at	3.977
hypothetical LOC100268168	LOC100268168	233491_at	3.975
placental growth factor	PGF	209652_s_at	3.963
bone morphogenetic protein receptor, type IB	BMPR1B	210523_at	3.961
immunoglobulin-like and fibronectin type III domain containing 1	IGFN1	229275_at	3.928
DnaJ (Hsp40) homolog, subfamily A, member 4	DNAJA4	1554334_a_at	3.921
parathyroid hormone-like hormone	PTHLH	211756_at	3.915

Table S2.2 cont'd.

transducin-like enhancer of split 6 (E(sp1) homolog, Drosophila)	TLE6	1553813_s_at	3.895
aggrecan	ACAN	207692_s_at	3.883
protein phosphatase 1, regulatory (inhibitor) subunit 14C	PPP1R14C	226907_at	3.88
similar to hCG41624	LOC100128071	1556560_a_at	3.865
isopentenyl-diphosphate delta isomerase 2	IDI2	1552491_at	3.86
Triple functional domain (PTPRF interacting)	TRIO	216700_at	3.845
discoidin, CUB and LCCL domain containing 2	DCBLD2	213873_at	3.841
cholecystokinin	CCK	205827_at	3.831
T-box, brain, 1	TBR1	220025_at	3.801
Phospholamban	PLN	228202_at	3.777
aldo-keto reductase family 1, member C2 (dihydrodiol dehydrogenase 2; bile acid binding protein; 3-alpha	AKR1C2	209699_x_at	3.771
nescient helix loop helix 2	NHLH2	215228_at	3.765
AT rich interactive domain 1A (SWI-like)	ARID1A	207591_s_at	3.739
hairy/enhancer-of-split related with YRPW motif 1	HEY1	44783_s_at	3.736
dynein, axonemal, heavy chain 1	DNAH1	239059_at	3.729
aldo-keto reductase family 1, member C1 (dihydrodiol dehydrogenase 1; 20-alpha (3-alpha)-hydroxysteroi	AKR1C1	216594_x_at	3.725
DiGeorge syndrome critical region gene 12	DGCR12	1566235_at	3.722
frizzled homolog 8 (Drosophila)	FZD8	227405_s_at	3.713
acid phosphatase 5, tartrate resistant	ACP5	204638_at	3.709
frizzled homolog 8 (Drosophila)	FZD8	224325_at	3.698
distal-less homeobox 3	DLX3	231778_at	3.698
cAMP responsive element binding protein 5	CREB5	229228_at	3.695
similar to hCG1815045	LOC100131781	240320_at	3.694
epiplakin 1	EPPK1	208156_x_at	3.684
chromodomain helicase DNA binding protein 5	CHD5	213965_s_at	3.683
KH domain containing, RNA binding, signal transduction associated 2	KHDRBS2	215527_at	3.679
peptidase domain containing associated with muscle regeneration 1	PAMR1	213661_at	3.667
WNK lysine deficient protein kinase 2	WNK2	1557536_at	3.665
catenin (cadherin-associated protein), delta 2 (neural plakophilin-related arm-repeat protein)	CTNND2	209617_s_at	3.665
HECT, C2 and WW domain containing E3 ubiquitin protein ligase 2	HECW2	232080_at	3.641
parathyroid hormone-like hormone	PTHLH	206300_s_at	3.641
calsequestrin 1 (fast-twitch, skeletal muscle)	CASQ1	219645_at	3.64
synovial sarcoma, X breakpoint 2 interacting protein	SSX2IP	203015_s_at	3.625
heat shock 70kDa protein 1A	HSPA1A	200799_at	3.62
Hypothetical LOC150538	FLJ32063	235147_at	3.618
gap junction protein, gamma 1, 45kDa	GJC1	228563_at	3.617
transmembrane protein 132E	TMEM132E	243708_at	3.56
gamma-aminobutyric acid (GABA) B receptor, 2	GABBR2	217077_s_at	3.544
microtubule-associated protein 1B	MAP1B	226084_at	3.528
chromosome 1 open reading frame 129	C1orf129	221182_at	3.525
signal transducer and activator of transcription 3 (acute-phase response factor)	STAT3	243213_at	3.509
insulin-like growth factor binding protein 5	IGFBP5	1555997_s_at	3.487
calmodulin binding transcription activator 1	CAMTA1	213268_at	3.465
chymotrypsin-like elastase family, member 3A	CELA3A	210080_x_at	3.457
homeobox C13	HOXC13	219832_s_at	3.44
talin 2	TLN2	212701_at	3.438
chondroitin sulfate proteoglycan 4	CSPG4	214297_at	3.436
atlastin GTPase 2	ATL2	237968_at	3.429
elastin microfibril interfacer 2	EMILIN2	224374_s_at	3.429
ArfGAP with dual PH domains 1	ADAP1	219150_s_at	3.411
Neural cell adhesion molecule 1	NCAM1	231532_at	3.405
Kruppel-like factor 6	KLF6	208960_s_at	3.401
growth arrest and DNA-damage-inducible, beta	GADD45B	209304_x_at	3.387
hypothetical protein LOC144481	LOC144481	1559315_s_at	3.383
UL16 binding protein 2	ULBP2	238542_at	3.378
oxytocin, prepropeptide	OXT	207576_x_at	3.368
met proto-oncogene (hepatocyte growth factor receptor)	MET	203510_at	3.364
copine IV	CPNE4	231336_at	3.362
Na+/H+ exchanger domain containing 2	NHEDC2	1564746_at	3.347
makorin ring finger protein 2	MKRN2	216995_x_at	3.338
potassium voltage-gated channel, Shaw-related subfamily, member 4	KCNC4	208251_at	3.335
neuron navigator 2	NAV2	222598_s_at	3.326
hypothetical LOC100126784	LOC100126784	240407_at	3.326
Fc receptor-like A	FCRLA	235400_at	3.312
eukaryotic translation initiation factor 4A, isoform 2	EIF4A2	1556350_a_at	3.305
melanoma cell adhesion molecule	MCAM	209087_x_at	3.3
dual specificity phosphatase 5 pseudogene	DUSP5P	1553299_at	3.296
glycoprotein, alpha-galactosyltransferase 1	GGTA1	228376_at	3.291
Hypothetical protein LOC203274	LOC203274	232034_at	3.29
kazrin	RP1-21O18.1	229144_at	3.286
brain-derived neurotrophic factor	BDNF	206382_s_at	3.278
AF4/FMR2 family, member 2	AFF2	206105_at	3.267
ATPase type 13A3	ATP13A3	219558_at	3.262
GPRIN family member 3	GPRIN3	1556697_at	3.253
Atonal homolog 8 (Drosophila)	ATOH8	1558705_at	3.247

Table S2.2 cont'd.

keratin 73	KRT73	1553537_at	3.238
adrenergic, beta-1-, receptor	ADRB1	229309_at	3.225
tropomyosin 1 (alpha)	TPM1	206117_at	3.223
kazrin	RP1-21O18.1	213478_at	3.222
muscle RAS oncogene homolog	MRAS	225185_at	3.218
hairy/enhancer-of-split related with YRPW motif 1	HEY1	218839_at	3.216
mitogen-activated protein kinase kinase kinase kinase 1	MAP4K1	214339_s_at	3.207
echinoderm microtubule associated protein like 2	EML2	204399_s_at	3.204
hyaluronoglucosaminidase 1	HYAL1	210619_s_at	3.197
synovial sarcoma, X breakpoint 2 interacting protein	SSX2IP	203019_x_at	3.195
stimulated by retinoic acid gene 6 homolog (mouse)	STRA6	1569334_at	3.185
Kruppel-like factor 6	KLF6	208961_s_at	3.185
tripartite motif-containing 14	TRIM14	211044_at	3.184
SERTA domain containing 4	SERTAD4	229674_at	3.181
cAMP responsive element binding protein 5	CREB5	205931_s_at	3.167
histone cluster 1, H3g	HIST1H3G	208496_x_at	3.156
cysteinyl-tRNA synthetase	CARS	240982_at	3.155
synovial sarcoma, X breakpoint 2 interacting protein	SSX2IP	210871_x_at	3.153
hypothetical protein LOC149086	LOC149086	1566647_s_at	3.152
hypothetical protein LOC731477	LOC731477	237312_at	3.146
Glycoprotein, synaptic 2	GPSN2	231556_at	3.146
growth arrest and DNA-damage-inducible, beta	GADD45B	209305_s_at	3.14
cartilage acidic protein 1	CRTAC1	221204_s_at	3.131
synovial sarcoma, X breakpoint 2 interacting protein	SSX2IP	203018_s_at	3.122
msh homeobox 1	MSX1	205932_s_at	3.121
Hypothetical protein DKFZp686O24166	DKFZp686O24	229715_at	3.115
SLAM family member 9	SLAMF9	1553770_a_at	3.113
keratin associated protein 2-4	KRTAP2-4	1555673_at	3.112
family with sequence similarity 83, member G	FAM83G	228587_at	3.108
SMAD family member 9	SMAD9	227719_at	3.101
interleukin 1 family, member 5 (delta)	IL1F5	222223_s_at	3.098
v-myb myeloblastosis viral oncogene homolog (avian)	MYB	204798_at	3.094
natriuretic peptide receptor A/guanylate cyclase A (atrionatriuretic peptide receptor A)	NPR1	32625_at	3.083
heat shock protein 90kDa alpha (cytosolic), class A member 1	HSP90AA1	211968_s_at	3.081
stimulated by retinoic acid gene 6 homolog (mouse)	STRA6	221701_s_at	3.08
hypothetical protein MGC16121	MGC16121	227488_at	3.072
peptidylprolyl isomerase A (cyclophilin A)-like 4A /// peptidylprolyl isomerase A (cyclophilin A)-like 4B /// pe	PPIAL4A /// PP	217136_at	3.066
HHIP-like 2	HHIPL2	220283_at	3.056
synovial sarcoma, X breakpoint 2 interacting protein	SSX2IP	203016_s_at	3.056
microtubule-associated protein 1B	MAP1B	212233_at	3.056
hypothetical protein LOC100132388	LOC100132388	224241_s_at	3.045
phospholipase C, epsilon 1	PLCE1	205111_s_at	3.04
tousled-like kinase 2	TLK2	233349_at	3.038
leucine zipper protein 2	LUZP2	215323_at	3.034
GATA binding protein 3	GATA3	209602_s_at	3.034
Kruppel-like factor 4 (gut)	KLF4	220266_s_at	3.033
solute carrier family 4, sodium bicarbonate cotransporter, member 7	SLC4A7	207604_s_at	3.033
kinesin family member 23	KIF23	204709_s_at	3.031
hypothetical gene supported by AK098783	FLJ25917	1564295_at	3.03
nuclear receptor interacting protein 3	NRIP3	222900_at	3.023
methylenetetrahydrofolate dehydrogenase (NADP+ dependent) 1, methenyltetrahydrofolate cyclohydrolas	MTHFD1	202309_at	3.005
dual specificity phosphatase 1	DUSP1	201044_x_at	2.985
gremlin 2, cysteine knot superfamily, homolog (Xenopus laevis)	GREM2	235504_at	2.982
UDP-N-acetyl-alpha-D-galactosamine:polypeptide N-acetylgalactosaminyltransferase 9 (GalNAc-T9) /// si	GALNT9 /// LO	229451_at	2.974
matrix metallopeptidase 25	MMP25	207890_s_at	2.973
growth arrest and DNA-damage-inducible, beta	GADD45B	207574_s_at	2.973
ovo-like 1(Drosophila)	OVOL1	229396_at	2.969
progesterone receptor	PGR	228554_at	2.967
Kruppel-like factor 2 (lung)	KLF2	219371_s_at	2.967
3-hydroxy-3-methylglutaryl-Coenzyme A synthase 1 (soluble)	HMGCS1	205822_s_at	2.964
Kruppel-like factor 4 (gut)	KLF4	221841_s_at	2.962
heat shock 27kDa protein 1	HSPB1	201841_s_at	2.961
interleukin 8	IL8	202859_x_at	2.956
glycerol kinase	GK	215977_x_at	2.955
Kruppel-like factor 6	KLF6	1555832_s_at	2.953
secretogranin II (chromogranin C)	SCG2	204035_at	2.94
plexin A2	PLXNA2	227032_at	2.938
pleckstrin homology-like domain, family A, member 1	PHLDA1	218000_s_at	2.933
somatostatin receptor 1	SSTR1	235591_at	2.932
chromosome 18 open reading frame 1	C18orf1	207996_s_at	2.927
brain-derived neurotrophic factor	BDNF	239367_at	2.919
fibulin 2	FBLN2	203886_s_at	2.905
parathyroid hormone-like hormone	PTHLH	210355_at	2.896
hairy and enhancer of split 6 (Drosophila)	HES6	226446_at	2.89
ArfGAP with dual PH domains 1	ADAP1	90265_at	2.888

Table S2.2 cont'd.

poliovirus receptor	PVR	212662_at	2.888
solute carrier family 25 (mitochondrial carrier; ornithine transporter) member 15	SLC25A15	222705_s_at	2.879
insulin-like 3 (Leydig cell)	INSL3	1553594_a_at	2.875
similar to hCG2042915	LOC100129673	236611_at	2.871
Collagen, type XXVII, alpha 1	COL27A1	1564008_at	2.87
adaptor-related protein complex 1, sigma 3 subunit	AP1S3	1555731_a_at	2.866
prolactin receptor	PRLR	216638_s_at	2.865
tubulin tyrosine ligase-like family, member 5	TTLL5	1566102_at	2.851
Threonyl-tRNA synthetase	TARS	240206_at	2.847
glycine-N-acyltransferase-like 1	GLYATL1	227794_at	2.843
one cut homeobox 2	ONECUT2	233441_at	2.842
transient receptor potential cation channel, subfamily C, member 3	TRPC3	206425_s_at	2.834
F-box protein 27	FBXO27	235169_at	2.825
synaptotagmin XV	SYT15	1560878_at	2.825
chromosome 17 open reading frame 53	C17orf53	219879_s_at	2.823
mucin 12, cell surface associated	MUC12	226654_at	2.816
SMAD family member 7	SMAD7	204790_at	2.813
cysteine-rich, angiogenic inducer, 61	CYR61	210764_s_at	2.813
DnaJ (Hsp40) homolog, subfamily C, member 6	DNAJC6	204720_s_at	2.807
Kruppel-like factor 6	KLF6	224606_at	2.798
carbonic anhydrase II	CA2	209301_at	2.796
TIMP metallopeptidase inhibitor 3	TIMP3	201150_s_at	2.787
scavenger receptor class A, member 5 (putative)	SCARA5	235849_at	2.778
chimerin (chimaerin) 2	CHN2	213385_at	2.776
chromosome 1 open reading frame 114	C1orf114	1555112_a_at	2.774
discoidin, CUB and LCCL domain containing 2	DCBLD2	213865_at	2.769
SHC (Src homology 2 domain containing) family, member 4	SHC4	230538_at	2.765
aldehyde dehydrogenase 3 family, member B2	ALDH3B2	204941_s_at	2.76
PDZ and LIM domain 3	PDLIM3	238592_at	2.758
prostaglandin E synthase	PTGES	207388_s_at	2.757
ubiquitin-like modifier activating enzyme 6	UBA6	1555441_at	2.756
sema domain, seven thrombospondin repeats (type 1 and type 1-like), transmembrane domain (TM) and s	SEMA5B	223610_at	2.752
KIAA1826	KIAA1826	223799_at	2.752
serine/threonine kinase 35	STK35	1553673_at	2.741
hairy and enhancer of split 4 (Drosophila)	HES4	227347_x_at	2.737
fatty acid binding protein 3, muscle and heart (mammary-derived growth inhibitor)	FABP3	214285_at	2.727
phosphatidylinositol transfer protein, cytoplasmic 1	PITPNC1	229414_at	2.725
brix domain containing 5	BXDC5	234243_at	2.718
echinoderm microtubule associated protein like 1	EML1	204797_s_at	2.712
tyrosine 3-monooxygenase/tryptophan 5-monooxygenase activation protein, eta polypeptide	YWHAH	201020_at	2.704
KIT ligand	KITLG	226534_at	2.702
protein phosphatase 4, regulatory subunit 1-like	PPP4R1L	223733_s_at	2.7
hyaluronan synthase 2	HAS2	206432_at	2.696
Similar to programmed cell death 6 interacting protein	LOC731884	217520_x_at	2.689
mucin 17, cell surface associated	MUC17	232321_at	2.688
chromosome 20 open reading frame 195	C20orf195	220426_at	2.685
tubulin, beta 2A	TUBB2A	204141_at	2.682
poly(A) binding protein, cytoplasmic 1-like	PABPC1L	233104_at	2.682
progestin and adipoQ receptor family member IX	PAQR9	1558322_a_at	2.681
neuron navigator 2	NAV2	222599_s_at	2.678
interleukin 1 receptor accessory protein-like 1	IL1RAPL1	222963_s_at	2.666
heat shock 60kDa protein 1 (chaperonin) /// heat shock 60kDa protein 1 (chaperonin) pseudogene 4	HSPD1 /// HSP	243372_at	2.642
gamma-aminobutyric acid (GABA) B receptor, 2	GABBR2	211679_x_at	2.641
actinin, alpha 2	ACTN2	203863_at	2.635
annexin A1	ANXA1	201012_at	2.631
NPC1 (Niemann-Pick disease, type C1, gene)-like 1	NPC1L1	220106_at	2.631
protocadherin 10	PCDH10	1552925_at	2.624
lin-7 homolog B (C. elegans)	LIN7B	219760_at	2.621
aminolevulinate, delta-, synthase 2	ALAS2	244205_at	2.621
hypothetical protein LOC100132356	hCG_2039148	1558310_s_at	2.611
v-yes-1 Yamaguchi sarcoma viral related oncogene homolog	LYN	202626_s_at	2.609
family with sequence similarity 84, member B	FAM84B	225864_at	2.594
calpain 5	CAPN5	205166_at	2.584
glycerol kinase	GK	207387_s_at	2.583
phosphatidylinositol transfer protein, membrane-associated 2	PITPNM2	1552924_a_at	2.579
leucine-rich repeat LGI family, member 2	LGI2	219699_at	2.579
oxidative stress induced growth inhibitor 1	OSGIN1	219475_at	2.578
serine incorporator 2	SERINC2	224762_at	2.578
KIAA2018	KIAA2018	242508_at	2.571
oxysterol binding protein-like 6	OSBPL6	238575_at	2.563
dual specificity phosphatase 26 (putative)	DUSP26	219144_at	2.56
Kruppel-like factor 13	KLF13	219878_s_at	2.551
KIAA1310	KIAA1310	1558652_at	2.548
jagged 1 (Alagille syndrome)	JAG1	209098_s_at	2.546
tubulin, beta 2A /// tubulin, beta 2B	TUBB2A /// TUE	209372_x_at	2.546

Table S2.2 cont'd.

deleted in liver cancer 1	DLC1	224822_at	2.543
UL16 binding protein 2	ULBP2	221291_at	2.537
cysteine and glycine-rich protein 2	CSRP2	207030_s_at	2.537
gremlin 2, cysteine knot superfamily, homolog (Xenopus laevis)	GREM2	240509_s_at	2.535
hypothetical LOC401317	LOC401317	242329_at	2.533
protocadherin 9	PCDH9	219737_s_at	2.533
cysteine and glycine-rich protein 2	CSRP2	211126_s_at	2.532
lipopolysaccharide-induced TNF factor	LITAF	200706_s_at	2.532
ADAM metallopeptidase domain 28	ADAM28	208269_s_at	2.531
vaccinia related kinase 3	VRK3	239190_at	2.523
zinc finger and BTB domain containing 1	ZBTB1	213376_at	2.516
Anthrax toxin receptor 1	ANTXR1	234832_at	2.512
armadillo repeat gene deletes in velocardiofacial syndrome	ARVCF	217516_x_at	2.508
C-type lectin domain family 4, member E	CLEC4E	222934_s_at	2.507
GATA binding protein 2	GATA2	209710_at	2.501
nuclear receptor interacting protein 3	NRIP3	219557_s_at	2.495
GINS complex subunit 3 (Psf3 homolog)	GINS3	218719_s_at	2.481
family with sequence similarity 62 (C2 domain containing), member C	FAM62C	239770_at	2.457
carbohydrate (N-acetylgalactosamine 4-0) sulfotransferase 8	CHST8	221065_s_at	2.451
gamma-aminobutyric acid (GABA) A receptor, beta 1	GABRB1	207010_at	2.448
stanniocalcin 2	STC2	203439_s_at	2.441
calmodulin binding transcription activator 1	CAMTA1	1555370_a_at	2.439
T cell receptor beta variable 27	TRBV27	241133_at	2.439
D-aspartate oxidase	DDO	207418_s_at	2.435
Transforming, acidic coiled-coil containing protein 1	TACC1	1557305_at	2.433
GATA binding protein 5	GATA5	238095_at	2.432
insulin-like growth factor binding protein 5	IGFBP5	203424_s_at	2.423
spectrin, beta, non-erythrocytic 1	SPTBN1	226342_at	2.422
cancer susceptibility candidate 5	CASC5	1552680_a_at	2.42
phospholipase inhibitor	LOC646627	238143_at	2.417
T-box 3	TBX3	229576_s_at	2.416
KN motif and ankyrin repeat domains 4	KANK4	229125_at	2.414
Norrie disease (pseudoglioma)	NDP	206022_at	2.408
solute carrier family 7 (cationic amino acid transporter, y+ system), member 1	SLC7A1	212290_at	2.408
solute carrier family 25 (mitochondrial carrier; ornithine transporter) member 15	SLC25A15	218653_at	2.4
MHC class I polypeptide-related sequence A	MICA	205904_at	2.396
aquaporin 1 (Colton blood group)	AQP1	209047_at	2.395
angiotensinogen (serpin peptidase inhibitor, clade A, member 8)	AGT	202834_at	2.393
MAP/microtubule affinity-regulating kinase 1	MARK1	226653_at	2.386
schlafen family member 5	SLFN5	243999_at	2.384
semaphorin 7A, GPI membrane anchor (John Milton Hagen blood group)	SEMA7A	230345_at	2.382
deleted in liver cancer 1	DLC1	220511_s_at	2.379
PDZ and LIM domain 3	PDLIM3	210170_at	2.378
mal, T-cell differentiation protein	MAL	204777_s_at	2.376
zinc finger, MYM-type 2	ZMYM2	210281_s_at	2.375
ATPase, class V, type 10A	ATP10A	214255_at	2.375
bone morphogenetic protein 7	BMP7	211259_s_at	2.374
glycine amidinotransferase (L-arginine:glycine amidinotransferase)	GATM	216733_s_at	2.371
heat shock 70kD protein 12B	HSPA12B	234610_at	2.371
mex-3 homolog C (C. elegans)	MEX3C	1556874_a_at	2.37
tetraspanin 12	TSPAN12	219274_at	2.368
matrix metallopeptidase 7 (matrilysin, uterine)	MMP7	204259_at	2.368
tetraspanin 10	TSPAN10	223795_at	2.366
insulin-like growth factor binding protein 5	IGFBP5	203426_s_at	2.363
cyclic nucleotide gated channel beta 1	CNGB1	207342_at	2.359
ChaC, cation transport regulator homolog 1 (E. coli)	CHAC1	219270_at	2.358
RAB27B, member RAS oncogene family	RAB27B	207017_at	2.357
spire homolog 2 (Drosophila)	SPIRE2	227706_at	2.353
small VCP/p97-interacting protein	SVIP	230285_at	2.353
phosphatidylinositol transfer protein, cytoplasmic 1	PITPNC1	238649_at	2.351
pyruvate dehydrogenase (lipoamide) alpha 2	PDHA2	214518_at	2.348
rhodopsin	RHO	206454_s_at	2.344
glycerol kinase	GK	217167_x_at	2.343
small glutamine-rich tetratricopeptide repeat (TPR)-containing, beta	SGTB	228745_at	2.342
N-acetylglucosamine-1-phosphate transferase, alpha and beta subunits	GNPTAB	220398_at	2.342
tubulin tyrosine ligase-like family, member 7	TTLL7	219882_at	2.339
PH domain and leucine rich repeat protein phosphatase-like	PHLPPL	213407_at	2.337
v-yes-1 Yamaguchi sarcoma viral related oncogene homolog	LYN	210754_s_at	2.337
chloride intracellular channel 3	CLIC3	219529_at	2.336
plasticity-related gene 2	PRG2	220798_x_at	2.336
microRNA host gene 1 (non-protein coding)	MIRHG1	232291_at	2.334
Janus kinase 2	JAK2	205841_at	2.333
serine/threonine protein kinase MST4	RP6-213H19.1	224407_s_at	2.332
RAB27B, member RAS oncogene family	RAB27B	207018_s_at	2.331
solute carrier family 14 (urea transporter), member 2	SLC14A2	208409_at	2.331

Table S2.2 cont'd.

phosphatidylinositol transfer protein, cytoplasmic 1	PITPNC1	219155_at	2.312
Tropomyosin 1 (alpha)	TPM1	238688_at	2.312
methyl-CpG binding domain protein 2	MBD2	214397_at	2.31
T-box 2	TBX2	213417_at	2.309
Jagged 1 (Alagille syndrome)	JAG1	231183_s_at	2.306
GATA binding protein 3	GATA3	209604_s_at	2.301
tensin 4	TNS4	230398_at	2.297
v-yes-1 Yamaguchi sarcoma viral related oncogene homolog	LYN	202625_at	2.295
jumonji domain containing 4	JMJD4	230810_at	2.295
small VCP/p97-interacting protein	SVIP	226278_at	2.293
chromosome 20 open reading frame 57	C20orf57	234829_at	2.293
contactin 3 (plasmacytoma associated)	CNTN3	229831_at	2.292
jun D proto-oncogene	JUND	203751_x_at	2.291
nuclear receptor subfamily 1, group D, member 1 /// thyroid hormone receptor, alpha (erythroblastic leuke	NR1D1 /// THRA	204760_s_at	2.291
chondroitin sulfate proteoglycan 4	CSPG4	204736_s_at	2.282
heparin-binding EGF-like growth factor	HBEGF	38037_at	2.28
MHC class I polypeptide-related sequence A /// MHC class I polypeptide-related sequence B	MICA /// MICB	205905_s_at	2.277
dishevelled associated activator of morphogenesis 1	DAAM1	244062_at	2.276
natural cytotoxicity triggering receptor 2	NCR2	217493_x_at	2.269
inhibitor of DNA binding 3, dominant negative helix-loop-helix protein	ID3	207826_s_at	2.269
acylphosphatase 1, erythrocyte (common) type	ACYP1	205260_s_at	2.268
pleckstrin homology-like domain, family A, member 1	PHLDA1	217997_at	2.268
UDP glucuronosyltransferase 1 family, polypeptide A1 /// UDP glucuronosyltransferase 1 family, polypepti	UGT1A1 /// UG	208596_s_at	2.265
choroideremia-like (Rab escort protein 2)	CHML	226350_at	2.262
echinoderm microtubule associated protein like 6	EML6	229656_s_at	2.261
prostaglandin I2 (prostacyclin) synthase	PTGIS	211892_s_at	2.26
karyopherin alpha 4 (importin alpha 3)	KPNA4	209653_at	2.259
ubiquitin specific peptidase 53	USP53	231817_at	2.258
blood vessel epicardial substance	BVES	223853_at	2.256
tetratricopeptide repeat domain 32	TTC32	226838_at	2.25
glutamate receptor, ionotropic, kainate 2	GRIK2	1563754_at	2.25
v-ets erythroblastosis virus E26 oncogene homolog 1 (avian)	ETS1	1555355_a_at	2.249
Hyaluronan synthase 2	HAS2	230372_at	2.244
syndecan 1	SDC1	201287_s_at	2.244
pleckstrin 2	PLEK2	218644_at	2.24
T-box 18	TBX18	1559840_s_at	2.238
fibroblast growth factor receptor 3	FGFR3	204379_s_at	2.227
myosin X	MYO10	201976_s_at	2.225
kinesin family member 7	KIF7	229405_at	2.224
GNAS complex locus	GNAS	217673_x_at	2.223
non imprinted in Prader-Willi/Angelman syndrome 1	NIPA1	225752_at	2.223
glycogen synthase kinase 3 alpha	GSK3A	202210_x_at	2.22
radical S-adenosyl methionine domain containing 2	RSAD2	213797_at	2.22
peptidoglycan recognition protein 4	PGLYRP4	220944_at	2.218
WD repeat domain 69	WDR69	242162_at	2.215
ADP-ribosylarginine hydrolase	ADPRH	228042_at	2.214
tight junction protein 2 (zona occludens 2)	TJP2	202085_at	2.213
KIAA0182	KIAA0182	212056_at	2.209
tubulin, beta 3	TUBB3	202154_x_at	2.204
keratin 24	KRT24	220267_at	2.191
malic enzyme 2, NAD(+)-dependent, mitochondrial	ME2	210154_at	2.187
abhydrolase domain containing 5	ABHD5	218739_at	2.185
T-box 3	TBX3	225544_at	2.183
cadherin-like 24	CDH24	1553166_at	2.181
cadherin 4, type 1, R-cadherin (retinal)	CDH4	1563587_at	2.177
synovial sarcoma, X breakpoint 2 interacting protein	SSX2IP	203017_s_at	2.175
blood vessel epicardial substance	BVES	228783_at	2.173
similar to MCT /// solute carrier family 16, member 5 (monocarboxylic acid transporter 6)	LOC100133772	206600_s_at	2.166
transmembrane protein 70	TMEM70	219449_s_at	2.162
inhibitor of DNA binding 4, dominant negative helix-loop-helix protein	ID4	209291_at	2.158
protein phosphatase 1, regulatory (inhibitor) subunit 15A	PPP1R15A	202014_at	2.157
integrin, alpha 6	ITGA6	201656_at	2.155
synaptotagmin XI	SYT11	209198_s_at	2.15
kelch domain containing 10	KLHDC10	209254_at	2.15
transient receptor potential cation channel, subfamily V, member 2	TRPV2	219282_s_at	2.149
tropomyosin 1 (alpha)	TPM1	1558532_at	2.145
serine hydrolase-like 2	SERHL2	217276_x_at	2.144
beta-1,4-N-acetyl-galactosaminyl transferase 1	B4GALNT1	206435_at	2.14
dual specificity phosphatase 8	DUSP8	206374_at	2.133
progestin and adipoQ receptor family member V	PAQR5	220333_at	2.132
hypothetical protein LOC149684	LOC149684	244231_at	2.132
stanniocalcin 2	STC2	203438_at	2.131
glutamate receptor interacting protein 2	GRIP2	216481_at	2.131
connective tissue growth factor	CTGF	209101_at	2.131
glycophorin B (MNS blood group)	GYPB	207459_x_at	2.121

Table S2.2 cont'd.

staufen, RNA binding protein, homolog 2 (Drosophila)	STAU2	227179_at	2.119
zinc finger protein 83	ZNF83	236429_at	2.118
transmembrane protein 8 (five membrane-spanning domains)	TMEM8	221882_s_at	2.118
myeloid/lymphoid or mixed-lineage leukemia (trithorax homolog, Drosophila); translocated to, 11	MLLT11	211071_s_at	2.115
Rho-guanine nucleotide exchange factor	RGNEF	1560348_at	2.112
ubiquilin 1	UBQLN1	222989_s_at	2.112
lipopolysaccharide-induced TNF factor	LITAF	200704_at	2.11
zinc finger CCCH-type containing 12C	ZC3H12C	231899_at	2.108
paternally expressed 10	PEG10	212092_at	2.108
Fraser syndrome 1	FRAS1	226145_s_at	2.106
WD repeat domain 64	WDR64	1553373_at	2.105
general transcription factor IIA, 1, 19/37kDa	GTF2A1	206521_s_at	2.104
anoctamin 10	ANO10	218910_at	2.102
metastasis associated lung adenocarcinoma transcript 1 (non-protein coding)	MALAT1	224558_s_at	2.099
keratin 9	KRT9	208188_at	2.096
acyl-CoA thioesterase 9	ACOT9	221641_s_at	2.093
GA binding protein transcription factor, alpha subunit 60kDa	GABPA	210188_at	2.091
thioredoxin-related transmembrane protein 3	TMX3	1552822_at	2.09
zinc finger and BTB domain containing 1	ZBTB1	205092_x_at	2.086
tropomyosin 1 (alpha)	TPM1	206116_s_at	2.071
hypothetical LOC284837	LOC284837	1563088_a_at	2.069
coiled-coil domain containing 68	CCDC68	220180_at	2.067
olfactory receptor, family 51, subfamily J, member 1 (gene/pseudogene)	OR51J1	233736_at	2.066
non imprinted in Prader-Willi/Angelman syndrome 1	NIPA1	1552696_at	2.065
hairy and enhancer of split 1, (Drosophila)	HES1	203394_s_at	2.064
sprouty homolog 2 (Drosophila)	SPRY2	204011_at	2.061
Strawberry notch homolog 1 (Drosophila)	SBNO1	216162_at	2.056
nicalin homolog (zebrafish)	NCLN	222206_s_at	2.055
cell division cycle 42 (GTP binding protein, 25kDa)	CDC42	210232_at	2.055
wingless-type MMTV integration site family, member 4	WNT4	208606_s_at	2.054
forkhead box D1	FOXD1	206307_s_at	2.052
v-Ki-ras2 Kirsten rat sarcoma viral oncogene homolog	KRAS	214352_s_at	2.05
erythrocyte membrane protein band 4.1 like 4B	EPB41L4B	220161_s_at	2.049
chromosome 16 open reading frame 11	C16orf11	1553826_a_at	2.042
progestin and adipoQ receptor family member III	PAQR3	213372_at	2.04
prefoldin subunit 2	PFDN2	218336_at	2.038
cerebellar degeneration-related protein 2-like	CDR2L	213230_at	2.036
heat shock protein 90kDa alpha (cytosolic), class A member 1	HSP90AA1	211969_at	2.031
Kruppel-like factor 7 (ubiquitous)	KLF7	204334_at	2.031
hypothetical protein KIAA1434	RP5-1022P6.2	224826_at	2.031
glycerol kinase 3 pseudogene	GK3P	215966_x_at	2.025
pyruvate dehydrogenase kinase, isozyme 4	PDK4	205960_at	2.025
heat shock 22kDa protein 8	HSPB8	221667_s_at	2.025
zinc finger protein 606	ZNF606	229707_at	2.024
hypothetical protein FLJ23519 /// ribonuclease/angiogenin inhibitor 1	FLJ23519 /// RN	216798_at	2.021
myosin X	MYO10	244350_at	2.02
pregnancy specific beta-1-glycoprotein 6	PSG6	208106_x_at	2.017
Fraser syndrome 1	FRAS1	1560153_at	2.016
forkhead box F2	FOXF2	206377_at	2.013
BMP and activin membrane-bound inhibitor homolog (Xenopus laevis)	BAMBI	203304_at	2.011
ring finger protein 112	RNF112	223603_at	2.01
synaptotagmin XI	SYT11	209197_at	2.007
similar to mCG134545	LOC342918	230814_at	2.006
myotubularin related protein 9	MTMR9	204837_at	2.006
KIAA0182	KIAA0182	212057_at	2.006
thrombospondin, type I, domain containing 4	THSD4	222835_at	2.003
Inhibitor of DNA binding 4, dominant negative helix-loop-helix protein	ID4	226933_s_at	2.003
aryl hydrocarbon receptor	AHR	202820_at	2.002
splicing factor, arginine/serine-rich 15	SFRS15	233753_at	2.001
forkhead box C1	FOXC1	1553613_s_at	2.001

Table S2.3: Genes with decreased expression due to Alk3QD in adherent EOC cells.

Gene Title	Gene Symbol	Probe Set ID	Fold Change
RAP1A, member of RAS oncogene family	RAP1A	1555340_x_at	1000.000
RAP1A, member of RAS oncogene family	RAP1A	1555339_at	333.333
serum amyloid A1 /// serum amyloid A2	SAA1 /// SAA2	214456_x_at	25.000
chitinase 3-like 1 (cartilage glycoprotein-39)	CHI3L1	209396_s_at	23.810
major histocompatibility complex, class II, DR alpha	HLA-DRA	210982_s_at	20.000
dipeptidyl-peptidase 6	DPP6	228546_at	19.231
protein kinase (cAMP-dependent, catalytic) inhibitor beta	PKIB	231120_x_at	18.182
periplakin	PPL	203407_at	15.152
chitinase 3-like 1 (cartilage glycoprotein-39)	CHI3L1	209395_at	14.085
chloride channel accessory 2	CLCA2	206165_s_at	13.699
serum amyloid A1 /// serum amyloid A2	SAA1 /// SAA2	208607_s_at	13.699
toll-like receptor 7	TLR7	220146_at	12.821
selenoprotein P, plasma, 1	SEPP1	201427_s_at	9.615
family with sequence similarity 5, member B	FAM5B	214822_at	9.009
hydroxy-delta-5-steroid dehydrogenase, 3 beta- and steroid delta-isomerase 2	HSD3B2	206294_at	9.009
chloride channel accessory 2	CLCA2	217528_at	8.475
dipeptidyl-peptidase 6	DPP6	207789_s_at	8.333
alpha-2-macroglobulin	A2M	217757_at	7.634
haptoglobin /// haptoglobin-related protein	HP /// HPR	208470_s_at	7.463
chromosome 13 open reading frame 36	C13orf36	241672_at	6.536
complement component 8, alpha polypeptide	C8A	206305_s_at	6.410
asp (abnormal spindle) homolog, microcephaly associated (Drosophila)	ASPM	232238_at	6.369
RALBP1 associated Eps domain containing 2	REPS2	227425_at	6.211
chromosome 9 open reading frame 38	C9orf38	208077_at	6.098
calbindin 1, 28kDa	CALB1	205625_s_at	6.024
benzodiazapine receptor (peripheral) associated protein 1	BZRAP1	205839_s_at	5.988
podoplanin	PDPN	221898_at	5.882
cadherin 1, type 1, E-cadherin (epithelial)	CDH1	201131_s_at	5.814
immunoglobulin heavy constant delta	IGHD	214973_x_at	5.714
serine PI Kazal type 5-like 3	SPINK5L3	233340_at	5.682
pyruvate carboxylase	PC	204476_s_at	5.682
asp (abnormal spindle) homolog, microcephaly associated (Drosophila)	ASPM	219918_s_at	5.435
bone morphogenetic protein 7	BMP7	211259_s_at	5.376
netrin 3	NTN3	207640_x_at	5.319
insulin-like growth factor 1 receptor	IGF1R	203628_at	5.181
piwi-like 1 (Drosophila)	PIWIL1	214868_at	5.128
testicular cell adhesion molecule 1 homolog (mouse)	TCAM1	233320_at	5.000
ATPase, class I, type 8B, member 4	ATP8B4	220416_at	4.902
keratin 36	KRT36	214576_at	4.785
calcium/calmodulin-dependent protein kinase II beta	CAMK2B	210404_x_at	4.762
carboxylesterase 8 (putative)	CES8	228903_at	4.739
thioredoxin interacting protein	TXNIP	201010_s_at	4.739
chromosome 19 open reading frame 59	C19orf59	235568_at	4.717
keratin 20	KRT20	213953_at	4.695
sema domain, immunoglobulin domain (Ig), transmembrane domain (TM) and short cytoplasmic domain	SEMA4D	228891_at	4.673
solute carrier family 39 (zinc transporter), member 2	SLC39A2	220413_at	4.630
transmembrane and tetratricopeptide repeat containing 4	TMTC4	225666_at	4.630
RALBP1 associated Eps domain containing 2	REPS2	205645_at	4.608
haptoglobin /// haptoglobin-related protein	HP /// HPR	206697_s_at	4.608
zinc finger protein 29 pseudogene	ZNF29	1567856_x_at	4.587
WD repeat domain 41	WDR41	240637_at	4.545
platelet derived growth factor D	PDGFD	219304_s_at	4.545
protein disulfide isomerase-like, testis expressed	PDILT	1554970_at	4.505
retinoschisin 1	RS1	216937_s_at	4.484
aryl-hydrocarbon receptor nuclear translocator 2	ARNT2	202986_at	4.464
Oligodendrocyte myelin glycoprotein	OMG	238720_at	4.444
heterogeneous nuclear ribonucleoprotein C (C1/C2)	HNRNPC	235500_at	4.425
Immunoglobulin heavy constant gamma 1 (G1m marker)	IGHG1	217320_at	4.367
potassium voltage-gated channel, subfamily H (eag-related), member 2	KCNH2	210036_s_at	4.367
solute carrier family 47, member 1	SLC47A1	219525_at	4.348
chromosome 2 open reading frame 58	C2orf58	1553829_at	4.348
hemoglobin, epsilon 1	HBE1	205919_at	4.348
insulin-like growth factor binding protein 2, 36kDa	IGFBP2	202718_at	4.310
leucine-rich repeats and immunoglobulin-like domains 3	LRIG3	226908_at	4.310
brain peptide A1	BPA-1	1555547_at	4.292
chloride channel accessory 2	CLCA2	206166_s_at	4.255
interferon stimulated exonuclease gene 20kDa-like 2	ISG20L2	216502_at	4.167

Table S2.3 cont'd.

interleukin 18 (interferon-gamma-inducing factor)	IL18	206295_at	4.167
chromosome 14 open reading frame 162	C14orf162	220887_at	4.149
transforming growth factor, beta receptor III	TGFBR3	204731_at	4.132
solute carrier family 27 (fatty acid transporter), member 2	SLC27A2	205768_s_at	4.065
chromosome 14 open reading frame 83	C14orf83	227544_at	4.065
NEDD4 binding protein 2-like 1	N4BP2L1	213375_s_at	4.016
superoxide dismutase 2, mitochondrial	SOD2	221477_s_at	4.016
Hypothetical protein LOC100130458	LOC100130458	239214_at	3.968
family with sequence similarity 84, member A	FAM84A	234331_s_at	3.953
solute carrier family 4, sodium bicarbonate cotransporter, member 5	SLC4A5	221723_s_at	3.937
vascular cell adhesion molecule 1	VCAM1	203868_s_at	3.817
lysyl oxidase-like 4	LOXL4	227145_at	3.774
solute carrier family 46, member 3	SLC46A3	214719_at	3.774
Tripartite motif-containing 8	TRIM8	228015_s_at	3.731
discs, large (Drosophila) homolog-associated protein 1	DLGAP1	206490_at	3.690
CD28 molecule	CD28	206545_at	3.690
aldehyde dehydrogenase 6 family, member A1	ALDH6A1	221589_s_at	3.676
potassium voltage-gated channel, Shal-related subfamily, member 3	KCND3	213832_at	3.663
collagen, type XIV, alpha 1	COL14A1	216866_s_at	3.663
cytochrome P450, family 7, subfamily B, polypeptide 1	CYP7B1	207386_at	3.636
growth arrest-specific 7	GAS7	202191_s_at	3.636
angiopoietin-like 1	ANGPTL1	239183_at	3.636
vacuolar protein sorting 36 homolog (S. cerevisiae)	VPS36	240086_at	3.623
complement component 1, s subcomponent	C1S	1555229_a_at	3.623
potassium voltage-gated channel, Shal-related subfamily, member 3	KCND3	215014_at	3.623
synovial sarcoma, X breakpoint 3	SSX3	207666_x_at	3.623
hook homolog 1 (Drosophila)	HOOK1	219976_at	3.597
chemokine (C-X-C motif) ligand 16	CXCL16	223454_at	3.571
family with sequence similarity 170, member B	FAM170B	1559828_at	3.546
sema domain, immunoglobulin domain (Ig), transmembrane domain (TM) and short cytoplasmic domain	SEMA4D	203528_at	3.534
chromosome 13 open reading frame 31	C13orf31	1553142_at	3.521
vanin 1	VNN1	205844_at	3.484
endothelin 2	EDN2	206758_at	3.484
synaptopodin 2	SYNPO2	227662_at	3.472
cytochrome b5 type A (microsomal)	CYB5A	217021_at	3.472
podoplanin	PDPN	204879_at	3.460
3-hydroxymethyl-3-methylglutaryl-Coenzyme A lyase-like 1	HMGCLL1	232305_at	3.413
major facilitator superfamily domain containing 4	MFSD4	229254_at	3.401
cytidine monophosphate-N-acetylneuraminic acid hydroxylase (CMP-N-acetylneuraminate monooxygen	CMAH	205518_s_at	3.401
G protein-coupled receptor 112	GPR112	1553006_at	3.356
E74-like factor 3 (ets domain transcription factor, epithelial-specific)	ELF3	210827_s_at	3.344
cyclin-dependent kinase 2	CDK2	211803_at	3.322
KIAA1324	KIAA1324	226248_s_at	3.322
chromosome 5 open reading frame 4	C5orf4	220751_s_at	3.322
caspase 12 (gene/pseudogene)	CASP12	1564736_a_at	3.322
complement factor H /// complement factor H-related 1	CFH /// CFHR1	215388_s_at	3.322
immunoglobulin kappa constant	IGKC	214836_x_at	3.300
WW and C2 domain containing 1	WWC1	216074_x_at	3.300
CUG triplet repeat, RNA binding protein 2	CUGBP2	242268_at	3.289
vanin 1	VNN1	1558549_s_at	3.257
cytochrome b reductase 1	CYBRD1	222453_at	3.247
STEAP family member 4	STEAP4	220187_at	3.226
interferon-induced protein with tetratricopeptide repeats 1	IFIT1	203153_at	3.195
phospholipid scramblase 4	PLSCR4	218901_at	3.175
baculoviral IAP repeat-containing 3	BIRC3	210538_s_at	3.175
hypothetical LOC728475	LOC728475	242010_at	3.165
interleukin-1 receptor-associated kinase 3	IRAK3	213817_at	3.165
discs, large (Drosophila) homolog-associated protein 1 /// hypothetical protein LOC284214	DLGAP1 /// LOC	235527_at	3.145
chromosome X open reading frame 56	CXorf56	239444_at	3.145
ring finger protein 125	RNF125	235199_at	3.135
hypothetical LOC653602	LOC653602	229546_at	3.115
B-cell CLL/lymphoma 8	BCL8	1560683_at	3.086
nuclear factor (erythroid-derived 2)-like 3	NFE2L3	204702_s_at	3.058
tescalcin	TESC	218872_at	3.040
myosin VB	MYO5B	225299_at	3.040
myosin VB	MYO5B	225301_s_at	3.040
sprouty homolog 1, antagonist of FGF signaling (Drosophila)	SPRY1	212558_at	3.021
hypothetical LOC401312	LOC401312	1560520_at	3.012
golgi phosphoprotein 3-like	GOLPH3L	218361_at	3.012

Table S2.3 cont'd.

SWI/SNF related, matrix associated, actin dependent regulator of chromatin, subfamily a, member 4	SMARCA4	213719_s_at	3.003
coiled-coil domain containing 80	CCDC80	225241_at	3.003
chromobox homolog 2 (Pc class homolog, Drosophila)	CBX2	224138_at	2.994
interferon, alpha-inducible protein 6	IFI6	204415_at	2.985
BCL2-interacting killer (apoptosis-inducing)	BIK	205780_at	2.976
myelin basic protein	MBP	210136_at	2.967
solute carrier family 44, member 3	SLC44A3	228221_at	2.967
hypothetical protein LOC100129827	LOC100129827	231595_at	2.950
calcyphosine	CAPS	226424_at	2.941
calbindin 2	CALB2	205428_s_at	2.941
OTU domain containing 1	OTUD1	226140_s_at	2.924
WW and C2 domain containing 1	WWC1	229180_at	2.924
armadillo repeat containing, X-linked 4	ARMCX4	1552327_at	2.924
chromosome 13 open reading frame 31	C13orf31	228937_at	2.915
Fc fragment of IgA, receptor for	FCAR	211816_x_at	2.915
sphingomyelin phosphodiesterase 3, neutral membrane (neutral sphingomyelinase II)	SMPD3	231732_at	2.915
superoxide dismutase 2, mitochondrial	SOD2	215223_s_at	2.915
EPH receptor B3	EPHB3	204600_at	2.907
potassium voltage-gated channel, subfamily H (eag-related), member 6	KCNH6	211045_s_at	2.899
tumor necrosis factor, alpha-induced protein 2	TNFAIP2	202510_s_at	2.890
plasticity related gene 3	RP11-35N6.1	1570250_at	2.890
chromosome 5 open reading frame 4	C5orf4	48031_r_at	2.890
E74-like factor 3 (ets domain transcription factor, epithelial-specific)	ELF3	201510_at	2.874
olfactory receptor, family 7, subfamily E, member 47 pseudogene	OR7E47P	222304_x_at	2.874
cytidine monophosphate-N-acetylneuraminic acid hydroxylase (CMP-N-acetylneuraminate monooxygen	CMAH	210571_s_at	2.874
chromosome 13 open reading frame 31	C13orf31	1553141_at	2.865
par-6 partitioning defective 6 homolog beta (C. elegans)	PARD6B	235165_at	2.857
aldehyde dehydrogenase 6 family, member A1	ALDH6A1	221588_x_at	2.841
sushi, von Willebrand factor type A, EGF and pentraxin domain containing 1	SVEP1	219552_at	2.817
synaptotagmin III	SYT3	223901_at	2.817
phospholipid scramblase 1	PLSCR1	202430_s_at	2.809
Hypothetical protein LOC100128484	LOC100128484	239308_at	2.809
solute carrier family 22 (organic cation transporter), member 2	SLC22A2	207429_at	2.809
interleukin 23 receptor	IL23R	1561853_a_at	2.801
glutamate receptor, ionotropic, N-methyl D-aspartate 2A	GRIN2A	206534_at	2.793
EF-hand domain (C-terminal) containing 2	EFHC2	220591_s_at	2.770
par-3 partitioning defective 3 homolog B (C. elegans)	PARD3B	1553188_s_at	2.762
Solute carrier family 25, member 29	SLC25A29	232280_at	2.762
E74-like factor 3 (ets domain transcription factor, epithelial-specific)	ELF3	229842_at	2.762
furry homolog (Drosophila)	FRY	204072_s_at	2.755
transmembrane protein 140	TMEM140	218999_at	2.755
collectin sub-family member 12	COLEC12	221019_s_at	2.740
cytochrome P450, family 39, subfamily A, polypeptide 1	CYP39A1	1553977_a_at	2.732
transforming growth factor, beta 3	TGFB3	209747_at	2.732
solute carrier family 22, member 23	SLC22A23	223194_s_at	2.717
KIAA1462	KIAA1462	213316_at	2.717
colony stimulating factor 2 receptor, alpha, low-affinity (granulocyte-macrophage) /// hypothetical protein	CSF2RA /// LOC	210340_s_at	2.710
annexin A4	ANXA4	201302_at	2.703
glutaminase	GLS	203157_s_at	2.688
interferon-induced protein with tetratricopeptide repeats 2	IFIT2	226757_at	2.688
chromosome 10 open reading frame 11	C10orf11	223703_at	2.688
ERO1-like beta (S. cerevisiae)	ERO1LB	231944_at	2.688
transmembrane protein 37	TMEM37	227190_at	2.681
T-cell activation RhoGTPase activating protein	TAGAP	1552541_at	2.674
vitronectin	VTN	204534_at	2.674
obscurin, cytoskeletal calmodulin and titin-interacting RhoGEF	OBSCN	229854_at	2.674
vav 3 guanine nucleotide exchange factor	VAV3	218807_at	2.667
islet cell autoantigen 1,69kDa-like	ICA1L	223881_at	2.660
PTPRF interacting protein, binding protein 2 (liprin beta 2)	PPFIBP2	212841_s_at	2.660
histone cluster 1, H2bc	HIST1H2BC	236193_at	2.660
prostaglandin F2 receptor negative regulator	PTGFRN	224937_at	2.660
cytochrome P450, family 27, subfamily A, polypeptide 1	CYP27A1	203979_at	2.639
spectrin, beta, non-erythrocytic 4	SPTBN4	224297_s_at	2.632
mesoderm specific transcript homolog (mouse)	MEST	202016_at	2.604
chromosome 9 open reading frame 125	C9orf125	224458_at	2.597
ferritin, heavy polypeptide 1	FTH1	214211_at	2.591
ATP-binding cassette, sub-family B (MDR/TAP), member 1	ABCB1	209993_at	2.584
Mannosidase, alpha, class 1A, member 1	MAN1A1	221760_at	2.577
family with sequence similarity 38, member B	FAM38B	219602_s_at	2.571

Table S2.3 cont'd.

MACRO domain containing 2	MACROD2	235278_at	2.564
myelin basic protein	MBP	1554544_a_at	2.558
cyclin-dependent kinase inhibitor 1C (p57, Kip2)	CDKN1C	219534_x_at	2.551
RAB7B, member RAS oncogene family	RAB7B	1553982_a_at	2.551
ubiquitin protein ligase E3 component n-recognin 4	UBR4	231889_at	2.551
hypothetical LOC151658	LOC151658	238283_at	2.545
tensin 3	TNS3	217853_at	2.545
calcium/calmodulin-dependent protein kinase kinase 2, beta	CAMKK2	207359_at	2.538
dymeclin	DYM	220774_at	2.538
unc-51-like kinase 2 (C. elegans)	ULK2	215154_at	2.538
ATP/GTP binding protein-like 2	AGBL2	220390_at	2.538
discs, large (Drosophila) homolog-associated protein 1	DLGAP1	206489_s_at	2.538
hypothetical LOC100129550	LOC100129550	229699_at	2.532
low density lipoprotein-related protein 2	LRP2	205710_at	2.525
TAP binding protein (tapasin)	TAPBP	210294_at	2.525
transmembrane protein 163	TMEM163	1552626_a_at	2.519
chromosome 11 open reading frame 35	C11orf35	236050_at	2.519
tumor necrosis factor receptor superfamily, member 21	TNFRSF21	214581_x_at	2.519
potassium inwardly-rectifying channel, subfamily J, member 12	KCNJ12	232289_at	2.513
chromosome 17 open reading frame 103	C17orf103	226657_at	2.513
cathepsin F	CTSF	203657_s_at	2.506
aldehyde dehydrogenase 6 family, member A1	ALDH6A1	204290_s_at	2.506
4-hydroxyphenylpyruvate dioxygenase	HPD	206024_at	2.500
Mov10l1, Moloney leukemia virus 10-like 1, homolog (mouse)	MOV10L1	239257_at	2.500
potassium inwardly-rectifying channel, subfamily J, member 12	KCNJ12	207110_at	2.500
LRRN4 C-terminal like	LRRN4CL	1556427_s_at	2.500
microtubule-associated protein 7	MAP7	202890_at	2.500
WW and C2 domain containing 1	WWC1	213085_s_at	2.494
spermatid perinuclear RNA binding protein	STRBP	223246_s_at	2.494
chromosome 8 open reading frame 83	C8orf83	224158_s_at	2.494
growth arrest-specific 7	GAS7	202192_s_at	2.488
paired box 8	PAX8	221990_at	2.488
glutamate decarboxylase 1 (brain, 67kDa)	GAD1	205278_at	2.481
ATP-binding cassette, sub-family A (ABC1), member 9	ABCA9	235335_at	2.481
hypothetical gene supported by AK026416	FLJ22763	233604_at	2.475
complement component 1, s subcomponent	C1S	208747_s_at	2.475
ets variant 4	ETV4	1554576_a_at	2.463
collagen, type XVI, alpha 1	COL16A1	204345_at	2.457
acyl-CoA thioesterase 4	ACOT4	229534_at	2.457
Kallmann syndrome 1 sequence	KAL1	205206_at	2.457
carboxymethylenebutenolidase homolog (Pseudomonas)	CMBL	227522_at	2.457
chromosome 5 open reading frame 13	C5orf13	201310_s_at	2.457
phospholipase A2, group X	PLA2G10	207222_at	2.451
CD6 molecule	CD6	213958_at	2.445
proprotein convertase subtilisin/kexin type 6	PCSK6	211262_at	2.445
GM2 ganglioside activator	GM2A	209727_at	2.439
caspase 10, apoptosis-related cysteine peptidase	CASP10	205467_at	2.433
receptor tyrosine kinase-like orphan receptor 1	ROR1	232060_at	2.433
hydroxy-delta-5-steroid dehydrogenase, 3 beta- and steroid delta-isomerase 1 /// hydroxy-delta-5-steroi	HSD3B1 /// HSI	215665_at	2.433
ureidopropionase, beta	UPB1	220507_s_at	2.433
C-terminal binding protein 1	CTBP1	1557714_at	2.427
glutaminase	GLS	203159_at	2.421
chromosome 10 open reading frame 54	C10orf54	225372_at	2.415
family with sequence similarity 38, member B	FAM38B	222908_at	2.410
ring finger protein 144B	RNF144B	228153_at	2.398
keratinocyte growth factor-like protein 2	KGFLP2	231031_at	2.398
cell adhesion molecule 4	CADM4	222293_at	2.398
K(lysine) acetyltransferase 2B	KAT2B	203845_at	2.392
aldehyde oxidase 1	AOX1	205082_s_at	2.392
ubiquitin specific peptidase 2	USP2	229337_at	2.392
chromosome 6 open reading frame 123	C6orf123	207698_at	2.387
tumor necrosis factor receptor superfamily, member 21	TNFRSF21	218856_at	2.387
ADAM metallopeptidase domain 12	ADAM12	215613_at	2.387
phosphoinositide-3-kinase, regulatory subunit 3 (gamma)	PIK3R3	202743_at	2.381
solute carrier family 39 (metal ion transporter), member 11	SLC39A11	227046_at	2.381
myelin-associated oligodendrocyte basic protein	MOBP	242765_at	2.375
chromosome 18 open reading frame 2	C18orf2	224045_x_at	2.375
superoxide dismutase 2, mitochondrial	SOD2	216841_s_at	2.375
coiled-coil domain containing 80	CCDC80	225242_s_at	2.375

Table S2.3 cont'd.

programmed cell death 4 (neoplastic transformation inhibitor)	PDCD4	212594_at	2.370
dual adaptor of phosphotyrosine and 3-phosphoinositides	DAPP1	219290_x_at	2.370
synovial sarcoma, X breakpoint 4 /// synovial sarcoma, X breakpoint 4B	SSX4 /// SSX4B	211425_x_at	2.364
syndecan 4	SDC4	202071_at	2.358
signal-regulatory protein gamma	SIRPG	220485_s_at	2.358
palmdelphin	PALMD	218736_s_at	2.358
par-3 partitioning defective 3 homolog B (C. elegans)	PARD3B	228411_at	2.353
hyaluronan and proteoglycan link protein 1	HAPLN1	230204_at	2.353
mannosidase, alpha, class 1A, member 1	MAN1A1	208116_s_at	2.342
chromosome 12 open reading frame 35	C12orf35	227152_at	2.342
family with sequence similarity 35, member A	FAM35A	233048_at	2.336
endoplasmic reticulum metallopeptidase 1	ERMP1	222603_at	2.331
ribosomal modification protein rimK-like family member A	RIMKLA	241075_at	2.331
mitogen-activated protein kinase kinase kinase 7 interacting protein 3	MAP3K7IP3	1558518_at	2.326
hypothetical LOC79150	MGC4859	207775_at	2.326
chromosome 5 open reading frame 13	C5orf13	201309_x_at	2.320
ADAM metallopeptidase domain 12	ADAM12	213790_at	2.315
cyclin-dependent kinase-like 2 (CDC2-related kinase)	CDKL2	236331_at	2.309
dopachrome tautomerase (dopachrome delta-isomerase, tyrosine-related protein 2)	DCT	205338_s_at	2.304
yippee-like 3 (Drosophila)	YPEL3	223179_at	2.304
phospholipid scramblase 1	PLSCR1	202446_s_at	2.299
histone cluster 1, H2bc	HIST1H2BC	214455_at	2.294
serpin peptidase inhibitor, clade B (ovalbumin), member 9	SERPINB9	242814_at	2.294
FERM domain containing 4B	FRMD4B	213056_at	2.294
protein-L-isoaspartate (D-aspartate) O-methyltransferase domain containing 1	PCMTD1	232382_s_at	2.288
copine VIII	CPNE8	243727_at	2.288
KIAA0247	KIAA0247	202181_at	2.288
glutaminase	GLS	203158_s_at	2.288
ST3 beta-galactoside alpha-2,3-sialyltransferase 5	ST3GAL5	203217_s_at	2.283
ectonucleotide pyrophosphatase/phosphodiesterase 3	ENPP3	232737_s_at	2.283
phospholipase D1, phosphatidylcholine-specific	PLD1	226636_at	2.278
endoplasmic reticulum metallopeptidase 1	ERMP1	218342_s_at	2.278
KIAA0895	KIAA0895	213424_at	2.278
aldehyde oxidase 1	AOX1	205083_at	2.278
unc-51-like kinase 2 (C. elegans)	ULK2	1554112_a_at	2.268
transmembrane protein 151A	TMEM151A	235614_at	2.268
six transmembrane epithelial antigen of the prostate 2	STEAP2	225871_at	2.262
solute carrier family 27 (fatty acid transporter), member 2	SLC27A2	205769_at	2.262
growth arrest-specific 6 /// similar to growth arrest-specific 6	GAS6 /// LOC10	1598_g_at	2.262
interleukin 1 receptor, type I	IL1R1	202948_at	2.262
Hypothetical protein LOC100130353	LOC100130353	1564449_at	2.262
Family with sequence similarity 92, member A1	FAM92A1	237910_x_at	2.257
MAX dimerization protein 4	MXD4	210778_s_at	2.257
mal, T-cell differentiation protein 2	MAL2	224650_at	2.257
poly (ADP-ribose) polymerase family, member 14	PARP14	224701_at	2.252
zinc finger and BTB domain containing 44	ZBTB44	225845_at	2.252
annexin A4	ANXA4	201301_s_at	2.252
myelin basic protein	MBP	225408_at	2.247
UDP-N-acetyl-alpha-D-galactosamine:polypeptide N-acetylgalactosaminyltransferase 1 (GalNAc-T1)	GALNT1	201724_s_at	2.242
ubiquitously transcribed tetratricopeptide repeat gene, Y-linked	UTY	210322_x_at	2.242
G protein-coupled receptor 87	GPR87	219936_s_at	2.237
Tissue factor pathway inhibitor (lipoprotein-associated coagulation inhibitor)	TFPI	215447_at	2.232
macrophage stimulating 1 receptor (c-met-related tyrosine kinase)	MST1R	205455_at	2.232
DEAD (Asp-Glu-Ala-Asp) box polypeptide 60	DDX60	218986_s_at	2.232
cyclin-dependent kinase inhibitor 2B (p15, inhibits CDK4)	CDKN2B	236313_at	2.222
post-GPI attachment to proteins 1	PGAP1	220576_at	2.217
engulfment and cell motility 1	ELMO1	204513_s_at	2.217
actin-like 8	ACTL8	214957_at	2.217
TP53 target 1 (non-protein coding)	TP53TG1	210241_s_at	2.212
macrophage stimulating 1 (hepatocyte growth factor-like)	MST1	205614_x_at	2.212
secretory leukocyte peptidase inhibitor	SLPI	203021_at	2.212
solute carrier family 15, member 3	SLC15A3	219593_at	2.212
integrin, beta 8	ITGB8	226189_at	2.208
hypothetical LOC541472	LOC541472	243977_at	2.208
aquaporin 2 (collecting duct)	AQP2	206672_at	2.203
solute carrier family 27 (fatty acid transporter), member 1	SLC27A1	226728_at	2.203
fibroblast growth factor 7 (keratinocyte growth factor)	FGF7	205782_at	2.203
neuroblastoma, suppression of tumorigenicity 1	NBL1	201621_at	2.203
cyclin-dependent kinase inhibitor 1C (p57, Kip2)	CDKN1C	216894_x_at	2.203

Table S2.3 cont'd.

fibulin 1	FBLN1	207835_at	2.198
peroxisome proliferator-activated receptor gamma, coactivator 1 beta	PPARGC1B	1553639_a_at	2.193
Rho guanine nucleotide exchange factor (GEF) 3	ARHGEF3	218501_at	2.193
ciliary neurotrophic factor receptor	CNTFR	205723_at	2.188
SH3 domain binding glutamic acid-rich protein like 2	SH3BGRL2	225354_s_at	2.188
TNFSF12-TNFSF13 readthrough transcript /// tumor necrosis factor (ligand) superfamily, member 13	TNFSF12-TNFS	209500_x_at	2.188
hexose-6-phosphate dehydrogenase (glucose 1-dehydrogenase)	H6PD	221892_at	2.188
sema domain, immunoglobulin domain (Ig), short basic domain, secreted, (semaphorin) 3E	SEMA3E	206941_x_at	2.183
guanine nucleotide binding protein (G protein), gamma 7	GNG7	228831_s_at	2.183
endothelin receptor type A	EDNRA	204464_s_at	2.183
CD40 molecule, TNF receptor superfamily member 5	CD40	222292_at	2.179
chromosome 9 open reading frame 126	C9orf126	228174_at	2.174
solute carrier family 25, member 27	SLC25A27	1554161_at	2.174
collagen, type XXII, alpha 1	COL22A1	228873_at	2.169
pre T-cell antigen receptor alpha	PTCRA	211837_s_at	2.169
mannosidase, alpha, class 2A, member 2	MAN2A2	219999_at	2.169
interferon regulatory factor 1	IRF1	238725_at	2.169
interleukin 16 (lymphocyte chemoattractant factor)	IL16	1555016_at	2.169
sortilin 1	SORT1	224818_at	2.169
pleckstrin homology domain containing, family G (with RhoGef domain) member 1	PLEKHG1	226122_at	2.155
phosphoinositide-3-kinase interacting protein 1	PIK3IP1	221757_at	2.155
hypothetical LOC729970	LOC729970	230433_at	2.155
leucine rich repeat containing 1	LRRC1	218816_at	2.146
2-5-oligoadenylate synthetase 3, 100kDa	OAS3	218400_at	2.146
zinc finger and BTB domain containing 44	ZBTB44	226148_at	2.146
furry homolog (Drosophila)	FRY	214318_s_at	2.141
zinc finger, FYVE domain containing 16	ZFYVE16	1555982_at	2.141
growth arrest-specific 6 /// similar to growth arrest-specific 6	GAS6 /// LOC10	202177_at	2.137
chromosome 12 open reading frame 35	C12orf35	218614_at	2.132
interleukin 20	IL20	224071_at	2.132
Transcription factor Dp-2 (E2F dimerization partner 2)	TFDP2	226157_at	2.132
plexin B1	PLXNB1	215807_s_at	2.132
phosphoinositide-3-kinase, catalytic, delta polypeptide	PIK3CD	203879_at	2.128
thioredoxin-related transmembrane protein 4	TMX4	201580_s_at	2.123
complement factor H	CFH	213800_at	2.119
T-cell lymphoma invasion and metastasis 2	TIAM2	222942_s_at	2.114
hypothetical LOC283070	LOC283070	226382_at	2.114
ezrin	EZR	208621_s_at	2.114
ribonuclease T2	RNASET2	217984_at	2.114
islet cell autoantigen 1,69kDa-like	ICA1L	230454_at	2.105
transmembrane phosphatase with tensin homology	TPTE	220205_at	2.105
basonuclin 1	BNC1	1552487_a_at	2.101
cordon-bleu homolog (mouse)	COBL	213050_at	2.101
ATPase, Cu++ transporting, beta polypeptide	ATP7B	204624_at	2.101
mannan-binding lectin serine peptidase 1 (C4/C2 activating component of Ra-reactive factor)	MASP1	210680_s_at	2.096
chromosome 6 open reading frame 170	C6orf170	232038_at	2.096
regulator of calcineurin 1	RCAN1	215253_s_at	2.092
chromosome 1 open reading frame 133	C1orf133	230121_at	2.092
Spermatid perinuclear RNA binding protein	STRBP	229513_at	2.092
hypothetical protein DKFZp586I1420	DKFZP586I142(	213546_at	2.092
C-terminal binding protein 2	CTBP2	215377_at	2.079
serpin peptidase inhibitor, clade B (ovalbumin), member 3	SERPINB3	209719_x_at	2.079
KIAA1217	KIAA1217	231807_at	2.079
tumor necrosis factor receptor superfamily, member 8	TNFRSF8	206729_at	2.079
prostaglandin F2 receptor negative regulator	PTGFRN	224950_at	2.079
WD repeat and SOCS box-containing 1	WSB1	201295_s_at	2.075
hypothetical protein LOC283867	LOC283867	231518_at	2.075
KIAA1324	KIAA1324	221874_at	2.075
protocadherin alpha 1 /// protocadherin alpha 10 /// protocadherin alpha 11 /// protocadherin alpha 12 ///	PCDHA1 /// PCI	224212_s_at	2.075
UDP-GlcNAc:betaGal beta-1,3-N-acetylglucosaminyltransferase 1	B3GNT1	203188_at	2.075
hemoglobin, alpha 1 /// hemoglobin, alpha 2	HBA1 /// HBA2	209458_x_at	2.070
Ral GEF with PH domain and SH3 binding motif 1	RALGPS1	204199_at	2.070
gastrokine 1	GKN1	220191_at	2.066
UDP-Gal:betaGlcNAc beta 1,4- galactosyltransferase, polypeptide 6	B4GALT6	235333_at	2.066
pre-B-cell leukemia homeobox 1	PBX1	212148_at	2.066
HBV preS1-transactivated protein 4	PS1TP4	226381_at	2.062
thioredoxin-related transmembrane protein 4	TMX4	201581_at	2.058
salt-inducible kinase 2	SIK2	213221_s_at	2.058
StAR-related lipid transfer (START) domain containing 10	STARD10	232322_x_at	2.058

Table S2.3 cont'd.

protein-L-isoaspartate (D-aspartate) O-methyltransferase domain containing 1	PCMTD1	226119_at	2.053
RUN domain containing 3B	RUNDC3B	241703_at	2.053
major facilitator superfamily domain containing 6	MFSD6	225325_at	2.049
phospholipase A2 receptor 1, 180kDa	PLA2R1	210194_at	2.049
SPARC related modular calcium binding 2	SMOC2	243946_at	2.049
hypothetical protein LOC90246	LOC90246	233830_at	2.049
transient receptor potential cation channel, subfamily M, member 3	TRPM3	216452_at	2.049
caspase 1, apoptosis-related cysteine peptidase (interleukin 1, beta, convertase)	CASP1	206011_at	2.045
complement component 3	C3	217767_at	2.045
family with sequence similarity 53, member A	FAM53A	1569139_s_at	2.041
cyclin D2	CCND2	200953_s_at	2.041
progesterone receptor membrane component 2	PGRMC2	213227_at	2.037
chromosome 12 open reading frame 26	C12orf26	229018_at	2.037
isochorismatase domain containing 1	ISOC1	218170_at	2.037
programmed cell death 4 (neoplastic transformation inhibitor)	PDCD4	202731_at	2.033
MU-2/AP1M2 domain containing, death-inducing	MUDENG	232156_at	2.033
CCAAT/enhancer binding protein (C/EBP), delta	CEBPD	203973_s_at	2.033
fibroblast growth factor receptor substrate 2	FRS2	226045_at	2.033
KIAA0146	KIAA0146	228325_at	2.028
phospholipase C, delta 3	PLCD3	234971_x_at	2.028
family with sequence similarity 111, member A	FAM111A	218248_at	2.024
regulator of calcineurin 1	RCAN1	215254_at	2.024
dishevelled associated activator of morphogenesis 1	DAAM1	216060_s_at	2.024
chromosome 11 open reading frame 54	C11orf54	223268_at	2.020
hyaluronan synthase 3	HAS3	223541_at	2.020
chromosome 8 open reading frame 68	C8orf68	1557679_at	2.016
Cyclin E1	CCNE1	242105_at	2.016
fucosidase, alpha-L- 1, tissue	FUCA1	202838_at	2.016
LAG1 homolog, ceramide synthase 6	LASS6	212446_s_at	2.012
zinc finger protein 720	ZNF720	242091_at	2.012
interleukin 2 receptor, gamma (severe combined immunodeficiency)	IL2RG	204116_at	2.012
chromosome 10 open reading frame 4	C10orf4	238596_at	2.012
chromosome 9 open reading frame 125	C9orf125	213386_at	2.008
hypothetical LOC651250	LOC651250	1566987_s_at	2.004
MAX dimerization protein 4	MXD4	212346_s_at	2.004

Table S2.4: Genes with decreased expression due to Alk3QD in EOC spheroids.

Gene Title	Gene Symbol	Probe Set ID	Fold Change
RAP1A, member of RAS oncogene family	RAP1A	1555340_x_at	333.333
RAP1A, member of RAS oncogene family	RAP1A	1555339_at	333.333
centromere protein I	CENPI	1555046_at	10.870
glutamate receptor, metabotropic 1	GRM1	207299_s_at	9.709
interferon stimulated exonuclease gene 20kDa	ISG20	204698_at	9.346
chromosome 4 open reading frame 37	C4orf37	1555096_at	8.547
UDP-N-acetyl-alpha-D-galactosamine:polypeptide N-acetylgalactosaminyltransferase-like	GALNTL6	1555273_at	8.065
platelet-derived growth factor receptor-like	PDGFRL	205226_at	7.752
hydroxysteroid (17-beta) dehydrogenase 6 homolog (mouse)	HSD17B6	205700_at	7.576
folate hydrolase (prostate-specific membrane antigen) 1	FOLH1	215363_x_at	7.407
hydroxysteroid (17-beta) dehydrogenase 6 homolog (mouse)	HSD17B6	37512_at	7.194
tumor necrosis factor (ligand) superfamily, member 10	TNFSF10	202687_s_at	6.667
tumor necrosis factor (ligand) superfamily, member 10	TNFSF10	202688_at	6.452
folate hydrolase (prostate-specific membrane antigen) 1	FOLH1	205860_x_at	6.289
aldehyde oxidase 1	AOX1	205083_at	6.250
EPH receptor B3	EPHB3	204600_at	5.952
ATP-binding cassette, sub-family A (ABC1), member 9	ABCA9	242541_at	5.882
similar to hCG2041313	LOC10012817[illegible]	235891_at	5.814
tumor necrosis factor (ligand) superfamily, member 10	TNFSF10	214329_x_at	5.714
SH3 domain containing ring finger 2	SH3RF2	228892_at	5.587
butyrobetaine (gamma), 2-oxoglutarate dioxygenase (gamma-butyrobetaine hydroxylase)	BBOX1	205363_at	5.435
transmembrane protein 170B	TMEM170B	235798_at	5.376
ankyrin 1, erythrocytic	ANK1	205390_s_at	5.155
chromosome 18 open reading frame 20	C18orf20	1553934_at	5.128
RALBP1 associated Eps domain containing 2	REPS2	227425_at	5.076
actin filament associated protein 1-like 2	AFAP1L2	226829_at	4.902
transmembrane protein 176B	TMEM176B	220532_s_at	4.878
PRP18 pre-mRNA processing factor 18 homolog (S. cerevisiae)	PRPF18	232473_at	4.854
pre-B-cell leukemia homeobox 1	PBX1	205253_at	4.831
protein kinase (cAMP-dependent, catalytic) inhibitor beta	PKIB	223551_at	4.762
Hypothetical protein LOC650392	LOC650392	1558463_s_at	4.762
signal transducer and activator of transcription 5B	STAT5B	1555088_x_at	4.717
sperm protein associated with the nucleus, X-linked, family member A1 /// SPANX family,	SPANXA1 /// SI	224032_x_at	4.673
MAM domain containing glycosylphosphatidylinositol anchor 1	MDGA1	238543_x_at	4.608
katanin p60 subunit A-like 2	KATNAL2	1554234_at	4.608
transmembrane protein 176A	TMEM176A	218345_at	4.608
interferon-induced protein 44-like	IFI44L	204439_at	4.587
wingless-type MMTV integration site family, member 6	WNT6	221608_at	4.587
Protein tyrosine phosphatase, non-receptor type 9	PTPN9	230140_at	4.545
plasticity related gene 3	RP11-35N6.1	219732_at	4.525
periplakin	PPL	203407_at	4.425
G0/G1switch 2	G0S2	213524_s_at	4.386
dedicator of cytokinesis 2	DOCK2	213160_at	4.348
chitinase 3-like 1 (cartilage glycoprotein-39)	CHI3L1	209396_s_at	4.348
phosphatase and actin regulator 3	PHACTR3	227949_at	4.329
family with sequence similarity 20, member A	FAM20A	226804_at	4.237
immunoglobulin heavy locus /// immunoglobulin heavy constant gamma 1 (G1m marker) /	IGH@ /// IGHG	211430_s_at	4.237
hypothetical LOC154872	LOC154872	237271_at	4.237
MYC induced nuclear antigen	MINA	229675_at	4.219
Rho GTPase activating protein 25	ARHGAP25	204882_at	4.202
phosphodiesterase 3B, cGMP-inhibited	PDE3B	214582_at	4.202
hypothetical LOC79100	MGC4473	224020_at	4.098
protein tyrosine phosphatase, receptor type, F	PTPRF	215066_at	4.082
lipocalin-like 1	LCNL1	1564431_a_at	3.984
ATP-binding cassette, sub-family B (MDR/TAP), member 6	ABCB6	203191_at	3.968
neuropeptide Y receptor Y1	NPY1R	205440_s_at	3.937
protein tyrosine phosphatase, non-receptor type 22 (lymphoid)	PTPN22	206060_s_at	3.906
aquaporin 3 (Gill blood group)	AQP3	39248_at	3.861
calcitonin receptor-like	CALCRL	206331_at	3.846

Table S2.4 cont'd.

postmeiotic segregation increased 2-like 5-like /// PMS2 postmeiotic segregation increase	LOC100132832	216039_at	3.831
RIMS binding protein 2	RIMBP2	214811_at	3.817
thyroid hormone receptor, beta (erythroblastic leukemia viral (v-erb-a) oncogene homolog	THRB	207044_at	3.817
ATP-binding cassette, sub-family A (ABC1), member 6	ABCA6	217504_at	3.817
prematurely terminated mRNA decay factor-like	LOC91431	1565935_at	3.802
DNA-damage-inducible transcript 4-like	DDIT4L	228057_at	3.802
ring finger protein 8	RNF8	203161_s_at	3.774
protogenin homolog (Gallus gallus)	PRTG	229073_at	3.759
decorin	DCN	209335_at	3.745
IKAROS family zinc finger 2 (Helios)	IKZF2	231929_at	3.731
vanin 1	VNN1	205844_at	3.717
myosin VB	MYO5B	225301_s_at	3.704
zinc finger protein 224	ZNF224	216991_at	3.690
leucine-rich repeats and immunoglobulin-like domains 3	LRIG3	226908_at	3.650
podoplanin	PDPN	221898_at	3.636
prostaglandin F receptor (FP)	PTGFR	207177_at	3.571
Mdm2, transformed 3T3 cell double minute 2, p53 binding protein (mouse) binding protein	MTBP	233436_at	3.559
SH3 domain containing ring finger 2	SH3RF2	243582_at	3.472
Hypothetical gene supported by BC008048	LOC440934	244159_at	3.460
A kinase (PRKA) anchor protein 13	AKAP13	232188_at	3.436
spastic paraplegia 11 (autosomal recessive)	SPG11	1559747_at	3.436
vascular cell adhesion molecule 1	VCAM1	203868_s_at	3.378
dpy-19-like 2 (C. elegans)	DPY19L2	230158_at	3.378
odontogenic, ameloblast asssociated	ODAM	220133_at	3.378
casein alpha s1	CSN1S1	208350_at	3.367
proteasome (prosome, macropain) subunit, alpha type, 3	PSMA3	232648_at	3.356
laminin, beta 4	LAMB4	215516_at	3.356
prostaglandin D2 synthase 21kDa (brain)	PTGDS	211663_x_at	3.356
cyclin-dependent kinase-like 2 (CDC2-related kinase)	CDKL2	207073_at	3.344
formin-like 1	FMNL1	204789_at	3.333
potassium voltage-gated channel, KQT-like subfamily, member 4	KCNQ4	243209_at	3.322
baculoviral IAP repeat-containing 5	BIRC5	202095_s_at	3.322
v-maf musculoaponeurotic fibrosarcoma oncogene homolog (avian)	MAF	209347_s_at	3.311
DENN/MADD domain containing 2A	DENND2A	221886_at	3.311
platelet derived growth factor D	PDGFD	219304_s_at	3.300
homeobox D1	HOXD1	205974_at	3.289
coiled-coil domain containing 80	CCDC80	225241_at	3.268
chitinase 3-like 1 (cartilage glycoprotein-39)	CHI3L1	209395_at	3.247
protein kinase (cAMP-dependent, catalytic) inhibitor beta	PKIB	231120_x_at	3.226
extracellular matrix protein 2, female organ and adipocyte specific	ECM2	206101_at	3.215
KIAA0644 gene product	KIAA0644	205151_s_at	3.205
potassium voltage-gated channel, subfamily H (eag-related), member 2	KCNH2	210036_s_at	3.205
RALBP1 associated Eps domain containing 2	REPS2	205645_at	3.195
TBC1 domain family, member 8 (with GRAM domain)	TBC1D8	204526_s_at	3.175
lipoprotein lipase	LPL	203549_s_at	3.155
myelin basic protein	MBP	1554544_a_at	3.155
heparan sulfate 6-O-sulfotransferase 2	HS6ST2	230030_at	3.125
GTPase, IMAP family member 2	GIMAP2	232024_at	3.106
kelch repeat and BTB (POZ) domain containing 10	KBTBD10	219106_s_at	3.106
synaptotagmin XVII	SYT17	205613_at	3.096
myosin VB	MYO5B	225299_at	3.096
V-ets erythroblastosis virus E26 oncogene homolog 2 (avian)	ETS2	241193_at	3.086
decorin	DCN	211896_s_at	3.067
phosphodiesterase 1A, calmodulin-dependent	PDE1A	233547_x_at	3.040
myosin light chain kinase family, member 4	MYLK4	1556136_at	3.030
T-box 1	TBX1	236926_at	3.021
teratocarcinoma-derived growth factor 1 /// teratocarcinoma-derived growth factor 3, pseu	TDGF1 /// TDG	206286_s_at	3.021
coxsackie virus and adenovirus receptor	CXADR	203917_at	3.012
GABA(A) receptors associated protein like 3 (pseudogene)	GABARAPL3	211457_at	3.012
chromosome 9 open reading frame 100	C9orf100	230521_at	3.003
phosphorylase kinase, alpha 1 (muscle)	PHKA1	229876_at	3.003

Table S2.4 cont'd.

KIAA1409	KIAA1409	229550_at	2.985
hypothetical LOC100192378	LOC100192378	1559965_at	2.976
WD repeat domain 91	WDR91	222799_at	2.967
protein tyrosine phosphatase, receptor type, N polypeptide 2	PTPRN2	203029_s_at	2.959
carboxypeptidase A4	CPA4	205832_at	2.950
chromosome 1 open reading frame 88	C1orf88	228100_at	2.950
dpy-19-like 2 pseudogene 2 (C. elegans)	DPY19L2P2	215143_at	2.941
potassium channel tetramerisation domain containing 12	KCTD12	212192_at	2.933
coiled-coil domain containing 102B	CCDC102B	220301_at	2.933
complement component 5	C5	205500_at	2.924
dipeptidyl-peptidase 4	DPP4	203717_at	2.915
protein tyrosine phosphatase, non-receptor type 13 (APO-1/CD95 (Fas)-associated phosp	PTPN13	204201_s_at	2.915
UDP-GlcNAc:betaGal beta-1,3-N-acetylglucosaminyltransferase 1	B3GNT1	203188_at	2.915
ADAMTS-like 1	ADAMTSL1	224371_at	2.899
hypothetical LOC285780	RP3-398D13.1	1553428_at	2.890
regulator of G-protein signaling 2, 24kDa	RGS2	202388_at	2.890
hypothetical protein FLJ10489	FLJ10489	1562433_at	2.890
phosphodiesterase 7A	PDE7A	1552343_s_at	2.882
epoxide hydrolase 2, cytoplasmic	EPHX2	209368_at	2.865
aldehyde dehydrogenase 6 family, member A1	ALDH6A1	221589_s_at	2.857
Carbohydrate (chondroitin 4) sulfotransferase 11	CHST11	226372_at	2.857
chemokine (C-X-C motif) ligand 16	CXCL16	223454_at	2.849
Collagen, type III, alpha 1	COL3A1	232458_at	2.833
family with sequence similarity 111, member B	FAM111B	1557129_a_at	2.825
retinoic acid receptor responder (tazarotene induced) 3	RARRES3	204070_at	2.817
ATP-binding cassette, sub-family A (ABC1), member 8	ABCA8	204719_at	2.817
complement component 2 /// complement factor B	C2 /// CFB	202357_s_at	2.801
tudor domain containing 6	TDRD6	232692_at	2.801
ATP/GTP binding protein-like 3	AGBL3	220649_at	2.801
podoplanin	PDPN	226658_at	2.793
matrix metallopeptidase 8 (neutrophil collagenase)	MMP8	207329_at	2.793
dehydrogenase/reductase (SDR family) member 2	DHRS2	214079_at	2.778
CD36 molecule (thrombospondin receptor)	CD36	206488_s_at	2.770
inter-alpha (globulin) inhibitor H5	ITIH5	219064_at	2.755
K(lysine) acetyltransferase 2B	KAT2B	203845_at	2.755
dihydropyrimidine dehydrogenase	DPYD	204646_at	2.747
CD9 molecule	CD9	233322_at	2.747
1-acylglycerol-3-phosphate O-acyltransferase 3	AGPAT3	224282_s_at	2.747
carboxymethylenebutenolidase homolog (Pseudomonas)	CMBL	227522_at	2.740
podocan-like 1	PODNL1	220411_x_at	2.740
thyroglobulin	TG	203673_at	2.732
sperm adhesion molecule 1 (PH-20 hyaluronidase, zona pellucida binding)	SPAM1	216989_at	2.725
RAB26, member RAS oncogene family	RAB26	50965_at	2.725
tumor necrosis factor receptor superfamily, member 21	TNFRSF21	218856_at	2.717
podoplanin	PDPN	204879_at	2.717
coiled-coil domain containing 80	CCDC80	225242_s_at	2.717
collagen-like tail subunit (single strand of homotrimer) of asymmetric acetylcholinesterase	COLQ	206073_at	2.717
fin bud initiation factor homolog (zebrafish)	FIBIN	226769_at	2.710
coiled-coil domain-containing-like	hCG_29977	227043_at	2.703
interferon-induced protein with tetratricopeptide repeats 1	IFIT1	203153_at	2.703
G protein-coupled receptor 115	GPR115	237690_at	2.695
phospholipase C, beta 4	PLCB4	203896_s_at	2.688
chromosome 14 open reading frame 143	C14orf143	210525_x_at	2.688
neural precursor cell expressed, developmentally down-regulated 4-like	NEDD4L	241396_at	2.681
BTG family, member 3	BTG3	215425_at	2.681
similar to hCG2041586	LOC730124	231337_at	2.674
mucin 12, cell surface associated	MUC12	1557906_at	2.674
DEAD (Asp-Glu-Ala-Asp) box polypeptide 50	DDX50	1568814_at	2.667
formin-like 1	FMNL1	1569257_at	2.667
paired immunoglobin-like type 2 receptor alpha	PILRA	219788_at	2.667
cytochrome P450, family 7, subfamily B, polypeptide 1	CYP7B1	207386_at	2.667

Table S2.4 cont'd.

zinc finger protein 3	ZNF3	232497_at	2.667
heat shock 70kDa protein 12A	HSPA12A	214434_at	2.660
protocadherin 18	PCDH18	225975_at	2.660
Phospholipase C, beta 4	PLCB4	240728_at	2.646
myosin light chain kinase	MYLK	202555_s_at	2.639
myosin light chain kinase	MYLK	224823_at	2.632
obscurin-like 1	OBSL1	227573_s_at	2.625
cytochrome P450, family 39, subfamily A, polypeptide 1	CYP39A1	220432_s_at	2.618
collagen, type I, alpha 2	COL1A2	229218_at	2.611
platelet-derived growth factor beta polypeptide (simian sarcoma viral (v-sis) oncogene hor	PDGFB	216055_at	2.611
zinc finger, matrin type 1	ZMAT1	226344_at	2.611
chromosome 3 open reading frame 65	C3orf65	1563207_at	2.591
ribonucleotide reductase M2 polypeptide	RRM2	209773_s_at	2.591
sortilin 1	SORT1	224818_at	2.571
CAP, adenylate cyclase-associated protein, 2 (yeast)	CAP2	212554_at	2.571
JMJD7-PLA2G4B readthrough transcript /// phospholipase A2, group IVB (cytosolic)	JMJD7-PLA2G4	219095_at	2.564
nicotinamide N-methyltransferase	NNMT	202237_at	2.558
cholinergic receptor, nicotinic, alpha 6	CHRNA6	207568_at	2.558
coiled-coil domain containing 69	CCDC69	1553102_a_at	2.551
cysteine conjugate-beta lyase 2 /// similar to RNA binding motif protein, X-linked /// RNA b	CCBL2 /// LOC'	1556336_at	2.545
coiled-coil domain containing 69	CCDC69	212886_at	2.538
Zinc finger protein 64 homolog (mouse)	ZFP64	229186_s_at	2.538
BCL2-like 11 (apoptosis facilitator)	BCL2L11	225606_at	2.538
ribonuclease H2, subunit B	RNASEH2B	229210_at	2.525
chromosome 18 open reading frame 24	C18orf24	217640_x_at	2.525
hypothetical protein LOC284898	LOC284898	1562030_at	2.513
myelin basic protein	MBP	210136_at	2.506
pyridine nucleotide-disulphide oxidoreductase domain 2	PYROXD2	228384_s_at	2.506
SH3-domain GRB2-like 3	SH3GL3	211565_at	2.506
ets variant 3	ETV3	214480_at	2.506
frizzled homolog 7 (Drosophila)	FZD7	203706_s_at	2.500
ectonucleotide pyrophosphatase/phosphodiesterase 5 (putative function)	ENPP5	237054_at	2.494
hypothetical protein LOC100129444	LOC100129444	236272_at	2.488
cation channel, sperm-associated, beta	CATSPERB	1570470_at	2.481
hypothetical LOC653602	LOC653602	229546_at	2.475
chromosome 9 open reading frame 126	C9orf126	228174_at	2.463
ADAMTS-like 1	ADAMTSL1	1552808_at	2.463
fin bud initiation factor homolog (zebrafish)	FIBIN	231001_at	2.457
Rho GTPase activating protein 18	ARHGAP18	225171_at	2.445
family with sequence similarity 65, member C	FAM65C	227654_at	2.439
prostaglandin F2 receptor negative regulator	PTGFRN	224937_at	2.433
MANSC domain containing 1	MANSC1	220945_x_at	2.427
phospholipid scramblase 4	PLSCR4	218901_at	2.427
chromosome 11 open reading frame 21	C11orf21	220560_at	2.421
mitogen-activated protein kinase kinase 6	MAP2K6	205698_s_at	2.421
arsenic (+3 oxidation state) methyltransferase	AS3MT	223652_at	2.415
Parkinson disease (autosomal recessive, juvenile) 2, parkin	PARK2	207058_s_at	2.415
coiled-coil domain containing 138	CCDC138	235644_at	2.415
glycosyltransferase 8 domain containing 2	GLT8D2	221447_s_at	2.415
glycosyltransferase 8 domain containing 2	GLT8D2	227070_at	2.415
integrin, beta 8	ITGB8	226189_at	2.410
P antigen family, member 1 (prostate associated)	PAGE1	206897_at	2.404
hypothetical FLJ13197	FLJ13197	219871_at	2.392
zinc finger protein 541	ZNF541	232604_at	2.392
V-set and transmembrane domain containing 2A	VSTM2A	230117_at	2.392
microtubule-associated protein 7	MAP7	202890_at	2.392
Synaptotagmin XVII	SYT17	229053_at	2.392
aldehyde dehydrogenase 6 family, member A1	ALDH6A1	221588_x_at	2.387
BRF1 homolog, subunit of RNA polymerase III transcription initiation factor IIIB (S. cerevis	BRF1	215676_at	2.381
paraneoplastic antigen MA2	PNMA2	209598_at	2.381
GLE1 RNA export mediator homolog (yeast)	GLE1	206920_s_at	2.381

Table S2.4 cont'd.

synaptotagmin XII	SYT12	228072_at	2.375
MOCO sulphurase C-terminal domain containing 2	MOSC2	227417_at	2.370
ribosomal protein L13	RPL13	229590_at	2.364
dehydrogenase/reductase (SDR family) member 2	DHRS2	206463_s_at	2.358
chromosome 4 open reading frame 23	C4orf23	220891_at	2.358
elongation of very long chain fatty acids (FEN1/Elo2, SUR4/Elo3, yeast)-like 3	ELOVL3	234513_at	2.358
testis specific, 14	TSGA14	215637_at	2.353
gap junction protein, alpha 3, 46kDa	GJA3	239572_at	2.353
hypothetical protein LOC100130506	LOC100130506	236656_s_at	2.353
integrin, beta 4	ITGB4	204990_s_at	2.353
phospholipase C, beta 4	PLCB4	203895_at	2.353
hypothetical LOC401052	LOC401052	232812_at	2.353
Fanconi anemia, complementation group D2	FANCD2	242560_at	2.353
hypothetical LOC346547	FLJ42291	238648_at	2.347
SEC31 homolog B (S. cerevisiae)	SEC31B	209889_at	2.347
sphingomyelin synthase 2	SGMS2	227038_at	2.347
chromosome 14 open reading frame 147	C14orf147	213508_at	2.342
SEC16 homolog B (S. cerevisiae)	SEC16B	228150_at	2.342
chromosome 11 open reading frame 54	C11orf54	223268_at	2.342
transmembrane protein 190	TMEM190	1552594_at	2.342
non-metastatic cells 5, protein expressed in (nucleoside-diphosphate kinase)	NME5	206197_at	2.336
chromosome 4 open reading frame 12	C4orf12	241401_at	2.331
Spectrin, beta, non-erythrocytic 1	SPTBN1	213914_s_at	2.331
2,5-oligoadenylate synthetase 1, 40/46kDa	OAS1	205552_s_at	2.331
KIAA1652 protein	KIAA1652	1560671_at	2.326
toll-interleukin 1 receptor (TIR) domain containing adaptor protein	TIRAP	1552804_a_at	2.326
chromosome 6 open reading frame 64	C6orf64	218784_s_at	2.326
progesterone receptor membrane component 2	PGRMC2	213227_at	2.320
5-nucleotidase domain containing 1	NT5DC1	223178_s_at	2.315
Protein kinase (cAMP-dependent, catalytic) inhibitor alpha	PKIA	226864_at	2.315
aldehyde dehydrogenase 6 family, member A1	ALDH6A1	204290_s_at	2.309
solute carrier family 25, member 27	SLC25A27	230624_at	2.304
solute carrier family 39 (zinc transporter), member 8	SLC39A8	209267_s_at	2.304
chromosome 10 open reading frame 11	C10orf11	223703_at	2.294
phospholipase C, beta 1 (phosphoinositide-specific)	PLCB1	215687_x_at	2.283
EF-hand calcium binding domain 3 /// similar to hypoxia-inducible protein 2	EFCAB3 /// LOC	1553392_at	2.283
SLIT and NTRK-like family, member 4	SLITRK4	232636_at	2.283
LIM and cysteine-rich domains 1	LMCD1	218574_s_at	2.283
caspase 10, apoptosis-related cysteine peptidase	CASP10	205467_at	2.278
tensin like C1 domain containing phosphatase (tensin 2)	TENC1	212494_at	2.278
hypothetical LOC151162 /// mannosyl (alpha-1,6-)-glycoprotein beta-1,6-N-acetyl-glucosa	LOC151162 ///	212098_at	2.278
CAP, adenylate cyclase-associated protein, 2 (yeast)	CAP2	212551_at	2.273
ephrin-A5	EFNA5	227955_s_at	2.268
phosphoinositide-3-kinase interacting protein 1	PIK3IP1	221756_at	2.262
CD302 molecule	CD302	203799_at	2.262
coxsackie virus and adenovirus receptor pseudogene 1	CXADRP1	239155_at	2.262
spermatogenesis associated 6	SPATA6	238459_x_at	2.252
nucleoredoxin	NXN	219489_s_at	2.252
mucin 1, cell surface associated	MUC1	213693_s_at	2.252
decorin	DCN	211813_x_at	2.252
neuropeptide Y receptor Y5	NPY5R	207400_at	2.252
septin 8	08-Sep	226627_at	2.252
nicotinamide N-methyltransferase	NNMT	202238_s_at	2.247
chromosome 1 open reading frame 53	C1orf53	1558507_at	2.247
mucin 1, cell surface associated	MUC1	207847_s_at	2.242
carbohydrate (chondroitin 4) sulfotransferase 11	CHST11	219634_at	2.242
dipeptidyl-peptidase 4	DPP4	203716_s_at	2.232
ELL associated factor 2	EAF2	219551_at	2.232
transducin (beta)-like 1X-linked	TBL1X	201868_s_at	2.232
OMA1 homolog, zinc metallopeptidase (S. cerevisiae)	OMA1	226019_at	2.232
retinoic acid receptor responder (tazarotene induced) 2	RARRES2	209496_at	2.232

Table S2.4 cont'd.

NADH dehydrogenase (ubiquinone) 1 beta subcomplex, 6, 17kDa	NDUFB6	1559042_at	2.227
solute carrier family 46, member 3	SLC46A3	214719_at	2.222
glycine C-acetyltransferase (2-amino-3-ketobutyrate coenzyme A ligase)	GCAT	205164_at	2.222
similar to pM5 (3 partial) /// NODAL modulator 1 /// NODAL modulator 2 /// NODAL modul	LOC100133864	242922_at	2.222
sidekick homolog 1, cell adhesion molecule (chicken)	SDK1	229912_at	2.217
SIX homeobox 4	SIX4	229796_at	2.212
cell cycle progression 1	CCPG1	221511_x_at	2.212
metallothionein 1M	MT1M	217546_at	2.203
potassium channel tetramerisation domain containing 12	KCTD12	212188_at	2.203
basonuclin 1	BNC1	1552487_a_at	2.198
basic helix-loop-helix family, member e41	BHLHE41	221530_s_at	2.193
zinc finger (CCCH type), RNA-binding motif and serine/arginine rich 1	ZRSR1	206512_at	2.193
nuclear factor (erythroid-derived 2)-like 3	NFE2L3	204702_s_at	2.193
prostaglandin D2 synthase 21kDa (brain)	PTGDS	211748_x_at	2.188
chromosome 12 open reading frame 35	C12orf35	218614_at	2.188
sema domain, immunoglobulin domain (Ig), short basic domain, secreted, (semaphorin) 3	SEMA3A	206805_at	2.174
hypothetical protein LOC100131731	LOC100131731	1557263_s_at	2.169
arachidonate 5-lipoxygenase-activating protein	ALOX5AP	204174_at	2.165
Rho GTPase activating protein 18	ARHGAP18	225173_at	2.165
methylcrotonoyl-Coenzyme A carboxylase 2 (beta)	MCCC2	1560033_at	2.165
bestrophin 4	BEST4	1552296_at	2.160
ferritin, heavy polypeptide 1	FTH1	214211_at	2.160
dipeptidyl-peptidase 4	DPP4	211478_s_at	2.160
ATP synthase, H+ transporting, mitochondrial F1 complex, delta subunit	ATP5D	203926_x_at	2.155
frizzled homolog 2 (Drosophila)	FZD2	210220_at	2.151
runt-related transcription factor 1	RUNX1	209360_s_at	2.151
engulfment and cell motility 1	ELMO1	204513_s_at	2.151
solute carrier family 27 (fatty acid transporter), member 1	SLC27A1	226728_at	2.151
flavin containing monooxygenase 4	FMO4	206263_at	2.151
RAB40B, member RAS oncogene family	RAB40B	204547_at	2.141
similar to Six transmembrane epithelial antigen of prostate	MGC87042	217553_at	2.141
zinc finger, FYVE domain containing 16	ZFYVE16	1555982_at	2.141
chromosome 12 open reading frame 72	C12orf72	1563474_at	2.137
smoothened homolog (Drosophila)	SMO	218629_at	2.132
V-set and immunoglobulin domain containing 1	VSIG1	243764_at	2.128
cytochrome P450, family 39, subfamily A, polypeptide 1	CYP39A1	1553977_a_at	2.123
hypothetical protein LOC283658	LOC283658	239741_at	2.123
intraflagellar transport 122 homolog (Chlamydomonas)	IFT122	220744_s_at	2.119
cell cycle progression 1	CCPG1	214151_s_at	2.114
transcription elongation factor A (SII), 3	TCEA3	226388_at	2.110
polymerase (DNA directed), mu	POLM	222238_s_at	2.110
Chromosome 12 open reading frame 32	C12orf32	241074_at	2.105
LIM domains containing 1	LIMD1	222762_x_at	2.105
von Willebrand factor A domain containing 5A	VWA5A	205011_at	2.105
spermatogenesis associated 17	SPATA17	230763_at	2.101
NHL repeat containing 3	NHLRC3	227040_at	2.096
Hypothetical LOC645513	LOC645513	1561761_x_at	2.096
C-type lectin domain family 7, member A	CLEC7A	1555213_a_at	2.096
phospholipid scramblase 1	PLSCR1	202430_s_at	2.096
syntrophin, beta 1 (dystrophin-associated protein A1, 59kDa, basic component 1)	SNTB1	226438_at	2.092
ubiquitin-like modifier activating enzyme 7	UBA7	203281_s_at	2.088
phosphoribosyl pyrophosphate synthetase 2	PRPS2	203401_at	2.083
SATB homeobox 1	SATB1	203408_s_at	2.083
Carbohydrate (chondroitin 4) sulfotransferase 11	CHST11	226368_at	2.083
formin binding protein 1	FNBP1	230389_at	2.083
prostaglandin D2 synthase 21kDa (brain)	PTGDS	212187_x_at	2.079
inhibin, alpha	INHA	210141_s_at	2.079
zinc finger protein 853	ZNF853	232884_s_at	2.079
chromosome 5 open reading frame 4	C5orf4	220751_s_at	2.075
nei endonuclease VIII-like 1 (E. coli)	NEIL1	219396_s_at	2.075
coiled-coil domain containing 82	CCDC82	220693_at	2.070

Table S2.4 cont'd.

zinc finger protein 658	ZNF658	231950_at	2.070
coiled-coil domain containing 109B	CCDC109B	218802_at	2.066
peroxisomal biogenesis factor 1	PEX1	204873_at	2.066
ERO1-like beta (S. cerevisiae)	ERO1LB	231944_at	2.062
fucosidase, alpha-L- 1, tissue	FUCA1	202838_at	2.062
cell division cycle associated 7-like	CDCA7L	225081_s_at	2.058
cancer susceptibility candidate 5	CASC5	228323_at	2.053
Hypothetical gene supported by BC043549; BX648102	DKFZp686O13	216874_at	2.053
transglutaminase 2 (C polypeptide, protein-glutamine-gamma-glutamyltransferase)	TGM2	201042_at	2.053
glutamate receptor, ionotrophic, AMPA 3	GRIA3	208032_s_at	2.049
RNA binding motif, single stranded interacting protein 2	RBMS2	225778_at	2.041
LSM5 homolog, U6 small nuclear RNA associated (S. cerevisiae)	LSM5	202903_at	2.041
phytanoyl-CoA dioxygenase domain containing 1	PHYHD1	226846_at	2.037
Nuclear autoantigenic sperm protein (histone-binding)	NASP	242918_at	2.037
HBV preS1-transactivated protein 4	PS1TP4	226381_at	2.037
hypothetical locus LOC401237	FLJ22536	229280_s_at	2.037
CUG triplet repeat, RNA binding protein 2	CUGBP2	227178_at	2.033
syndecan 3	SDC3	202898_at	2.033
cold inducible RNA binding protein	CIRBP	225191_at	2.024
elastin microfibril interfacer 1	EMILIN1	204163_at	2.020
melanoma associated antigen (mutated) 1-like 1	MUM1L1	229160_at	2.020
adaptor-related protein complex 2, alpha 1 subunit	AP2A1	223237_x_at	2.016
potassium inwardly-rectifying channel, subfamily J, member 12	KCNJ12	207110_at	2.008
ribonuclease H2, subunit B	RNASEH2B	219056_at	2.008
CTD (carboxy-terminal domain, RNA polymerase II, polypeptide A) small phosphatase-lik	CTDSPL	201906_s_at	2.008
myotubularin related protein 3	MTMR3	202198_s_at	2.008
Rho guanine nucleotide exchange factor (GEF) 3	ARHGEF3	218501_at	2.008
nuclear receptor subfamily 1, group H, member 3	NR1H3	203920_at	2.008
ATP-binding cassette, sub-family A (ABC1), member 5	ABCA5	213353_at	2.008
carbonic anhydrase XII	CA12	204509_at	2.008
cytochrome b5 type B (outer mitochondrial membrane)	CYB5B	227382_at	2.008
potassium inwardly-rectifying channel, subfamily J, member 12	KCNJ12	232289_at	2.000

Chapter 3

3 LKB1 signalling protects dormant ovarian cancer spheroids from cell death in an AMPK-independent manner

3.1 Introduction

Ovarian cancer is the most lethal gynecologic malignancy in the western world, the overall survival of which has remained unchanged for more than 50 years[1,2]. Models that can be used to uncover the molecular events important for disease dissemination are crucial since the majority of women with ovarian cancer (over 75%) are diagnosed at advanced stage[3]. Intraperitoneal implants identified in these patients with advanced-stage disease are the result of single cells and multicellular aggregates, or spheroids, that adhere to the mesothelial lining of various abdominal organs to establish secondary lesions[4-6]. In many cases, this is accompanied by accumulation of ascites fluid within the peritoneal cavity, where cells in suspension are exposed to a unique set of microenvironmental cues, allowing this population of cells to form secondary metastases[3-5,7]. These non-adherent metastatic cells provide unique therapeutic challenges for treatment of ovarian cancer[3].

The biological significance and clinical relevance of multicellular spheroids has been documented in many different tumour types[8-14]. It is well accepted that spheroids more closely mimic the cell-cell, cell-matrix interactions, metabolic gradients, cellular viability and differentiation of malignant cells within a solid tumour than do conventional monolayer cultures[15]. We have shown that ascites-derived ovarian cancer cells in suspension form dormant multicellular aggregates characterized by quiescence and decreased Akt activity[16]. These dormant cells are subsequently able to re-enter the cell cycle and grow when they reach an adherent substratum.[16]. Ovarian cancer cells that are able to resist anoikis and survive within ascitic fluid most likely have uniquely adapted key cell survival pathways to meet the nutrient and energy demands of this particular microenvironment.

A fundamental requirement of all cells is the ability to respond to various forms of metabolic stress and balance ATP consumption and generation in response. Under conditions where nutrients are low, AMPK acts as a metabolic checkpoint by activating catabolic processes and inhibiting anabolic metabolism[17,18]. AMPK is a heterotrimeric complex containing a catalytic α-subunit and two regulatory subunits, β and γ. When intracellular ATP levels are low, AMP or ADP directly bind to the γ regulatory subunits. This causes a conformation change in the complex that allows AMPK to be phosphorylated at threonine 172 on the α subunit[17]. The primary kinase responsible for phosphorylation at this site is LKB1[19-21].

It has been suggested that AMPK may function as a context-dependent tumour suppressor or oncogene[22]. Modest activation of AMPK may be cell protective, but prolonged or enhanced activation can be detrimental and result in growth arrest or cell death[18]. The most thoroughly characterized mechanism through which the LKB1/AMPK pathway regulates cell growth is by suppression of mTORC1 signalling. LKB1, on the other hand, is commonly regarded as a tumour suppressor, and is mutated in the rare hereditary autosomal dominant Peutz Jeghers Syndrome. These patients experience benign intestinal hamartomatous polyps and have an increased risk of developing malignant tumours[23]. Despite this, LKB1 mutations have been identified in relatively few sporadic cancers.

Previous studies have shown that metabolic stress is induced when normal epithelial cells lose ECM attachment, resulting in a decreased ATP:ADP ratio and subsequent activation of AMPK[24-26]. However, this suspension-induced AMPK activation has yet to be examined in tumour spheroids. In our study, we use a disease-relevant spheroid model to interrogate the function of the LKB1/AMPK pathway in ovarian cancer cells. Our results indicate that LKB1 and AMPK serve distinct functions in ovarian cancer cells and spheroids to promote dormancy and anoikis-resistance.

3.2 Materials and Methods

3.2.1 Culture of cell lines, ascites-derived cells and isolation of native ascites spheroids

Ascites fluid from patients diagnosed with advanced stage (II-IV), high-grade serous epithelial ovarian cancer (Table S1) was used to establish primary cell cultures as previously described[27]. The iOvCa147-E2 and iOvCa198 cell line were isolated from the EOC147 and EOC 198 ascites samples respectively. All work with patient materials has been approved by The University of Western Ontario Health Sciences Research Ethics Board (Protocol # 12668E and 16391E; Appendix B). Spheroids were isolated directly from ascites fluid by filtration through a 40 μm cell strainer (Becton Dickinson), washed with phosphate-buffered saline (PBS) into a collection tube with protein lysis buffer for immunoblot or embedded directly in OCT to obtain fresh frozen sections.

3.2.2 TCGA Analysis

Datasets from The Cancer Genome Atlas analysis of ovarian serous cystadenocarcinoma samples were downloaded from the University of California Santa Cruz Cancer Genomics Browser (https://genome- cancer.ucsc.edu)[28] and from the Memorial Sloan-Kettering Cancer Center's cBioPortal for Cancer Genomics (http://www.cbioportal.org/)[29]. Array comparative genomic hybridization data was acquired at the Broad TCGA genome characterization center using the Affymetrix Genome-Wide Human SNP Array 6.0 platform. Raw data was analyzed using the GISTIC2 method to generate gene-level copy-number variation (CNV) estimates and downloaded as either thresholded copy-number calls or as log2-transformed CNV values. Protein expression data was generated and processed at the MD Anderson Cancer Center TCGA proteome characterization center using reverse-phase protein array (RPPA) technology as described[30] and downloaded either natural log-transformed values or as z-scores.

3.2.3 Immunoblotting and Immunofluorescence

Whole cell protein lysates were generated from cell lines and ascites-derived cells in adherent and spheroid culture as previously described[31]. Antibodies used for immunoblot against p-AMPKα Thr172 (#2535), AMPKα (#5832), p-LKB1 Ser428 (#3482), LKB1 (#3050), p-p70S6K1 Thr 389 (#9234), p-ACC (#3661), ACC (#3676) and p70S6K1 (#2708) were obtained from Cell Signaling Technology (Danvers, MA). Anti-Tubulin antibody was obtained from Sigma. AICAR was purchased from Caymen Chemical Company (Ann Arbor, MI) and A-769662 from Tocris Bioscience (Bristol, UK). Immunofluorescent (IF) analysis was performed on fresh frozen sections that were fixed (4% formaldehyde), permeabilized (0.1% Triton X-100 in PBS), and blocked (5% BSA in 0.1% Triton X-100) before incubation with p-AMPKα antibody (#ab51110) from abcam® Inc. (Cambridge, MA). Following primary antibody incubation and PBS washes, sections were incubated for 1 hour with anti-rabbit FITC secondary antibody (1:250; Sigma-Aldrich). After further washing, sections were incubated with 4',6-diamidino-2-phenylindole (DAPI; 1:1000) and slides were mounted with Vectashield (Vector Laboratories, Burlingame CA, USA). Fluorescence images were captured using an Olympus AX70 upright microscope and ImagePro image capture software.

3.2.4 Cell Viability and ATP assays

Cells were seeded to either 24-well tissue culture plastic or ultra-low attachment (ULA) plates at a density of $1.0x10^4$ to form adherent cultures or $5.0x10^4$ per well to form spheroids, respectively.. Treatment was initiated at time of seeding for cells in suspension while cells under adherent conditions were given 12 hours to adhere prior to commencing treatment. CellTiter-Glo® reagent (Promega, Madison, WI) was prepared according to manufacturer's instructions. At 72h post-treatment, spheroids were collected, pelleted and left in a minimal volume of media (100 µL), at which point CellTiter-Glo® reagent was added in a 1:1 volume ratio. Under adherent conditions, cells were harvested directly in CellTiter-Glo® reagent (1:1 reagent/media) after a 20 minute incubation period. All samples were subject to a freeze/thaw cycle prior to analysis. Approximately 200µL of the mixture was added to a white-walled 96-well micro-plate and luminescence signal was detected using a microplate spectrophotometer (Wallac 1420 Victor 2; Perkin-Elmer,

Waltham, MA). Treatments were conducted in at least duplicate wells and luminescence readings normalized to cells treated with vehicle control.

3.2.5 siRNA transfections

All siRNA transfections were performed in a 6-well format. The day prior to transfection, cells were plated at a density of approximately 1×10^5 cells per well in antibiotic-free media. The next day, DharmaFECT transfection reagent (DharmaFECT1 for OVCA429 and iOVCA147-E2 and DharmaFECT3 for SKOV3) was used to transfect cells, as per manufactures protocol. Briefly, 1 µl of DharmaFECT1 or 4 µl of DharmaFECT3 was combined with 10nM siRNA in a volume of 1mL of media (Wisent) and incubated for 20 min; the complexes of DharmaFECT and siRNAs were then added directly to each well. Media was removed 24 hours following transfection and replaced with fresh antibiotic-free growth media. At this point, the cells were incubated until nearly confluent, approximately 72 hours following transfection. *PRKAA1* and *STK11* siRNAs (M-005027-02 and M-005035-02 respectively) were obtained from Dharmacon (Thermo Fisher Scientific Inc., Waltham, MA). All siRNAs used were siGENOME SMARTpool predesigned pools of four oligos.

3.2.6 Graphing and Statistical Analysis

All graphs were generated using GraphPad Prism 5 (GraphPad Software, San Diego, CA). Data were expressed as Mean ± SEM, as indicated. All statistical analysis (Student's *t*-test and Analysis of Variance (ANOVA) with Tukey's Multiple Comparison Test) was performed using GraphPad Prism 5. Tests of significance were set at $p < 0.05$.

3.3 Results

3.3.1 AMPKα1 is expressed in metastatic ovarian tumour samples and is associated with a high frequency of copy-number gains and amplifications.

AMPK has been described in many instances to serve as a tumour suppressor despite the lack of genetic evidence to demonstrate a loss of AMPK function in cancer[18]. In order to assess AMPK activity in a large number of serous ovarian tumours, the majority of which (91.1%) are from metastatic, stage III-IV cases, we made use of level 3 array comparative genomic hybridization (aCGH) and reverse phase protein array (RPPA) data from The Cancer Genome Atlas (TCGA). This analysis revealed copy-number gain of the *PRKAA1* gene (encoding AMPKα1) in 36% (111/311) of samples (Figure 3.1A). To determine whether *PRKAA1* copy-number correlated with protein expression, we plotted RPPA data against copy-number calls for both phosphorylated (T172) and total AMPKα1. This demonstrated a significant increase in both phosphorylated (Figure 3.1B) and total AMPKα1 (Figure 3.1C) in samples with copy-number gain. Using log2-transformed copy-number data, we also performed regression analysis to measure the correlation between *PRKAA1* copy-number and protein expression. This revealed a positive correlation between copy-number and AMPKα1 protein expression (both phosphorylated and total; Figure 3.1D&E). In addition, we also noted a positive correlation between AMPKα1 protein expression and activity (Figure 3.1F). To verify AMPKα1 expression and activity in fresh tumour specimens, we performed western blots on lysates harvested from metastatic tumour samples obtained by our lab (Figure 3.1G). Indeed, our direct results demonstrate that AMPKα1 is expressed and active in metastatic ovarian tumours.

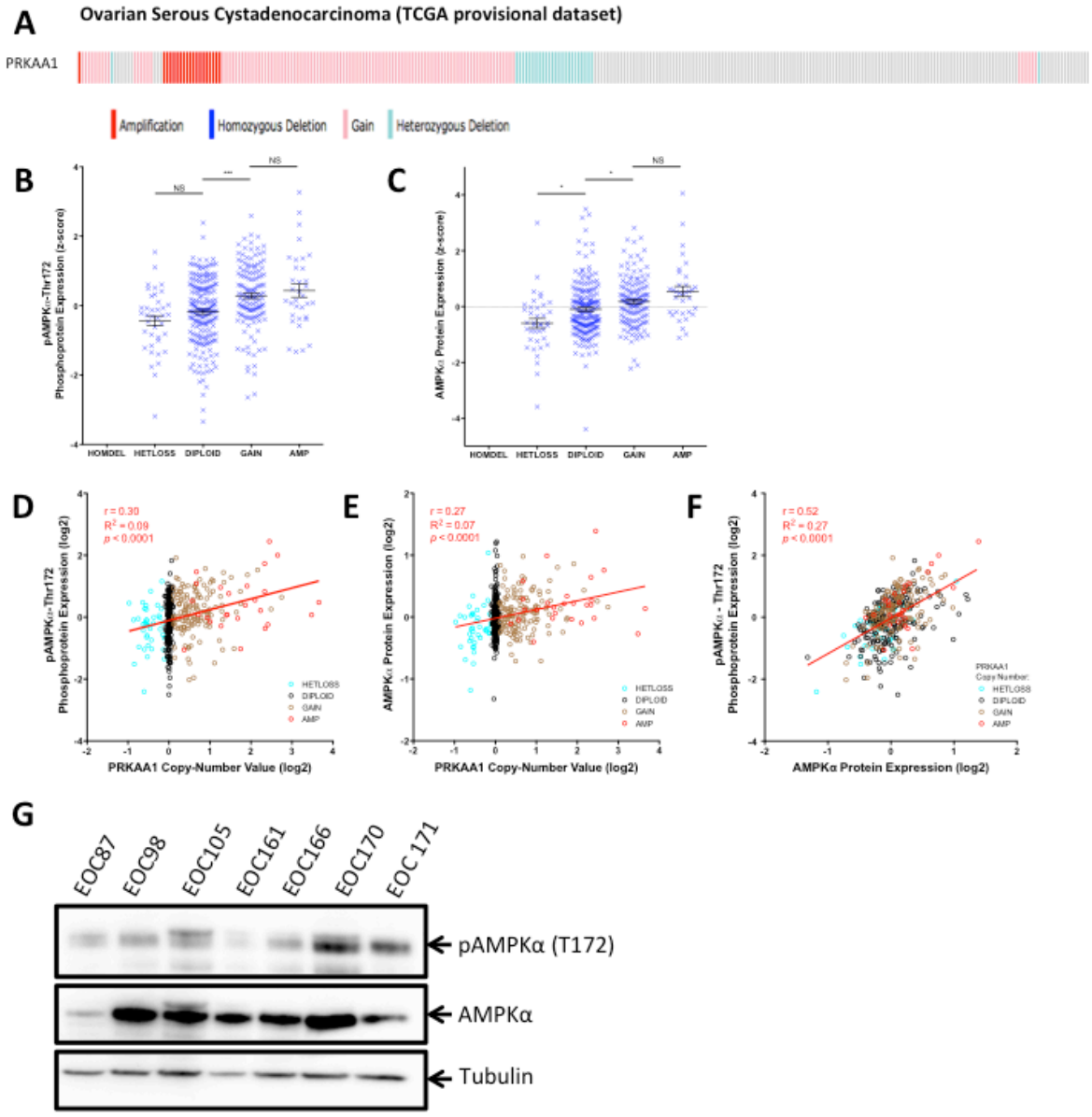

Figure 3.1: The AMPK pathway is active in mestatic ovarian tumour samples.
(A) Gene copy-number calls at the *PRKAA1* locus are depicted for 311 ovarian serous cystadenocarcinoma tumors (red & pink = high-level & low-level amplification, respectively; teal &blue = heterozygous & homozygous deletion, respectively). OncoPrint obtained from cBioPortal.org. (B,C) Phosphorylated and total AMPKα1 protein (quantitative RPPA; n=398) expression data were transformed to z-scores and depicted as functions of copy-number. One-way ANOVA with Tukey's Test was performed (*p<0.05; ***p<0.001). (D,E) ln-transformed protein expression (n=397;re-transformed to $\log_2$ values) data depicted as a function of $\log_2$-transformed copy number values. (F) Phosphorylated AMPKα1 protein expression depicted as a function of total protein. Correlation and linear regression analysis performed: line of best fit, Pearson's r, Goodness-of-fit R^2, and p values all reported. (G) Lysates were generated from metastatic tumour samples from seven ovarian cancer patients and immunoblot was performed to examine AMPK activity in these samples.

3.3.2 Multicellular aggregates filtered from patient ascites fluid exhibit enhanced AMPK activity.

Our lab has previously demonstrated that ovarian cancer cells which form multicellular aggregates *in vitro* enter a dormant state, a process which is aided by decreased AKT activity[16]. Herein, we postulate that the AMPK pathway is another pathway, that mediates spheroid formation-induced dormancy. due to its unique ability to respond to stresses, such as nutrient deprivation and hypoxia. In order to evaluate this, we analyzed AMPK activity in native ascites spheroids filtered directly from patient ascites fluid by western blot and immunofluorescence. Lysates generated from ascites spheroids filtered directly from a number of different patient ascites samples revealed a significant increase in AMPK activity in spheroids compared to matched adherent samples from the same patient (Figure 3.2A). Additionally, immunofluorescence on ascites-derived spheroids revealed intense expression of phosphorylated AMPKα1 in the cytoplasm and along the cell membrane (Figure 3.2B). These data indicate that AMPK activity is enhanced is actively metastatic cells in spheroids within malignant ascites fluid.

3.3.3 Ovarian cancer cell lines and ascites-derived cells in suspension exhibit decreased levels of ATP and enhanced AMPK activity.

Following our observation that AMPK activity is enhanced in native ascites spheroids, we sought to investigate regulation of this phenomenon further using spheroids formed *in vitro*. We hypothesized that as a result of spheroid formation induced-dormancy, the metabolic state of cells within these multicellular aggregates is decreased. To assess this, we used Cell Titer Glo® luminescence-based ATP assay to determine levels of intracellular ATP in ovarian cancer cells in adherent and spheroid form. Indeed, ATP levels were significantly lower in spheroids compared to their adherent counterparts (Figure 3.3A). Correspondingly, western blot analysis of adherent and spheroid ovarian cancer cells revealed a significant increase in AMPK activity associated with spheroid formation (Figure 3.3B,C). Taken together, these data demonstrate decreased ATP levels that are associated with increased AMPK activity when ovarian cancer cells aggregate to form multicellular clusters or spheroids.

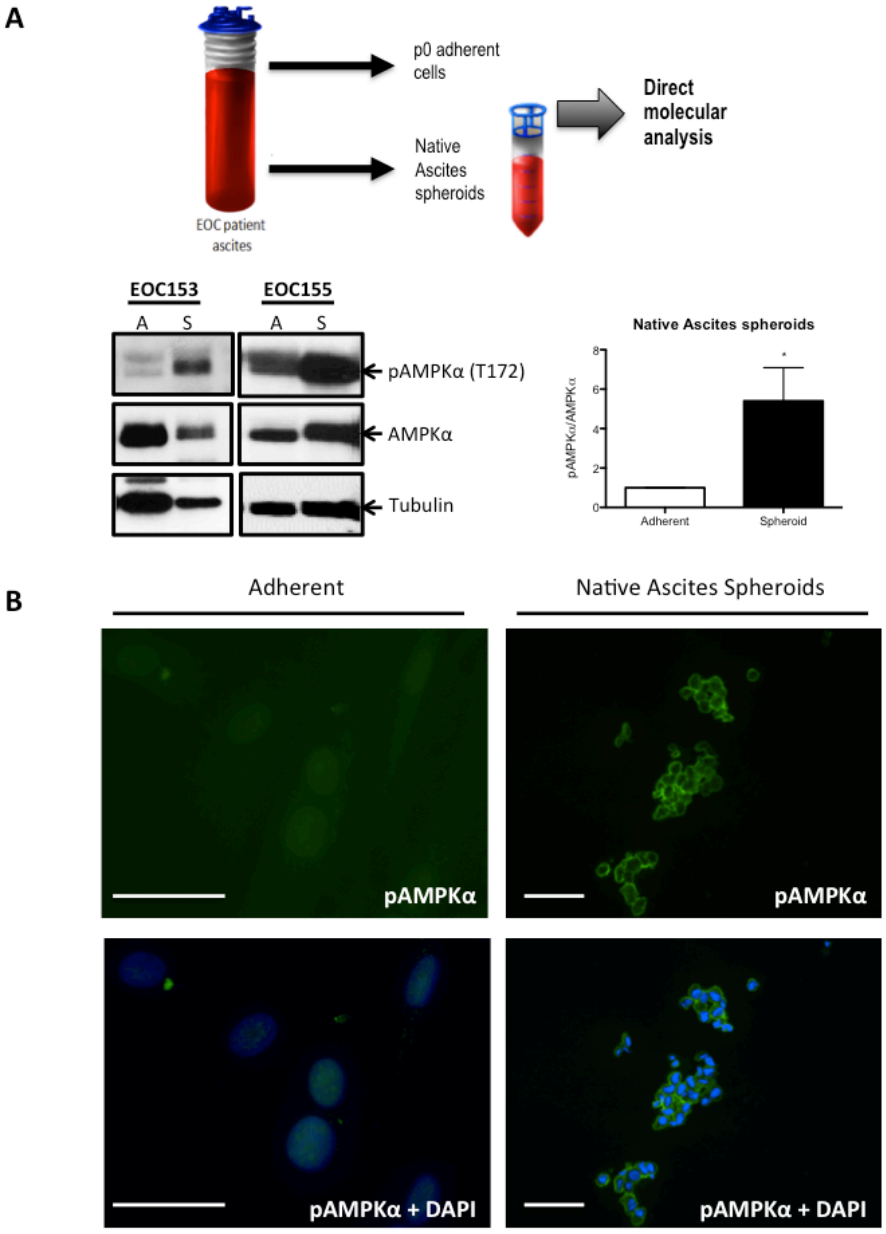

Figure 3.2: Native ascites spheroids have enhanced AMPK activity compared to adherent cells.

(A) Lysates were prepared from filtered spheroids [S] and passage 0 adherent cells [A] from 5 independent patient ascites samples. Immunoblot (shown representative image from two samples) and subsequent densitometry were performed to determine levels of phosphorylated AMPKα1 compared to total protein. Bars: Mean ± SEM. Levels of phosphorylated AMPKα1 were compared using Student's t-test (*$p<0.05$). (B) Spheroids filtered from patient ascites fluid for immunofluorescence analysis compared to early passage adherent cells from the same patient [EOC 169]. Nuclei (blue) and pAMPKα1 (green) are visible. Scale bar: 100μm.

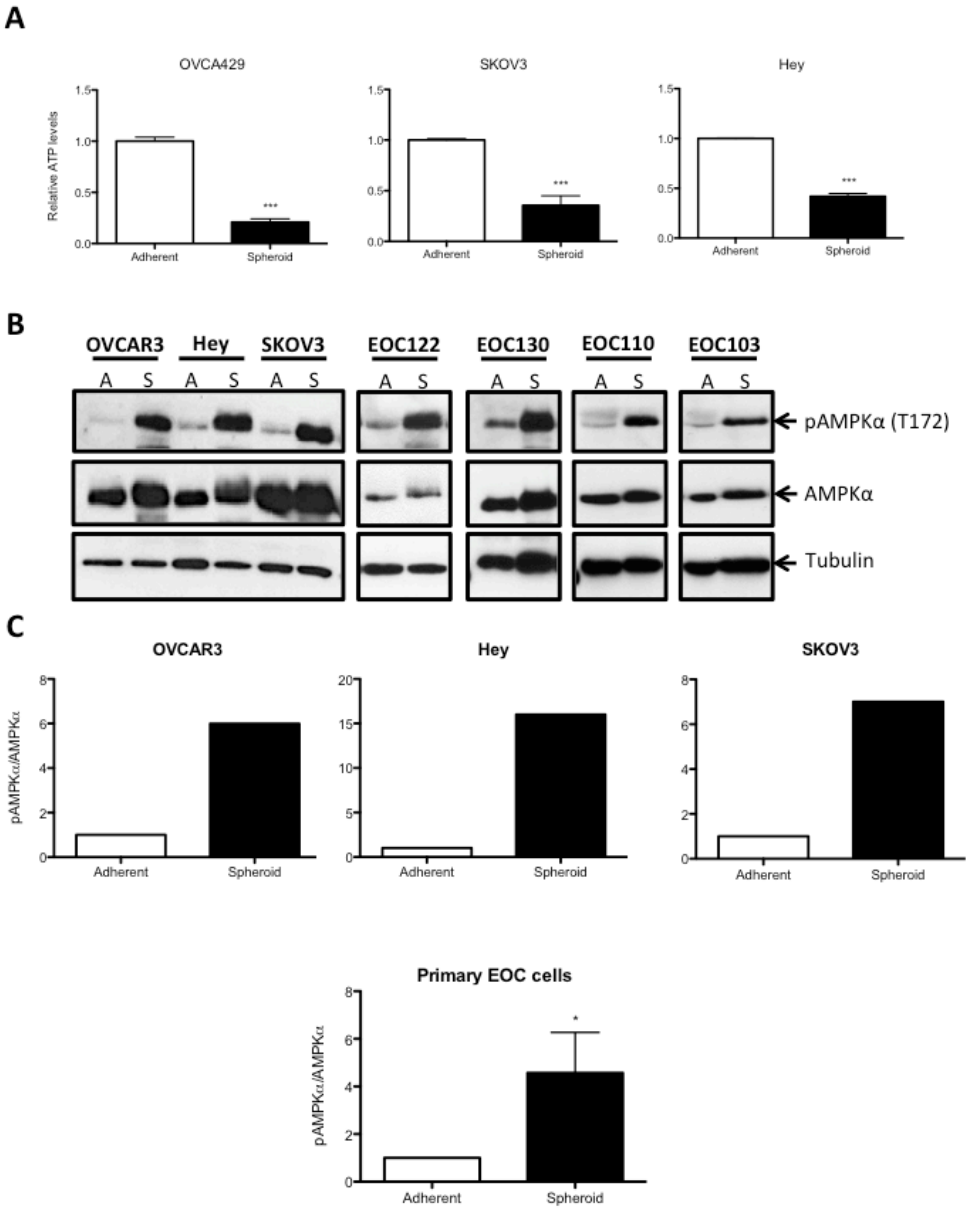

Figure 3.3: Spheroids formed from EOC cell lines and ascites-derived cells have decreased levels of ATP and corresponding increases in AMPK activity.
(A) Quantification of ATP levels in EOC cell lines cultured in both adherent and spheroid conditions using luminescence-based ATP assay CellTiter Glo®. Difference in viable cells between each culture condition was accounted for by normalizing results to total protein levels for each sample. Bars: Mean ± SEM. Student's t-test was used to compare levels of ATP between culture conditions (***$p<0.001$). (B) Immunoblot performed on EOC cell lines and ascites-derived EOC cells to determine levels of phosphorylated and total AMPKα1 protein. (C) Densitometry was performed on cell lines and primary EOC cells (n=14) to compare levels of phosphorylated AMPKα1 between adherent and spheroid cultured cells. Bars: Mean ± SEM. Student's t-test was used to determine statistical significance (*$p<0.05$).

3.3.4 LKB1 protein is expressed in metastatic ovarian tumour samples.

Activity of the key upstream AMPK kinase LKB1 is commonly thought to be tumour suppressive[32]. Multiple studies have suggested that single allelic inactivation of the *STK11* gene encoding LKB1 is sufficient to promote tumorigenesis, while other data suggests that biallelic loss may be required[33-36]. In order to examine status of LKB1 in serous ovarian tumours we again made use of data from the TCGA. Whereas copy-number gain was common for *PRKAA1*, heterozygous deletion of *STK11* was detected in 84% of samples (262/311; Figure 3.4A). This single allelic loss correlated with decreased protein expression compared to samples with normal copy-number (Figure 3.4B), and a positive correlation between *STK11* copy-number and LKB1 protein expression when we performed regression analysis on log2-transformed copy-number data (Figure 3.4C). When we sought to determine LKB1 expression in metastatic tumour samples obtained by our lab, however, we consistently observed expression of phosphorylated and total LKB1 (Figure 3.4D). Therefore, despite single allele loss of *STK11*, LKB1 protein expression is maintained in metastatic ovarian cancer cells and may in fact serve an important function in late-stage disease.

3.3.5 Suspension-induced activation of AMPK signalling is accompanied by enhanced LKB1 signalling and inhibition of mTORC1.

We next wanted to determine the specific components of the AMPK pathway that may also be altered when ovarian cancer cells are put in suspension. We first focused on LKB1 as a critical upstream activator of AMPK signalling. Immunoblot revealed increased phosphorylation of LKB1 at Serine 428 in spheroids formed from a number of ovarian cancer cell lines and ascites-derived cells compared to cells grown under adherent conditions (Figure 3.5A,B). Although its phosphorylation state does not affect its catalytic activity, phosphorylation at Ser428 has been shown to be important for the tumour suppressive functions of LKB1[37]. LKB1 can be localized to the nucleus or cytoplasm, and the cytoplasmic pool of LKB1 has been shown to contribute to the tumour suppressive function of this kinase[32]. We determined by cellular fractionation and

immunoblotting that LKB1protein in adherent and spheroid-cultured cells is located in the cytoplasm (Figure S3.1).

Since the LKB1/AMPK signalling pathway has been identified as a key negative regulator of mTORC1 signalling, we next focused on this pathway as a downstream readout for AMPK's ability to rewire cellular metabolism in these clusters of cells. Immunoblot performed on spheroids from cell lines and ascites-derived cells revealed a significant decrease in mTORC1 activity as determined by p70S6K1 phosphorylation (Figure 3.5C). Taken together, these results provide additional evidence for decreased anabolic metabolism that occurs when cells detach into suspension and form spheroids, indicating that the LKB1/AMPK/mTORC1 signalling axis may be a crucial mediator of cell survival in this context.

3.3.6 Spheroids are much less sensitive to further activation of the AMPK pathway than adherent ovarian cancer cells.

It has been previously demonstrated that treatment of ovarian cancer cells with AMP mimetic AICAR results in increased AMPK activity and decreased viability of adherent cells[38,39]. Similarly, in our study, we demonstrate robust activation of AMPK after treatment of ovarian cancer cells with 1 mM AICAR, which corresponds with decreased mTORC1 activity (Figure 3.6A). In addition, AICAR treatment of various ovarian cancer cell lines and ascites-derived cells results in decreased viability in cells cultured under both adherent and suspension conditions. Importantly, the detrimental effects of AICAR treatment on spheroid cell viability are not observed until later time points compared to their adherent counterparts (Figure 3.6B). When spheroids are treated with AICAR during reattachment, however, a significant reduction in dispersion area was observed highlighting the detrimental effect that AMPK activation has on cell proliferation (Figure 3.6C).

To further explore mechanisms of AMPK activation, we also tested a more specific allosteric AMPK activator, A-769662, which stimulates AMPK directly without affecting the kinase domain[40]. Treatment of ovarian cancer cells with A-769662 (100μM) results in activation of AMPK as indicated by enhanced phosphorylation of ACC (Figure

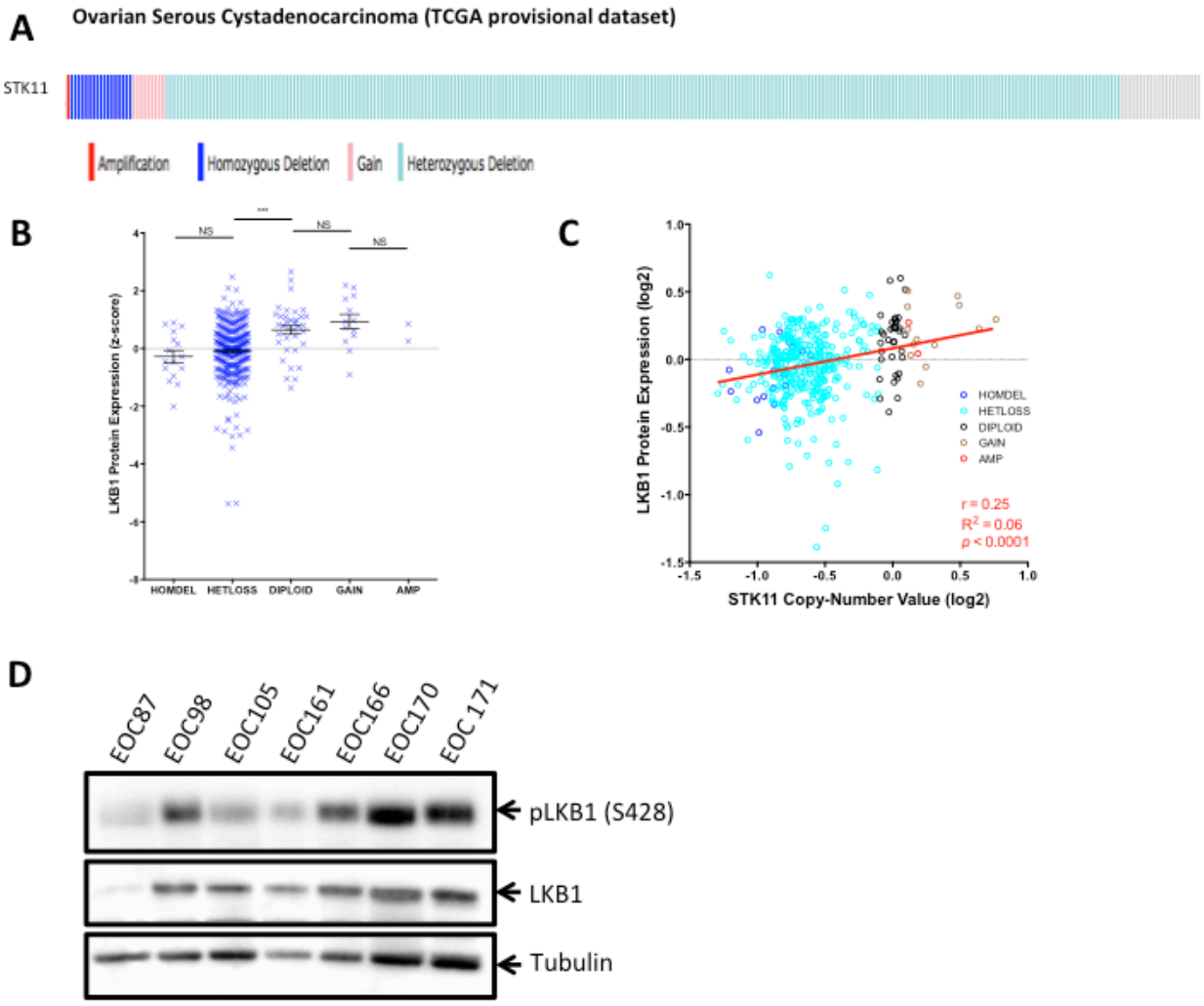

Figure 3.4: Despite heterozygous deletion, LKB1 protein is expressed in metastatic ovarian tumour samples.

(A) Gene copy-number calls at the *STK11* locus are depicted for 311 ovarian serous cystadenocarcinoma tumors (red & pink = high-level & low-level amplification, respectively; teal &blue = heterozygous & homozygous deletion, respectively). OncoPrint obtained from cBioPortal.org. (B) STK11 protein (quantitative RPPA; n=398) expression data was transformed to z-scores and depicted as functions of copy-number. One-way ANOVA with Tukey's Test was performed (***p<0.001). (C) ln-transformed protein expression (n=397;re-transformed to $\log_2$ values) data depicted as a function of $\log_2$-transformed copy number values. Correlation and linear regression analysis performed: line of best fit, Pearson's r, Goodness-of-fit R^2, and p values all reported. (D) Lysates were generated from metastatic tumour samples from seven ovarian cancer patients and immunoblot was performed to examine LKB1 expression in these samples.

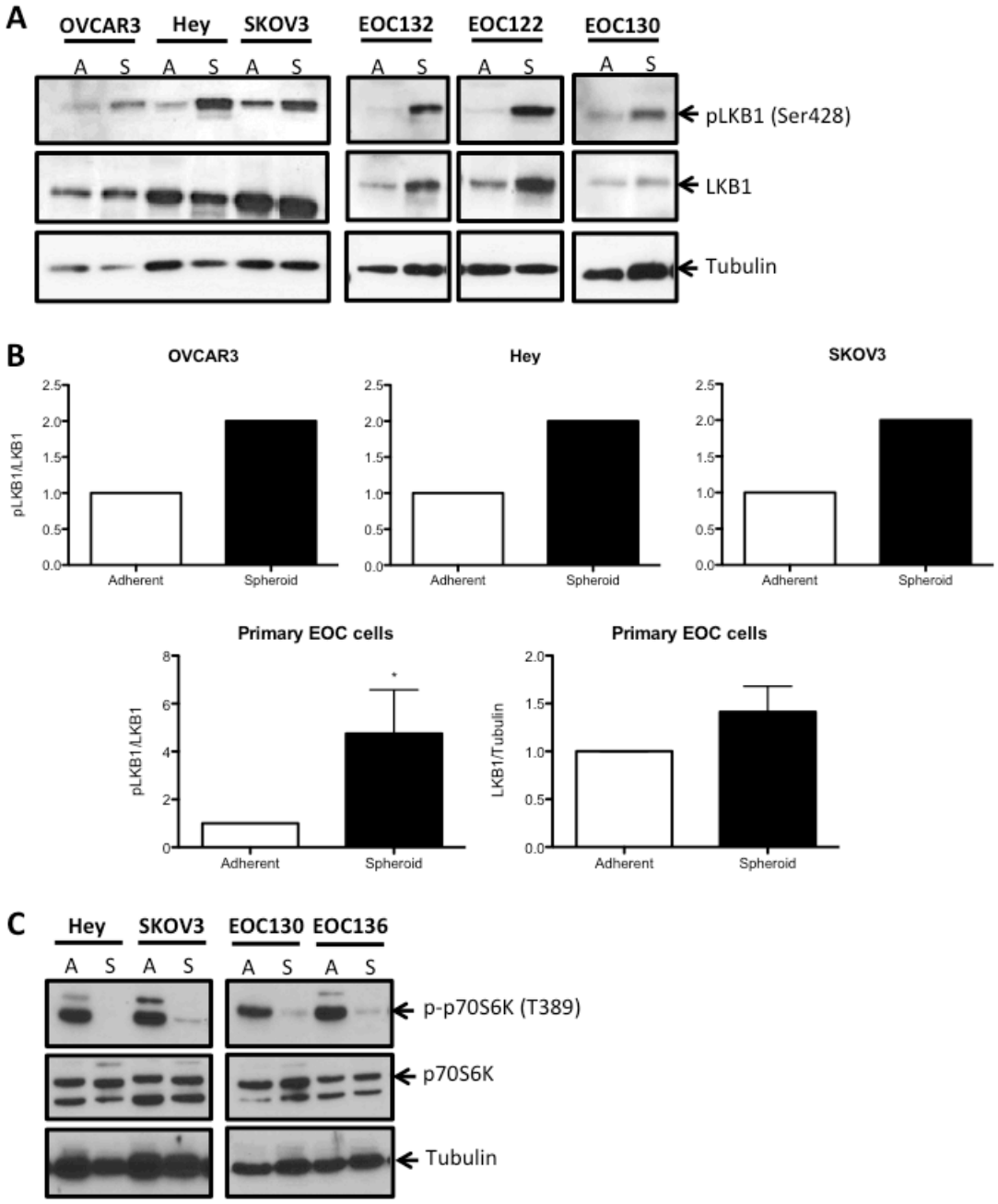

Figure 3.5: Spheroids formed from EOC cell lines and ascites-derived cells express LKB1 protein and have decreased levels of mTORC1 signalling.
(A) Immunoblot performed on EOC cell lines and ascites-derived EOC cells to determine levels of phosphorylated and total LKB1 protein. (B) Densitometry was performed on cell lines and primary EOC cells (n=16) to compare levels of phosphorylated and total LKB1 between adherent and spheroid cultured cells. Bars: Mean ± SEM. Student's t-test was used to determine statistical significance (*$p<0.05$). (C) Immunoblot performed on EOC cell lines and ascites-derived EOC cells to determine levels of phosphorylated and total p70S6K1 protein as a read-out of mTORC1 activity.

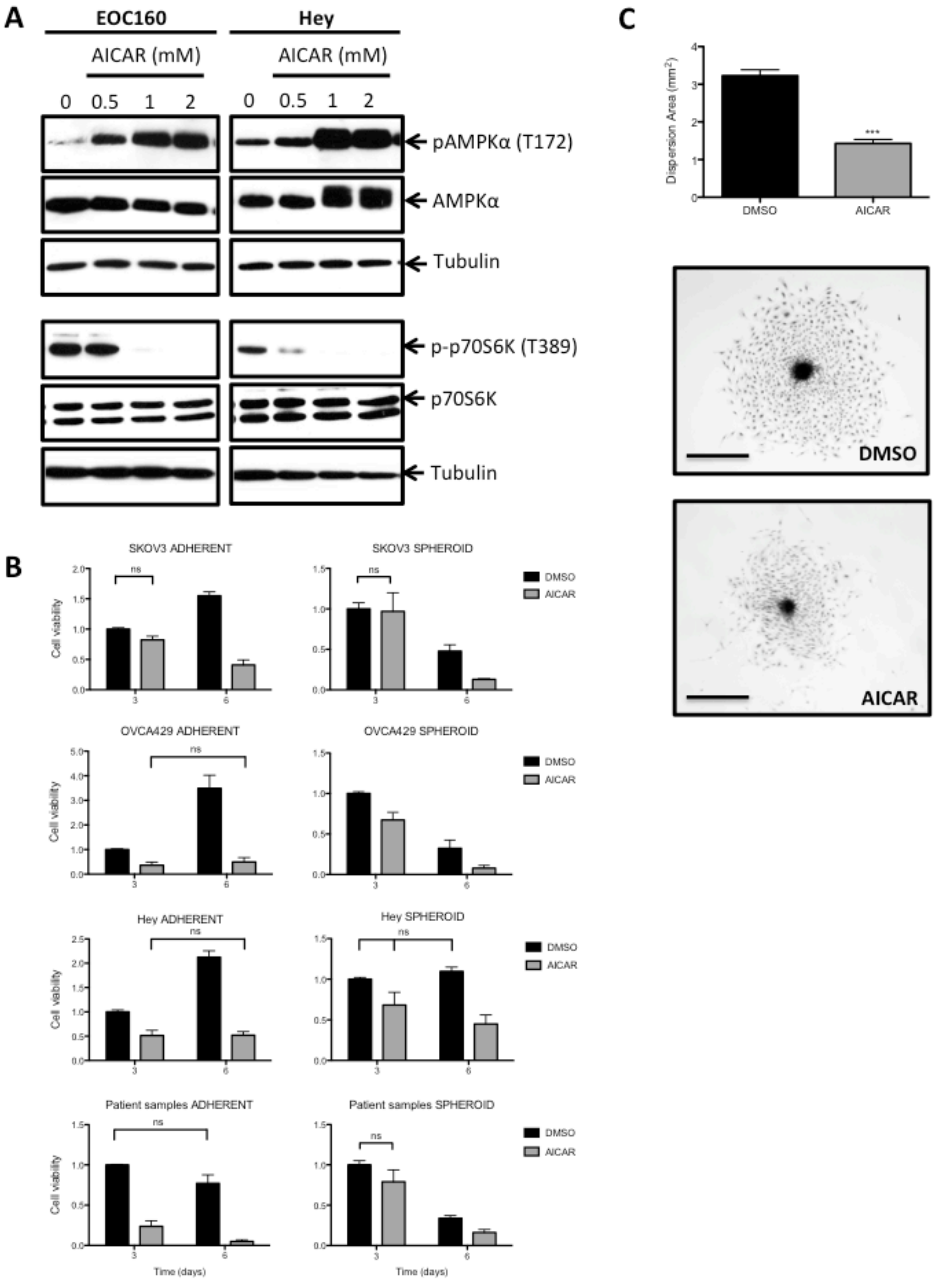

Figure 3.6: AICAR treatment of EOC cell lines and ascites-derived cells decreases cell viability in adherent and spheroid cells.

(A) Immunoblot performed on EOC cells treated for 24 hours with various doses of AICAR as indicated. (B) Viability of ovarian cancer cell lines and ascites-derived cells following 3 and 6 days of AICAR (1mM) treatment in adherent and spheroid culture conditions. Bars: Mean ± SEM. Effect of treatment at each timepoint was determined using Student's t-test. Results are significant ($p<0.05$) unless otherwise indicated. (C) Reattachment of spheroids (72h) formed from ascites-derived cells (n=9) treated with AICAR (1mM) at time of seeding to suspension culture. Quantifications performed using ImageJ and Student's t-test used to compare areas between groups (***$p<0.001$). Representative image of one patient sample (EOC154) depicted. Scale bar: 100µm.

3.7A). Similarly to AICAR treatment, this compound also reduces viability of ovarian cancer cells in adherent culture. However, there is no effect of A-769662 treatment on viability of cells in spheroids (Figure 3.7B). These results suggest that actively proliferating, adherent ovarian cancer cells are more sensitive to AMPK activation, but quiescent cells in multicellular spheroids are less impacted by a further increase in the activation state of this pathway.

Following the observation that both AICAR and A-769662 have detrimental effects on ovarian cancer cells in adherent culture, we further characterized this reduced viability by determining whether cells were undergoing apoptosis or arresting in a particular phase of the cell cycle. Both compounds result in a decreased proportion of cells in the S-phase of the cell cycle as early as 24 hours after treatment. The effect observed with AICAR treatment is more robust across different cell lines than that observed with A-769662 (Figure S3.2). We also used Caspase-Glo® luminescence-based assay which uses caspase 3/7 activity as a read-out for apoptosis. We found that 72 hours following treatment with AICAR (1mM), there was a significant induction of apoptosis, an effect which was not observed in A-769662-treated cells (Figure S3.2). These results suggest that these two compounds have different mechanisms of action in ovarian cancer cells: AICAR decreases ovarian cancer cell viability largely by apoptosis, whereas A-769662 elicits a cytostatic response thereby blocking ovarian cancer cell growth.

3.3.7 LKB1, but not AMPK, is required for ovarian cancer cell survival in suspension.

Given the relative insensitivity of ovarian cancer cells in suspension to further activation of AMPK, we assessed the functional impact of attenuation of the LKB1/AMPK pathway in spheroids. In order to do this we transfected ovarian cancer cell lines with siRNAs targeting either *PRKAA1* (AMPKα1) or *STK11* (LKB1). A number of established ovarian cancer cell lines were screened for LKB1 and AMPK expression and activity in adherent culture (Figure S3.3) and those with the highest activity were used in knockdown experiments. Effective knockdown of *STK11* and *PRKAA1* was achieved in cells in both adherent (Figure 3.8A) and suspension (Figure 3.8B) cultures. Cells in adherent culture were not sensitive to knockdown of either AMPKα1 or LKB1 with

respect to cell viability, most likely since these cells are proliferating and not under metabolic stress, therefore not requiring this pathway. Surprisingly, knockdown of AMPKα1 had no impact on the survival of cells in suspension, while loss of LKB1 significantly reduced viability of cells in spheroids (Figure 3.8C). These results point to AMPK-independent LKB1 signalling as an important stress adaptation used by ovarian cancer cells in suspension in order to avoid anoikis.

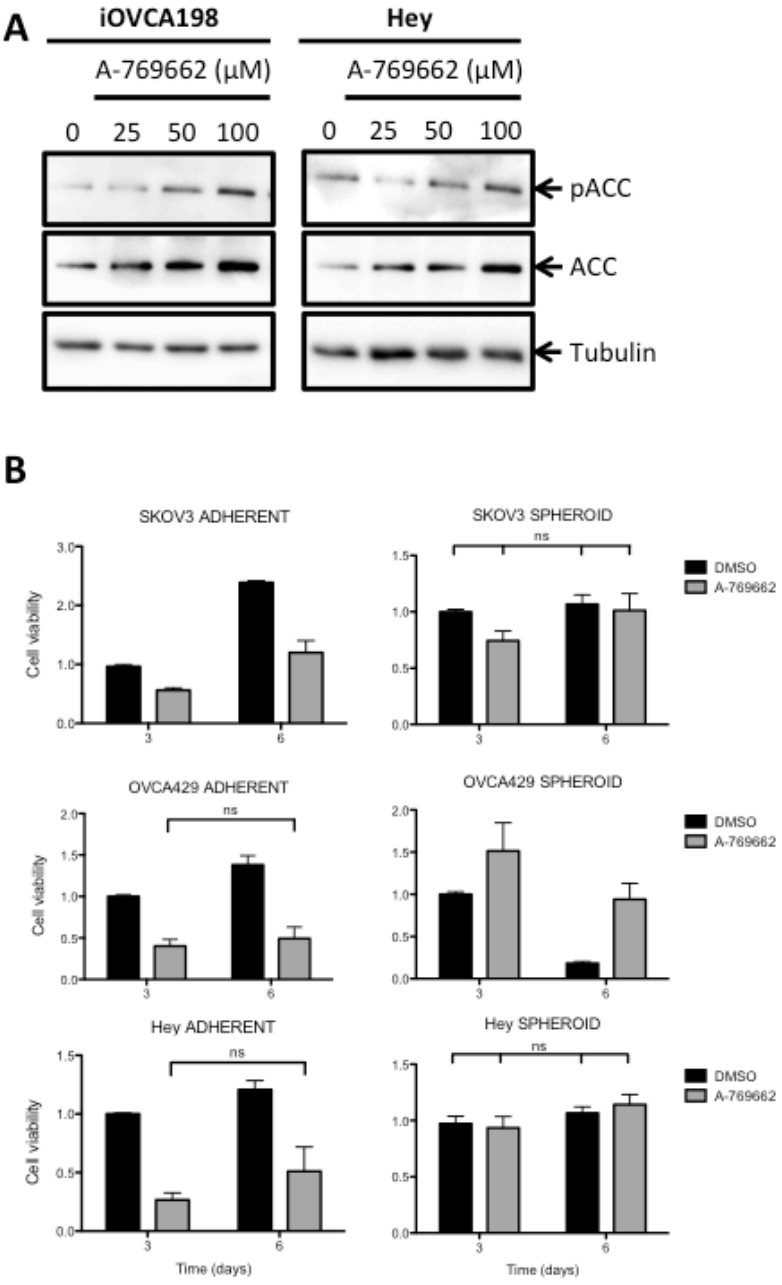

Figure 3.7: Allosteric AMPK activator A-769662 decreases viability of EOC cells in a context-dependent manner.
(A) Immunoblot performed on EOC cells treated for 24 hours with various doses of A-769662 as indicated. AMPK activation determined by levels of phosphorylated ACC. (B) Viability of ovarian cancer cell lines following 3 and 6 days of A-769662 (100μM) treatment in adherent and spheroid culture conditions. Bars: Mean ± SEM. Effect of treatment at each timepoint was determined using Student's t-test. Results are significant ($p<0.05$) unless otherwise indicated.

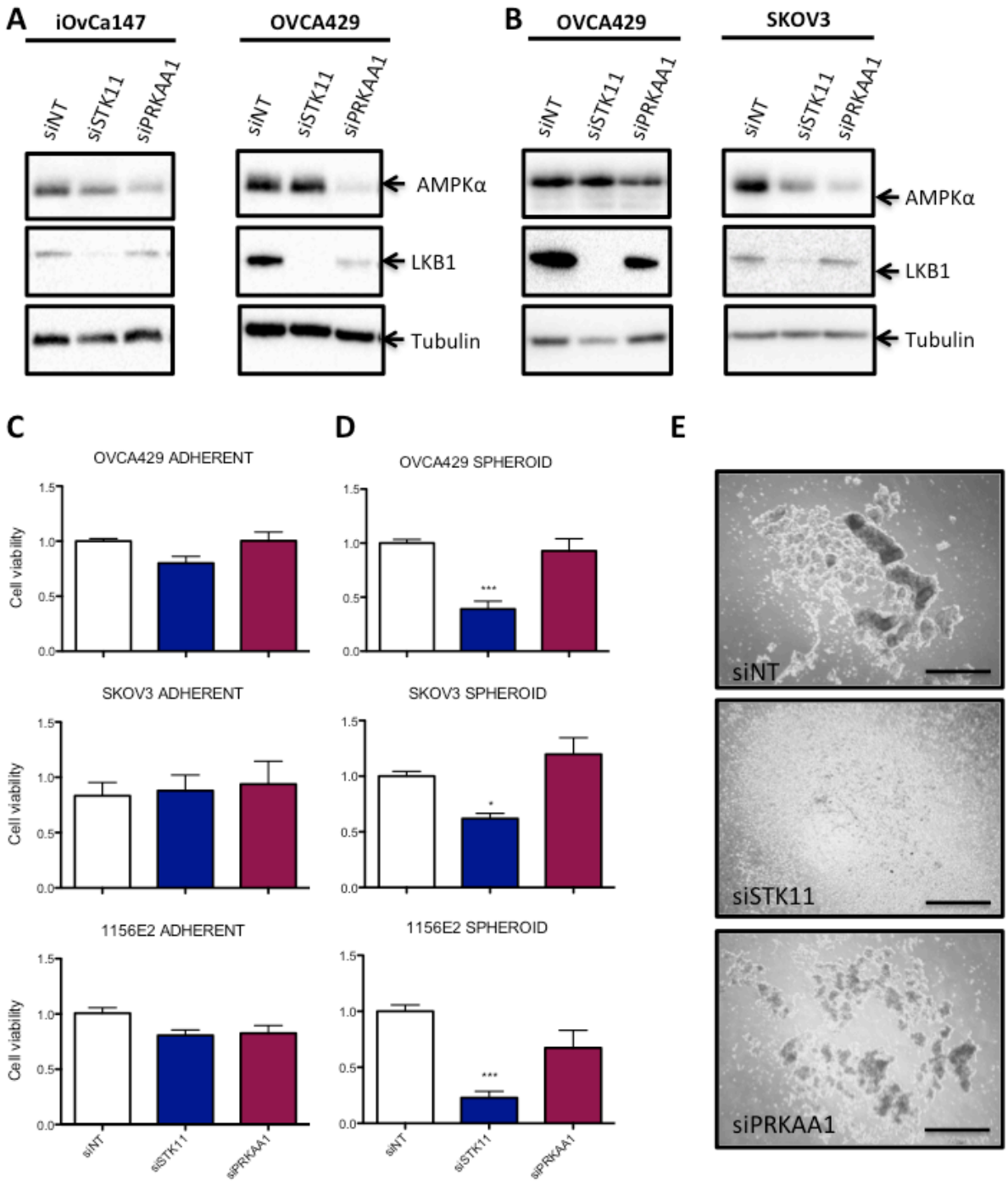

Figure 3.8: siRNA-mediated knockdown of *STK11* but not *PRKAA1* results in a decrease in viability of ovarian cancer spheroids.
(A,B) Immunoblot performed for proteins as indicated on adherent and spheroid ovarian cancer cells 72 hours after transfection or 3 days after spheroid formation respectively. (C,D) Cell viability as determined by Cell Titer Glo® assay on ovarian cancer cell lines in adherent or suspension culture respectively after three days (seeded to these conditions 72 hours after transfection). (E) Images of day 3 OVCA429 spheroids following siRNA knockdown as indicated. Scale Bar: 100μm.

3.4 Discussion

The distinct mode of metastatic spread whereby EOC cells transit the peritoneal cavity in suspension, presents unique therapeutic challenges for treatment of advanced-stage ovarian cancer. Characterization of this unique population of non-adherent cells will provide insights into novel targets for treatment of this deadly disease. Our laboratory has previously shown that ovarian cancer cells in suspension have a propensity to aggregate and form dormant multicellular clusters or spheroids. This dormancy is reversible upon reattachment to an adherent substratum, a process that is dependent upon AKT[16]. Following up on this observation, we show in this report that cells in dormant EOC spheroids have reduced metabolic activity and as such induce the LKB1/AMPK metabolic stress response pathway. Indeed, we demonstrate that AMPK activity is enhanced in quiescent ovarian cancer spheroids. Also, direct pharmacologic activation of AMPK in proliferating adherent ovarian cancer cells to leads to cytostasis and ultimately a decrease in cell viability. Our surprising new result, however, is that where maintenance of LKB1 expression is required for ovarian cancer cell survival in suspension, AMPK is not necessary. This implies an AMPK-independent role for LKB1 in mediating anoikis-resistance in ovarian cancer cells. This is the first study to demonstrate a pro-survival function for LKB1, a kinase that has been traditionally considered to be a tumour suppressor.

Expansive tumour growth is typically dependent on over-proliferative malignant cells that lack the normal response to induce protective growth arrest. Under nutrient-rich conditions, proliferative cancer cells should have low to absent levels of active AMPK signalling. Indeed, we show that expression of phosphorylated AMPKα is marginal in the majority of cultured EOC cells assessed; however, AMPK activity is significantly elevated upon spheroid formation. Ectopic activation of this pathway in proliferating cells using the AMP mimetic AICAR or an allosteric AMPKα activator A-769662 result in decreased viability. These agents most likely produce this effect through different mechanisms. Although both compounds induce a potent cytostatic response, AICAR treatment eventually results in significant cell death due to induction of apoptosis whereas A-769662 does not. A recent report highlighted the difference between these two

compounds, demonstrating that the growth-suppressive effects of AICAR are actually independent of AMPK in a glioma model[41]. Thus, the decreased viability observed in ovarian cancer spheroids treated with AICAR may in fact occur via AMPK-independent mechanisms. Taken together, this indicates that suppressed AMPK signalling is required to sustain active tumour growth, and supports a general idea that this pathway possesses classical tumour suppressor function under these conditions. However, when cells are in suspension AMPK is activated to facilitate cellular quiescence, and further activation is of lesser consequence on viability. These results indicate that AMPK acts like a typical tumour suppressor, yet its function may be utilized to promote protection from apoptosis during later stages of ovarian cancer progression.

Along this same reasoning, it is not unreasonable to postulate that LKB1 function may be context-specific during ovarian cancer progression given its array of downstream targets. A recent report of a conditional mouse model for serous ovarian carcinoma determined that loss of one *Stk11* allele in the context of *Pten* loss within the OSE leads to the development of high-grade papillary serous ovarian carcinomas[42]. This is not the first study to demonstrate synergism between LKB1 and other tumour suppressors or oncogenes. In fact, LKB1 has been shown to accelerate tumorigenesis in conjunction with p53[43], *Kras*[44], and c-myc[45]. This provides additional support for the complex function of this important kinase. Indeed, the molecular signature of a particular tumour is likely another factor that impacts the operational role of LKB1 in a particular type or stage of cancer[18]. Although the study by Tanwar and colleagues[42] implicates loss of LKB1 function in the initiation of ovarian cancer, knockout is performed in the ovarian surface epithelium and not the secretory epithelium of oviduct; the secretory epithelial cells of the distal fallopian tube is now considered the site of origin for high-grade serous ovarian cancer[46-48]. Since loss of *STK11* in premalignant serous tubal intraepithelial carcinoma lesions in humans has not yet been documented, studies in this regard would provide additional insight into the role of LKB1 in ovarian cancer initiation.

In this report, we show that analysis of the serous ovarian cancer provisional dataset from cBioPortal indicated that 84% of tumours exhibit heterozygous loss of *STK11* the gene encoding LKB1[29]. Despite this, we show that numerous EOC solid tumour

specimens, as well as established ovarian cancer cell lines, express LKB1 protein. Interestingly, we also show copy number gains or amplifications in *PRKAA1*, which encodes AMPKα1, in 36% of samples. This suggests that there may be compensatory mechanisms to upregulate AMPK activity in late-stage ovarian tumours which harbour reduced LKB1 in order to maintain a functional pathway for tumour cell survival during metastasis. It is also possible that this discordance in LKB1 and AMPK copy number variations indicates that these kinases may not necessarily be acting in concert in advanced-stage ovarian cancer. Our data imply that although *STK11* haploinsufficiency may occur and predispose to ovarian cancer initiation, maintenance of functional LKB1 signalling pathway is likely essential during metastatic progression particularly to fuel recurrence of chemoresistant ovarian cancer.

The LKB1/AMPK signalling pathway represents an immediate response to metabolic stress and reduced energy supply to downregulate anabolic metabolism and shunt pathways to utilize alternative energy substrates[18]. Previous data from our laboratory has shown a decrease in AKT activity upon spheroid formation and an accompanying induction of dormancy[16] and autophagy (Correa, Shepherd, DiMattia, unpublished). We now show that the LKB1/AMPK pathway is induced in EOC spheroids, which has opposing regulatory effects on mTORC1 compared with what would be observed by AKT. Indeed, we show that mTORC1 activity is reduced in spheroids. This result indicates that the LKB1/AMPK signalling cascade acts to reduce protein translation and induce autophagy, likely in concert with downregulated AKT activity.

It has been shown in other cell systems that LKB1/AMPK is an important mediator of protecting detached epithelial cells from anoikis[24,26]. Interestingly, targeted knockdown of *STK11* (LKB1) in our study demonstrated a significant reduction in spheroid cell viability yet there was no effect when AMPKα1 activity was reduced. We confirmed that there was no compensatory effect of AMPKα2 expression in *PRKAA1*-knockdown spheroid cells that could explain this lack of effect (Appendix A). This implies that LKB1 plays an important role in mediating anoikis-resistance and dormancy in EOC spheroids independent of AMPK. AMPK is the most studied downstream target of LKB1. However, LKB1 has been called a “master kinase” given its ability to phosphorylate at

least 12 other downstream proteins, referred to as AMPK-related kinases (ARKs: MARK1, MARK2, MARK3, MARK4, SIK1, SIK2, SIK3, BRSK1, BRSK2, SNRK, NUAK1, NUAK2)[49]. The ARKs have been shown to play roles in many important aspects of cell function including cell polarity (MARK, BRSK)[50,51], cell proliferation (NUAKs)[52,53] and CREB-regulated gene transcription (SIKs)[54-56]. It seems likely that one or more of these ARKs are important downstream mediators of the LKB1-dependent decrease in cell viability we observe in ovarian cancer spheroids. One likely candidate, microtubule affinity-regulating kinase 4 (MARK4), is able to phosphorylate Raptor on the same residue as AMPK, resulting in inhibition of mTORC1 signalling[57]. Another of these kinases, NUAK1 may also be an interesting target to investigate in our system, as it is able to promote cell survival during periods of nutrient deprivation[58]. Further studies are needed to determine which of the numerous substrates downstream from LKB1 are mediating this requirement to maintain cell viability in ovarian cancer spheroids.

Although literature supports the idea that *STK11* acts as a tumour suppressor during early steps of tumorigenesis, our *STK11* knockdown results provide yet another example of a protein, in this case LKB1, exhibiting an important reciprocal metastasis-promoting function during late-stage disease. EOC spheroids have the capacity to harbour a niche of chemotherapy-resistant cells. Our data supports this idea, and importantly we provide the first evidence that AMPK-independent LKB1 signalling may play a significant role in adaptive resistance mechanisms in these metastasis-promoting structures.

3.5 References

1. Statistics, C.C.S.s.A.C.o.C. Canadian Cancer Statistics 2013. *Canadian Cancer Society* (2013).
2. Nik, N.N., Vang, R., Shih, I.M. & Kurman, R.J. Origin and Pathogenesis of Pelvic (Ovarian, Tubal, and Primary Peritoneal) Serous Carcinoma. *Annu Rev Pathol* (2013).
3. Lengyel, E.*, et al.* Epithelial ovarian cancer experimental models. *Oncogene* (2013).
4. Burleson, K.M.*, et al.* Ovarian carcinoma ascites spheroids adhere to extracellular matrix components and mesothelial cell monolayers. *Gynecol Oncol* **93**, 170-181 (2004).
5. Burleson, K.M., Hansen, L.K. & Skubitz, A.P. Ovarian carcinoma spheroids disaggregate on type I collagen and invade live human mesothelial cell monolayers. *Clinical & experimental metastasis* **21**, 685-697 (2004).
6. Kenny, H.A., Nieman, K.M., Mitra, A.K. & Lengyel, E. The first line of intra-abdominal metastatic attack: breaching the mesothelial cell layer. *Cancer Discov* **1**, 100-102 (2011).
7. Landen, C.N., Jr., Birrer, M.J. & Sood, A.K. Early events in the pathogenesis of epithelial ovarian cancer. *Journal of clinical oncology : official journal of the American Society of Clinical Oncology* **26**, 995-1005 (2008).
8. Barbone, D.*, et al.* The Bcl-2 repertoire of mesothelioma spheroids underlies acquired apoptotic multicellular resistance. *Cell death & disease* **2**, e174.
9. Bertuzzi, A., Fasano, A., Gandolfi, A. & Sinisgalli, C. Necrotic core in EMT6/Ro tumour spheroids: Is it caused by an ATP deficit? *Journal of theoretical biology* **262**, 142-150.
10. Dolznig, H.*, et al.* Modeling Colon Adenocarcinomas in Vitro A 3D Co-Culture System Induces Cancer-Relevant Pathways upon Tumor Cell and Stromal Fibroblast Interaction. *Am J Pathol* **179**, 487-501.
11. Grun, B.*, et al.* Three-dimensional in vitro cell biology models of ovarian and endometrial cancer. *Cell Prolif* **42**, 219-228 (2009).
12. Sodek, K.L., Ringuette, M.J. & Brown, T.J. Compact spheroid formation by ovarian cancer cells is associated with contractile behavior and an invasive phenotype. *International journal of cancer* **124**, 2060-2070 (2009).
13. Valcarcel, M.*, et al.* Three-dimensional growth as multicellular spheroid activates the proangiogenic phenotype of colorectal carcinoma cells via LFA-1-dependent VEGF: implications on hepatic micrometastasis. *Journal of translational medicine* **6**, 57 (2008).
14. Waite, C.L. & Roth, C.M. PAMAM-RGD conjugates enhance siRNA delivery through a multicellular spheroid model of malignant glioma. *Bioconjug Chem* **20**, 1908-1916 (2009).
15. Kunz-Schughart, L.A., Doetsch, J., Mueller-Klieser, W. & Groebe, K. Proliferative activity and tumorigenic conversion: impact on cellular metabolism in 3-D culture. *American journal of physiology* **278**, C765-780 (2000).

16. Correa, R.J., Peart, T., Valdes, Y.R., Dimattia, G.E. & Shepherd, T.G. Modulation of AKT activity is associated with reversible dormancy in ascites-derived epithelial ovarian cancer spheroids. *Carcinogenesis* **33**, 49-58 (2012).
17. Mihaylova, M.M. & Shaw, R.J. The AMPK signalling pathway coordinates cell growth, autophagy and metabolism. *Nat Cell Biol* **13**, 1016-1023 (2011).
18. Liang, J. & Mills, G.B. AMPK: a contextual oncogene or tumor suppressor? *Cancer Res* **73**, 2929-2935 (2013).
19. Hawley, S.A.*, et al.* Complexes between the LKB1 tumor suppressor, STRAD alpha/beta and MO25 alpha/beta are upstream kinases in the AMP-activated protein kinase cascade. *J Biol* **2**, 28 (2003).
20. Shaw, T.J., Senterman, M.K., Dawson, K., Crane, C.A. & Vanderhyden, B.C. Characterization of intraperitoneal, orthotopic, and metastatic xenograft models of human ovarian cancer. *Mol Ther* **10**, 1032-1042 (2004).
21. Woods, A.*, et al.* LKB1 is the upstream kinase in the AMP-activated protein kinase cascade. *Current biology : CB* **13**, 2004-2008 (2003).
22. Mandal, S., Guptan, P., Owusu-Ansah, E. & Banerjee, U. Mitochondrial regulation of cell cycle progression during development as revealed by the tenured mutation in Drosophila. *Developmental cell* **9**, 843-854 (2005).
23. Hemminki, A.*, et al.* A serine/threonine kinase gene defective in Peutz-Jeghers syndrome. *Nature* **391**, 184-187 (1998).
24. Ng, T.L.*, et al.* The AMPK stress response pathway mediates anoikis resistance through inhibition of mTOR and suppression of protein synthesis. *Cell Death Differ* **19**, 501-510 (2012).
25. Schafer, Z.T.*, et al.* Antioxidant and oncogene rescue of metabolic defects caused by loss of matrix attachment. *Nature* **461**, 109-113 (2009).
26. Avivar-Valderas, A.*, et al.* Regulation of autophagy during ECM detachment is linked to a selective inhibition of mTORC1 by PERK. *Oncogene* **32**, 4932-4940 (2013).
27. Shepherd, T.G., Theriault, B.L., Campbell, E.J. & Nachtigal, M.W. Primary culture of ovarian surface epithelial cells and ascites-derived ovarian cancer cells from patients. *Nat Protoc* **1**, 2643-2649 (2006).
28. Goldman, M.*, et al.* The UCSC Cancer Genomics Browser: update 2013. *Nucleic Acids Res* **41**, D949-954 (2013).
29. Gao, J.*, et al.* Integrative analysis of complex cancer genomics and clinical profiles using the cBioPortal. *Science signaling* **6**, pl1 (2013).
30. Tibes, R.*, et al.* Reverse phase protein array: validation of a novel proteomic technology and utility for analysis of primary leukemia specimens and hematopoietic stem cells. *Molecular cancer therapeutics* **5**, 2512-2521 (2006).
31. Peart, T.M., Correa, R.J., Valdes, Y.R., Dimattia, G.E. & Shepherd, T.G. BMP signalling controls the malignant potential of ascites-derived human epithelial ovarian cancer spheroids via AKT kinase activation. *Clinical & experimental metastasis* **29**, 293-313 (2012).
32. Alessi, D.R., Sakamoto, K. & Bayascas, J.R. LKB1-dependent signaling pathways. *Annu Rev Biochem* **75**, 137-163 (2006).
33. Bardeesy, N.*, et al.* Loss of the Lkb1 tumour suppressor provokes intestinal polyposis but resistance to transformation. *Nature* **419**, 162-167 (2002).

34. Hernan, I.*, et al.* De novo germline mutation in the serine-threonine kinase STK11/LKB1 gene associated with Peutz-Jeghers syndrome. *Clin Genet* **66**, 58-62 (2004).
35. Jishage, K.*, et al.* Role of Lkb1, the causative gene of Peutz-Jegher's syndrome, in embryogenesis and polyposis. *Proceedings of the National Academy of Sciences of the United States of America* **99**, 8903-8908 (2002).
36. Miyoshi, H.*, et al.* Gastrointestinal hamartomatous polyposis in Lkb1 heterozygous knockout mice. *Cancer Res* **62**, 2261-2266 (2002).
37. Sapkota, G.P.*, et al.* Phosphorylation of the protein kinase mutated in Peutz-Jeghers cancer syndrome, LKB1/STK11, at Ser431 by p90(RSK) and cAMP-dependent protein kinase, but not its farnesylation at Cys(433), is essential for LKB1 to suppress cell vrowth. *J Biol Chem* **276**, 19469-19482 (2001).
38. Cheong, J.H.*, et al.* Dual inhibition of tumor energy pathway by 2-deoxyglucose and metformin is effective against a broad spectrum of preclinical cancer models. *Molecular cancer therapeutics* **10**, 2350-2362 (2011).
39. Priebe, A.*, et al.* Glucose deprivation activates AMPK and induces cell death through modulation of Akt in ovarian cancer cells. *Gynecol Oncol* **122**, 389-395 (2011).
40. Goransson, O.*, et al.* Mechanism of action of A-769662, a valuable tool for activation of AMP-activated protein kinase. *J Biol Chem* **282**, 32549-32560 (2007).
41. Liu, X.*, et al.* Discrete mechanisms of mTOR and cell cycle regulation by AMPK agonists independent of AMPK. *Proceedings of the National Academy of Sciences* (2014).
42. Tanwar, P.S.*, et al.* Loss of LKB1 and PTEN tumor suppressor genes in the ovarian surface epithelium induces papillary serous ovarian cancer. *Carcinogenesis* (2013).
43. Wei, C.*, et al.* Mutation of Lkb1 and p53 genes exert a cooperative effect on tumorigenesis. *Cancer Res* **65**, 11297-11303 (2005).
44. Ji, H.*, et al.* LKB1 modulates lung cancer differentiation and metastasis. *Nature* **448**, 807-810 (2007).
45. Partanen, J.I., Nieminen, A.I. & Klefstrom, J. 3D view to tumor suppression: Lkb1, polarity and the arrest of oncogenic c-Myc. *Cell cycle (Georgetown, Tex* **8**, 716-724 (2009).
46. Erickson, B.K., Conner, M.G. & Landen, C.N., Jr. The role of the fallopian tube in the origin of ovarian cancer. *Am J Obstet Gynecol* (2013).
47. Kessler, M., Fotopoulou, C. & Meyer, T. The molecular fingerprint of high grade serous ovarian cancer reflects its fallopian tube origin. *Int J Mol Sci* **14**, 6571-6596 (2013).
48. Piek, J.M.*, et al.* BRCA1/2-related ovarian cancers are of tubal origin: a hypothesis. *Gynecologic oncology* **90**, 491 (2003).
49. Lizcano, J.M.*, et al.* LKB1 is a master kinase that activates 13 kinases of the AMPK subfamily, including MARK/PAR-1. *The EMBO journal* **23**, 833-843 (2004).

50. Hayashi, K., Suzuki, A. & Ohno, S. A novel function of the cell polarity-regulating kinase PAR-1/MARK in dendritic spines. *Bioarchitecture* **1**, 261-266 (2011).
51. Saadat, I.*, et al.* Helicobacter pylori CagA targets PAR1/MARK kinase to disrupt epithelial cell polarity. *Nature* **447**, 330-333 (2007).
52. Hou, X.*, et al.* A new role of NUAK1: directly phosphorylating p53 and regulating cell proliferation. *Oncogene* **30**, 2933-2942 (2011).
53. Sun, X., Gao, L., Chien, H.Y., Li, W.C. & Zhao, J. The regulation and function of the NUAK family. *J Mol Endocrinol* **51**, R15-22 (2013).
54. Katoh, Y.*, et al.* Silencing the constitutive active transcription factor CREB by the LKB1-SIK signaling cascade. *Febs J* **273**, 2730-2748 (2006).
55. Katoh, Y.*, et al.* Salt-inducible kinase-1 represses cAMP response element-binding protein activity both in the nucleus and in the cytoplasm. *Eur J Biochem* **271**, 4307-4319 (2004).
56. Takemori, H., Kajimura, J. & Okamoto, M. TORC-SIK cascade regulates CREB activity through the basic leucine zipper domain. *Febs J* **274**, 3202-3209 (2007).
57. Li, L. & Guan, K.L. Microtubule-associated protein/microtubule affinity-regulating kinase 4 (MARK4) is a negative regulator of the mammalian target of rapamycin complex 1 (mTORC1). *J Biol Chem* **288**, 703-708 (2013).
58. Suzuki, A.*, et al.* ARK5 suppresses the cell death induced by nutrient starvation and death receptors via inhibition of caspase 8 activation, but not by chemotherapeutic agents or UV irradiation. *Oncogene* **22**, 6177-6182 (2003).

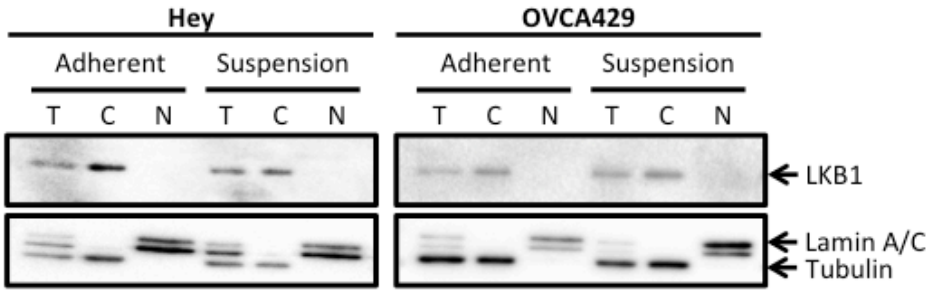

Figure S3.1: LKB1 is located in the cytoplasm in adherent and spheroid EOC cells. Immunoblot performed on whole-cell (T), cytoplasmic (C), and nuclear (N) protein extracts isolated from ovarian cancer cell lines to determine subcellular localization of LKB1 protein. Lamin A/C and tubulin used as nuclear and cytoplasmic loading controls, respectively.

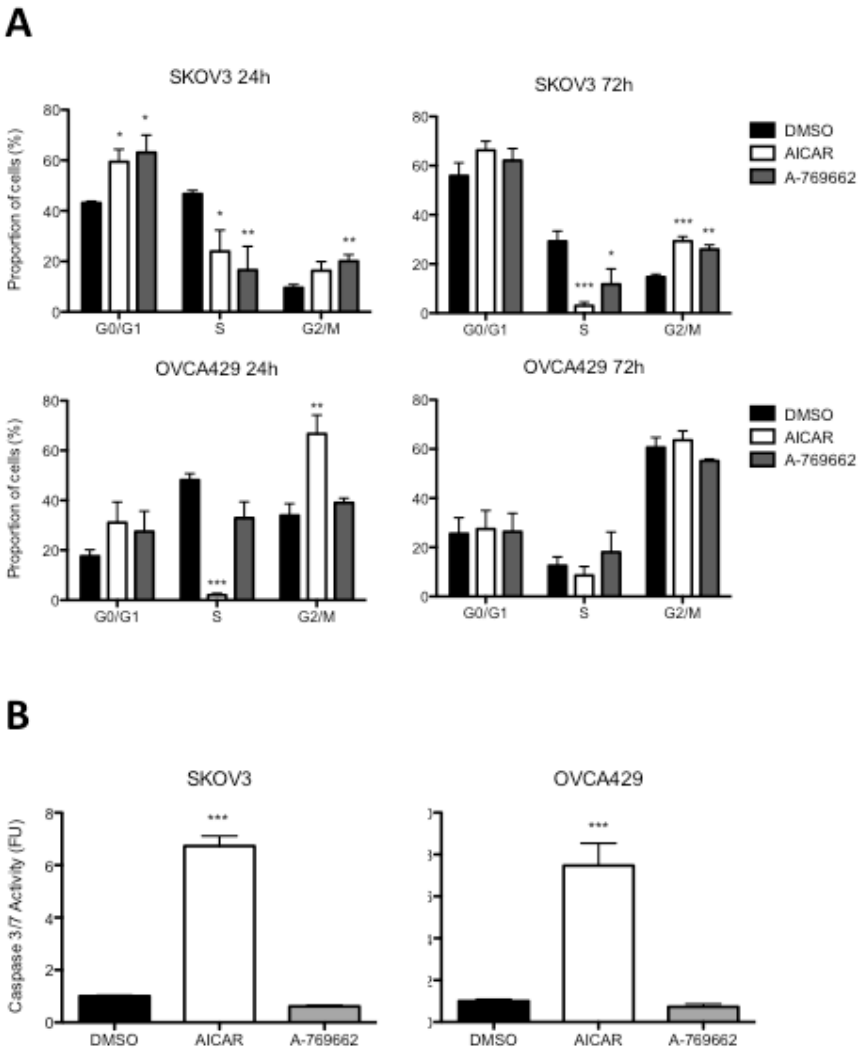

Figure S3.2: AICAR and A-769662 have different effects on cell cycle progression and apoptosis in adherent ovarian cancer cells.
(A) Cell cycle analysis (BrdU and PI) by flow cytometry on ovarian cancer cells following 24 and 72 hours of treatment with either AICAR or A-769662 (n=2 for each cell line). (B) Caspase 3/7 activity 72 hours following treatment with either AICAR or A-769662 as determined by Caspase-Glo®. Bars: Mean ± SEM. Effect of treatment determined by One-way ANOVA (*$p<0.05$; **$p<0.01$; ***$p<0.001$).

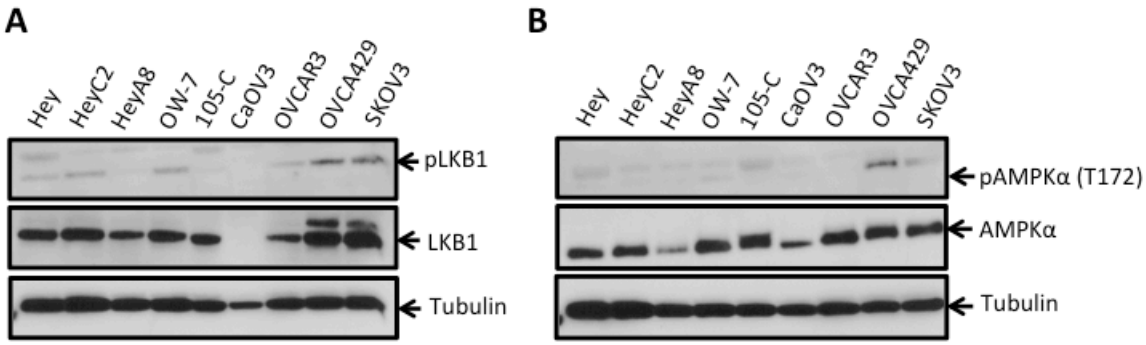

Figure S3.3: LKB1 and AMPK are expressed in EOC cell lines under adherent conditions but activity is low.
(A, B) Immunoblot performed on a number of ovarian cancer cell lines cultured under adherent conditions in order to determine levels of phosphorylated and total LKB1 and AMPK as indicated.

Chapter 4

4 Discussion

4.1 Summary of findings

The high level of a mortality associated with high-grade serous ovarian cancer has been directly attributed to intra-abdominal metastases, which recur despite aggressive surgical and chemotherapeutic interventions. The presence of microscopic disease and dormant, chemotherapy-resistant cancer cells is likely the cause of these recurrences. Therefore, experimental models that allow us to better understand the biology and pathogenesis of dormant high-grade ovarian cancer cells are crucial to uncover more effective treatment options for patients with advanced-stage disease. Our studies use a highly-relevant, tractable, non-adherent culture system to examine the molecular underpinnings of multicellular spheroid formation and subsequent reattachment to an adherent substratum. These structures induce dormancy and mimic the spheroid state of ovarian cancer cells in ascites, which facilitates the spread of this cancer.

I focused on two distinct cellular signalling systems and discovered in the first instance that BMP signalling is decreased upon spheroid formation, a process that is reversed when these clusters reattach to an adherent substratum (Chapter 2). To examine the functional implications of this dynamic regulation, I constitutively activated BMP signalling and discovered a detrimental effect on spheroid formation, resulting in smaller, more loosely aggregated clusters. Activation of this pathway during spheroid reattachment on the other hand, resulted in increased cellular dispersion. These phenotypic alterations in spheroid formation and reattachment observed in response to BMP signalling, were shown to be mediated, in part, by interaction with the PI3K/AKT signalling pathway. Specifically, constitutive activation of BMP signalling resulted in enhanced AKT activity, which was shown to contribute to increased spheroid reattachment observed as a result of overactive BMP signalling.

Given the ability of the PI3K/AKT and BMP signalling pathways to act together to alter spheroid formation and reattachment, I chose to examine other key cell survival pathways, which might act in concert with AKT in EOC cells. The objective was to

identify signalling pathways that may interact to maintain the viability of ovarian cancer cells and allow seeding of recurrent disease. In doing so, we expect to identify new potential therapeutic targets for which drugs may already exist or lay the ground work for use of specific combinatorial treatments. Additional rationale for this route of investigation was provided by other work in our laboratory demonstrating an AKT-dependent induction of dormancy and autophagy in EOC spheroids[1]. Investigating this area of research revealed number of studies that reported AMPK-dependent induction of autophagy under conditions of stress such as glucose deprivation and hypoxia[2,3]. Therefore, I hypothesized that, in addition to the AKT pathway, the LKB1/AMPK signalling cascade would be an important contributor to spheroid-formation induced dormancy.

AMPK has a unique ability integrate extracellular nutrient and energy signals in order to control the metabolic function of cells. I discovered that AMPK activity is greatly enhanced in ovarian cancer spheroids and this is associated with enhanced phosphorylation of its upstream kinase, LKB1 (Chapter 3). Activation of AMPK is detrimental in adherent, proliferating cells but has little effect on dormant, multicellular spheroids. On the other hand, targeted knockdown experiments highlight an AMPK-independent role for LKB1 in survival of cells in suspension. This is the first demonstration of a pro-survival function for LKB1, a kinase that has been primarily considered to be a tumour suppressor.

The data presented in this thesis discusses two signalling pathways that play distinct roles in EOC spheroid formation and survival. Both pathways however, present potential therapeutic targets for the unique population of non-adherent ovarian cancer cells within ascites fluid.

4.2 BMP signalling plays context-specific roles during ovarian cancer spheroid formation and reattachment

Although a dichotomous role for TGF-β in carcinogenesis is well-established, this is not the case for BMP signalling. More *in vitro* and *in vivo* evidence is required to determine whether this pathway is indeed oncogenic or tumour suppressive and in which

types and stages of cancers this is true. BMP signalling is generally considered a critical pathway during development controlling cell differentiation. Therefore, it is reasonable to suppose that induction of BMP signalling in cancer cells might be anti-oncogenic causing a differentiation-related program to force cancer cells out of the cell cycle. It is also possible that BMP signalling has been co-opted by cancer cells in a pro-oncogenic manner to facilitate maintenance of the cancer cell phenotype.

Our study focused on dissecting the contribution of the BMP signalling cascade during the various phases of ovarian cancer progression using a biologically-relevant, tractable *in vitro* model system. This model takes into account the unique mode of ovarian cancer metastasis, whereby multicellular spheroids represent an important conduit through which cells are able to survive until they reach a mesothelial surface where re-implantation and invasion are possible. It has been suggested that ovarian cancer cells within multicellular aggregates or spheroids undergo EMT, acquiring more mesenchymal characteristics, preparing them to reattach and invade, forming secondary metastases when conditions are favourable[4,5].

The data presented in Chapter 2 confirms that spheroids formed from primary ovarian cancer cells undergo EMT, characterized by decreased expression of the E-cadherin gene. This is supported by previous evidence that E-cadherin expression is reduced in cells isolated from ascites compared to their solid tumour counterparts[6] as well as other studies demonstrating that ovarian cancer cell lines with more mesenchymal characteristics have an increased propensity for compact spheroid formation[5]. The autonomous down-regulation of BMP signalling during spheroid formation and the decreased propensity for compact spheroid formation when this pathway is activated suggests that BMP signalling may in fact be opposing the natural EMT response of EOC spheroids. This is concordance with a study published in 2011 by the Weinburg lab in which they documented that the BMP pathway had the ability to antagonize TGF-β-induced EMT in mammary epithelial cells[7]. Indeed, activation of BMP signalling within EOC spheroids results in increased E-cadherin expression when compared to controls, suggesting that inhibition of EMT could be a potential mechanism through which BMP signalling decreases spheroid compaction.

Although activated BMP signalling in spheroids results in smaller, more loosely aggregated clusters this does not result in an overall decrease in cell viability. Therefore, it should not be assumed that activation of this pathway is detrimental. Rather, it may 'prime' cells within these aggregates to more readily attach and disperse. Indeed, when spheroids with constitutively active BMP signalling are exposed to an adherent substratum, they have an increased propensity for reattachment and dispersion. This is supported by previous work demonstrating that BMP4 has the ability to enhance motility and invasion of adherent primary ovarian cancer cells[8,9].

Taken together, these findings suggest that inhibition of BMP signalling may in fact be a viable therapeutic target through which to prevent EOC spheroid reattachment and formation of secondary metastatic lesions. We show that inhibition of the BMP pathway using a small molecule inhibitor as well as BMP antagonist, noggin, does in fact decrease the ability of cells to disperse from a spheroid following re-introduction to an adherent substratum. Since this does not completely prevent spheroids from reattaching, it is likely that the BMP signalling pathway acts in conjunction with other pathways during this process.

Our studies uncovered an interaction between the BMP and AKT signalling cascades and demonstrated that these two pathways act in concert to promote EOC spheroid reattachment. This finding is supported by other reports demonstrating that the PI3K/AKT pathway is required for BMP-induced migration and invasion in gastric, colon and pancreatic cancer cells[10,11]. This highlights the potential for targeting these pathways in combination for treatment of metastatic ovarian cancer. Xenograft models will be important to determine whether this interaction is translatable in an *in vivo* setting. Weroha and colleagues recently published elegant work validating the use of a novel 'tumourgraft' model whereby ovarian cancer patient tumour material is minced and intraperitoneally injected into immune-compromised mice[12]. The tumours formed in mice recapitulate the clinical and molecular characteristics of the patient tumour but also mimic the patient's clinical response to chemotherapeutic treatment. This is an extremely exciting, highly translatable *in vivo* model with which to test the potential response of an patient's tumour to a targeted therapeutic. Using this model, we would be able to test the

therapeutic response of a number of ovarian cancer tumour specimens to treatment with the small molecule inhibitors of BMP and AKT signalling that I have in the studies described in this thesis. Molecular analysis of these 'tumourgrafts' would allow us to determine patient-specific responses to modulation of these two signalling pathways prior to and following treatment.

This work highlights the fact that the BMP signalling pathway exerts the majority of its effects during spheroid reattachment and dispersion. Therefore, it would be interest to examine the contribution of tumour-stroma interactions in this process and the role that the BMP signalling pathway plays in mediating these interactions. Carcinoma-associated fibroblasts (CAFs) have become increasingly recognized as important components of the tumour microenvironment that can aid in the initiation and progression of a number of different cancers including breast, prostate and ovarian[13-16]. Interestingly, normal fibroblasts co-cultured with carcinoma cells results in an irreversible conversion to a CAF phenotype, suggesting that fibroblasts exposed to cancer cells exhibit permanent, heritable changes[13,14,16]. Recent studies in ovarian cancer have demonstrated that the presence of CAFs can contribute to tumour progression, omental and lymph node metastases, in addition to being associated with poor patient prognosis[17,18]. Fu and colleagues were able to obtain primary cultures of CAFs from ovarian cancer patients and co-culture these with EOC cells[19]. Analysis of conditioned medium from this co-culture system revealed the presence of number of soluble factors including TGF-β and a number of BMPs. Using our *in vitro* system, it would be of interest to determine the effects of this co-culture media on spheroid reattachment both under ambient conditions as well in spheroids with constitutively activated BMP signalling and those treated with noggin. These studies would provide an additional layer of complexity to our model system, allowing us to not only determine the contribution of CAFs to spheroid reattachment and dispersion but also allow us to determine the interaction between the BMP signalling pathway and this population of cells (Figure 4.1).

The results presented in this thesis have uncovered an important role for BMP signalling in cellular cohesion and EMT during spheroid formation and cellular motility

during reattachment. This has laid the groundwork for preclinical models to investigate the utility of targeting this pathway for treatment of advanced-stage ovarian cancer.

4.3 LKB1 has AMPK-independent effects on cellular viability in ovarian cancer spheroids

Given the important roles that the AKT signalling pathway plays in EOC spheroids both in mediating responses to BMP signalling but also in contributing to spheroid formation-induced dormancy, I wanted to identify other candidate pathways known to interact with the PI3K/AKT pathway. Taking into account the dormant state of the cells within spheroids and their decreased metabolism an obvious candidate for investigation was the AMPK signalling cascade given its unique ability to respond to changes in extracellular energy and nutrient supply. The AMPK and PI3K/AKT signalling pathways converge on mTORC1 and have opposing regulatory effects on this complex[20]. We have demonstrated that in ovarian cancer spheroids decreased AKT activity and induction of cellular dormancy is associated with enhanced and sustained AMPK activity (Figure 4.1).

Other studies in our laboratory have linked cellular dormancy and quiescence within multicellular spheroids with induction of autophagy (Correa, DiMattia, and Shepherd, unpublished data). AMPK has the ability to directly induce autophagy by phosphorylating and positively regulating ULK1, a critical protein for autophagy initiation[21-23]. AMPK can also indirectly induce autophagy through its ability to inhibit mTORC1 by phosphorylation of TSC2 and Raptor. A study by Avivar-Valderas and colleagues in 2012 highlighted the potential for interaction between mTORC1, AMPK and a member of the unfolded protein response (UPR) pathway, protein kinase (PKR)-like endoplasmic reticulum kinase (PERK) in autophagy induction and anoikis-resistance in mammary epithelial cells[24]. It was noted that in response to loss of ECM attachment PERK was able to activate AMPK through its upstream kinase, LKB1 although the precise mechanism through which this occurs remains unclear. This suspension-induced AMPK activity was required for inhibition of mTORC1 and induction of autophagy. This was the first study to implicate the LKB1/AMPK/mTORC1 signalling cascade as a key regulator of anoikis in epithelial cells.

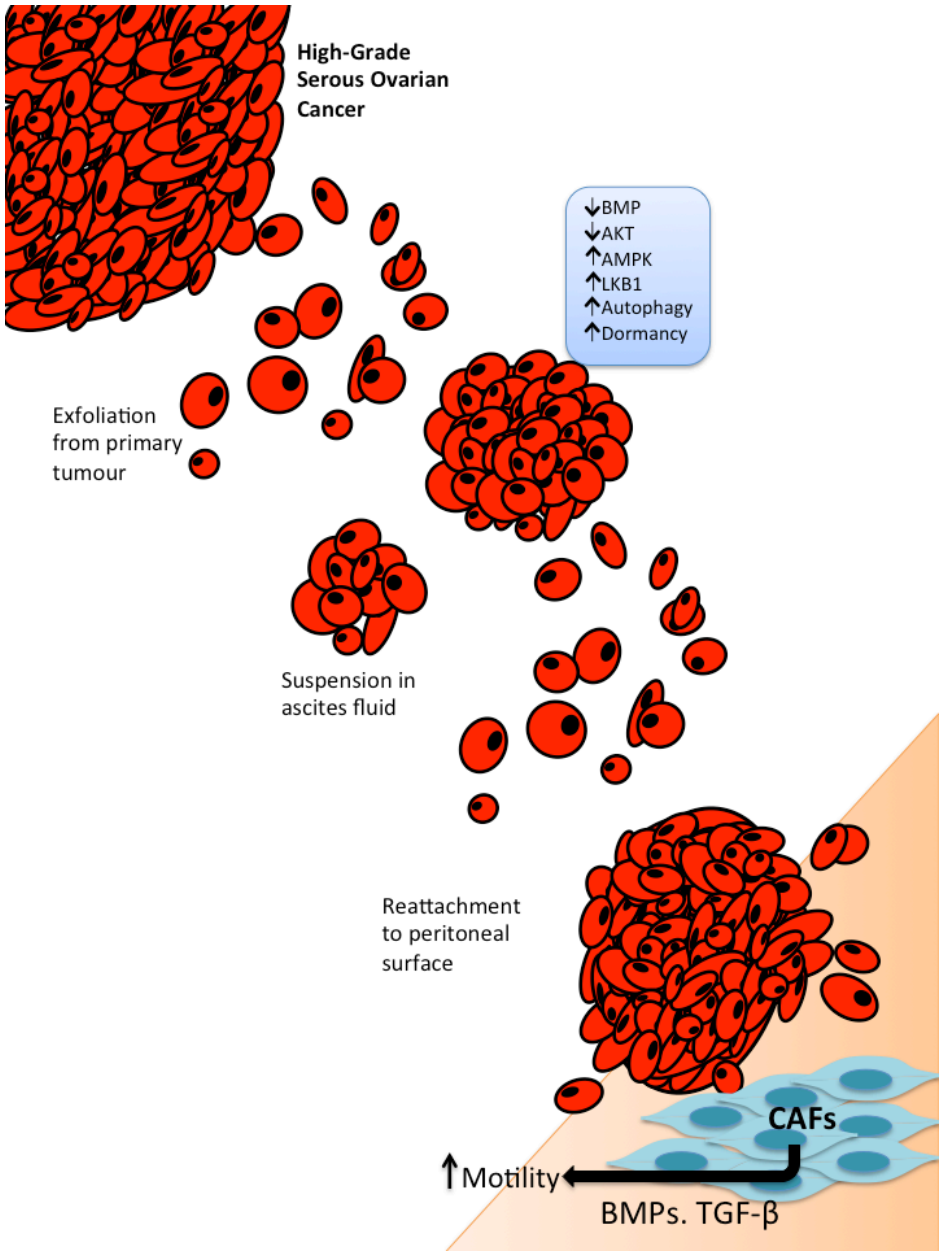

Figure 4.1: Contribution of BMP and LKB1/AMPK signalling pathways to ovarian cancer metastasis.
A number of pathways and processes are uniquely altered in ovarian cancer spheroids, aiding in cellular aggregation and induction of dormancy. Specifically, the BMP signalling pathway is down-regulated during ovarian cancer spheroid formation and aids in cellular aggregation and cohesion. Alternatively, the LKB1/AMPK signalling cascade is up-regulated during spheroid formation and contributes to spheroid formation-induced dormancy. Many of these signalling aberrations are reversed during spheroid reattachment. We propose that upon spheroid reattachment to serosal surfaces of various peritoneal organs (omentum, appendix, intestine), carcinoma-associated fibroblasts (CAFs) secrete a number of cytokines, such as BMPs and TGF-βs, to enhance proliferation, motility and invasion.

Applying these findings to our system, I chose to focus on LKB1 and mTORC1 as critical upstream and downstream mediators of AMPK signalling in EOC spheroids. As discussed in this thesis, suspension-induced AMPK activation in ovarian cancer cells is in fact associated with enhanced phosphorylation of its upstream kinase LKB1 and decreased activity of mTORC1. Surprisingly, targeted knockdown of AMPK did not have any effect on viability of cells within ovarian cancer spheroids. This was unexpected given the important role AMPK is known to play in cell survival under nutrient replete conditions. However, targeted knockdown of LKB1 results in significant reduction in viability of cells within multicellular aggregates, indicating an important role for this kinase in anoikis-resistance of ovarian cancer cells independent of AMPK.

As described in the introduction to this thesis, LKB1 phosphorylates 12 other kinases in addition to AMPK, termed the AMPK-related kinases (ARKs). Interestingly, one of these kinases, microtubule affinity-regulating kinase 4 (MARK4) has very recently been shown to phosphorylate Raptor on the same residue as AMPK, resulting in inhibition of mTORC1 signalling[25] (Figure 4.2). Another of these kinases, NUAK1 may also be an interesting target to investigate in our system as it has been shown to be a target of AKT in addition to LKB1[26]. Similar to AMPK, NUAK1 is able to promote cell survival during times of nutrient deprivation[27]. Although their functions are not as well characterized as AMPK, it is likely that one or more of the ARKs may be important mediators of the pro-survival functions of LKB1 in our system. Targeted knockdown of each of these ARKs (MARK1-4, NUAK1, NUAK2, SIK 1-3, SNRK, BRSK1, BRSK2) and assessment of cell viability in suspension would be the most effective method through which to determine our target(s) of interest.

These studies are the first to identify a pro-survival function for the tumour suppressor LKB1 in a metastatic cancer setting. Further studies will focus on examining the effect that LKB1 loss has on cellular quiescence and autophagy induction in ovarian cancer spheroids, as well as determining downstream mediators of LKB1 in our system. Perhaps we have uncovered a unique LKB1 signalling axis crucial in mediating anoikis-resistance in ovarian cancer cells.

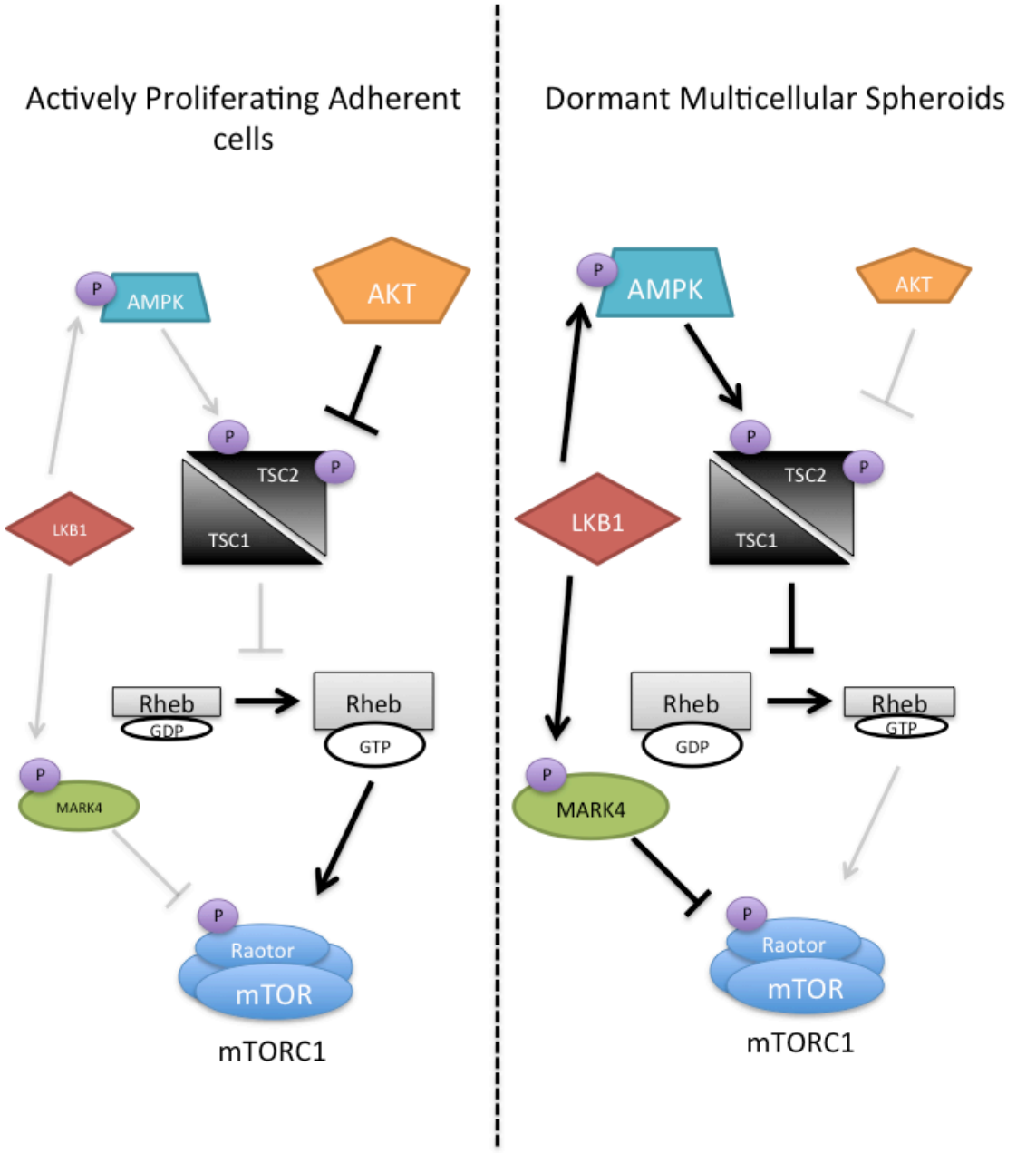

Figure 4.2: Proposed mechanisms of dormancy induction in ovarian cancer spheroids.
AMPK and AKT have opposing regulatory effects on mTORC1 via phosphorylation of TSC2. mTORC1 activity is decreased in multicellular spheroids and this corresponds with decreased AKT activity and enhanced AMPK activation. LKB1 not only functions as an upstream kinase for AMPK but also for a number of AMPK-related kinases (ARKs). One of these ARKs, MARK4, phosphorylates Raptor leading to inhibition of mTORC1. This is another potential kinase with elevated activity in dormant ovarian cancer spheroids. We propose that LKB1 is an important mediator of spheroid-formation induced dormancy independent of AMPK.

4.4 BMP and LKB1 signalling: Is there a connection?

The ability to avoid anoikis is an adaptation that is afforded to all metastatic ovarian cancer cells. In fact this biologic phenomenon is probably important in a variety of cancers that induce ascites formation or pleural effusions including mesothelioma[28], gastric cancer[29] and pancreatic cancer[30]. We have shown that under non-adherent conditions these cells have a propensity to aggregate and form multicellular clusters or spheroids, conferring them with a survival advantage. Therapeutic targeting of this population of cells while they are suspended within the peritoneal cavity or at the point of reattachment to form secondary metastatic lesions would be beneficial since the majority of ovarian cancer patients succumb to recurrent, metastatic disease. In this thesis I have specifically focused on two signalling pathways with diverse functions in ovarian cancer spheroid biology.

One of the few studies linking LKB1 to the TGF-β/BMP signalling pathway demonstrated that LKB1 is able to phosphorylate Smad4, preventing it from binding DNA, resulting in inhibition of both TGF-β and BMP signalling cascades[31]. Future studies could focus on examining potential interaction between these two signalling cascades through Smad4 or other transcriptional targets. It would also be important to determine whether there may be a functional link between these pathways. Perhaps decreased cellular cohesion that occurs as a result of activated BMP signalling will render cells in suspension even more susceptible to knockdown of LKB1. It would also be interesting to determine the activity of the TGF-β/BMP pathways in cells that have LKB1 knocked down. This may provide additional mechanistic evidence for the AMPK-independent effects of LKB1 in our system.

Both studies discussed in Chapter 2 and 3 of this thesis could be expanded with the use of the recent Pax8-Cre $p53^{mut}/PTEN^{-/-}/BRCA1/2^{-/-}$ mouse model of high grade serous cancer (HGSC)[32]. In this model, disease begins in the fallopian tube secretory epithelium with the development of STIC lesions which progress to HGSC, which metastasizes throughout the peritoneum, similar to the human disease. This is an extremely relevant model, as it highly resembles the progression of human ovarian cancer and provides opportunities to study the earliest events in initiation of HGSC.

The majority of studies to date have focused on BMPs in the ovary and OSE. However, now that it is clear the OSE is not the origin of high-grade serous ovarian cancer, it would be of interest to determine the role that the BMP signalling pathway plays in the fallopian tube. To set the stage it will be relevant to determine the expression of various BMPs and their receptors by IHC in STIC lesions from human and mouse fallopian tube. Based on the expression levels, knockout of these specific components of the pathway using the aforementioned mouse model would provide insight into the role of this pathway in initiation and early pathogenesis of high-grade serous ovarian cancer. This would nicely complement the studies presented in this thesis where we demonstrate a role for this pathway in advanced-stage HGSC.

Very little is known about the role of LKB1 in ovarian cancer pathogenesis. However, recent studies from the Teixeria lab demonstrate that loss of *Pten* and *STK11* in the OSE results in formation of high-grade papillary serous carcinomas[33]. This suggests that loss of LKB1 may be important in tumour establishment, but based on the findings presented in this thesis, LKB1 also aids in cell survival during later metastatic stages. However, the transgenic mouse model of high-grade serous ovarian cancer discussed above is a more relevant model with which to test this hypothesis since it provides a more accurate representation of disease initiation. Knockout of *STK11* in addition to *Pten Tp53* and *Brca1/2* specifically in the secretory epithelium of the fallopian tube may in fact result in more rapid disease progression in this model. Ideally, all combinations of this knockouts focusing on this gene set would provide the most relevant information regarding the importance of LKB1 in the initiation and progression of HGSC. These mouse models would indicate which genes, in combination with homozygous or heterozygous loss of LKB1 activity might predispose secretory epithelial cells to transformation and metastasis to the ovary and peritoneal cavity. These studies would help to determine at which stage of disease progression LKB1 activity is important for either disease progression or inhibition, providing additional support for the findings discussed in Chapter 3.

4.5 Synthesis

The goal of this thesis was to contribute to our knowledge of ovarian cancer metastasis, particularly focusing on multicellular spheroids as major contributors to formation of secondary metastatic lesions. The data presented in Chapters 2 and 3 characterizes two signalling pathways that are dysregulated in EOC spheroids and discusses the potential for targeting these pathways therapeutically. Overall, this body of work has contributed to the field of ovarian cancer metastasis by uncovering unique and complex interactions between a number of signalling cascades and provided rationale for investigating these pathways further in preclinical models. Understanding the unique characteristics afforded to non-adherent ovarian cancer cells is critical for the identification of more effective treatment regimes particularly for late-stage recurrent disease.

4.6 References

1. Correa, R.J., Peart, T., Valdes, Y.R., Dimattia, G.E. & Shepherd, T.G. Modulation of AKT activity is associated with reversible dormancy in ascites-derived epithelial ovarian cancer spheroids. *Carcinogenesis* **33**, 49-58 (2012).
2. Meijer, A.J. & Codogno, P. AMP-activated protein kinase and autophagy. *Autophagy* **3**, 238-240 (2007).
3. Papandreou, I., Lim, A.L., Laderoute, K. & Denko, N.C. Hypoxia signals autophagy in tumor cells via AMPK activity, independent of HIF-1, BNIP3, and BNIP3L. *Cell Death Differ* **15**, 1572-1581 (2008).
4. Shield, K., Ackland, M.L., Ahmed, N. & Rice, G.E. Multicellular spheroids in ovarian cancer metastases: Biology and pathology. *Gynecol Oncol* **113**, 143-148 (2009).
5. Sodek, K.L., Ringuette, M.J. & Brown, T.J. Compact spheroid formation by ovarian cancer cells is associated with contractile behavior and an invasive phenotype. *International journal of cancer* **124**, 2060-2070 (2009).
6. Veatch, A.L., Carson, L.F. & Ramakrishnan, S. Differential expression of the cell-cell adhesion molecule E-cadherin in ascites and solid human ovarian tumor cells. *International journal of cancer. Journal international du cancer* **58**, 393-399 (1994).
7. Scheel, C.*, et al.* Paracrine and autocrine signals induce and maintain mesenchymal and stem cell states in the breast. *Cell* **145**, 926-940 (2011).
8. Shepherd, T.G. & Nachtigal, M.W. Identification of a putative autocrine bone morphogenetic protein-signaling pathway in human ovarian surface epithelium and ovarian cancer cells. *Endocrinology* **144**, 3306-3314 (2003).

9. Theriault, B.L., Shepherd, T.G., Mujoomdar, M.L. & Nachtigal, M.W. BMP4 induces EMT and Rho GTPase activation in human ovarian cancer cells. *Carcinogenesis* **28**, 1153-1162 (2007).
10. Chen, X., Liao, J., Lu, Y., Duan, X. & Sun, W. Activation of the PI3K/Akt Pathway Mediates Bone Morphogenetic Protein 2-Induced Invasion of Pancreatic Cancer Cells Panc-1. *Pathol Oncol Res*.
11. Kang, M.H.*, et al.* Inhibition of PI3 kinase/Akt pathway is required for BMP2-induced EMT and invasion. *Oncol Rep* **22**, 525-534 (2009).
12. Weroha, S.J.*, et al.* Tumorgrafts as in vivo surrogates for women with ovarian cancer. *Clinical cancer research : an official journal of the American Association for Cancer Research* (2014).
13. Bhowmick, N.A., Neilson, E.G. & Moses, H.L. Stromal fibroblasts in cancer initiation and progression. *Nature* **432**, 332-337 (2004).
14. Hayward, S.W.*, et al.* Malignant transformation in a nontumorigenic human prostatic epithelial cell line. *Cancer Res* **61**, 8135-8142 (2001).
15. Kuperwasser, C.*, et al.* Reconstruction of functionally normal and malignant human breast tissues in mice. *Proceedings of the National Academy of Sciences of the United States of America* **101**, 4966-4971 (2004).
16. Olumi, A.F.*, et al.* Carcinoma-associated fibroblasts direct tumor progression of initiated human prostatic epithelium. *Cancer Res* **59**, 5002-5011 (1999).
17. Cai, J.*, et al.* Fibroblasts in omentum activated by tumor cells promote ovarian cancer growth, adhesion and invasiveness. *Carcinogenesis* **33**, 20-29 (2012).
18. Zhang, Y.*, et al.* Ovarian cancer-associated fibroblasts contribute to epithelial ovarian carcinoma metastasis by promoting angiogenesis, lymphangiogenesis and tumor cell invasion. *Cancer Lett* **303**, 47-55 (2011).
19. Fu, S.*, et al.* Stromal-epithelial crosstalk provides a suitable microenvironment for the progression of ovarian cancer cells in vitro. *Cancer Invest* **31**, 616-624 (2013).
20. Liang, J. & Mills, G.B. AMPK: a contextual oncogene or tumor suppressor? *Cancer Res* **73**, 2929-2935 (2013).
21. Egan, D.F.*, et al.* Phosphorylation of ULK1 (hATG1) by AMP-activated protein kinase connects energy sensing to mitophagy. *Science* **331**, 456-461 (2011).
22. Kim, J., Kundu, M., Viollet, B. & Guan, K.L. AMPK and mTOR regulate autophagy through direct phosphorylation of Ulk1. *Nat Cell Biol* **13**, 132-141 (2011).
23. Lee, J.W., Park, S., Takahashi, Y. & Wang, H.G. The association of AMPK with ULK1 regulates autophagy. *PLoS One* **5**, e15394 (2010).
24. Avivar-Valderas, A.*, et al.* Regulation of autophagy during ECM detachment is linked to a selective inhibition of mTORC1 by PERK. *Oncogene* **32**, 4932-4940 (2013).
25. Li, L. & Guan, K.L. Microtubule-associated protein/microtubule affinity-regulating kinase 4 (MARK4) is a negative regulator of the mammalian target of rapamycin complex 1 (mTORC1). *J Biol Chem* **288**, 703-708 (2013).
26. Suzuki, A.*, et al.* Identification of a novel protein kinase mediating Akt survival signaling to the ATM protein. *J Biol Chem* **278**, 48-53 (2003).

27. Suzuki, A.*, et al.* ARK5 suppresses the cell death induced by nutrient starvation and death receptors via inhibition of caspase 8 activation, but not by chemotherapeutic agents or UV irradiation. *Oncogene* **22**, 6177-6182 (2003).
28. Barbone, D.*, et al.* The Bcl-2 repertoire of mesothelioma spheroids underlies acquired apoptotic multicellular resistance. *Cell death & disease* **2**, e174.
29. Mayer, B.*, et al.* Multicellular gastric cancer spheroids recapitulate growth pattern and differentiation phenotype of human gastric carcinomas. *Gastroenterology* **121**, 839-852 (2001).
30. Tai, J., Cheung, S.S., Ou, D., Warnock, G.L. & Hasman, D. Antiproliferation activity of Devil's club (Oplopanax horridus) and anticancer agents on human pancreatic cancer multicellular spheroids. *Phytomedicine* (2013).
31. Moren, A., Raja, E., Heldin, C.H. & Moustakas, A. Negative regulation of TGFbeta signaling by the kinase LKB1 and the scaffolding protein LIP1. *J Biol Chem* **286**, 341-353 (2011).
32. Perets, R.*, et al.* Transformation of the fallopian tube secretory epithelium leads to high-grade serous ovarian cancer in brca;tp53;pten models. *Cancer cell* **24**, 751-765 (2013).
33. Tanwar, P.S.*, et al.* Loss of LKB1 and PTEN tumor suppressor genes in the ovarian surface epithelium induces papillary serous ovarian cancer. *Carcinogenesis* (2013).

Appendix A: Additional Figures

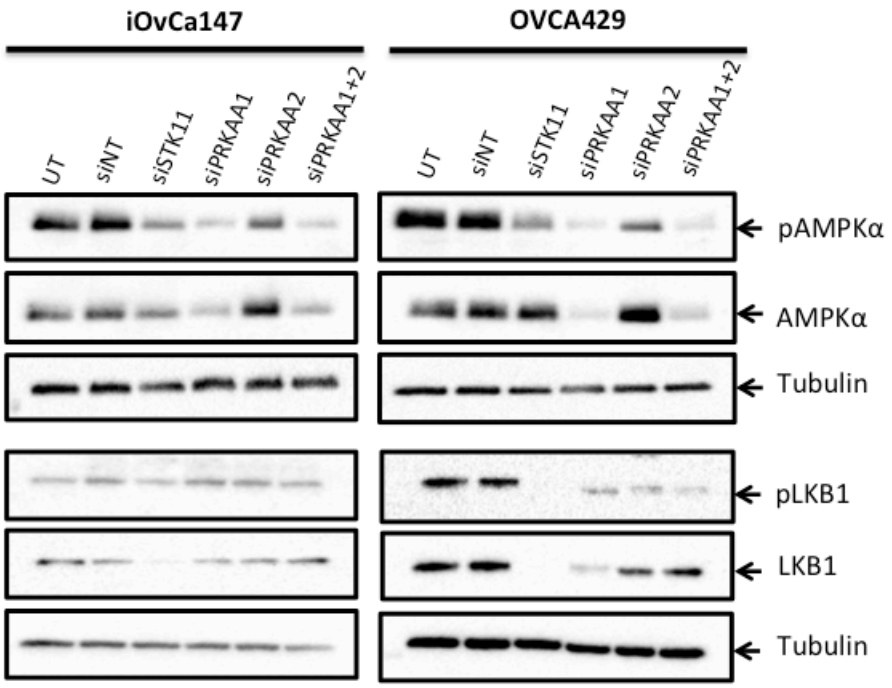

Figure 1: siRNA-mediated knockdown of *PRKAA2* does not affect levels of AMPKα. Immunoblot performed on proteins as indicated 72 hours after transfection of adherent EOC cells with siRNA. AMPKα expression and activity is decreased by *PRKAA1* knockdown but not *PRKAA2*.

Appendix B: Ethics Approval

Research Western

Use of Human Participants - Ethics Approval Notice

Principal Investigator: Dr. Gabriel DiMattia
Review Number: 12668E
Review Level: Delegated
Approved Local Adult Participants: 90
Approved Local Minor Participants: 0
Protocol Title: Development of Biological Models for the translation ovarian cancer research initiative.
Department & Institution: Biochemistry, University of Western Ontario
Sponsor:
Ethics Approval Date: December 09, 2011 **Expiry Date:** December 31, 2015
Documents Reviewed & Approved & Documents Received for Information:

Document Name	Comments	Version Date
Revised Study End Date	The study end date has been extended to December 31, 2015 to allow for project completion.	

This is to notify you that The University of Western Ontario Research Ethics Board for Health Sciences Research Involving Human Subjects (HSREB) which is organized and operates according to the Tri-Council Policy Statement: Ethical Conduct of Research Involving Humans and the Health Canada/ICH Good Clinical Practice Practices: Consolidated Guidelines; and the applicable laws and regulations of Ontario has reviewed and granted approval to the above referenced revision(s) or amendment(s) on the approval date noted above. The membership of this REB also complies with the membership requirements for REB's as defined in Division 5 of the Food and Drug Regulations.

The ethics approval for this study shall remain valid until the expiry date noted above assuming timely and acceptable responses to the HSREB's periodic requests for surveillance and monitoring information. If you require an updated approval notice prior to that time you must request it using the UWO Updated Approval Request Form.

Members of the HSREB who are named as investigators in research studies, or declare a conflict of interest, do not participate in discussion related to, nor vote on, such studies when they are presented to the HSREB.

The Chair of the HSREB is Dr. Joseph Gilbert. The UWO HSREB is registered with the U.S. Department of Health & Human Services under the IRB registration number IRB 00000940.

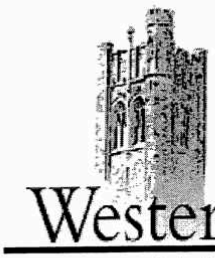

Office of Research Ethics

The University of Western Ontario
Room 4180 Support Services Building, London, ON, Canada N6A 5C1
Telephone: (519) 661-3036 Fax: (519) 850-2466 Email: ethics@uwo.ca
Website: www.uwo.ca/research/ethics

Use of Human Subjects - Ethics Approval Notice

Principal Investigator: Dr. T.G. Shepherd
Review Number: **16391E** **Review Level:** Expedited
Review Date: August 12, 2009
Protocol Title: Investigating key signalling pathways in secondary tumour implants formed during ovarian cancer metastasis
Department and Institution: Oncology, London Health Sciences Centre
Sponsor: CIHR-CANADIAN INSTITUTE OF HEALTH RESEARCH
Ethics Approval Date: August 28, 2009 **Expiry Date:** September 30, 2014
Documents Reviewed and Approved: UWO Protocol, Letter of Information and Consent.
Documents Received for Information:

This is to notify you that The University of Western Ontario Research Ethics Board for Health Sciences Research Involving Human Subjects (HSREB) which is organized and operates according to the Tri-Council Policy Statement: Ethical Conduct of Research Involving Humans and the Health Canada/ICH Good Clinical Practice Practices: Consolidated Guidelines; and the applicable laws and regulations of Ontario has reviewed and granted approval to the above referenced study on the approval date noted above. The membership of this REB also complies with the membership requirements for REB's as defined in Division 5 of the Food and Drug Regulations.

The ethics approval for this study shall remain valid until the expiry date noted above assuming timely and acceptable responses to the HSREB's periodic requests for surveillance and monitoring information. If you require an updated approval notice prior to that time you must request it using the UWO Updated Approval Request Form.

During the course of the research, no deviations from, or changes to, the protocol or consent form may be initiated without prior written approval from the HSREB except when necessary to eliminate immediate hazards to the subject or when the change(s) involve only logistical or administrative aspects of the study (e.g. change of monitor, telephone number). Expedited review of minor change(s) in ongoing studies will be considered. Subjects must receive a copy of the signed information/consent documentation.

Investigators must promptly also report to the HSREB:

a) changes increasing the risk to the participant(s) and/or affecting significantly the conduct of the study;
b) all adverse and unexpected experiences or events that are both serious and unexpected;
c) new information that may adversely affect the safety of the subjects or the conduct of the study.

If these changes/adverse events require a change to the information/consent documentation, and/or recruitment advertisement, the newly revised information/consent documentation, and/or advertisement, must be submitted to this office for approval.

Members of the HSREB who are named as investigators in research studies, or declare a conflict of interest, do not participate in discussion related to, nor vote on, such studies when they are presented to the HSREB.

Appendix C: Summary of Clinical Data for EOCs

Sample	Age	Histological Subtype	Grade	Stage
EOC57	46	Serous adenocarcinoma	3	IIIC
EOC61	78	Serous adenocarcinoma	3	IIIC
EOC63	70	Carcinosarcoma	3 (High)	IIIC
EOC116	64	Papillary serous	2	IIIC
EOC120	70	Goblet cell carcinoma	n.a.	n.a.
EOC122	56	Serous carcinoma	High	IIIC
EOC129	74	Serous carcinoma	High	IIIC
EOC132	59	Serous Adenocarcinoma	High	IIIC
EOC136	42	Serous ovarian carcinoma	High	IV
EOC137	77	Serous Carcinoma	High	IIIC
EOC140	76	poorly differentiated carcinoma	High	IIIC
EOC148	67	Bilateral ovarian serous carcinoma	High	IC*
EOC149	69	Serous adenocarcinoma	High	IIIC
EOC153	48	Serous (60%) and endometriod (40%)	High	IIA
EOC154	66	Serous intra-abdominal carcinomatosis	High	IIIC
EOC155	66	Serous adenocarcinoma (poorly-differentiated)	High	IIIC
EOC156	67	Serous	High	IIIC
EOC158	45	Papillary serous	2/3	IIIC
EOC159	57	Serous adenocarcinoma	High	n.a.
EOC160	47	Cystadenofibroma (benign)	n.a.	n.a.
EOC171	65	Serous carcinoma	High	IIIC
iOVCA130	59	Serous Carcinoma	High	IIIC
iOVCA147-E2	43	Serous (70%) and clear cell (30%) adenocarcinoma	2	IIC
iOVCA198	65	serous adenocarcinoma	High	n.a.

*, stage was defined as at least IC for this patient.
n.a., not available

Appendix D: Copyright Permissions

SPRINGER LICENSE
TERMS AND CONDITIONS

Jan 28, 2014

This is a License Agreement between Teresa M Peart ("You") and Springer ("Springer") provided by Copyright Clearance Center ("CCC"). The license consists of your order details, the terms and conditions provided by Springer, and the payment terms and conditions.

All payments must be made in full to CCC. For payment instructions, please see information listed at the bottom of this form.

License Number	3317810075785
License date	Jan 28, 2014
Licensed content publisher	Springer
Licensed content publication	Clinical & Experimental Metastasis
Licensed content title	BMP signalling controls the malignant potential of ascites-derived human epithelial ovarian cancer spheroids via AKT kinase activation
Licensed content author	Teresa M. Peart
Licensed content date	Jan 1, 2012
Volume number	29
Issue number	4
Type of Use	Thesis/Dissertation
Portion	Full text
Number of copies	5
Author of this Springer article	Yes and you are the sole author of the new work
Order reference number	
Title of your thesis / dissertation	Mechanisms of ovarian cancer spheroid formation and reattachment
Expected completion date	Apr 2014
Estimated size(pages)	150
Total	0.00 CAD
Terms and Conditions	

Introduction

The publisher for this copyrighted material is Springer Science + Business Media. By clicking "accept" in connection with completing this licensing transaction, you agree that the following terms and conditions apply to this transaction (along with the Billing and Payment terms and conditions established by Copyright Clearance Center, Inc. ("CCC"), at the time that you opened your Rightslink account and that are available at any time at http://myaccount.copyright.com).

Curriculum Vitae

Teresa Marie Peart

EDUCATION

University of Western Ontario, London, Ontario
PhD, Anatomy and Cell Biology Sept 2008-March 2014

University of Western Ontario, London, Ontario
Bachelor of Science, Honours Cell and Developmental Biology 2007

McKinnon Park Secondary School, Caledonia, Ontario
OSSD and Ontario Scholar Award 2003

RESEARCH-RELATED EXPERIENCE

University of Western Ontario, London, Ontario
Translational Ovarian Cancer Research Program Sept. 2008-March 2014

- My research examines the role of key signalling pathways and their relation to ovarian cancer pathogenesis
- Using novel cell culture methods to examine hypotheses
- Presented findings at a number of local and National conferences
- Author on several peer-reviewed publications

Fourth year thesis project Sept. 2006-May 2007

- Studied the muscle physiology of exercising grass carp
- Responsible for developing and carrying out methods for exercising grass carp as well as accurately sampling blood and muscle
- Performed various in-vitro tests
- Responsible for keeping accurate laboratory records
- Presented findings in two conferences

TEACHING EXPERIENCE

Undergraduate Teaching assistant, Medical Science 4461, University of Western Ontario

Jan 2012-Aptil 2012

Undergraduate Teaching assistant, Medical Science 4900, University of Western Ontario

Sept 2011-present

Honours Student Mentorship
Arlan Walsh, Department of Biochemistry, University of Western Ontario
Sept 2010-April 2011

- Responsible for training student in proper laboratory techniques, overseeing daily experiments as well as providing expertise crucial for project completion

Anton Shimanovsky, Department of Biology, McMaster University
Sept 2009-Aug 2010

- Responsible for training student in proper laboratory techniques as well as overseeing daily experiments

Dominik Dobransky, Department of Biochemistry, University of Western Ontario
Sept 2009-April 2010

- Responsible for training student in proper laboratory techniques, overseeing daily experiments as well as providing expertise crucial for project completion

Undergraduate Teaching assistant, Anatomy and Cell Biology 3319, University of Western Ontario
Sept 2008-April 2009

SCHOLARSHIPS

Ontario Graduate Scholarship Sept. 2012-Sept. 2013

CIHR student training program in Cancer Research Sept. 2009-Sept. 2013

PUBLICATIONS

Peer-Reviewed Publications

Correa RJ, Ramos Valdes Y, **Peart TM**, Fazio EN, Bertrand M, McGee J, Préfontaine M, Sugimoto A, Dimattia GE, Shepherd TG (2014). Combination of AKT inhibition with autophagy blockade effectively reduces ascites-derived ovarian cancer cell viability. *Carcinogenesis.*

Peart T, Correa R, DiMattia GE, Shepherd TG (2012). BMP signalling controls the malignant potential of ascites-derived human epithelial ovarian cancer cells via Akt kinase activation in an *in vitro* metastasis model. *Clinical and Experimental Metastasis*

Correa R, **Peart T**, Ramos-Valdes Y, DiMattia GE, Shepherd TG (2011). Modulation of AKT activity is associated with reversible dormancy in ascites-derived epithelial ovarian cancer spheroids. *Carcinogenesis.*

Abstracts

Peart T., Ramos-Valdés Y, Bertrand M, Sugimoto AK, Préfontaine M, DiMattia GE, and Shepherd TG (2010) Activated BMP signalling differentially modulates cellular adhesion and motility in epithelial ovarian cancer spheroids. *UWO department of Oncology Research and Education Day; awarded poster prize*

Peart T., Ramos-Valdés Y, Bertrand M, Sugimoto AK, Préfontaine M, DiMattia GE, and Shepherd TG (2010) Activated BMP signalling differentially modulates cell adhesion and motility during ovarian cancer spheroid formation and attachment. *5th Annual Canadian Conference on Ovarian Cancer Research; Toronto, Ontario.*

Peart T, Bertrand M, Sugimoto AK, Prefontaine M, DiMattia GE and Shepherd TG (2011) Activated BMP signalling modulates multicellular spheroid formation and reattachment of ascites-derived human epithelial ovarian cancer cells in an *in vitro* model of metastasis. *Published in AACR 102nd Annual Meeting Program; Denver, CO*.

Peart T, Bertrand M, Sugimoto AK, Prefontaine M, DiMattia GE and Shepherd TG (2011) Activated BMP signalling modulates multicellular spheroid formation and reattachment of ascites-derived human epithelial ovarian cancer cells in an *in vitro* model of metastasis. *Paul Harding Research Day; London, Ontario*.

Peart T, Bertrand M, Sugimoto AK, Prefontaine M, DiMattia GE and Shepherd TG (2011) Activated BMP signalling modulates multicellular spheroid formation and reattachment of ascites-derived human epithelial ovarian cancer cells in an *in vitro* model of metastasis. *Canadian Cancer Research Conference; Toronto, Ontario*.

Peart T, Bertrand M, Sugimoto AK, Prefontaine M, DiMattia GE and Shepherd TG (2012) The 5'-AMP-activated protein kinase (AMPK) pathway is upregulated in ovarian cancer spheroids to promote the dormant phenotype. *Paul Harding Research Day; London, Ontario; awarded poster prize.*

Peart T, Bertrand M, Sugimoto AK, Prefontaine M, DiMattia GE and Shepherd TG (2012) The 5'-AMP-activated protein kinase (AMPK) pathway is upregulated in ovarian cancer spheroids to promote the dormant phenotype. *Canadian Conference on Ovarian Cancer Research; Quebec City, Quebec; awarded prize for oral presentation.*

Peart T, Bertrand M, Sugimoto AK, Prefontaine M, DiMattia GE and Shepherd TG (2012) The 5'-AMP-activated protein kinase (AMPK) pathway is upregulated in ovarian cancer spheroids to promote the dormant phenotype*. UWO Oncology Research and Education Day.*